Novel Agonists and Potent Antagonists at $P2Y_{11}$ Purinergic Receptors: Synthesis and Biological Testing

Neue Agonisten und potente Antagonisten an $P2Y_{11}$ Purinergen Rezeptoren: Synthese und Biologische Untersuchung

Inaugural-Dissertation
zur
Erlangung des Doktorgrades
der Mathematisch-Naturwissenschaftlichen Fakultät
der Heinrich-Heine-Universität Düsseldorf

vorgelegt von
Sophi Damayanti
aus Bandung, Indonesien

Düsseldorf, 2008

Aus dem Institut für Pharmazeutische und Medizinische Chemie
der Heinrich-Heine-Universität-Düsseldorf

„Gedruckt mit Unterstützung der Islamic Development Bank (IDB)“

Gedruckt mit der Genehmigung
der Mathematisch-Naturwissenschaftlichen Fakultät
der Heinrich-Heine-Universität Düsseldorf

Referent: Prof. Dr. Matthias U. Kassack
Koreferent: Prof. Dr. Thomas Kurz

Tag der mündlichen Prüfung: 26.11.2008

Erklärung

Ehrenwörtlich erkläre ich hiermit, dass ich die vorgelegte Dissertation mit dem Titel: “Novel agonists and potent antagonists at $P2Y_{11}$ purinergic receptors: Synthesis and biological testing” selbst angefertigt und ohne fremde Hilfe verfasst habe. Quellen und Hilfsmittel sind vollständig angegeben. Weiterhin erkläre ich, dass ich bisher keine erfolglosen Promotionsversuche unternommen habe.

Düsseldorf, 27.10.2008
Sophi Damayanti

For my husband and my parents

I am truly blessed

LIST OF CONTENTS

1. INTRODUCTION 1

1.1. Purinergic receptors 1
1.1.1. General aspects 1
1.1.2. P2X receptors 2
1.1.2.1. Role and location 2
1.1.2.2. Ligands at P2X receptors 4
1.1.3. P2Y receptors 6
1.1.3.1. G protein-coupled receptors 6
1.1.3.2. Location and role of P2Y receptors 8
1.1.3.3. Ligands at P2Y receptors 10
1.2. $P2Y_{11}$ receptors 15
1.2.1. General aspects 15
1.2.2. Role of $P2Y_{11}$ receptors 15
1.2.3. Ligands at $P2Y_{11}$ receptors 16

2. AIM AND SCOPE OF THE STUDY 19

2.1. Synthesis of novel ligands 19
2.1.1. Synthesis of urea derivatives containing trisodium 7-naphthalene-1,3,5-trisulfonate substituent and 4-fluoro -3,1-phenylene-linker 19
2.1.2. Synthesis of urea derivatives containing trisodium 3-(2,4-disulfonatophenylcarbamoyl)benzoate substituent 21
2.2. Biological evaluation 21

3. CHEMISTRY 22

3.1. Synthesis of urea derivatives containing trisodium 7-naphthalene-1,3,5-trisulfonate substituent 22
3.1.1. Synthesis of “small urea” derivatives 24
3.1.1.1. Trisodium 7-(4-fluoro-3-nitrobenzamido)-naphthalene-1,3,5-trisulfonate 24
3.1.1.2. Trisodium 7-(3-amino-4-fluorobenzamido)-naphthalene-1,3,5-trisulfonate 33
3.1.1.3. Hexasodium 7,7’-{carbonylbis[azanediyl(4-fluoro-3,1-phenylene) carbonylazanediyl]}bis(naphthalene-1,3,5-trisulfonate) 40
3.1.2. Synthesis of “large urea” derivatives 47
3.1.2.1. Trisodium 7-[4-(3-nitrobenzamido)-benzamido]-naphthalene-1,3,5-trisulfonate 47
3.1.2.2. Trisodium 7-[4-(3-aminobenzamido)-benzamido]-naphthalene-1,3,5-trisulfonate 50
3.1.2.3. Hexasodium 7,7′-{carbonylbis[azanediyl-3,1-phenylene carbonylazanediyl(4,1-phenylene)carbonylazanediyl]}bis(naphthalene-1,3,5-trisulfonate) 53

3.2. Synthesis of urea derivatives containing 4-fluoro-3,1- phenylene-linker at benzene or naphthalene sulfonates 57
3.2.1. Disodium 2-(4-fluoro-3-nitrobenzamido)benzene-1,4-disulfonate 58
3.2.2. Disodium 2-(3-amino-4-fluorobenzamido)benzene-1,4-disulfonate 64
3.2.3. Tetrasodium 2,2'-{carbonylbis[azanediyl(4-fluoro-3,1-phenylene)carbonylazanediyl]}bis(benzene-1,4-disulfonate) 69
3.3. Synthesis of urea derivatives containing trisodium 3-(2,4-disulfonatophenylcarbamoyl)benzoate substituent 75
3.3.1. Trisodium 3-(2,4-disulfonatophenylcarbamoyl)-5-(4-nitrobenzamido)benzoate 77
3.3.2. Trisodium 3-(2,4-disulfonatophenylcarbamoyl)-5-(4-aminobenzamido)benzoate 81
3.3.3. Hexasodium 5,5′-[carbonylbis(azanedyl-4,1-phenylenecarbonylazanediyl]bis[3-(2,4-disulfonatophenylcarbamoyl)benzoat] 84

4. PHARMACOLOGY 89

4.1. Evaluation of the test system 89
4.2. Agonist screening of compounds at $P2Y_{11}$ receptors 91
4.2.1. Primary agonist screening of compounds at $P2Y_{11}$ receptors 91
4.2.2. Efficacy and potency testing 94
4.2.3. Concentration-response curves of compounds 8c and 9c 96
4.2.4. Schild analysis of compound 9c 99
4.3. Antagonist screening at $P2Y_{11}$ receptors 101
4.4. Urea derivatives containing trisodium 7-naphthalene-1,3,5-trisulfonate substituent 107
4.4.1. Apparent pK_i value of urea 1c -14c 107
4.4.2. Schild analysis of compound 5c 117
4.5. Urea derivatives containing 4-fluoro-3,1-phenylene-linker 118
4.6. Urea derivatives containing trisodium 3(2,4-disulfonatophenylcarbamoyl)benzoate substituent 123
4.7. Selectivity of the test compound 125
4.7.1. Selectivity test at $P2Y_1$ receptors 125
4.7.2. Selectivity test at $P2Y_2$ receptors 127
4.7.3. Selectivity test at $P2Y_4$ receptors 130

5. CONCLUSION 133

6. ABSTRACT 137

7. ZUSAMMENFASSUNG 138

8. MATERIALS AND METHODS 140

8.1. Chemistry 140
8.1.1. Instruments and analytical methods 140
8.1.1.1. pH stat 140
8.1.1.2. Thin layer chromatography 140

8.1.1.3. High performance liquid chromatography 141
8.1.1.4. UV-visible spectrophotometry 142
8.1.1.5. Titration method: NaCl determination 142
8.1.1.6. Elemental analysis 142
8.1.1.7. Infrared spectroscopy 143
8.1.1.8. Nuclear magnetic resonance spectroscopy 143
8.1.1.9. Mass spectrometry 143
8.1.2. Chemical 144
8.1.3. General reaction procedures (GRP) 145
8.1.3.1. GRP 1: Preparation of acylchloride 145
8.1.3.2. GRP 2: Synthesis of nitro derivative 145
8.1.3.3. GRP 3: Synthesis of amine derivative 145
8.1.3.4. GRP 4: Synthesis of urea compound 146
8.2. Biological testing 147
8.2.1. Instruments and materials 147
8.2.2. Chemicals 147
8.2.3. Buffers and solutions 148
8.2.4. Cell culture method 150
8.2.4.1. General aspects 150
8.2.4.2. Growth medium 150
8.2.4.3. Detaching process 151
8.2.4.4. Cryoconservation 151
8.2.4.5. Passaging cells 151
8.2.5. Biological testing technique 152
8.2.5.1. Preparation of the dilution series 152
8.2.5.2. Assay preparation 152
8.2.5.3. Screening of compounds 154
8.2.5.4. Assay condition 155
8.2.5.5. EC_{50} and IC_{50} 155
8.2.5.6. Data analysis 156
8.2.5.7. Schild-analyse 157

9. MONOGRAPHS 158

10. REFERENCES 253

11. ABBREVIATIONS 261

12. APPENDIX 263

1. Introduction

1.1. Purinergic receptors

1.1.1. General aspects

The first investigation of extracellular signaling by purines was done by Drury and Szent-Györgyi. They described effects of an extract of heart muscle and other tissues which contained adenosine and adenosinemonophosphate (AMP) on the cardiovascular system (Cheek, 2000). In 1976, Burnstock has suggested the new term of purinergic receptors (Burnstock, 1976). Two years later, the purinergic receptors were subdivided into P1 (adenosine) and P2 (ATP, UTP and ADP) receptors according to their agonists (Burnstock, 1978). Figure 1.1 shows an overview of the classification of purinergic receptors.

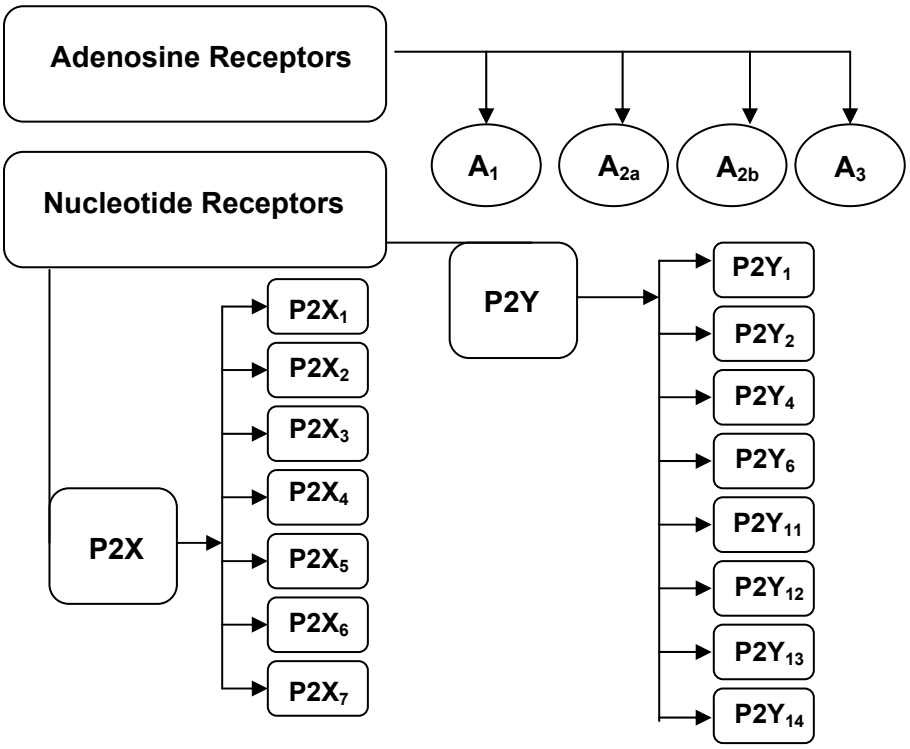

Figure 1.1 Classification of purinergic receptors. Adenosine P1 receptors consist of A_1, A_{2A}, A_{2B}, and A_3 receptors and nucleotide P2 receptors are divided into P2X receptors ($P2X_{1\text{-}7}$) and P2Y receptors ($P2Y_{1, 2, 4, 6, 11\text{-}14}$).

P1 receptors consist of four G protein-coupled receptors (GPCRs): A_1, A_{2A}, A_{2B}, and A_3 (Abbracchio, 1996). P2 receptors can be subdivided into P2X receptors, which are ligand gated ion channels and P2Y receptors, which belong to the group of GPCRs. Seven human P2X receptors ($P2X_{1-7}$) and eight P2Y receptors ($P2Y_{1, 2, 4, 6, 11-14}$) have been cloned (Abbrachio *et al.,* 2006; Ralevic and Burnstock, 1998).
P2 receptors are activated by nucleotides such as ATP, ADP, UTP, UDP, and UDP-glucose (Müller, 2002). Previously, ATP was only known as an important energy source molecule. In the recent decades, ATP and other nucleotides were recognized as native ligands at purinergic receptors (Burnstock, 2007; Abbracchio *et al*., 2006; Gever *et al*., 2006).

1.1.2. P2X receptors

1.1.2.1. Role and location

P2X receptors belong to the great class of ligand gated ion channels. A P2X receptor monomer consists of two transmembrane domains connected by a large extracellular loop containing the putative ATP binding site (Figure 1.2)

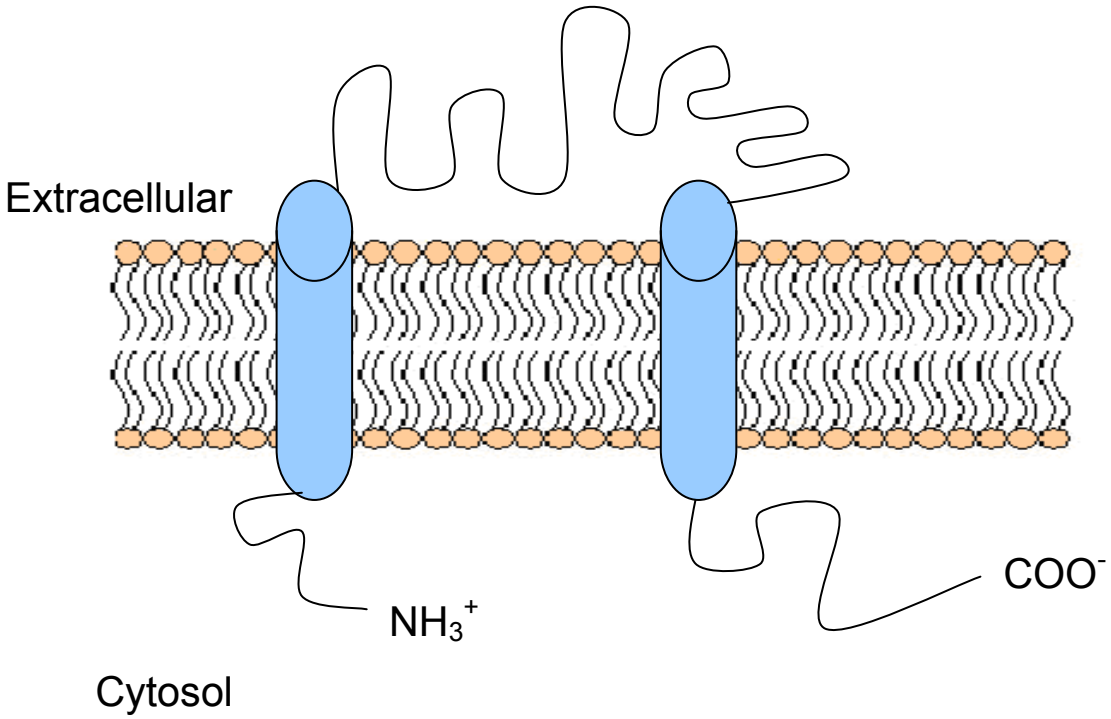

Figure 1.2 P2X ion channel monomer consists of intracellular carboxy and amino termini, two transmembrane spanning domains, and a large extracellular ligand-binding loop.

Three P2X receptor subunits are involved in forming a cation-selective ion channel, which is gated by extracellular ATP and some related nucleotides. The channel can be built by homotrimers ($P2X_1$, $P2X_2$, $P2X_3$, $P2X_4$, $P2X_5$, $P2X_7$ receptors) and heteromers ($P2X_{1/2}$, $P2X_{2/3}$, $P2X_{1/5}$, $P2X_{2/6}$, $P2X_{4/6}$, $P2X_{1/4}$ receptors) (Gever *et al.*, 2006; Egan *et al.*, 2004; North, 2002).

P2X receptors are located at autonomic, central, enteric and sensory neurons, cochlear and retinal cells, endothelium and epithelium, vascular and visceral smooth muscle, heart and developing skeletal muscle, bone, platelets, and hemopoietic cells (Clifford *et al.*, 1998; Gever *et al.,* 2006; North, 2002).

$P2X_1$ receptors contribute to platelet aggregation. They are involved in platelet shape change. However, they are unable to promote platelet aggregation by themselves (Gachet, 2005). ATP might be involved in acute pain. ATP was reported to be involved in migraine (Burnstock, 1981) and pain pathways in the spinal cord (Jahr and Jessel, 1983; Fyffe and Perl, 1984; Salter and Henry, 1985). Furthermore, the role of ATP in nociceptive signaling has been cleared when $P2X_3$ receptors were cloned (Kennedy 2005; Chen *et al.*, 1995; Lewis *et al.*, 1995). In particular, $P2X_3$ and $P2X_{2/3}$ receptors were reported as interesting targets for the

treatment of inflammatory, visceral, and probably neuropathic pain (Chizh and Illes, 2000). $P2X_7$ receptors are expressed in a variety of cell types and involved in pain, inflammatory processes, and neurodegeneration (Romagnoli *et al.*, 2008). In summary, P2X receptors are an appealing target for pharmacological intervention.

1.1.2.2. Ligands at P2X receptors

ATP acts as agonist at P2X receptors. $\alpha\beta$-Methylene ATP was also reported as a potent and selective agonist for receptors containing $P2X_1$ and $P2X_3$ subunits (North, 2002). The first described antagonist for this receptor subtype was suramin. NF023, NF279, and NF449 were reported as selective and increasingly potent antagonists at $P2X_1$ receptors (Figure 1.3) (Kassack *et al.*, 2004; Damer, 2002; Braun *et al.,* 2001).

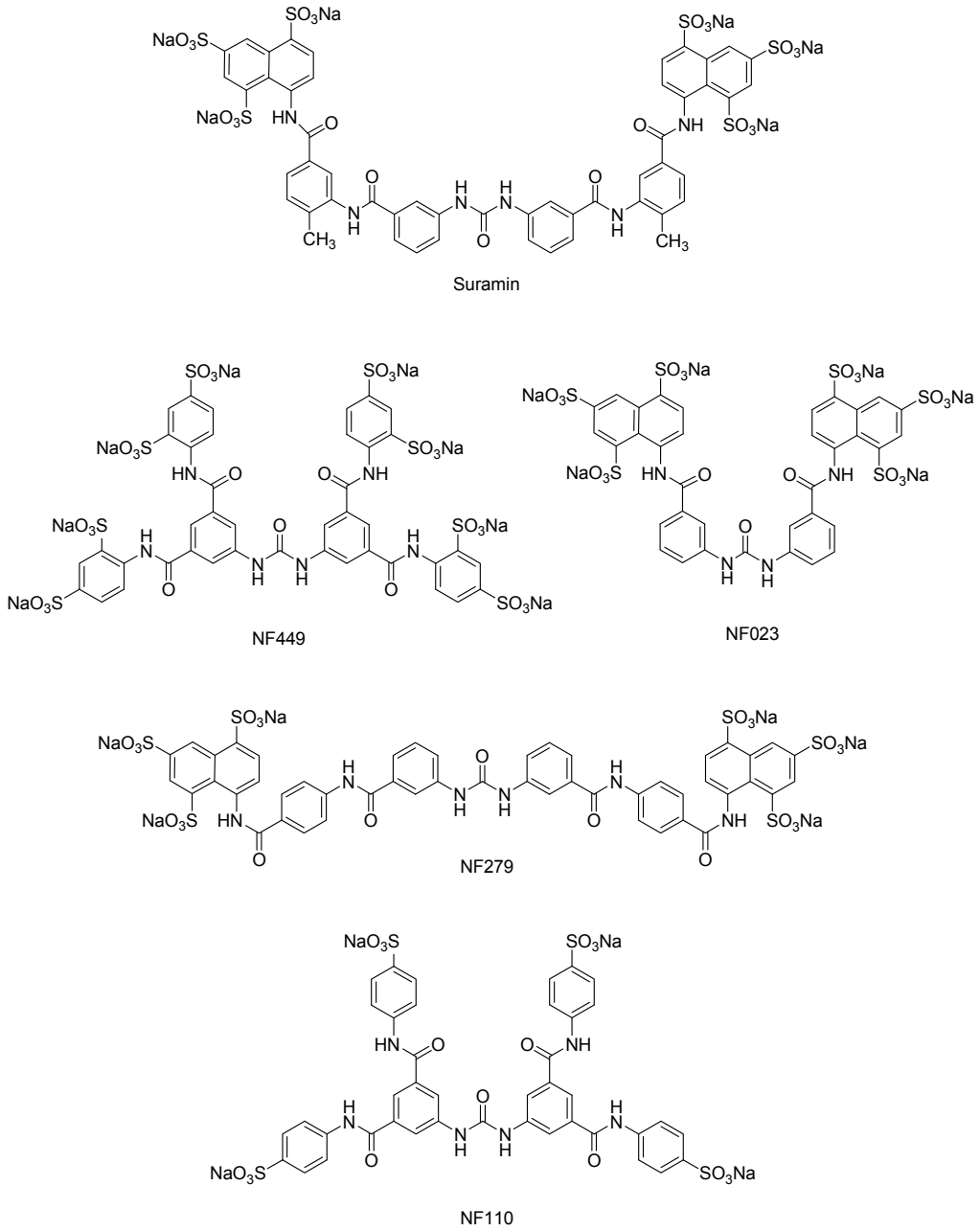

Figure 1.3 P2X receptor antagonists.

Among the described substances, NF449 is the most potent and selective antagonist at $P2X_1$ receptors with a K_i value of 0.3 nM (Braun *et al.*, 2001). At $P2X_3$ receptors, NF110 exhibited an antagonistic activity with a K_i value of 36.0 nM (Hausmann *et al.*, 2006). It is also known that pyridoxal-phosphate-6-azophenyl-2′,4′-disulfonic acid (PPADS) and its derivatives also have antagonistic activity at P2X receptors (Kim *et al.*, 2001; Brown *et al.*, 2001).

1.1.3. P2Y receptors

1.1.3.1. G protein-coupled receptors

All of the P2Y receptors belong to the family of G protein-coupled receptors (GPCRs). It is estimated that more than 50 % of all drugs regulate GPCR function and 30 % of these drugs are directly targeted to GPCRs (Fredholm *et al.*, 2007; Jacoby *et al.*, 2006, Flower, 1999). GPCRs are important based on their roles in human cell signaling (Milligan, 2003; Brink *et al.*, 2004). GPCRs play a key role for the translation of extracellular stimuli in intracellular signals. They are involved in the primary mechanism of eukaryotic cells to accept, interpret, and activate a broad range of different extracellular stimuli (Kostenis *et al.*, 2005). Structurally, GPCRs are seven transmembrane spanning receptors (7TM) (Figure 1.4).

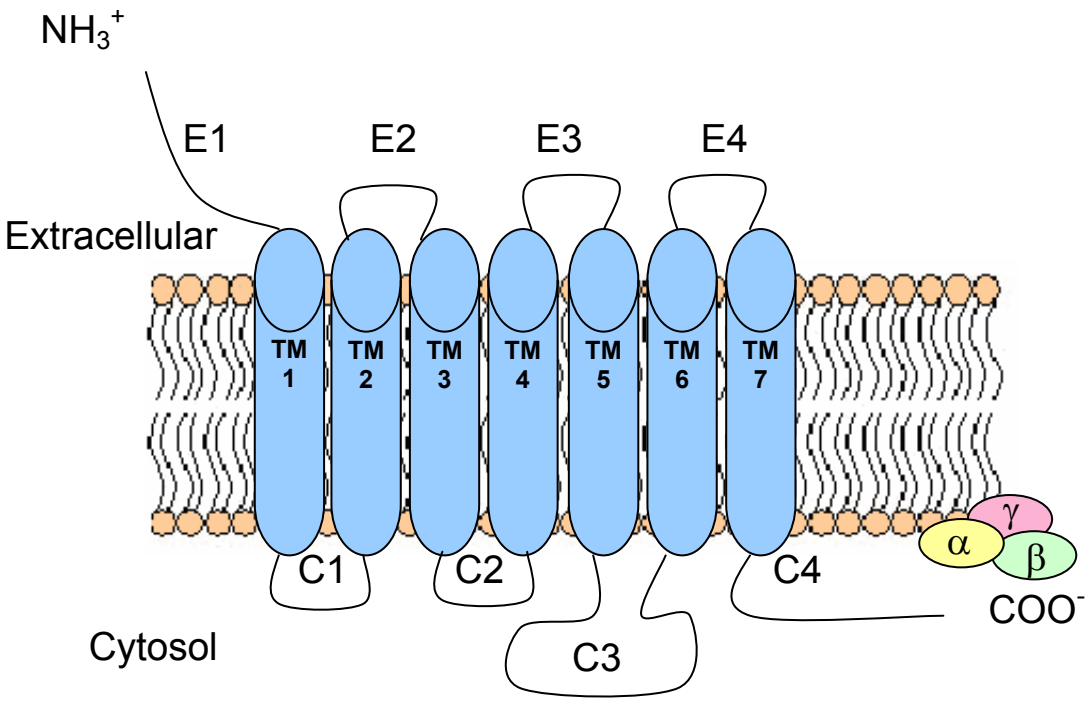

Figure 1.4 G-Protein coupled receptor consists of seven transmembrane spanning domains, an intracellular carboxy terminus, and extracellular amino terminus.

They activate heterotrimeric G proteins (guanine-nucleotide-binding proteins) which consist of three subunits: α, β, and γ. The α-subunit shows GTP-ase activity. It determines the intracellular signal transduction by inhibition or activation of different effector systems. G proteins can be subdivided into three families

according to their sequence homologies: G_s, G_i/G_o, and G_q. In the rest time, α subunits of G proteins are attached to GDP. Once an agonistic ligand binds to the specific site of a GPCR, the receptor is activated and a conformational change of the receptor protein leads to an exchange of GDP to GTP at the α subunit of the G protein. Thus, the α subunit dissociates from the β/γ subunit and both can be involved in the modulation of effector proteins such as adenylate cyclase or phospholipase C.

The G_s protein stimulates the enzymatic synthesis of the secondary messenger cyclic AMP (cAMP) by activating adenylate cyclase. The G_i/G_o protein has the opposite effect. The G_q-protein activates phospholipase C which catalyses hydrolysis of phosphatidylinositol-4,5-bisphosphate (PIP_2) into two second messengers, namely inositol-1,4,5-triphosphate (IP_3) and diacylglycerole (DAG) (Figure 1.5) (Fredholm *et al.*, 2007; Steinhilber *et al.*, 2005, Patrick, 1995).

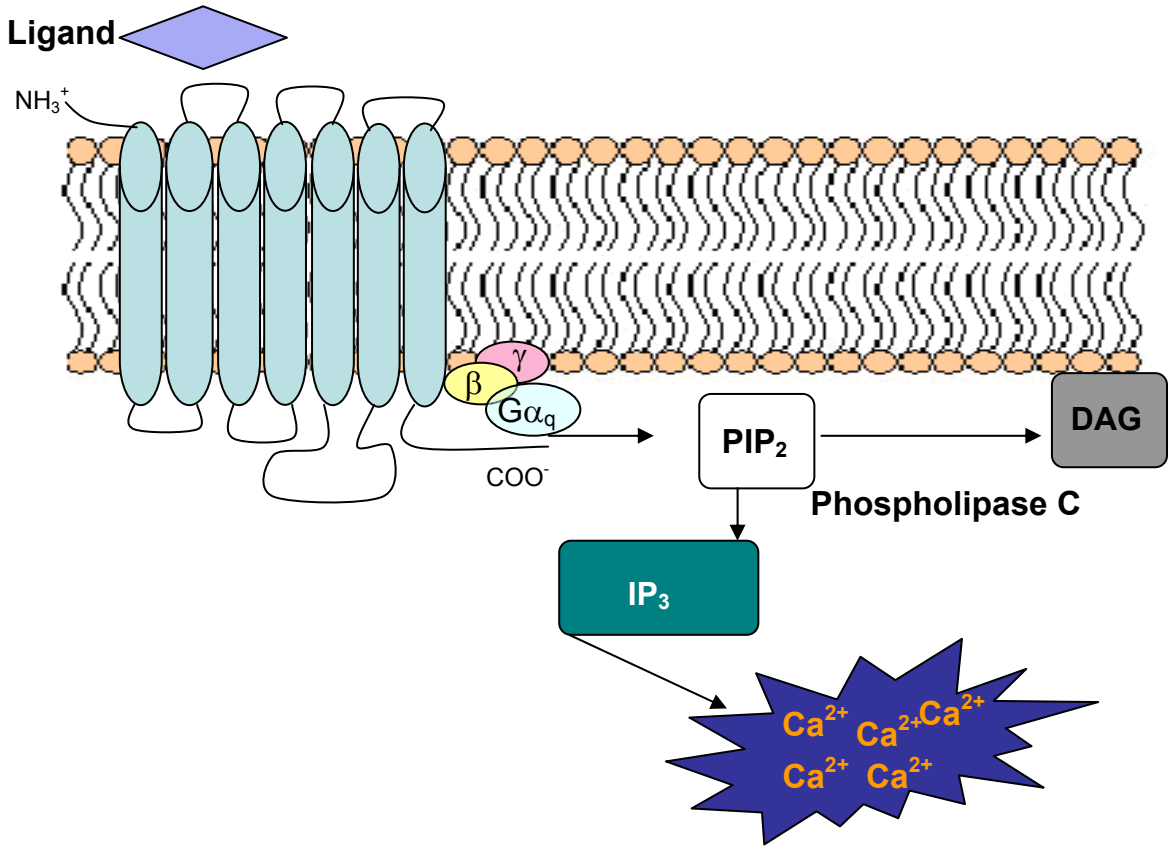

Figure 1.5 Signal transduction of G_q-coupling receptors. DAG = Diacylglycerol, IP_3 = Inositol-1,4,5-triphosphate, PIP_2 = Phosphatidylinositol-4,5-bisphosphate.

IP_3 is a hydrophilic molecule that mobilizes the release of intracellular Ca^{2+} from the endoplasmic reticulum. Ca^{2+} shows numerous regulations of diverse cellular functions. Meanwhile DAG activates protein kinase C (Steinhilber *et al.*, 2005; Patrick, 1995).

1.1.3.2. Location and role of P2Y receptors

Up to now, eight P2Y receptor subtypes are identified, cloned, and characterized. They can be divided into two phylogenetic groups. One group consists of $P2Y_1$, $P2Y_2$, $P2Y_4$, $P2Y_6$, and $P2Y_{11}$ receptors mainly coupled to phospholipase C (G_q-coupling) and the other consists of the $P2Y_{12}$, $P2Y_{13}$, and $P2Y_{14}$ receptors that inhibit adenylyl cyclase (G_i-coupling) (Abbrachio *et al.*, 2003). $P2Y_1$ receptors were detected mostly in placenta, platelets, brain, and prostate. This receptor was rarely found in liver, stomach, lymphocytes, bone marrow, and kidney. $P2Y_1$ receptors were reported to take part in platelet activation and aggregation. Platelet activation is important for the arrest of bleeding. It occurs in response to vessel injury (Gachet, 2005; Baurand *et al.*, 2000, Boeynaems *et al.*, 2001). $P2Y_2$ receptors were detected in the heart, skeletal muscle, and several brain areas at high level. These receptors were found in lymphocytes, spleen, bone marrow, lung, and macrophages at medium level. They were detected in pancreas, stomach, and liver at low level (Moore *et al.*, 2001). Agonists of $P2Y_2$ receptors were developed for the treatment of symptomatic cystic fibrosis (Parr *et al.*, 1994). $P2Y_2$ receptors were reported to have a role in the dry eye syndrome (Müller, 2002). A high expression of $P2Y_2$ receptors was found in different cell types of the eye. Activation of $P2Y_2$ receptors by their agonists appears to regulate ocular surface hydration. It stimulates chloride secretion and increases tear production (Fujihara *et al.*, 2001; Mundasad *et al.*, 2001).

$P2Y_4$ receptors have a limited distribution. These receptors are expressed almost specifically in placenta, intestine, and brain. Expression in lung was found at low level (Moore *et al.*, 2001) as well as in monocyte and lymphocytes (Jin *et al.*, 1998b). $P2Y_4$ receptors seem to be involved in the regulation of epithelial chloride transport in the jejunum (Robaye *et al.*, 2003). $P2Y_6$ receptors were found at high level in spleen, kidney, and placenta (Communi *et al.*, 1996). They were also

detected in the vascular system, smooth muscle, and lung at moderate level (Ralevic and Burnstock, 1998). These receptors were also found in the liver at low level and were detected in some brain regions (Moore *et al.*, 2001). $P2Y_6$ receptors were reported to have a role in stimulation of proliferation of human lung epithelial cells (Schäfer *et al.*, 2003).

The main receptors in this study are $P2Y_{11}$ receptors, which are expressed at high level in brain and intestine as well as in lymphocytes and spleen. $P2Y_{11}$ receptors are expressed in other tissues at moderate level and the lowest levels were detected in the spinal cord (Moore *et al.*, 2001). $P2Y_{11}$ receptors seem to have a role in maturation and migration of dendritic cells (Wilkin *et al.*, 2001; Schnurr *et al.*, 2003). Detailed information for $P2Y_{11}$ receptors is given in Chapter 1.2.

$P2Y_{12}$ receptors were found in brain, spinal cord, and platelets (Barnard and Simon, 2001; Takasaki *et al.*, 2001; Sasaki *et al.*, 2003). $P2Y_{12}$ receptors play a central role in platelet activation. These receptors were reported to take part in amplification and completion of platelet activation and aggregation (Schoeneberg *et al.*, 2007; Gachet, 2005). Antagonists of $P2Y_{12}$ receptors are metabolites of clopidogrel and ticlopidin. They have been widely used as antiplatelet drugs (Angiolillo *et al.*, 2008; Michelson, 2008; Sandros, 2008). Figure 1.6 shows the structure formulas of clopidogrel and ticlodipin.

Ticlodipin Clopidogrel

Figure 1.6 $P2Y_{12}$ receptor antagonists: ticlodipin and clopidogrel.

Clinical studies showed that clopidogrel is an effective antiplatelet agent and as safe as aspirin in medium dose (Caprie, 1996). A significant reduction of the risk of myocardial infarction, ischemic stroke, peripheral artery disease, or vascular death was reported in combination with aspirin. CURE (Clopidogrel in Unstable Angina to Prevent Recurrent Ischemic Events) has shown that a combination therapy of both clopidogrel and aspirin has raised beneficial effects. If given to everyone in the United States with acute coronary syndrome, the combination of

clopidogrel and aspirin could prevent between 50,000 and 100,000 new myocardial infarction, strokes and deaths annually (Mitka, 2001). Based on these result, FDA approved clopidogrel for the treatment of some acute coronary syndromes

$P2Y_{13}$ receptors were detected at high level in brain and spleen (Marteau *et al.*, 2003; Zhang *et.al.*, 2002). They are also expressed in bone marrow, heart, and peripheral leukocytes. So far, there is no precise evidence for their tissue function (Abbrachio *et al.*, 2006). Lastly, $P2Y_{14}$ receptors were detected at high level in adipose tissue, the intestine, stomach, and placenta. Spleen, heart, lung, and many brain regions showed moderate level (Moore *et al.*, 2003). They were reported to have an important role in peripheral and neuroimmune function (Moore *et al.*, 2003).

In conclusion, based on their role and expression in the human body, P2Y receptors are important targets for drug development.

1.1.3.3. Ligands at P2Y receptors

P2Y receptor ligands are classified as nucleotides, nucleotide derivates, and non-nucleotides. The triphosphates ATP and UTP as well as the diphosphates ADP and UDP belong to nucleotide ligands. 2-MeSADP and 2-MeSATP are known nucleotide derivatives. Meanwhile, suramin, reactive blue 2 (RB-2), and PPADS are categorized as non-nucleotide antagonists. Table 1.1 shows agonists and antagonists at P2Y receptors (Fredholm *et al.*, 1997; Boarder and Hourani, 1998; Hollopeter *et al.*, 2001; Zhang *et al.*, 2001).

Table 1.1 Ligands for P2Y receptors (King and Towsend-Nicholson, 2003; Abbrachio, 2006)

Subtype	Agonists	Antagonists
$hP2Y_1$	MRS2365, ADP, ADPβS, 2-MeSADP, 2-MeSATP	MRS2179, MRS2279, MRS2500
$hP2Y_2$	UTP, ATP, Ap4A	Suramin
$hP2Y_4$	UTP, UTPγS	PPADS, Reactive Blue-2
$hP2Y_6$	UDP, UDPβS	MRS 2567, Reactive Blue-2
$hP2Y_{11}$	AR-C67085, ATPγS, BzATP, ATP	Suramin, NF157, NF340
$hP2Y_{12}$	2-MeSATP, 2-MeSADP	Metabolite of ticlopidine, clopidogrel, suramin, AZD6140
$hP2Y_{13}$	ADP, 2-MeSADP, 2-MeSATP, ADPβS, ATP	Suramin, MRS2211
$hP2Y_{14}$	UDP - glucose, UDP - galactose, UDP - *N* - acetylglucosamine	-

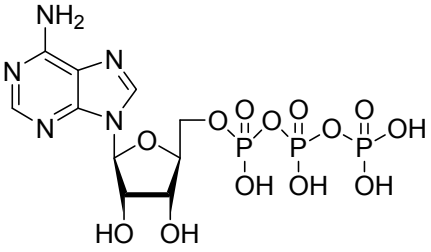

ATP

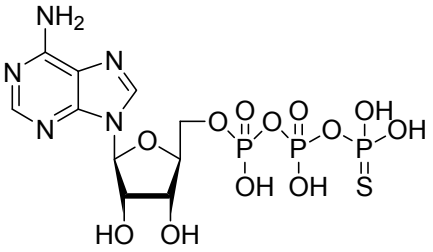

ATPγS

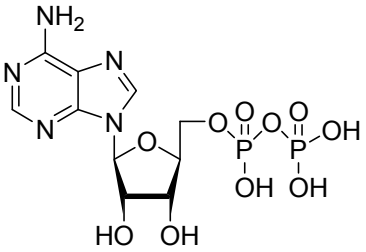

ADP

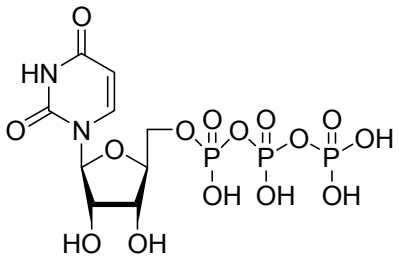

UTP

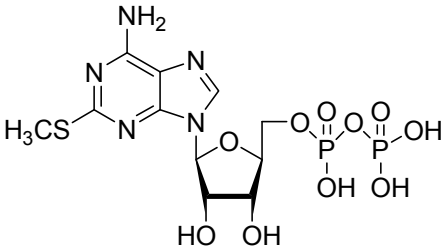

2-MeSADP

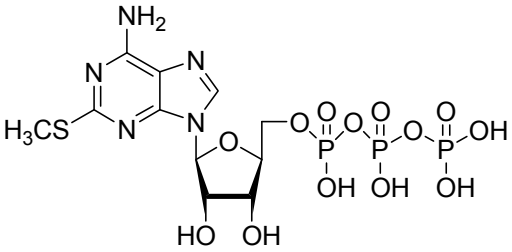

2-MeSATP

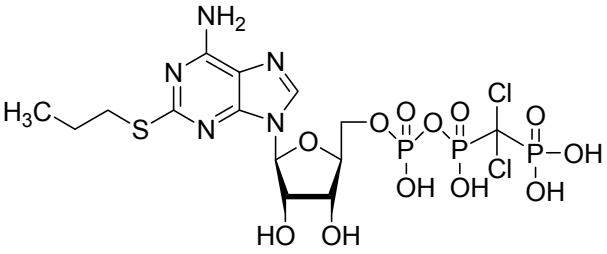

AR-C67085

Figure 1.7 P2Y receptor agonists.

Figure 1.7 shows the structure formulas of some agonists at P2Y receptors. Agonists at P2Y receptors are classified into four groups. $P2Y_1$, $P2Y_{11}$, $P2Y_{12}$, and $P2Y_{13}$ receptors are activated by adenine nucleotides (ADP and ATP). In the second group, $P2Y_4$ and $P2Y_6$ receptors are stimulated by uracil nucleotides

whereas $P2Y_2$ receptors are activated by both adenine and uracil nucleotides. $P2Y_{14}$ receptors are activated by UDP-glucose and other sugar coupled nucleotides (Abbrachio, 2006). $P2Y_{11}$ receptors are stimulated by ATP and ATPγS. ATPγS is the most potent agonist with an EC_{50} value of 261 nM in the cAMP assay and 55 nM at Ca-assay. EC_{50} value of ATP in Ca-assay was 214 nM (Meis, 2008). At $P2Y_2$ receptors, ATP and UTP act as agonist. $P2Y_4$ receptors are strongly stimulated by UTP. In the case of $P2Y_6$ receptors, UDP was identified as the most potent physiological nucleotide at these receptors. As mentioned above, $P2Y_{14}$ receptors are the receptors which are only activated by a complex of a nucleotide and sugar such as UDP-glucose, UDP-galactose, and UDP-*N*- acetylglucosamine (Abbracchio, 2006; King and Townsend-Nicholson, 2003).

Figure 1.8 shows structure formulas of some antagonists at P2Y receptors.

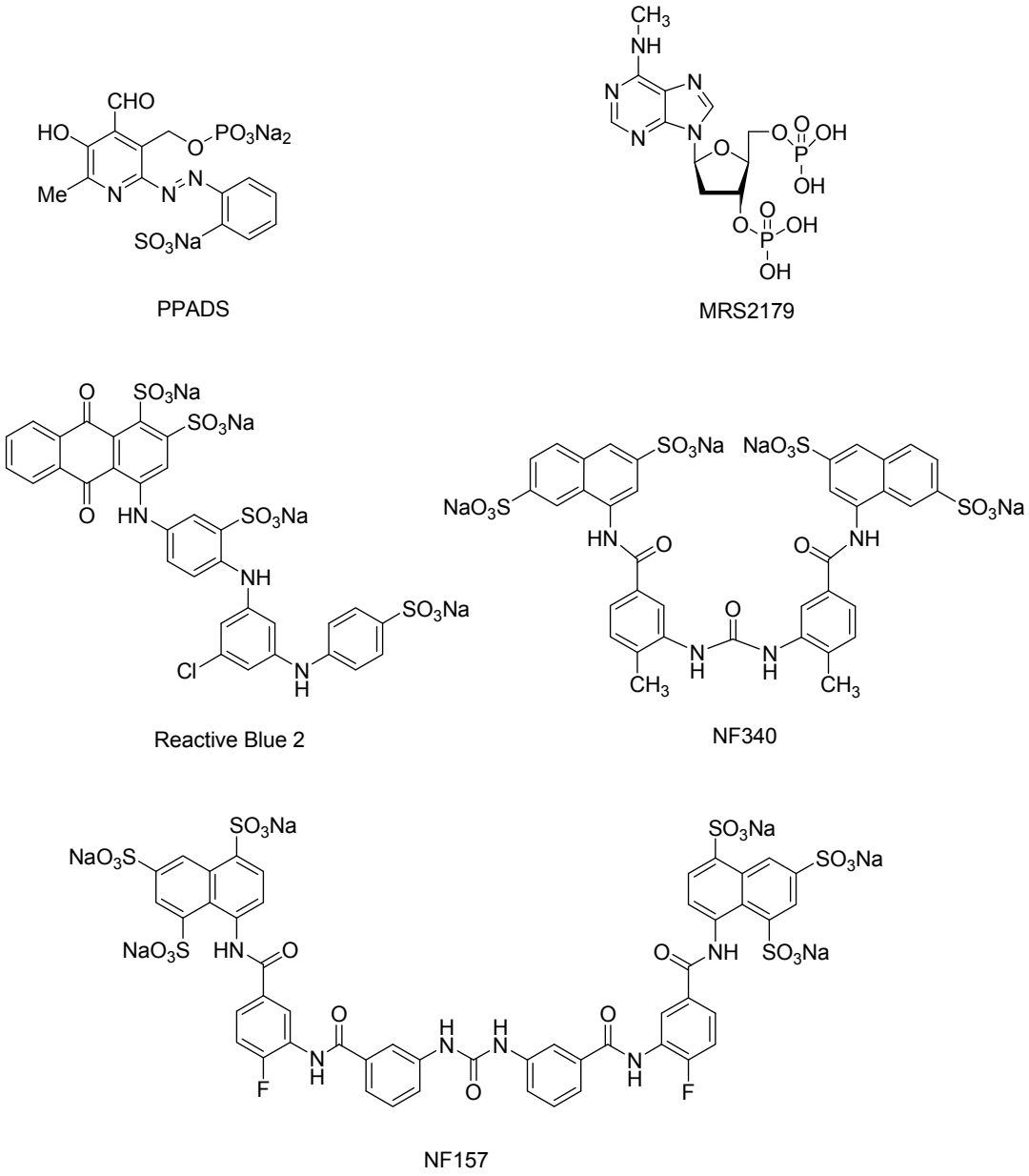

Figure 1.8 P2Y receptor antagonists.

2-MeSADP, MRS2179, and MRS2279 are known as selective antagonists at $P2Y_1$ receptors, whereas suramin is recognized as a non-selective antagonist at $P2Y_2$, $P2Y_{11}$, $P2Y_{12}$, and $P2Y_{13}$ receptors (King and Townsend-Nicholson, 2003; Dangelmaier *et al.*, 2001; Boyer *et al.*, 1998; Abracchio, 1996). PPADS and RB-2 are also known as antagonistic ligands at $P2Y_1$, $P2Y_4$ and $P2Y_6$ (Abbracchio, 2006; Nicholson, 2003). NF157 was introduced by our group as the first potent antagonist at $P2Y_{11}$ receptors (Ullmann e*t al.*, 2005).

1.2. $P2Y_{11}$ receptors

1.2.1. General aspects

$P2Y_{11}$ receptors are considered as unique receptors in comparison to other P2Y receptors. They are coupled to both phospholipase C and adenylyl cyclase pathways. Coupling to adenylyl cyclase is much weaker than to phospholipase C (Qi *et al.*, 2001). Secondly, the $P2Y_{11}$ receptor gene is the only one of the purinergic receptors containing an intron in the coding sequence (Communi *et al.*, 2001).

1.2.2. Role of $P2Y_{11}$ receptors

$P2Y_{11}$ receptors play a role in the maturation of dendritic cells. They are expressed in human monocyte-derived dendritic cells (Schnurr *et al.*, 2003; Wilkin *et al.*, 2001; Berchtold *et al.*, 1999). Dendritic cells (DC) are known as mononuclear phagocytic cells presenting antigen to T-lymphocytes. They are expressed in spleen as mononuclear phagocytes and the afferent lymphatics. In addition, they are widely distributed in the skin, lymph nodes, and paracortex as Langerhans' cells, interdigitating cells and veiled cells, respectively (Cruse, 2003).

DCs often function as a sensor of the immune system. They recognize exogenous antigens and mark them as a complex of peptide and major histocompatibility complex (MHC) on the cell surface (Cruse, 2003). It is known that ATP and TNF-α synergize in the activation and maturation of human dendritic cells (Schnurr *et al.*, 2000 and Wilkin *et al.*, 2001).

$P2Y_{11}$ receptors were reported as receptors for inhibiting TNF-α release. Activation of $P2Y_{11}$ receptors by ATP led to cAMP-induced PKA stimulation and subsequent down-regulation of TNF-α release (Swennen, 2006). The involvement of this receptor was demonstrated by pre-incubation of blood with 5′-adenosine monophosphate (5′-AMPS) prior to incubation with ATP. 5′-AMPS is a selective inhibitor of $P2Y_{11}$ receptors (Figure 1.9). Results showed that 5′-AMPS completely reversed the inhibitory effect of ATP on TNF-α release in blood. A confirmation of the involvement of the $P2Y_{11}$ receptor was further achieved by incubating blood with ATP in the presence of H-89, a potent inhibitor of cAMP-activated PKA. The

release of TNF-α was increased. The study concluded that inhibition of TNF-α release is dependent on PKA stimulation by cAMP, indicating the involvement of $P2Y_{11}$ receptors (Swennen, 2006). This result is an important implication for the treatment of chronic inflammatory diseases. Figure 1.9 shows the structure formulas of 5′-AMPS and H-89.

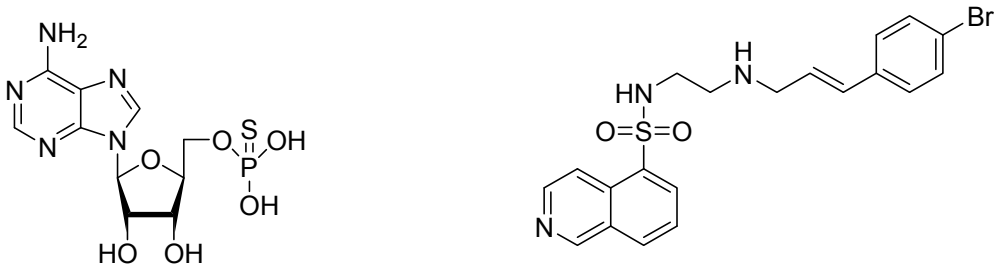

5'-AMPS H-89

Figure 1.9 Structure formulas of 5′ AMPS and H-89.

Furthermore, agonists of $P2Y_{11}$ receptors could possibly be used to improve cardiac output in patients with circulatory shock. On the other hand, P2Y receptor antagonists could be advantageous in patients with congestive heart failure (CHF) (Balogh *et al.*, 2005). $P2Y_{11}$ receptor expression in mice and other rodents is not detected. Cloning of the receptors was done only in man and dog (Zambon *et al.*, 2001; Communi *et al.*, 1999). According to the results of receptor stimulation in the mouse cardiomyocytes, $P2Y_{11}$-like receptors were discovered in mouse heart. They seem to have a role in controlling cardiomyocyte contractility. The order of agonist potency was AR-C67085 > ATPγS > 2-MeSATP >>> 2-MeSADP (structure formulas in Figure 1.7). This rank order is similar to the agonist profile of the $P2Y_{11}$ receptor (Communi *et al.,* 1999). These results suggest that $P2Y_{11}$ receptors might have potential as a therapeutic target in heart diseases (Amisten *et al.,* 2006; Balogh *et al.*, 2005).

1.2.3. Ligands at $P2Y_{11}$ receptors

At $P2Y_{11}$ receptors, ATP is the preferred native ligand (Communi *et al.*, 1999). The following amino acid residues were suggested to interact with the ATP molecule: Arg106, Phe109, Ser206, Arg268, Arg307, and Met310. The three positively

charged residues might interact electrostatically with the triphosphate moiety of ATP, while Ser206 possibly formed an H-bond with Pγ (Zylberg *et al*, 2007). The EC_{50} of ATP is 72 μM as determined by IP_3 whereas by cAMP accumulation assay is 17.4 μM (Communi *et al.*, 1999).

As well as in P2X receptors, the story of antagonist ligands at $P2Y_{11}$ receptors began with suramin. Suramin, a $P2Y_{11}$ receptor antagonist, is a polysulfonated naphthylurea with a K_i close to 1.0 μM. Unfortunately, it exhibits low selectivity at P2Y receptors (Communi *et al*., 1999). Synthesis of P2Y receptor ligands based on suramin showed an interesting result. The result could be used to derive structure-activity relationships (Ullmann *et al.,* 2005). NF157 is the first potent and selective antagonist at $P2Y_{11}$ receptors with nanomolar potency (Figure 1.8). Ullmann *et al.* described a K_i value of 44.3 nM for this compound which was about 7-fold more potent than suramin. In addition, it exhibited selectivity to $P2Y_{11}$ receptors over $P2Y_1$ and $P2Y_2$ receptors more than 650-fold higher (Ullmann *et al*, 2005).

Albeit NF157 has potent antagonistic effects at $P2Y_{11}$ receptors, it still has disadvantages. NF157 has the same potency at $P2X_1$ receptors. Another analogue, with a higher potency at $P2Y_{11}$ receptors, is NF340 (Figure 1.8). NF340 is a truncated urea analogue with nanomolar potency (K_i value of 19.5 nM, Meis, 2008). Besides NF340, Meis (Dissertation, 2008) also reported a high antagonistic activity of small urea of suramin derivative (NF294) with K_i value of 38.0 nM (Figure 1.10). NF340 and NF294 have a meta position between sulfonate and amido-linkage group.

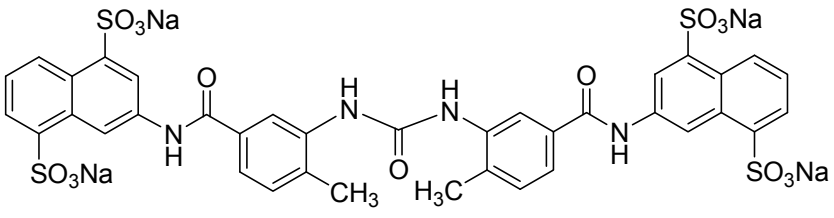

Figure 1.10 Structure formula of NF294.

Analogues of NF340 with variations of the sulfonate precursors have been synthesized by Hongwiset (2008). Hongwiset (Dissertation, 2008) reported a high potency urea derivative of NF340 (MK094) with a K_i value of 72.0 nM (Figure 1.11). At this stage, the research is still ongoing to discover still more potent suramin and NF340 analogues.

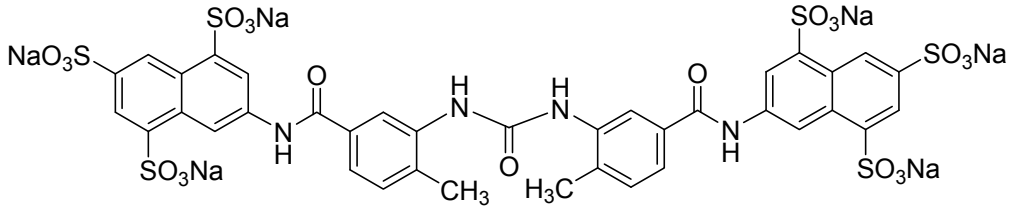

Figure 1.11 Structure formula of MK094.

So far, $P2Y_{11}$ receptors are less investigated than other P2Y receptors (Zylberg, 2007). Regarding the importance of $P2Y_{11}$ receptors, the exploration of their physiological role is one interesting step for drug development.

2. Aim and scope of the study

The unambiguous attribution of the $P2Y_{11}$ receptor with a specific effect is hampered by the lack of subtype-selective agonists and antagonists. Hence, novel antagonists or agonists to evaluate the physiological role of the $P2Y_{11}$ receptor are still required.

NF340, an antagonist with nanomolar potency, was recently identified (Meis, 2008). Analogues of NF340 with variation at the sulfonate precursor have been synthesized by Hongwiset (2008). Hongwiset synthesized with the variation at benzene or naphthalene sulfonate whereas in this study the phenylene-linker was varied. Moreover, the derivatives containing 4-fluoro phenylene-linker at benzene or naphthalene sulfonate were synthesized. Meis has reported the finding of non-nucleotide agonists (Meis, 2008). However the structure activity relationship was not fully understood. The aim of this study was to obtain a deeper insight in the structure activity relationship by using a further systematic variation of urea containing sulfonate group.

This study was divided into two parts: synthesis and biological evaluation.

2.1. Synthesis of novel ligands

2.1.1. Synthesis of urea derivatives containing trisodium 7-naphthalene-1,3,5-trisulfonate substituent and 4-fluoro -3,1-phenylene-linker

NF294 is a disulfonate derivative with methyl group at phenylene-linker with K_i value of 38.0 nM (Figure 1.10). MK094 is a trisulfonate derivative with the similar phenylene-linker with a K_i value of 72.0 nM (Figure 1.11). Both compounds have a sulfonate substitution in meta position to the amido-linkage group. The similar sulfonate precursor with MK094 was used in this study. Moreover, the fluorine analogue of suramin (NF157) showed high potency (Ullmann *et al.*, 2005). Therefore, it was interesting to study trisulfonate derivatives with a sulfonate substitution in meta position to the amido-linkage group and containing 4-fluoro-3,1- phenylene-linker. In this study, compound 5c was synthesized (Figure 2.1).

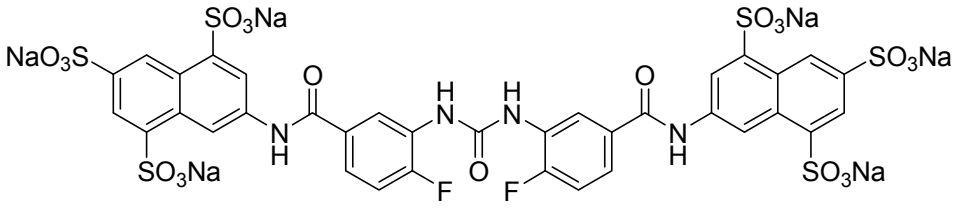

Figure 2.1 Structure formula of compound 5c.

Based on the result of the high antagonistic activity of compound 5c, further derivatives of compound 5c were designed and synthesized (Figure 2.2).

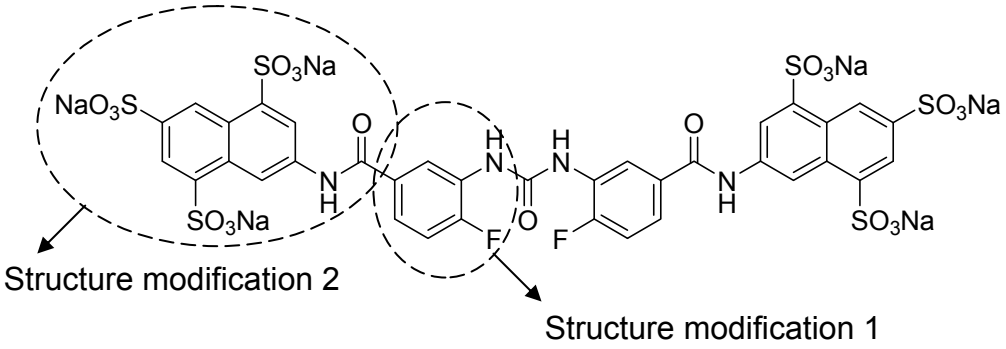

Figure 2.2 Structure modification 1 and 2 of compound 5c.

Modification 1: variation of the phenylene-linker. Symmetrical naphthalene sulfonate urea derivatives with variations of the phenylene-linker were planned to be synthesized. In addition, extended structures with a second phenylene-linker were further synthesized ("large urea").

Modification 2: variation of the numbers and positions of the sulfonate moieties of the naphthalene ring and benzene ring with the fluorinated phenylene-linker. This variation was planned to be synthesized in order to study which of the sulfonate moieties were important for $P2Y_{11}$ receptor activity. Moreover, it was investigated if the naphthalene could be substituted by a benzene ring.

2.1.2. Synthesis of urea derivatives containing trisodium 3-(2,4-disulfonatophenylcarbamoyl)benzoate substituent

Series of urea derivatives containing trisodium 3-(2,4-disulfonatophenyl-carbamoyl)benzoate substituent was synthesized. Ullmann (Dissertation, in process) reported a small urea containing this substituent. An extended structure of urea derivatives with variation of phenylene-linker extension were synthesized in this study (Figure 2.3).

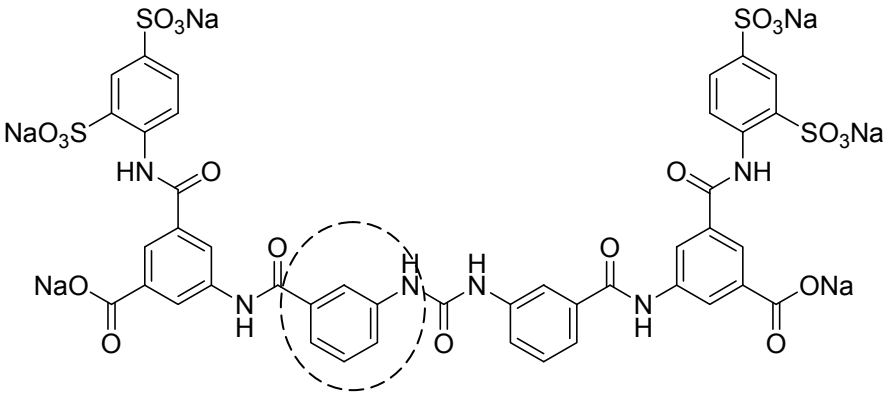

Figure 2.3 Structure modification 3: variation of the phenylene-linker.

Identification and purity of compounds were then analyzed by elemental analysis (C, H, and N), thin layer chromatography (TLC), high performance liquid chromatography (HPLC), infrared spectroscopy (IR), mass spectrometry (MS), and nuclear magnetic resonance (NMR) spectroscopy (^{1}H, ^{13}C).

2.2. Biological evaluation

Biological activities of the synthesized compounds were tested at $P2Y_{11}$ receptors recombinantly expressed in 1321N1 astrocytoma cells by measuring ligand induced changes in the intracellular calcium concentration. Furthermore, structure-activity relationships were discussed according to the biological results. The selectivity of the compounds for $P2Y_{11}$ receptors was investigated at $P2Y_1$, $P2Y_2$, and $P2Y_4$ receptors, each recombinantly expressed in 1321N1 astrocytoma cells.

3. Chemistry

3.1. Synthesis of urea derivatives containing trisodium 7-naphthalene-1,3,5-trisulfonate substituent

A series urea derivatives containing trisodium 7-naphthalene-1,3,5-trisulfonate substituent was synthesized by varying the phenylene-linker (Figure 3.1 and Figure 3.2). 14 ureas were synthesized. As an example of synthesis and structure conformation of compounds 5a, 5b, 5c, 9a, 9b and 9c are explained in detail in the following chapter.

.

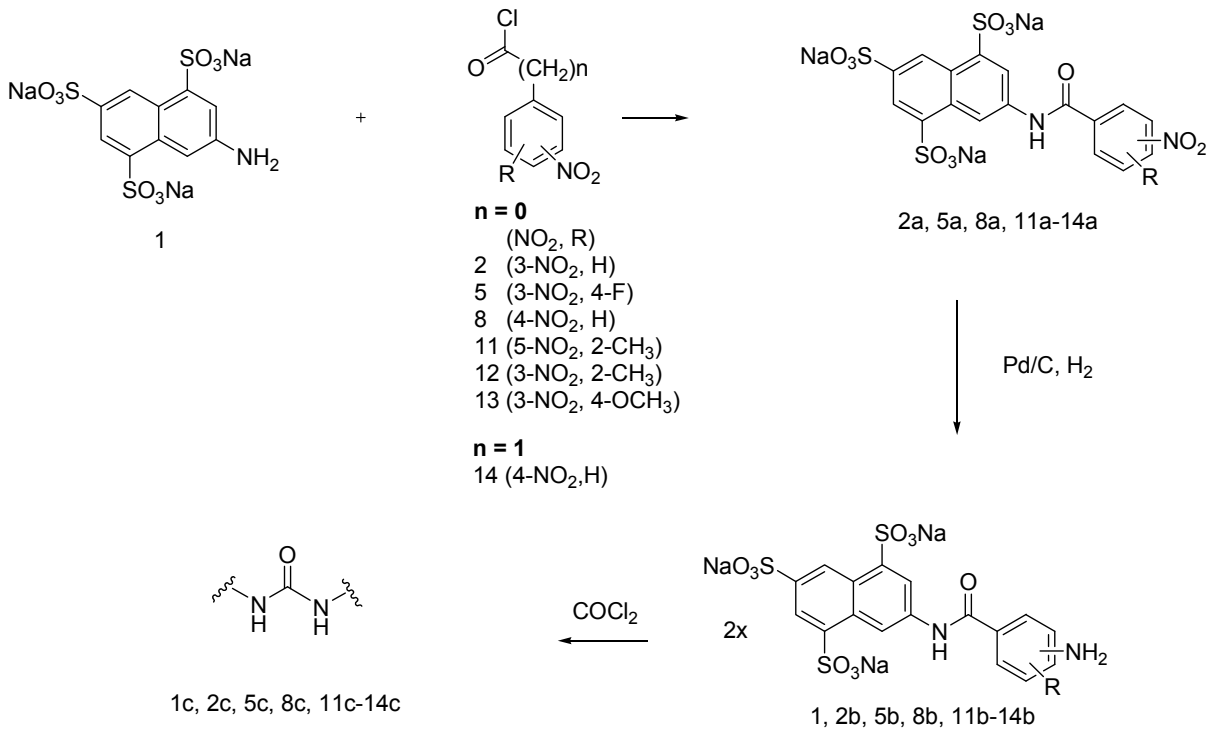

Figure 3.1 Synthesis pathways of small urea derivatives containing trisodium 7-naphthalene-1,3,5-trisulfonate substituent.

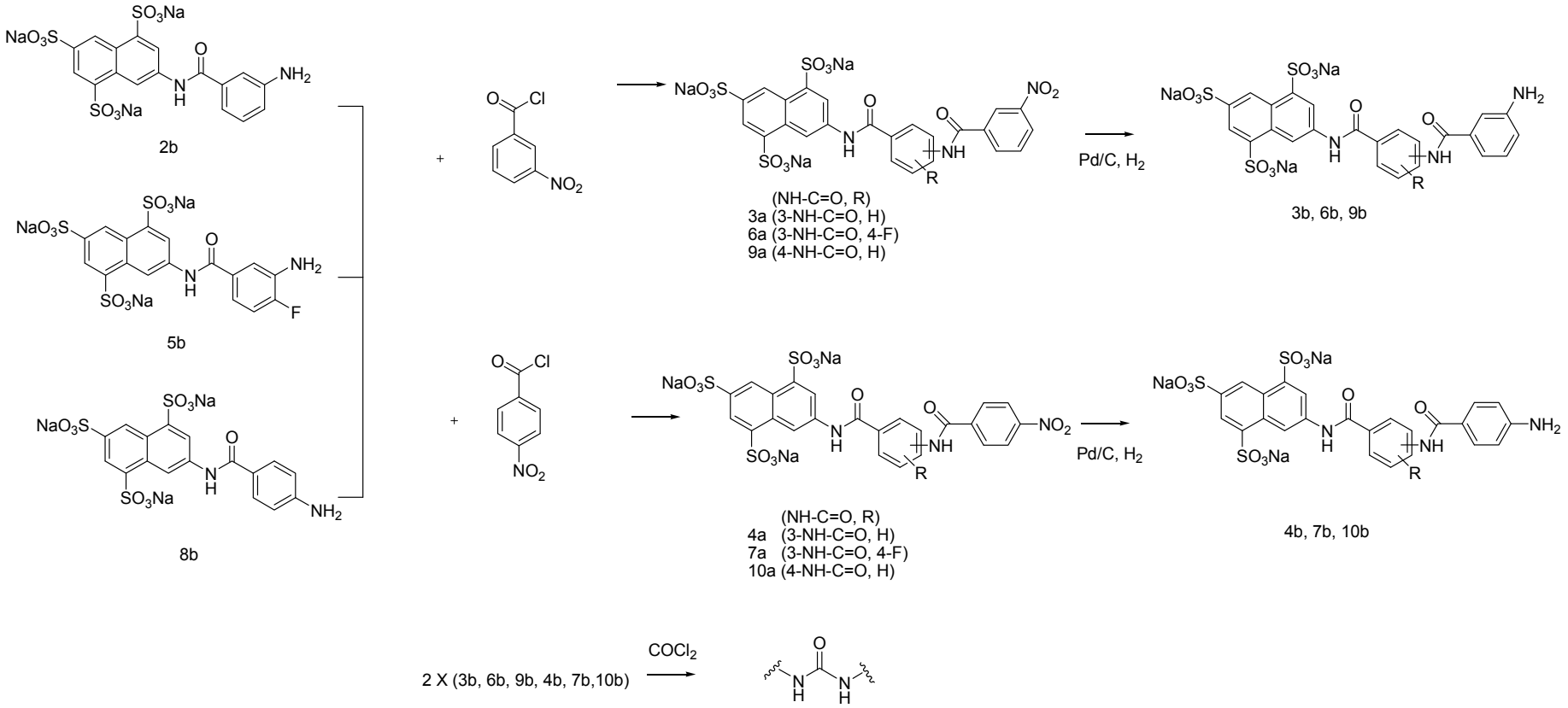

Figure 3.2 Synthesis pathways of large urea derivatives containing trisodium 7-naphthalene-1,3,5-trisulfonate substituent.

To synthesize compound 5a, 4-fluoro-3-nitrobenzoyl chlorid was needed. 4-Fluoro-3-nitrobenzoyl chlorid was resynthesized. This compound was formerly synthesized by Ullmann *et al.* and was used as phenylene-linker precursor of NF157 (Ullman *et al.*, 2005). 4-Fluoro-3-nitrobenzoyl chloride was synthesized from 4-fluoro-3-nitrobenzoic acid, which was obtained from nitration of 4-fluorobenzoic acid with a combination of nitric acid and sulphuric acid (Becker *et al.*, 2001) (Figure 3.3).

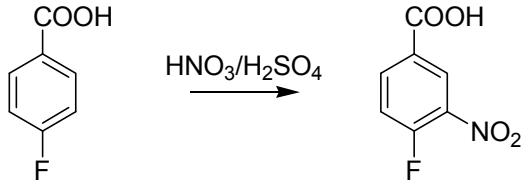

Figure 3.3 Nitration of 4-fluorobenzoic acid.

4-Fluoro-3-nitrobenzoic acid was then converted to 4-fluoro-3-nitrobenzoyl chloride (Figure 3.4).

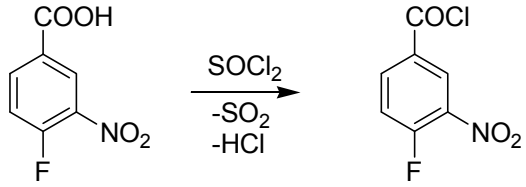

Figure 3.4 Formation of 4-fluoro-3-nitrobenzoyl chloride.

3.1.1. Synthesis of “small urea” derivatives

3.1.1.1. Trisodium 7-(4-fluoro-3-nitrobenzamido)-naphthalene-1,3,5-trisulfonate

Compound 5a is a nitro derivative which was obtained by amide formation of trisodium 7-aminonaphthalene-1,3,5-trisulfonate and 4-fluoro-3-nitrobenzoyl chloride (Figure 3.5).

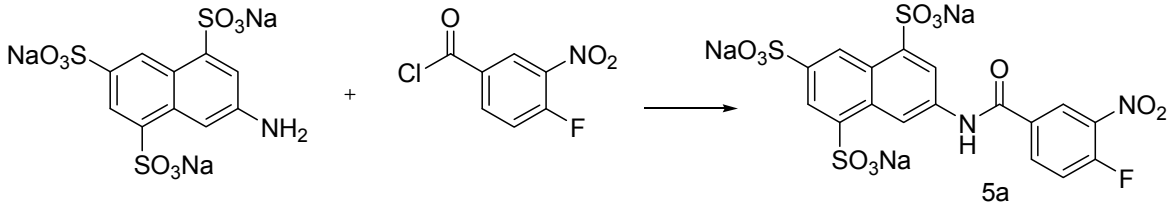

Figure 3.5 Acylation of trisodium 7-aminonaphthalene-1,3,5-trisulfonate with 4-fluoro-3-nitrobenzoic chlorid.

Trisodium 7-aminonaphthalene-1,3,5-trisulfonate was dissolved in water and was acylated with the acid chloride dissolved in toluene in a two-phase reaction. During the reaction, pH was maintained at 3.8 by automatically adding of 2 M Na_2CO_3 solution. pH 3.8 was a compromise to avoid the hydrolysis of the acid chloride at high pH and the protonation of the amine at low pH. After the reaction was completed (controlled by TLC and HPLC), the reaction mixture was extracted with diethylether to remove the side product 4-fluoro-3-nitrobenzoic acid. The aqueous phase was adjusted to pH 7.0 and the solvent was removed under vacuum. NaCl, as a side product, was separated by stirring in methanol. The amount of NaCl was measured by titration analysis. The product was obtained as white powder with a yield of 80.2 %.

Purity and structure confirmation

The purity of compound 5a was checked by TLC and HPLC. The HPLC chromatogram showed a single peak with a purity of 98.3 % at a retention time of 3.47 minutes (Figure 3.6). The UV spectrum showed a maximum absorption wavelength at 256.5 nm. This compound contained 3.84 % NaCl.

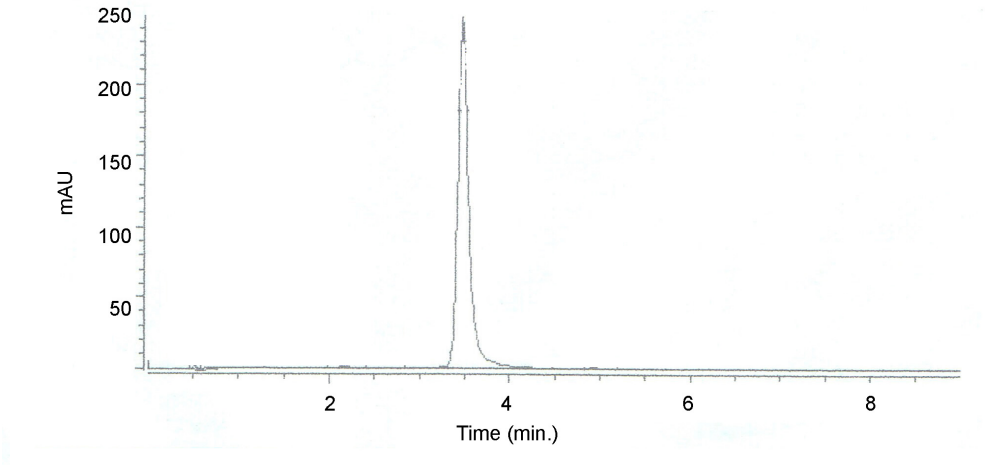

Figure 3.6 HPLC chromatogram of compound 5a.

Figure 3.7 shows the ^{1}H NMR spectrum of compound 5a

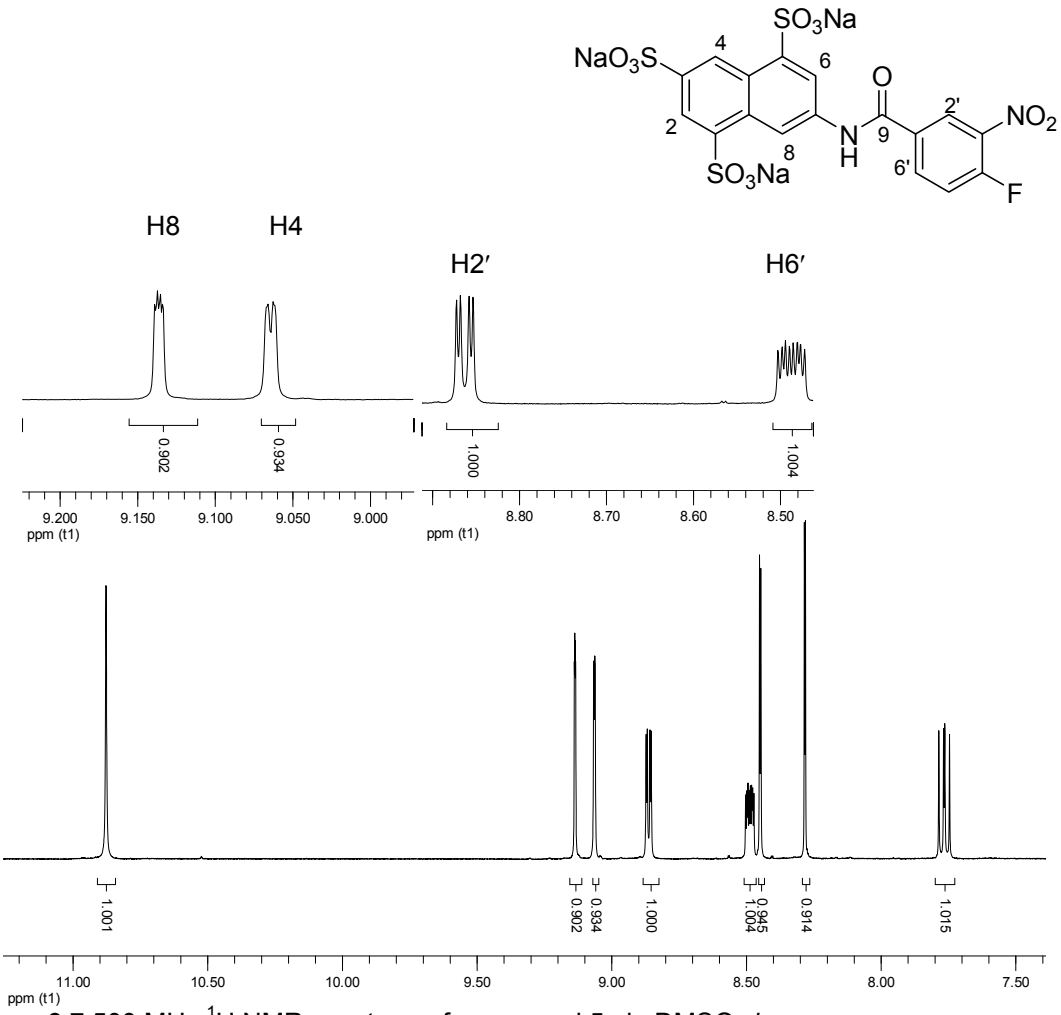

Figure 3.7 500 MHz ^{1}H NMR spectrum of compound 5a in DMSO-d_6.

Analysis of the ^{1}H NMR spectrum of compound 5a revealed the presence of eight signals with the integration of eight protons. The signal in the lowest field of the spectrum (10.80 ppm) appeared as a singlet, which disappeared upon the addition of D_2O. This signal represented the amide proton, which indicated the success of the reaction.

The signals of protons H2 and H6 of compound 5a appeared as two doublets at 8.45 ppm (^{4}J = 2.0 Hz) and 8.28 ppm (^{4}J = 1.8 Hz), respectively. The signal of the proton H8 appeared at 9.14 ppm as a doublet of doublet with one meta coupling (^{4}J = 1.8 Hz) to H6 and one zig-zag coupling (^{5}J = 0.8 Hz) to H4. The signal of proton H4 appeared as broad doublet at 9.06 ppm (^{4}J = 2.0 Hz). Figure 3.8 shows the possibility of zig-zag coupling of H4 and H8. Coupling through more than four bonds is normally difficult to observe. Coupling through "zig-zag bond" systems in unsaturated compounds can be observed (Manfred *et al.*, 1979).

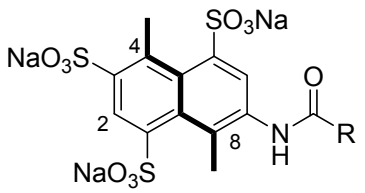

Figure 3.8 A "Zig-zag bond" between the proton H4 and H8 showed the ^{5}J coupling constant of 0.8 Hz.

The presence of the protons of the fluorine substituted phenylene-linker was confirmed by signals at 8.86 ppm, 8.49 ppm, and 7.75 ppm. The doublet of doublet at 8.86 ppm was interpreted as the signal of H-2′. This proton was coupled to H6′ with meta coupling (^{4}J = 2.2 Hz) and coupled to fluorine atom (^{4}J = 7.2 Hz). A multiplet signal at 8.49 ppm was assigned to the proton H6′ that coupled to H2′, H5′, and the fluorine atom. A doublet of doublet signal at 7.80 ppm referred to the signal of H5′, which coupled to H6′ and the fluorine atom (^{3}J = 8.8 Hz, ^{3}J = 11.0 Hz).

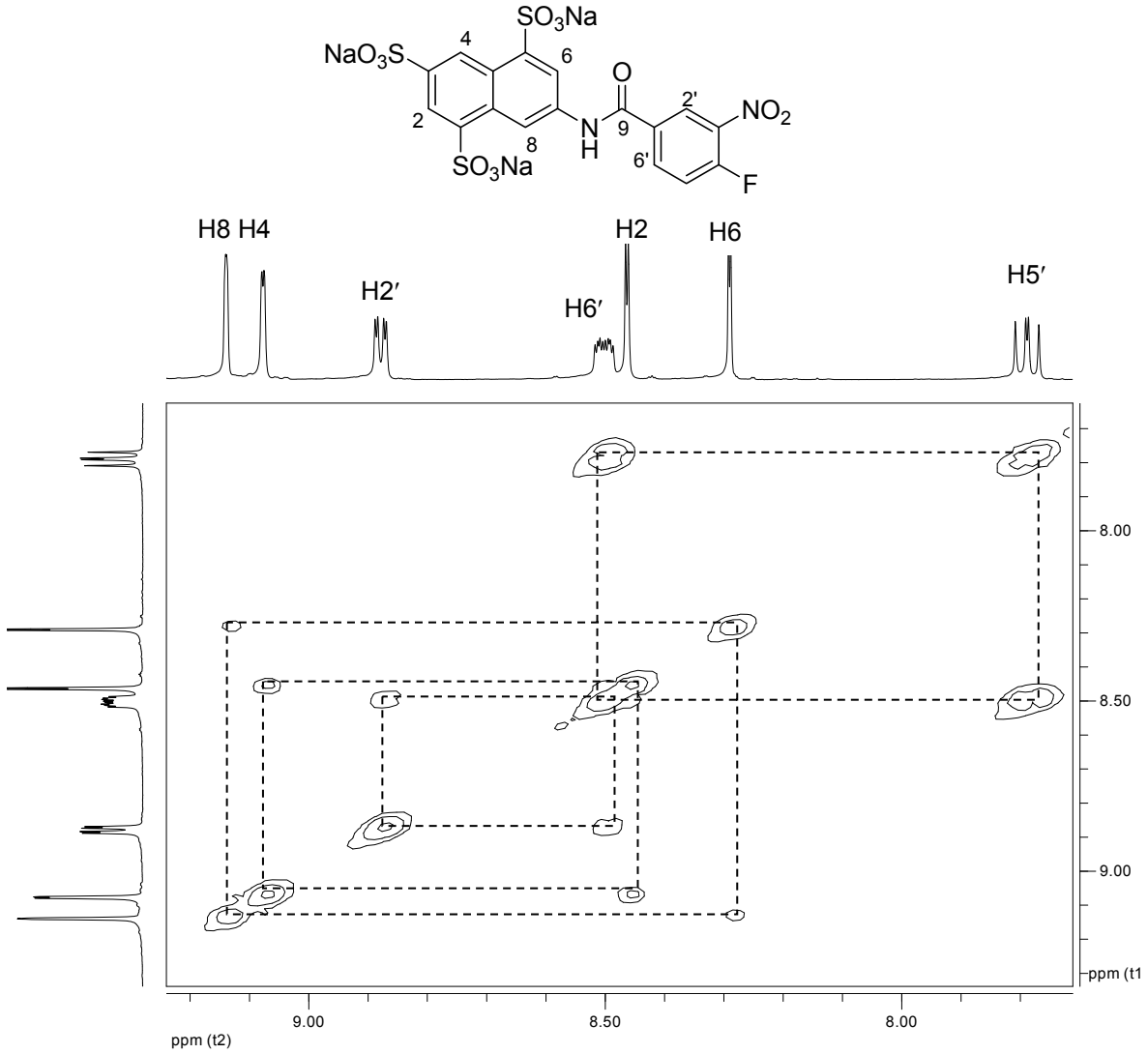

Figure 3.9 500 MHz H-H COSY spectrum of compound 5a shown as a contour plot. At the top and the left-hand edge is the one dimensional ^{1}H NMR spectrum with partial assignments.

The coupling character of the protons was confirmed by H, H-COSY spectrum (Figure 3.9). The cross peaks (dotted lines) in the spectrum showed the coupling of the protons H8 (δ = 9.14 ppm) to H6 (δ = 8.28 ppm), H2 (δ = 8.45 ppm) to H4 (δ = 9.06 ppm). Furthermore, the coupling of phenylene-linker proton H2′ (doublet), H5′ (doublet of doublet) and H6′ (multiplet) can be investigated by using the cross peaks. The zig-zag coupling of H4 and H8 was much better observed in the interpretation of compound 5b.

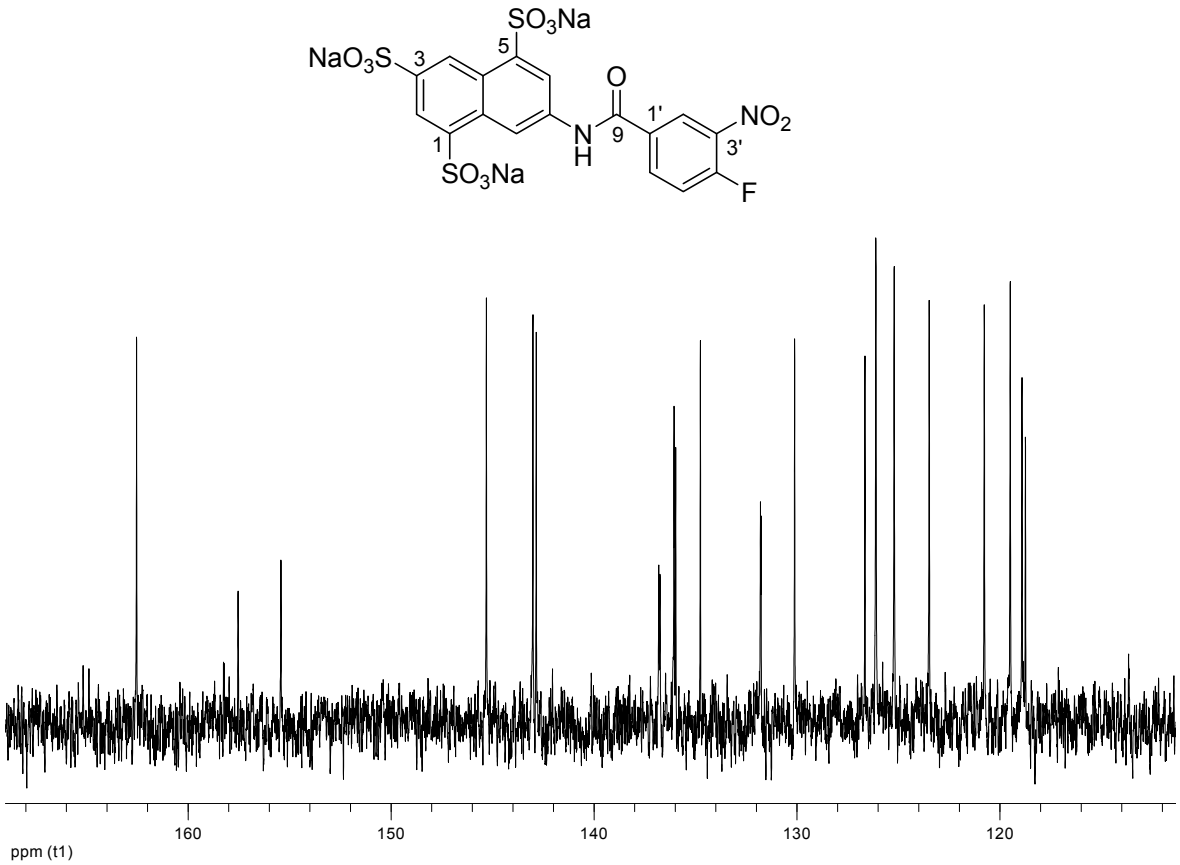

Figure 3.10 125 MHz ^{13}C NMR spectrum of compound 5a in DMSO-d_6.

Figure 3.10 shows the ^{13}C NMR spectrum of compound 5a. The carbon C4′ could couple to fluorine (Manfred *et al.*, 1979). Therefore, the signal appeared as a doublet at 156.4 ppm with ^{1}J = 264.5 ppm. Because of the -I effect of fluorine, the signal of C3′ was shifted to 136.8 ppm and showed ^{2}J coupling of fluorine with 8.0 Hz. The assignment of C2′, C5′, and C6′ was done by using HSQC spectrum (Figure 3.11). The signals at 126.6 ppm, 118.0 ppm, and 135.0 ppm could be interpreted as C2′, C5′, (^{2}J = 21 Hz), and C6′ (^{3}J = 10 Hz), respectively.

Table 3.1 shows the comparison of the calculated and found ^{13}C NMR chemical shift of the benzamido residue. Calculated signals were obtained by software ChemDraw 9.

Table 3.1 Comparison of the calculated, found ^{13}C NMR chemical shift δ (ppm) of benzamido residue of compound 5a, and HSQC spectra.

Position	**δ calculated (ppm)**	**δ found (ppm)**	**HSQC assignment**
C1′	130.7	131.8	-
C2′	122.7	126.6	H2′
C3′	137.0	136.8	-
C4′	158.9	156.5	-
C5′	116.5	118.0	H5′
C6′	135.2	135.0	H6′

The 10 signals of the naphthalene carbons could be interpreted by comparison to the calculated signals (ChemDraw 9.0) and HSQC (Figure 3.11).

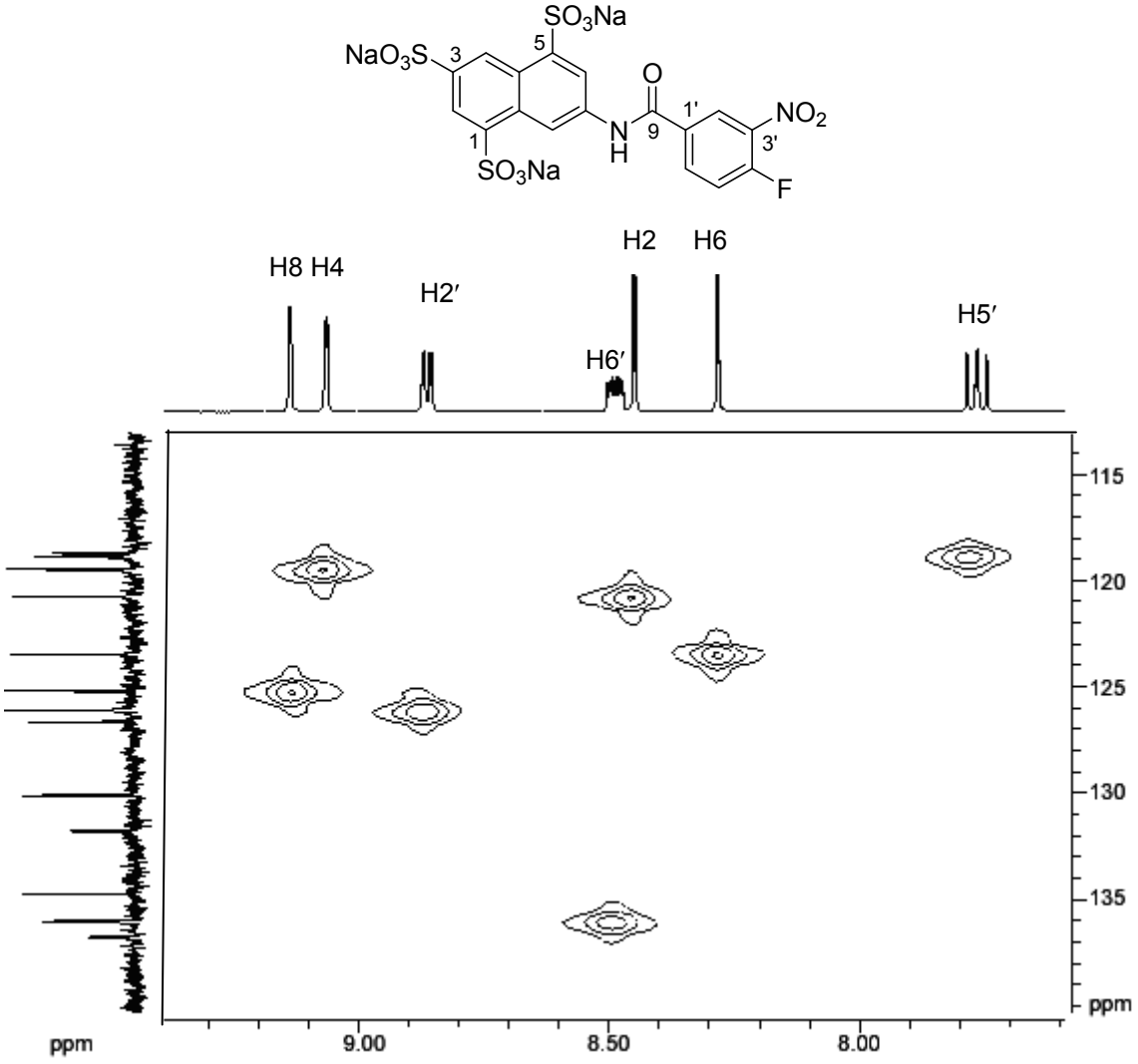

Figure 3.11 HSQC spectrum of compound 5a in DMSO-d_6. Only signals in the aromatic region are shown here. The one-dimensional 500 MHz ^{1}H NMR spectrum is shown at the top edge, while at the left-hand edge the one-dimensional 125 MHz ^{13}C NMR is shown.

The signals of C2, C4, C6, and C8 appeared at 120.7 ppm, 119.5 ppm, 123.5 ppm, and 125.8 ppm, respectively. Due to the effect of the sulfonate group, the signal C5 appeared in the lower field at 143.0 ppm. The similar effect was observed for signals C3 and C1. Their signals appeared at 142.8 ppm and 136.8 ppm, respectively. The signal at 145.3 ppm, 126.1 ppm and 130.1 ppm were interpreted as C7, C4a, and C8a, respectively. Table 3.2 shows the chemical shift

of carbons at the naphthalene ring of compound 5a according to ^{13}C and correlation between HSQC ^{1}H and ^{13}C from the HSQC spectrum.

Table 3.2 Chemical shift of carbons at the naphthalene ring of compound 5a according to ^{13}C and HSQC spectra.

Position	^{13}C δ (ppm)		HSQC assignment
	Found	Calculated	
C1	142.8	138.1	-
C2	120.7	122.5	H2
C3	134.7	135.5	-
C4	119.5	121.8	H4
C4a	126.1	126.2	-
C5	143.0	141.6	-
C6	123.5	117.1	H6
C7	145.3	138.7	-
C8	125.8	115.7	H8
C8a	130.1	130.1	-

The IR spectrum confirmed the presence of the amide functional group with the characteristic band of the C=O stretching vibration at 1679 cm^{-1} and the N-H bending vibration at 1540 cm^{-1}. The ESI-MS was measured in the negative mode. The spectrum showed the signal of $[M-Na]^-$ at m/z 593.3 and $[M-3Na+2H]^-$ at m/z 549.3 which was in accordance to the calculated $[M-Na]^-$ at m/z 592.9 and $[M-3Na+2H]^-$ at m/z 548.9).

3.1.1.2. Trisodium 7-(3-amino-4-fluorobenzamido)-naphthalene-1,3,5-trisulfonate

Catalytic hydrogenation of the nitro derivative 5a to the corresponding amine 5b was done in aqueous solution using Palladium (10%) on charcoal as the catalyst (Figure 3.12). Compound 5a was dissolved in water. Under heavy stirring the reaction mixture was hydrogenated under pressure (4.0 bar) in a Parr apparatus for approximately 12 hours. The reaction was controlled by TLC. Palladium/carbon was then filtrated and the solvent was removed under vacuum.

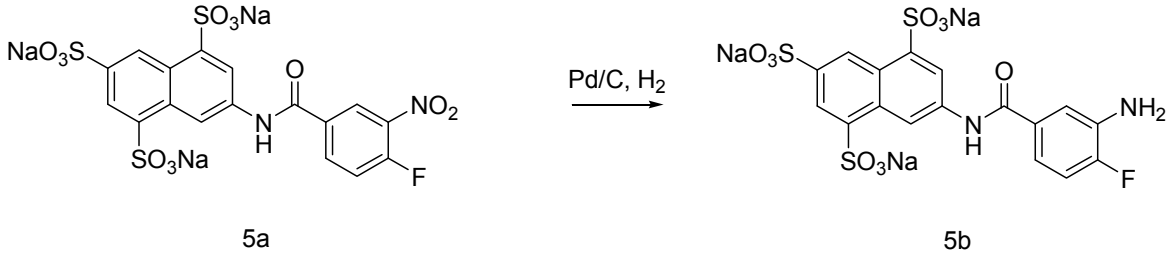

5a 5b

Figure 3.12 Hydrogenation of trisodium 7-(4-fluoro-3-nitrobenzamido)-naphthalene-1,3,5-trisulfonate.

5b was obtained as beige powder. The yield of the compound was 84.3 %.

Purity and structure confirmation

The TLC of amine 5b showed one spot and was detected with Ehrlich reagent. HPLC showed a purity of 95.6 % with a peak at a retention time of 2.24 minutes (Figure 3.13). 5b contained 5.50 % NaCl. The UV spectrum of 5b showed a maximum absorption wavelength at 258.5 nm.

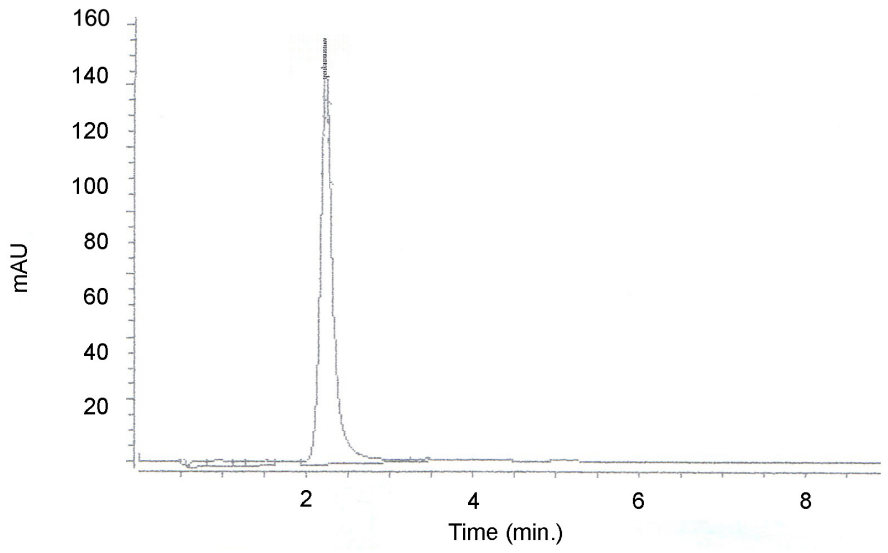

Figure 3.13 HPLC chromatogram of compound 5b.

Figure 3.14 shows the ^{1}H NMR spectrum of compound 5b.

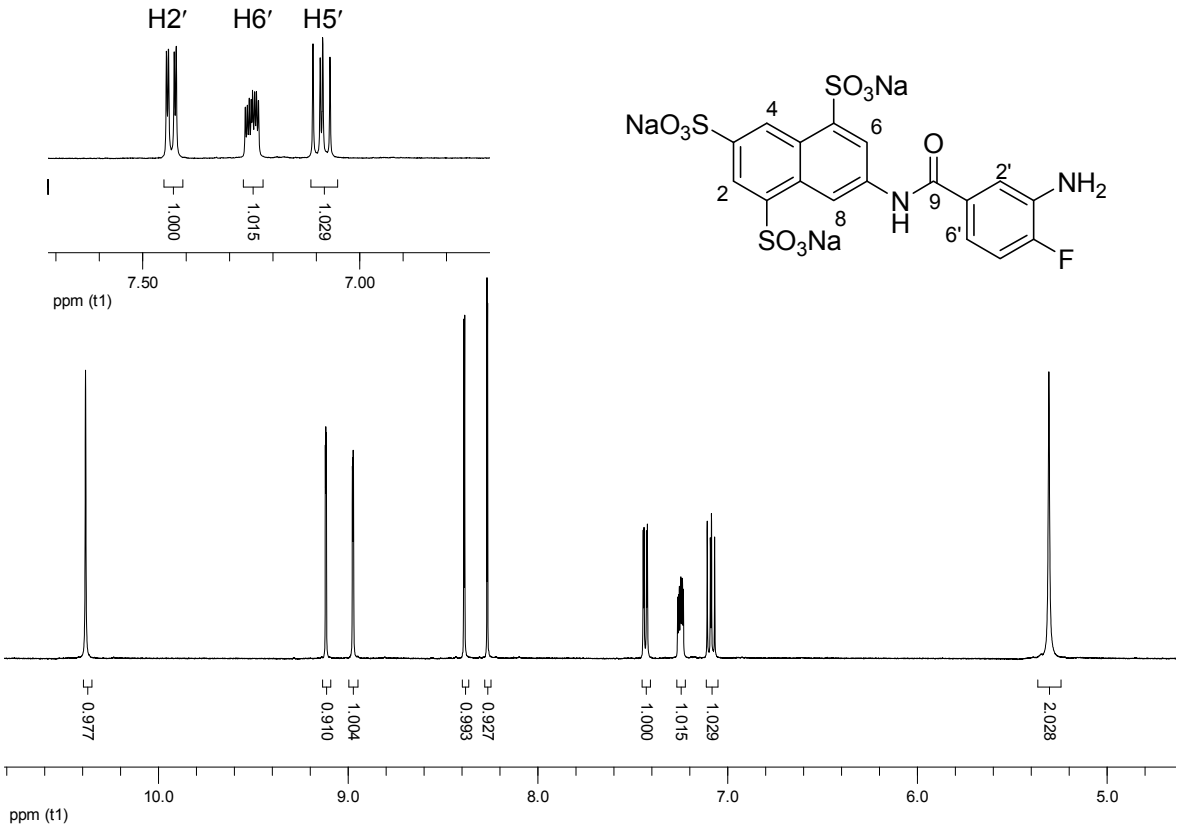

Figure 3.14 500 MHz ^{1}H NMR spectrum of compound 5b in DMSO-d_6.

The spectrum revealed the presence of 9 signals with the integration of 10 protons. The D_2O exchangeable singlet at 5.30 ppm with an integration of two protons was characterized as the signal of the $-NH_2$ protons. The amide proton appeared as a singlet at 10.40 ppm, which also disappeared in the D_2O exchange spectrum. The signals of the protons at the naphthalene ring appeared in nearly the same positions as the signals of the nitro compound (5a). Because of the +M effect of the amino group, the proton signals of the fluorine substituted phenylene-linker of 5b were shifted to the upper field in comparison with the nitro precursor (5a). The signal of the proton H2′ appeared as a doublet of doublet at 7.44 ppm (^4J = 1.9, ^4J = 7.2). The signal of H6′ was shifted to 7.25 ppm, whereas the signal of H5′ appeared as doublet of doublet at 7.09 ppm (^3J = 8.5 Hz, ^3J = 11.3 Hz).

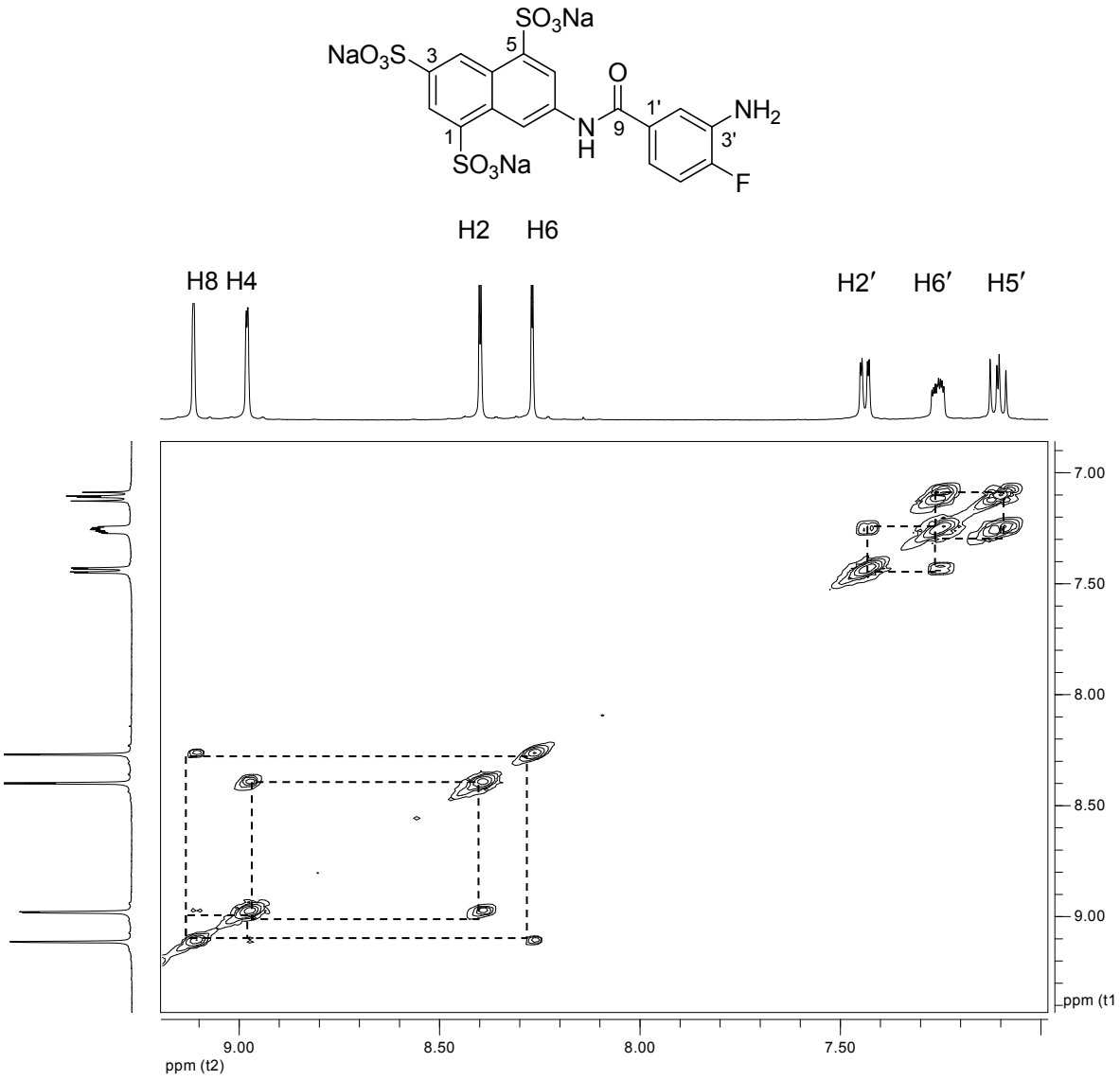

Figure 3.15 500 MHz H,H-COSY spectrum of compound 5b shown as a contour plot. At the top and the left-hand edge is the one-dimensional 1H NMR spectrum with partial assignments.

H-H COSY of compound 5b was measured to confirm the coupling of the protons (Figure 3.15). The cross peaks (dotted lines) in the spectrum showed the zig-zag coupling of H4 and H8. Furthermore, the coupling of the protons H8 (δ 9.12 ppm) to H6 (δ 8.26 ppm) and H2 (δ 8.39 ppm) to H4 (δ 8.98 ppm) can be observed. The coupling of phenylene-linker proton H2′ to H6′ (^4J = 1.9) can be observed as well as coupling of H5′ and H6′ (^3J = 8.5 Hz).

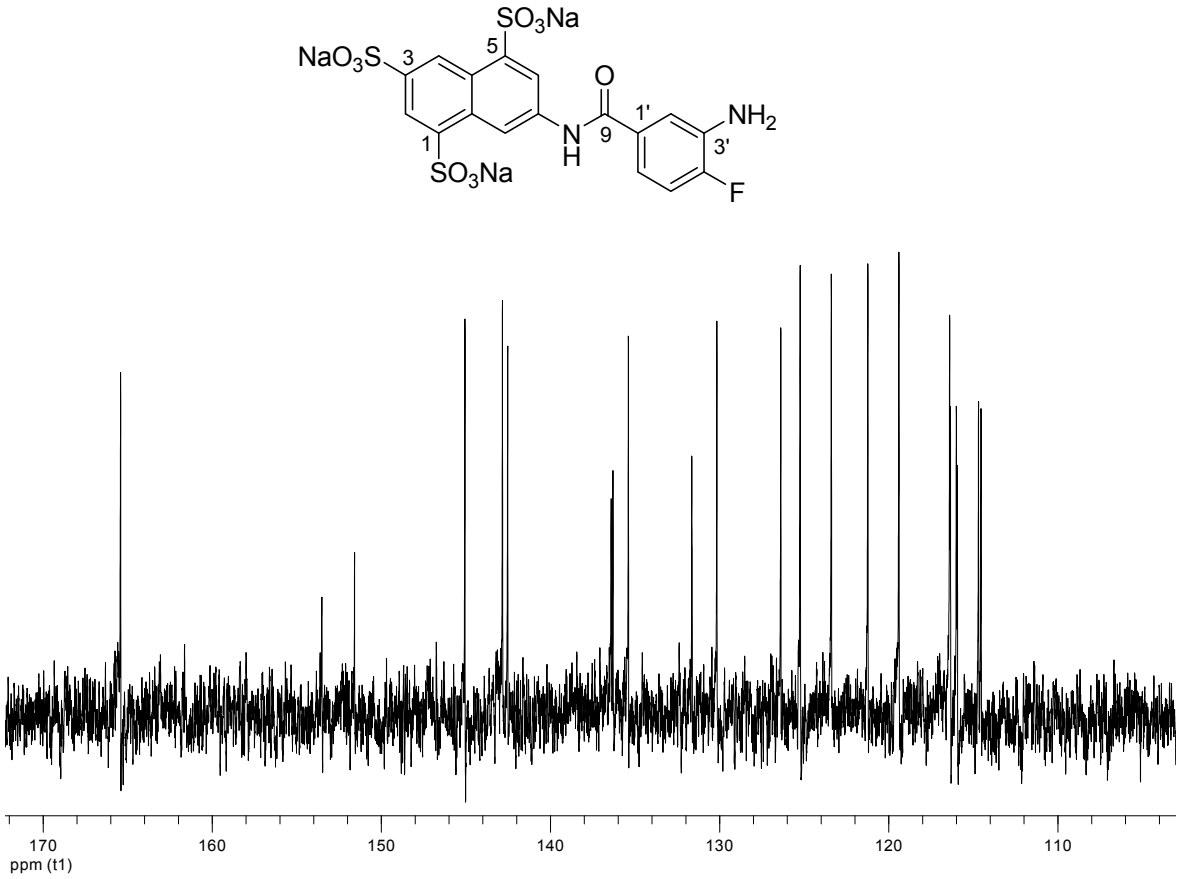

Figure 3.16 125 MHz ^{13}C NMR spectrum of compound 5b in DMSO-d_6.

Figure 3.16 shows the ^{13}C NMR spectrum of compound 5b. The signal of the carbonyl carbon C9 appeared in the lowest field (165.4 ppm). As observed in compound 5a, signal of C4′ was detected at 152.5 ppm, as a doublet with ^{1}J = 245 Hz. The signal of C3′ appeared at 136.5 ppm and showed ^{2}J coupling with fluorine with J = 13.5 Hz. For further interpretation of the remaining carbons, HSQC was performed (Figure 3.17, Table 3.3).

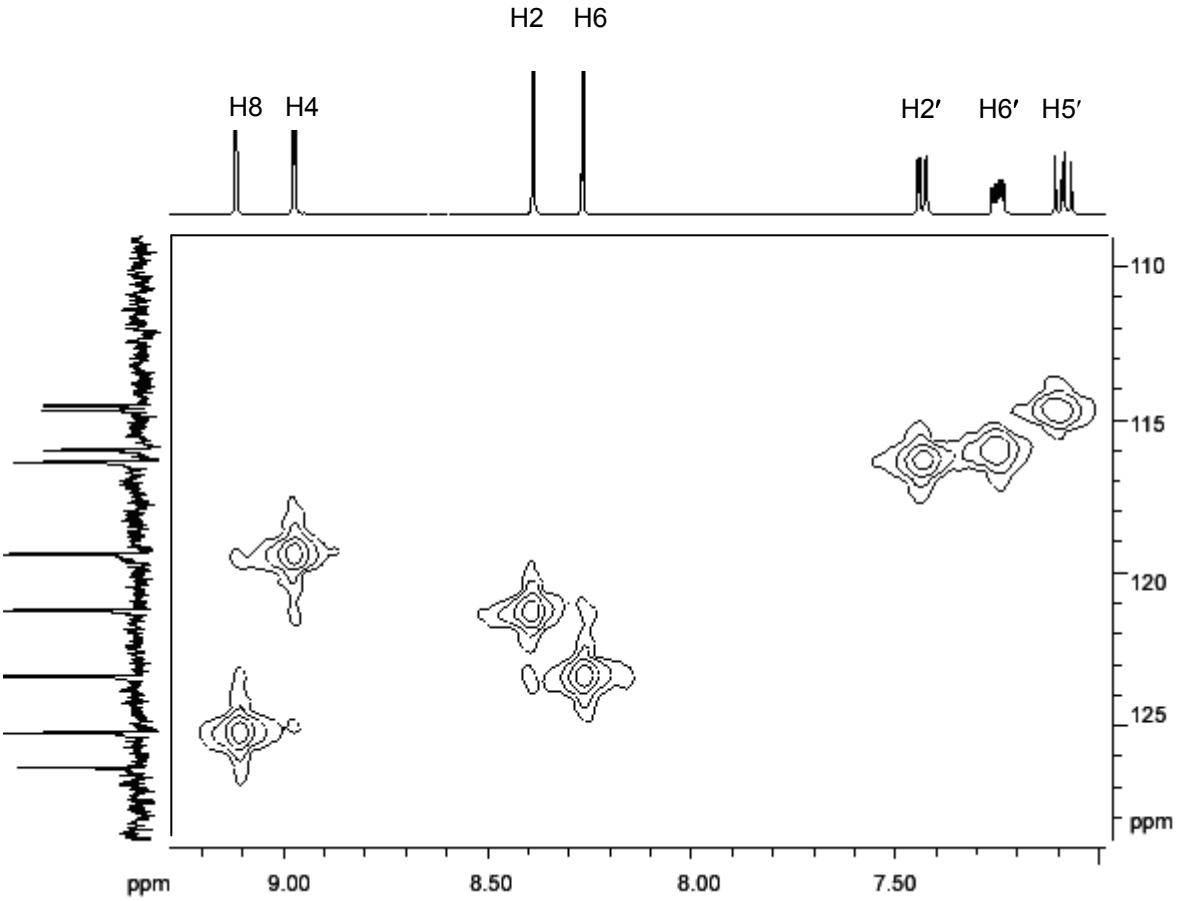

Figure 3.17 HSQC spectrum of compound 5b in DMSO-d_6. Only signals in the aromatic region are shown here. The one-dimensional 500 MHz ^{1}H NMR spectrum is shown at the top edge, while at the left-hand edge the one-dimensional 125 MHz ^{13}C NMR is shown.

The +M effect of the -NH_2 group caused a shift of carbon signals of the fluorine substituted phenylene-linker to the higher field. The signals of the naphthalene carbons appeared in the relatively same range as in the nitro derivative (compound 5a). The signals of C2, C4, C6, and C8 appeared at 121.2 ppm, 119.4 ppm, 123.3 ppm, and 125.2 ppm, respectively. The signal C5 appeared in the lower field at 142.7 ppm, while the other signals C3 and C1 appeared in a slightly higher field at 135.4 ppm and 142.5 ppm, respectively. The signal at 145.1 ppm, 126.4 ppm and 130.2 ppm were interpreted as C7, C4a, and C8a, respectively. Table 3.3 shows the chemical shift of carbons at the naphthalene ring of compound 5b according to ^{13}C and HSQC spectra.

Table 3.3 Chemical shift of carbons at the naphthalene ring of compound 5b according to ^{13}C NMR and HSQC spectra.

Position	^{13}C δ (ppm)		HSQC assignment
	Found	Calculated	
C1	142.5	138.1	-
C2	121.2	122.5	H2
C3	135.4	135.5	-
C4	119.4	121.8	H4
C4a	126.4	126.2	-
C5	142.7	141.6	-
C6	123.3	117.1	H6
C7	145.1	138.7	-
C8	125.2	115.7	H8
C8a	130.2	130.1	-

.

The interpretation of the carbons C2′, C5′, and C6′ was confirmed by the HSQC spectrum and the remaining carbons of the fluorine substituted phenylene-linker were assigned after substitution increment calculation (Table 3.4).

Table 3.4 Comparison of the calculated and found ^{13}C NMR chemical shift of the carbons of the fluorine substituted phenylene-linker of compound 5b.

Position	δ (ppm)	
	Calculated	Found
C1′	130.6	131.6
C2′	113.4	116.4
C3′	136.4	136.5
C4′	161.1	152.5
C5′	116.4	114.6
C6′	119.1	115.9

The IR spectrum revealed the presence of the amide functional group with the characteristic band of the C=O stretching vibration at 1652 cm^{-1}. The ESI-MS spectrum was measured in the negative mode. The spectrum showed signals of $[M-Na]^-$ at m/z 563.8, $[M-2Na+H]^-$ at m/z 541.6 and $[M-3Na+2H]^-$ at m/z 519.6 in comparison with calculated m/z of $[M-Na]^-$ at 563.4, $[M-2Na+H]^-$ at 541.5 and $[M-3Na+2H]^-$ at 519.0.

3.1.1.3. Hexasodium 7,7'-{carbonylbis[azanediyl(4-fluoro-3,1-phenylene)carbonylazanediyl]}bis(naphthalene-1,3,5-trisulfonate)

The urea derivative 5c was synthesized by phosgenation of amine 5b. A solution of phosgene in toluene (20 %) was slowly dropped to the aqueous solution of amine 5b (Figure 3.18). The pH of the reaction was kept constant at 3.7 to avoid the hydrolysis of phosgene and protonation of the amine at low pH. Compound 5c was obtained as beige powder with 66.0 % yield. After the reaction was completed, the solution was adjusted to pH 7 and solvent was removed under vacuum.

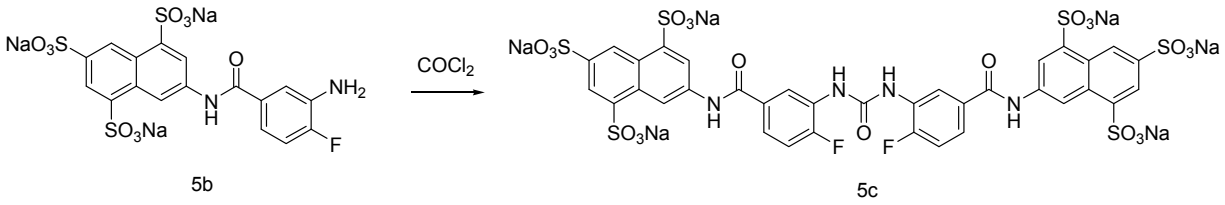

Figure 3.18 Phosgenation of trisodium 7-(3-amino-4-fluorobenzamido)-naphthalene-1,3,5-trisulfonate

Purity and structure confirmation

The TLC of urea 5c showed one spot. The HPLC chromatogram showed a single peak with a purity of 96.5 % at a retention time of 4.98 minutes (Figure 3.19). The UV spectrum showed a maximum absorption at the wavelength of 258.5 nm.

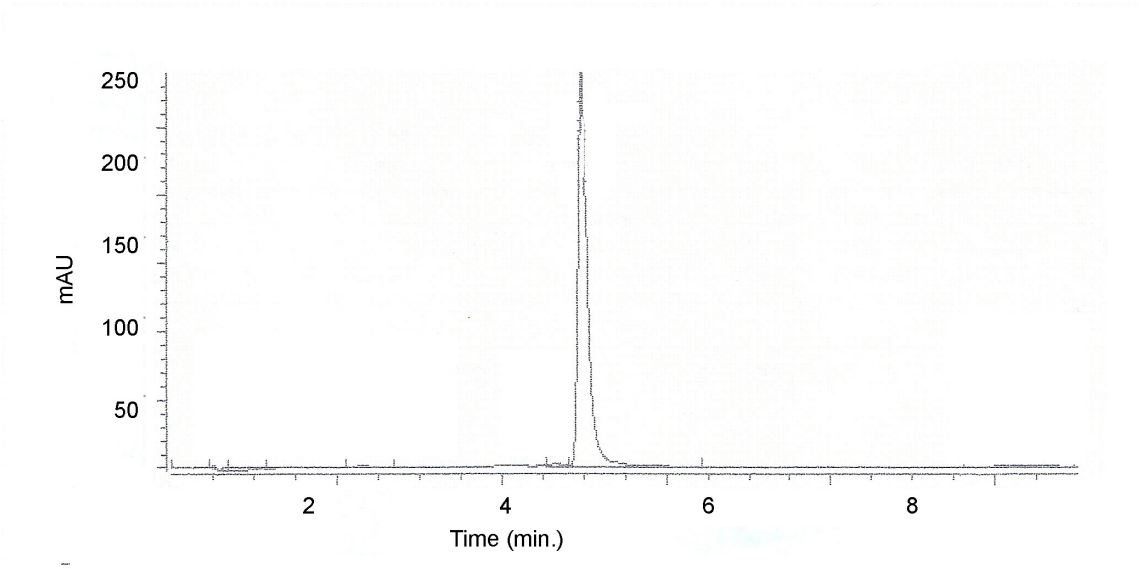

Figure 3.19 HPLC chromatogram of compound 5c.

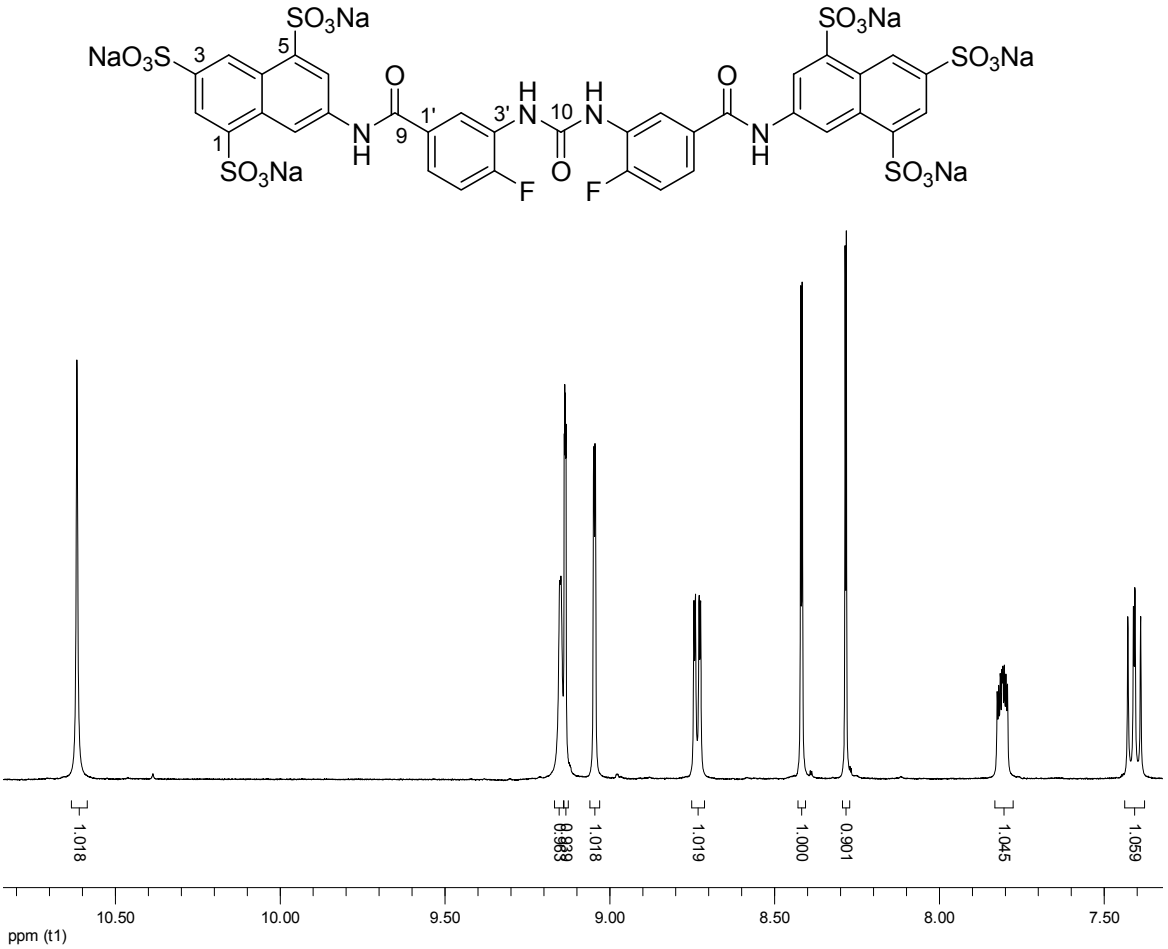

Figure 3.20 500 MHz ^{1}H NMR spectrum of compound 5c in DMSO-d_6.

Figure 3.20 shows the ^{1}H NMR of compound 5c. The spectrum revealed the presence of nine signals with integration of 18 protons. The signals of the amide proton at 10.61 ppm and urea at 9.16 ppm disappeared upon addition of D_2O. The interpretation of ^{1}H NMR of compound 5c was supported by COSY spectrum (Figure 3.21).

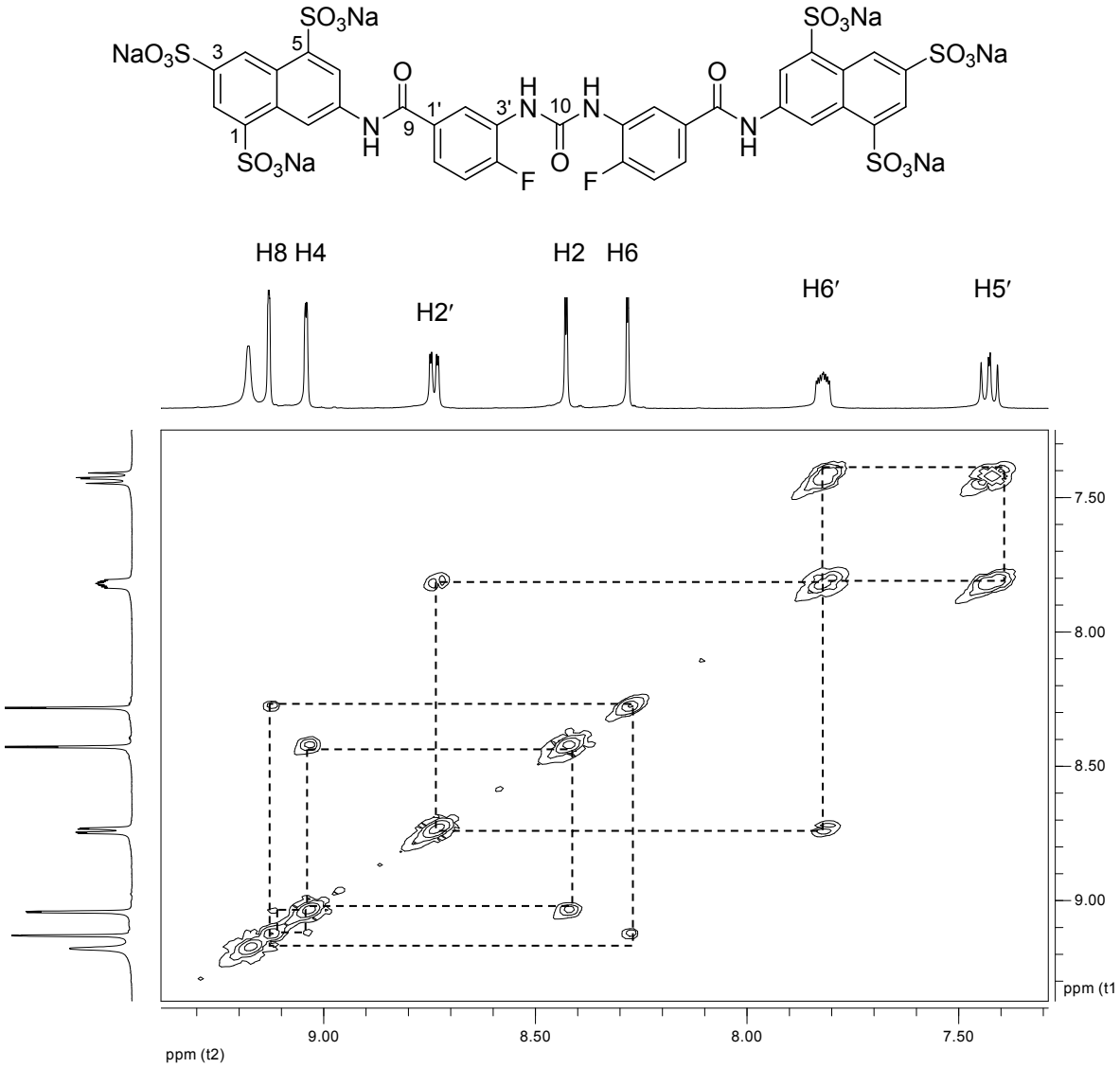

Figure 3.21 500 MHz H,H-COSY-90 spectrum of compound 5c shown as a contour plot. At the top and the left-hand edge is the one-dimensional 1H NMR spectrum with partial assignments.

The cross peaks (dotted lines) in the spectrum showed the zig-zag coupling of H4 and H8. Furthermore, the coupling of the protons H8 (δ 9.14 ppm) to H6 (δ = 8.28 ppm) and H2 (δ = 8.42 ppm) to H4 (δ = 9.05 ppm) can be observed. The coupling of phenylene-linker proton H2′ to H6′ (^4J = 1.6) can be observed as well as coupling of H5′ and H6′ (^3J = 8.5 Hz). H6′ appeared as multiplet signal. It coupled to H2′, H5′ and fluorine atom. H2′ appeared as doublet of doublet signal and coupled to H6′ and H5′. H5′ appeared as doublet of doublet signal and coupled to H6′ and fluorine atom. Table 3.5 shows the comparison of the chemical shifts of the benzamido residues of the nitro-, amino-, and urea-derivatives.

Table 3.5 Comparison of ^{1}H NMR signals (DMSO-d_6) of benzamido residues between compounds 5a-5c.

Position	δ (ppm) (5a) Nitro-derivative	δ (ppm) (5b) Amine-derivative	δ (ppm) (5c) Urea
H2′	8.86	7.44	8.73
H5′	8.49	7.25	7.81
H6′	7.75	7.09	7.41

The ^{13}C spectrum of 5c (Figure 3.22) shows the carbonyl urea carbon at 152.1 ppm whereas the signal of the carbonyl carbon of the amide group (C9) appeared at 164.5 ppm. The signals of the naphthalene carbons appeared in a similar range as the carbons of the precursors 5a and 5b.

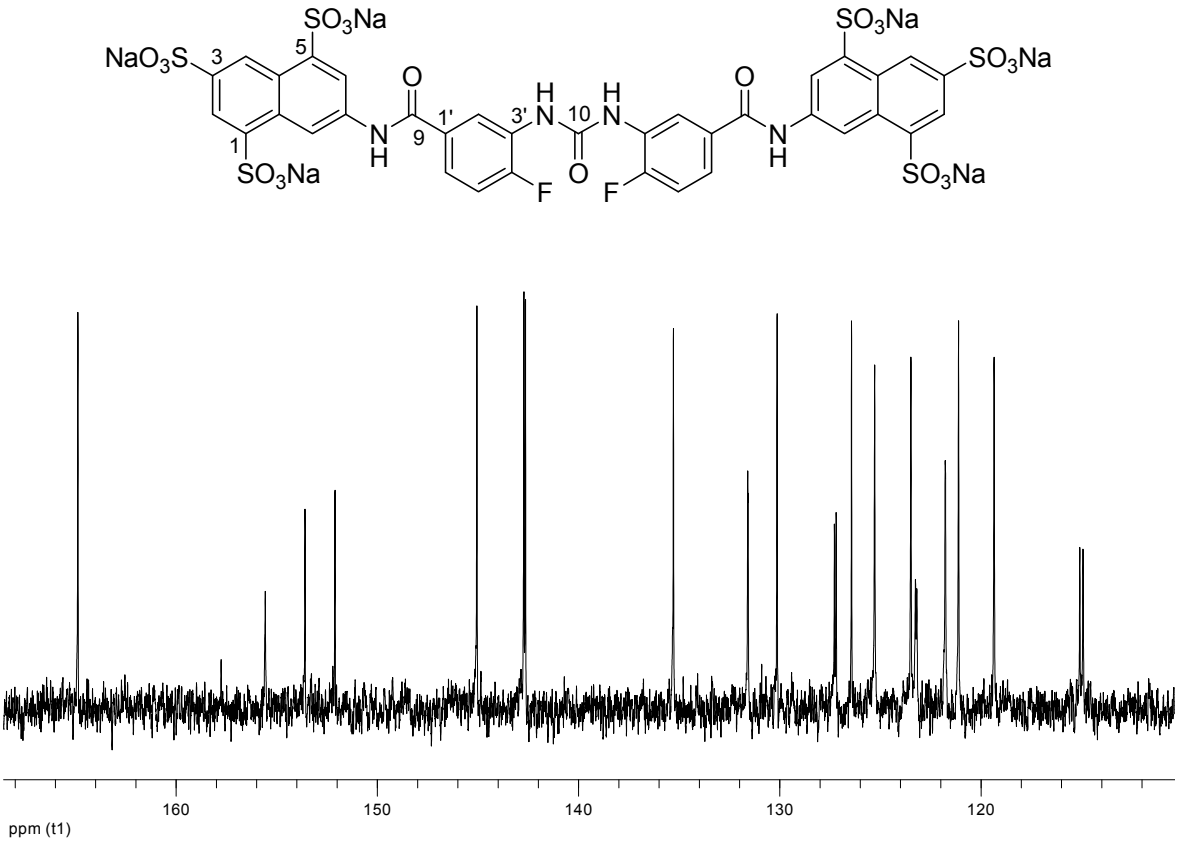

Figure 3.22 125 MHz ^{13}C NMR spectrum of compound 5c in DMSO-d_6.

The assignment of all carbon signals was performed by comparison with the calculated signals and HSQC spectrum (Figure 3.23). Table 3.6 shows the assignment of the carbon signals of the benzamido residue.

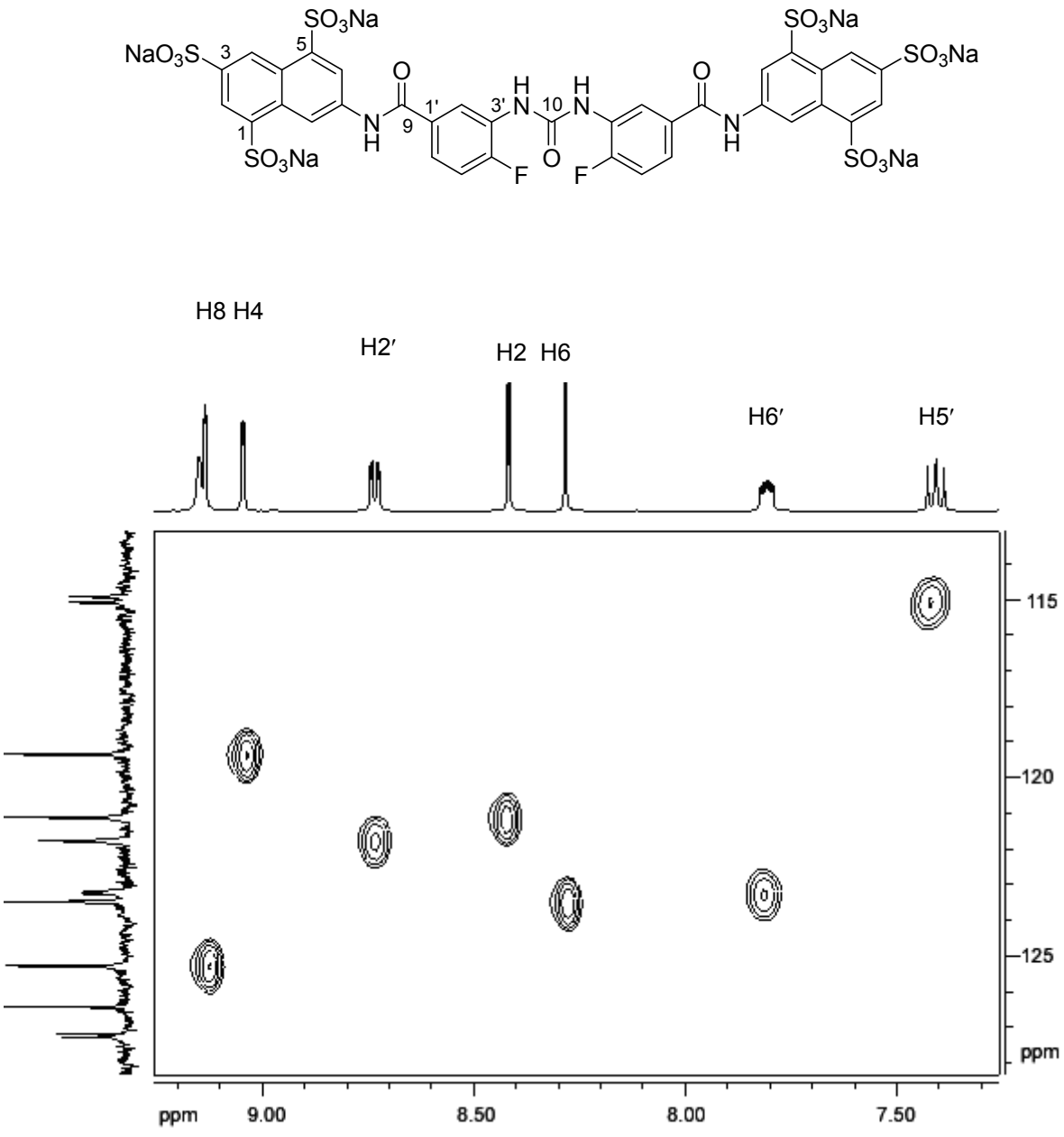

Figure 3.23 HSQC spectrum of compound 5c in DMSO-d_6. Only signals in the aromatic region are shown here. The one-dimensional 500 MHz ^{1}H NMR spectrum is shown at the top edge, while at the left-hand edge the one-dimensional 125 MHz ^{13}C NMR is shown.

HSQC spectrum showed the correlation between C2 - H2 and C4 - H4 as well as C6 – H6 and C8 - H8. The signals of C2, C4, C6, and C8 appeared at 121.1 ppm, 119.3 ppm, 123.5 ppm, and 115.1 ppm, respectively. Furthermore, the spectrum showed the coupling of C2′ (121.8 ppm), C5′ (115.1 ppm) and C6′ (123.2 ppm) to H2′ (8.73 ppm), H5′ (7.81 ppm) and H6′ (7.41 ppm), respectively. Coupling patterns of the phenylene-linker of compounds 5a, 5b and 5b can be observed (Table 3.6). The characteristic coupling of C4′ to fluorine was shown by the coupling constant of 264.5 Hz, 245 Hz and 246.9 Hz of compound 5a, 5b and 5c, respectively. Further coupling to fluorine was observed for C5′ with *J* = 21 Hz (5a), 18.9 Hz (5b) and 20 Hz (5c) whereas C6′ with *J* = 10 Hz (5a), 7.1 Hz (5b) and 8.5 Hz (5c), respectively.

Table 3.6 Comparison of ^{13}C NMR signals (DMSO-d_6) and coupling constants of carbons at benzamido residues of compounds 5a-5c.

Position	**5a**		**5b**		**5c**	
	δ (ppm)	***J*(Hz)**	**δ (ppm)**	***J*(Hz)**	**δ (ppm)**	***J*(Hz)**
C1′	131.8	3.6	131.6	5.6	131.6	2.14
C2′	126.6	-	116.4	-	121.8	-
C3′	136.8	8.0	136.5	13.5	127.2	10.9
C4′	156.5	264.5	152.5	245.0	154.6	246.9
C5′	118.0	21.0	114.6	18.9	115.1	20
C6′	135.0	10.0	115.9	7.1	123.2	8.5

The ESI-MS spectrum was measured in the negative mode. The spectrum showed a signal m/z of $[M-Na]^-$ at 1175.3 in comparison with calculated m/z 1174.8.

3.1.2. Synthesis of “large urea” derivatives

3.1.2.1. Trisodium 7-[4-(3-nitrobenzamido)-benzamido]-naphthalene-1,3,5-trisulfonate

Urea compound 9c was found as a novel agonist at $P2Y_{11}$ receptors in this study. Precursors of compound 9c are nitro 9a and amine 9b. Compound 9a is an extended structure (“large urea”) of compound 8b (structure in Appendix B) with a second phenylene-linker (Figure 3.24). Trisodium 7-(4-aminobenzamido)-naphthalene-1,3,5-trisulfonate (8b) was dissolved in water and acylated with the 3-nitrobenzoylchloride dissolved in toluene in a two-phase reaction. Compound 9a was obtained as white powder. The yield of the compound was 78.4 %.

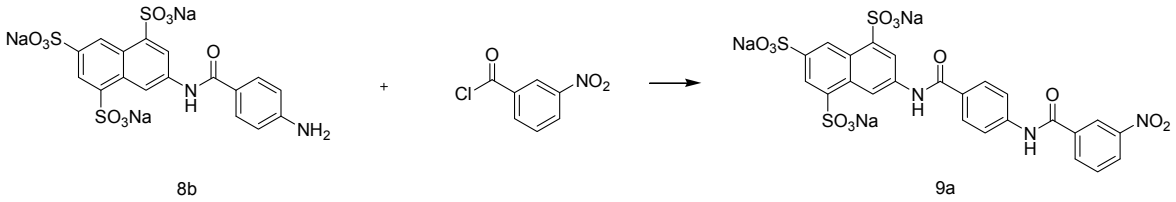

Figure 3.24 Acylation of trisodium 7-(4-aminobenzamido)-naphthalene-1,3,5-trisulfonate with 3-nitrobenzoyl chloride

Purity and structure confirmation

The TLC of compound 9a showed one spot. The HPLC chromatogram showed 98.1 % of purity at a retention time of 5.66 minutes. The UV spectrum showed a maximum absorption wavelength at 258 nm.

Figure 3.25 shows the ^{1}H NMR spectrum of compound 9a.

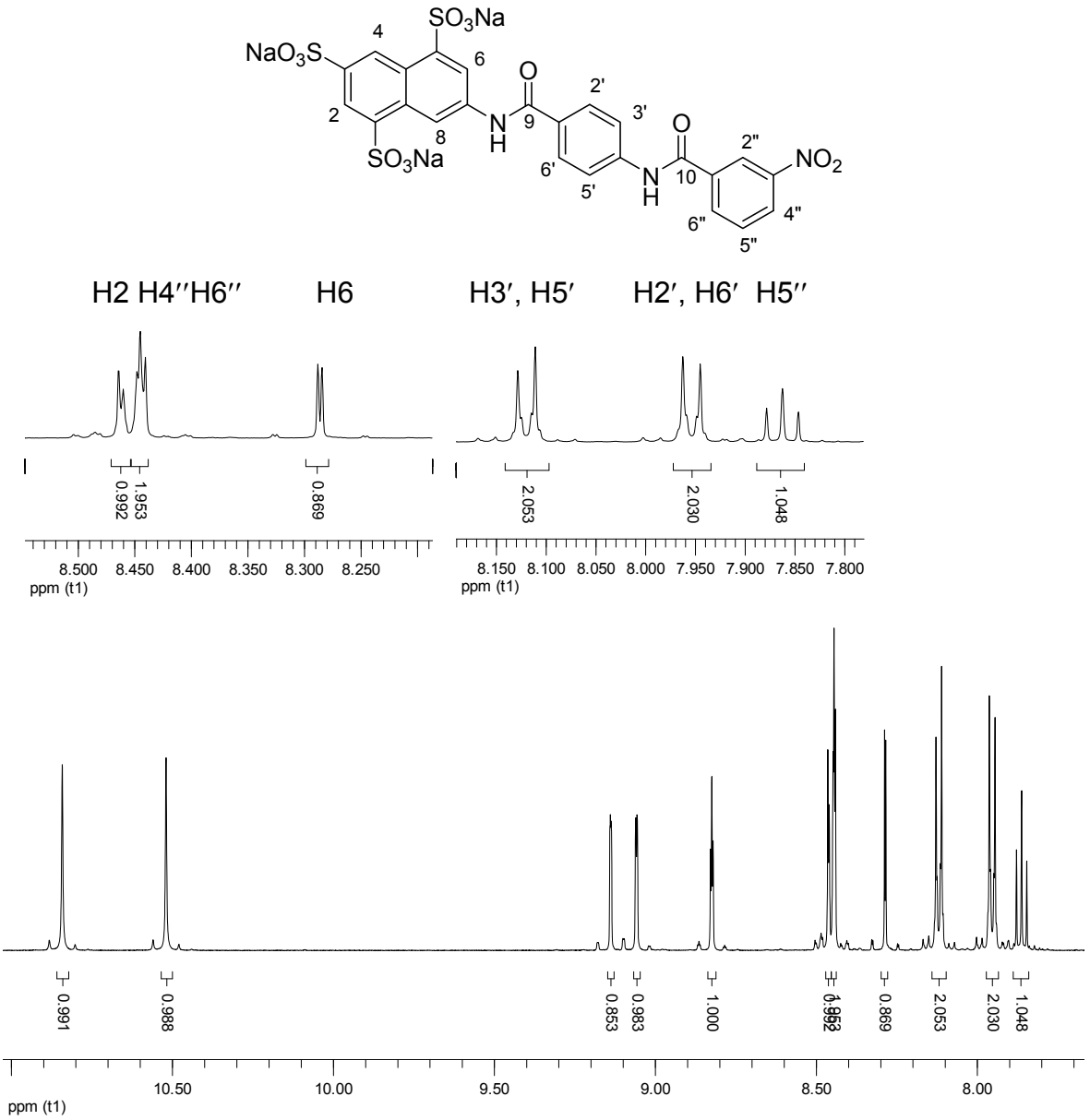

Figure 3.25 500 MHz ^{1}H NMR spectrum of compound 9a in DMSO-d_6.

Analysis of the ^{1}H NMR spectrum revealed the presence of 11 signals with the integration of 14 protons. The signals in the lowest field of the spectrum (10.84 ppm and 10.52 ppm) appeared as singlet, which disappeared upon the addition of D_2O. The signal represented both amide protons of compound 9a. The signal of protons H2, H4, H6 and H8 appeared at the similar range with the protons of compound 5a. The first phenylene ring formed a AA′BB′ system. Two

signals were assigned to protons H2′, H6′ and H3′, H5′ at 7.95 ppm and 8.44 ppm, respectively. The signals appeared as doublet of doublet with ^{3}J = 6.9 and ^{4}J = 1.9. Signal H2′′ appeared at 8.82 ppm as a triplet which coupled to H4′′ and H6′′ with ^{4}J = 2.2. The triplet signal at 7.85 ppm was assigned to H5′′ which coupled to H4′′ and H6′′. Due to the poor resolution, proton H4′′ and H6′′ appeared as a not separated signal at 8.45 ppm. The better resolution was much better observed in compound 9b and 9c.

Figure 3.26 shows the ^{13}C NMR spectrum of compound 9a.

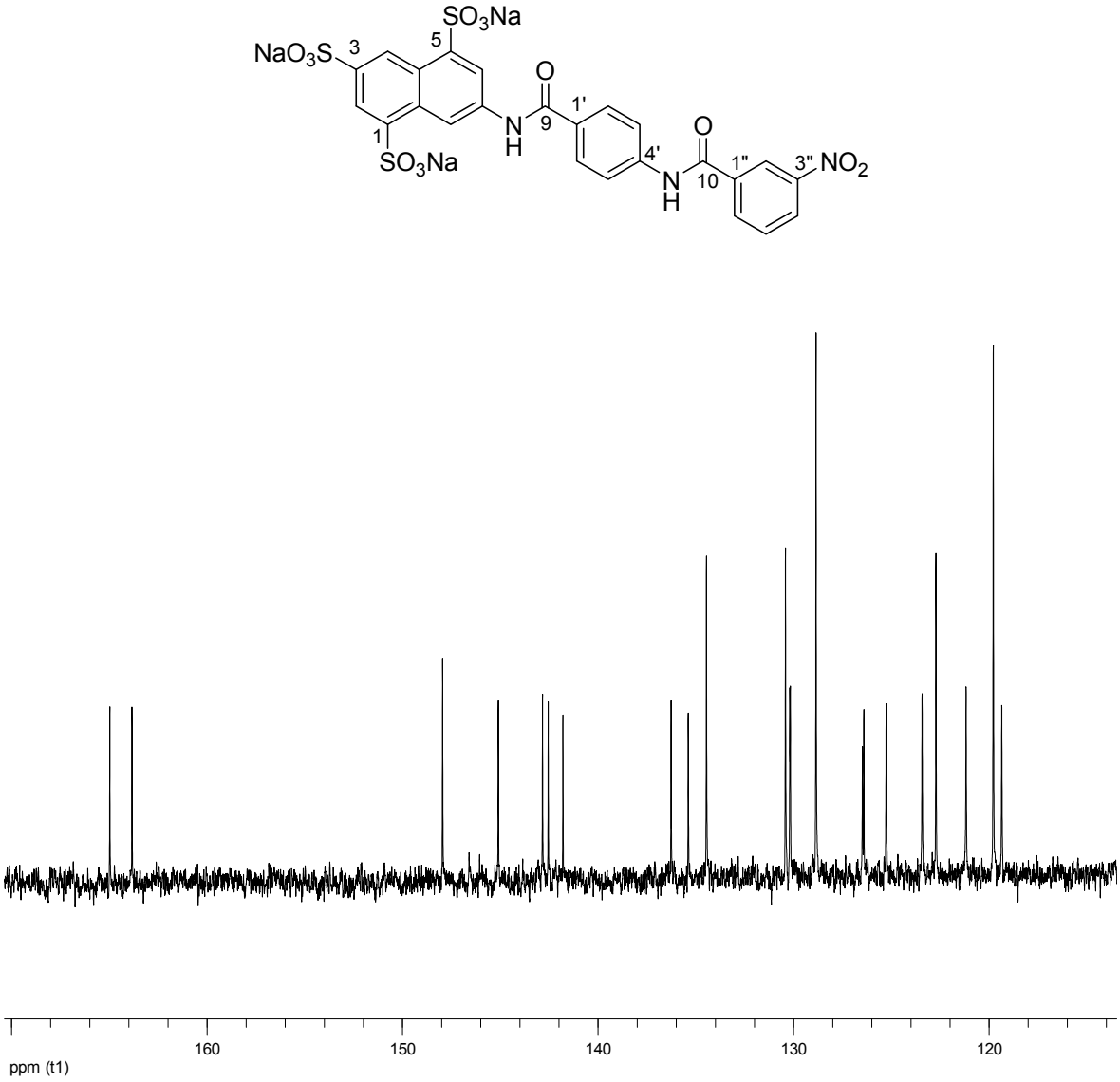

Figure 3.26 125 MHz ^{13}C NMR spectrum of compound 9a in DMSO-d_6.

The ^{13}C spectrum of compound 9a shows the carbonyl carbons appeared in the lower field at 164.9 ppm and 163.8 ppm. Carbons C1-C8 appeared in similar range with compound 5a. The AA′BB′ system can be observed at signals of carbons C2′, C6′ (128.9 ppm) and carbons C3′, C5′ (122.7 ppm). The assignment of other signals was performed by comparison of the found signals with the estimated signals from the software ChemDraw Ultra 9.0 which explained in chapter 3.1.2.3. The IR spectrum confirmed the presence of the amide functional group with the characteristic band of the C=O stretching vibration at 1662 cm^{-1} and the N-H bending vibration at 1527 cm^{-1}.

3.1.2.2. Trisodium 7-[4-(3-aminobenzamido)-benzamido]-naphthalene-1,3,5-trisulfonate

Compound 9b was hydrogenated in water using palladium/carbon as catalyst. The same method as explained for the synthesis of compound 5b was used (Figure 3.27). 9b was obtained as beige powder with 93.3 % yield of compound.

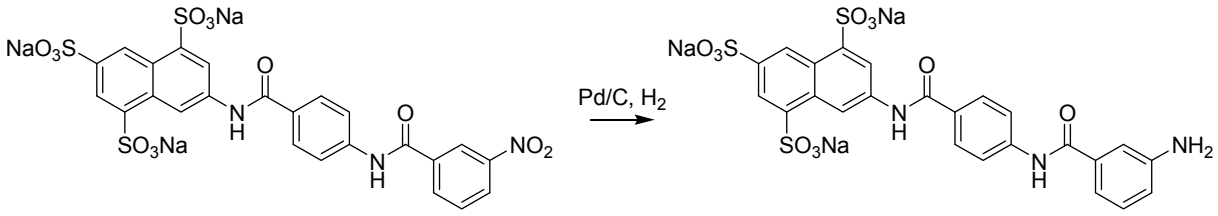

Figure 3.27 Hydrogenation of trisodium 7-[4-(3-nitrobenzamido)-benzamido)]-naphthalene-1,3,5-trisulfonate.

Purity and structure confirmation

The TLC of 9b showed one spot. HPLC showed a purity of 98.0 % with a peak at a retention time of 2.38 minutes. The UV spectrum showed a maximum absorption wavelength at 254.5 nm.

Figure 3.28 shows the ^{1}H NMR spectrum of compound 9b.

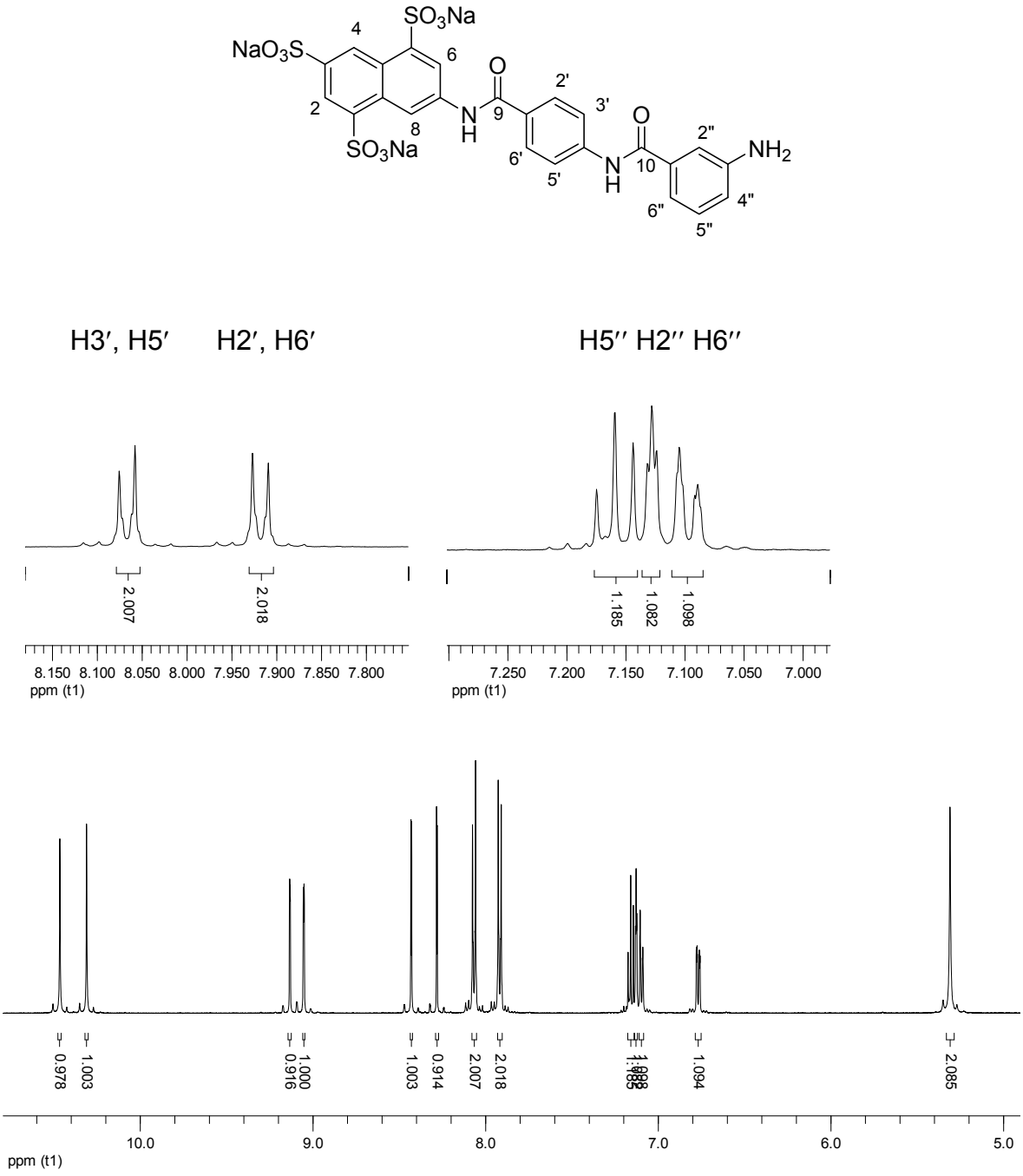

Figure 3.28 500 MHz ^{1}H NMR spectrum of compound 9b in DMSO-d_6.

The spectrum revealed the presence of 13 signals with the integration of 16 protons. The D_2O exchangeable singlets at 10.46 ppm and 10.31 ppm were characterized as the signal of amine protons. The amine protons appeared as a singlet with integration of two protons, which also disappeared in the D_2O exchange spectrum. The signals of the protons at the naphthalene ring appeared

in nearly the same potions as the signal of the nitro compound 9a. Because of the +M effect of the amino group, the proton signals of the H4′′ were shifted to the upper field in comparison to 9a. H4′′ coupled to H2′′ and H6′′ (^4J = 2.2, ^3J = 7.5). Proton H5′′ appeared as triplet at 7.15 ppm with *J* coupling = 7.5 ppm. The AA′BB′ system was also observed in this amino compound. Protons H3′, H5′ and H2′, H6′ appeared at 8.08 ppm and 7.92 ppm, respectively.
Figure 3.29 shows the ^{13}C NMR of compound 9b.

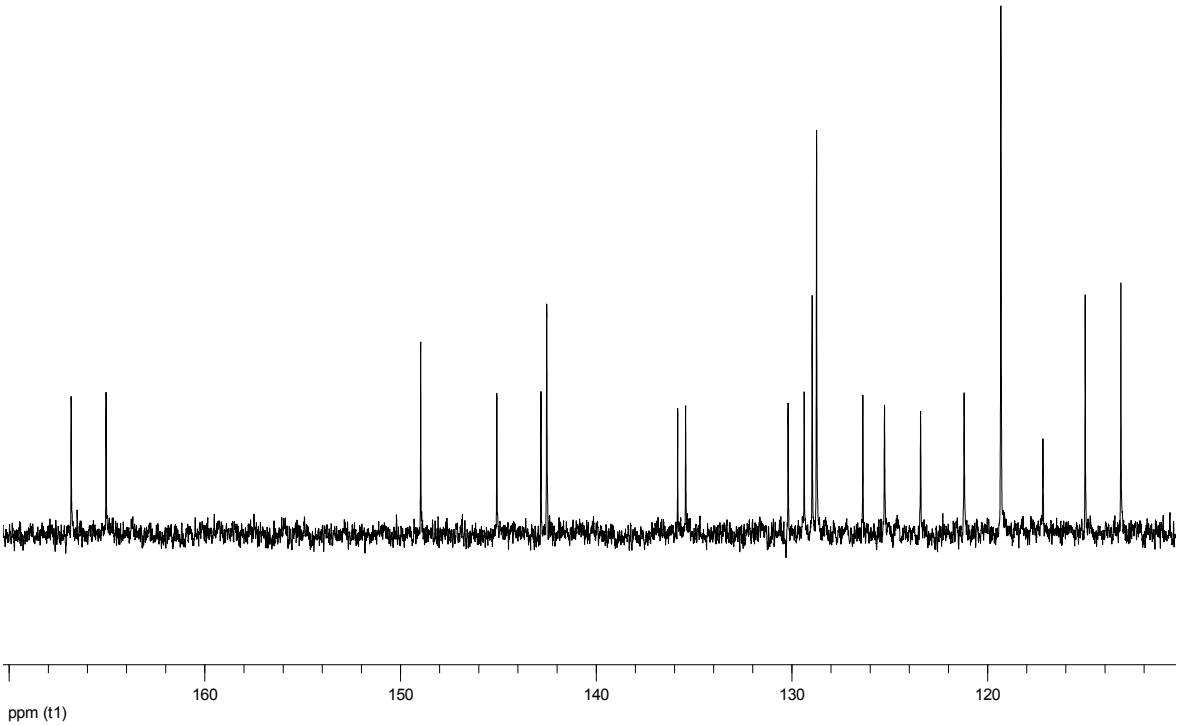

Figure 3.29 125 MHz ^{13}C NMR spectrum of compound 9b in DMSO-d_6.

The signals of carbonyl carbons appeared at 166.8 ppm and 165.1 ppm. As observed in compound 9a, the AA′BB′ system can be observed at carbons C2′, C6′ and C3′, 5′ at 128.7 ppm and 119.3 ppm, respectively. The interpretation of other signals was performed by comparison of the found signals with the estimated signals from the software ChemDraw Ultra 9.0 which is explained in Chapter 3.1.2.3.

3.1.2.3. Hexasodium 7,7′-{carbonylbis[azanediyl-3,1-phenylenecarbonylazanediyl(4,1-phenylene)carbonylazanediyl]} bis(naphthalene-1,3,5-trisulfonate)

The urea derivative 9c was synthesized by phosgenation of amine 9b. Urea 9c is an extended structure (“large urea”) of compound 8c (structure in Appendix B) with a second phenylene-linker. A solution of phosgene in toluene solution (20 %) was slowly dropped to the aqueous solution of amine 9b (Figure 3.30). The pH of the reaction was kept constant at 3.7 to avoid the hydrolysis of phosgene. Compound 9c was obtained as grey powder with 89.0 % yield. After the reaction was completed, the solution was adjusted to pH 7 and solvent was removed under vacuum.

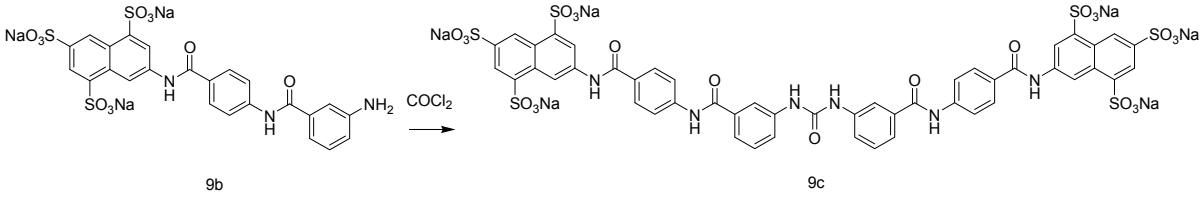

Figure 3.30 Phosgenation of trisodium 7-(4-(3-nitrobenzamido)-naphthalene-1,3,5-trisulfonate.

Purity and structure confirmation

The TLC of urea 9c showed one spot. The HPLC chromatogram showed a single peak with purity of 98.3 % at a retention time of 5.08 minutes. The UV spectrum showed a maximum absorption at the wavelength of 260.5 nm.

Structure confirmation

Figure 3.31 shows the ^{1}H spectrum of compound 9c.

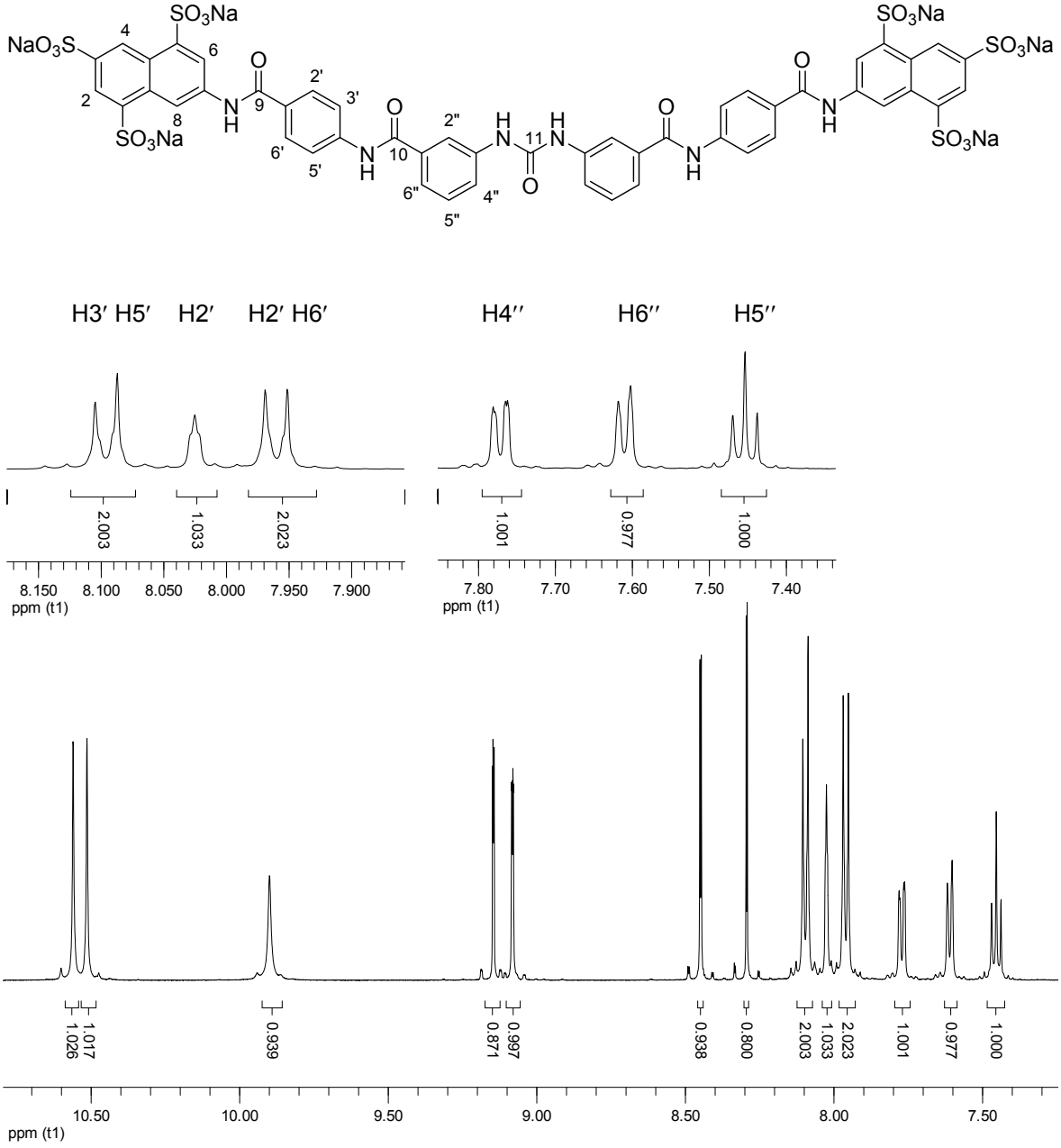

Figure 3.31 500 MHz ^{1}H NMR spectrum of compound 9c in DMSO-d_6.

The spectrum of compound 9c revealed 13 signals with the integration of 30 protons. Signals at 10.56 ppm and 10.52 ppm were assigned to amide proton. Signal of urea proton appeared at 9.89 ppm. Amide and urea signals disappeared upon addition of D_2O. The proton signals of H8, H4, H6 and H2 appeared in nearly the same range as the signals of the proton compounds 5a-5c. H8, H4, H2 and H6

were assigned to signal at 9.14 ppm, 9.08 ppm, 8.43 ppm and 8.28 ppm, respectively. The para phenylene-linker formed a AA′BB′ system. Signals at 8.08 ppm were assigned to H3′, H5′ and at 7.96 ppm to H2′ and H6′ with ^{3}J = 8.8. The signals of the meta phenylene-linker protons appeared at 7.77 ppm (H4′′), 7.61 ppm (H6′′), and 7.45 ppm (H6′′), respectively. The signal of proton H5′′ appeared as triplet and coupled to H6′′ and H5′′ with ^{3}J = 8.5 ppm.

Figure 3.32 shows the ^{13}C NMR of compound 9c.

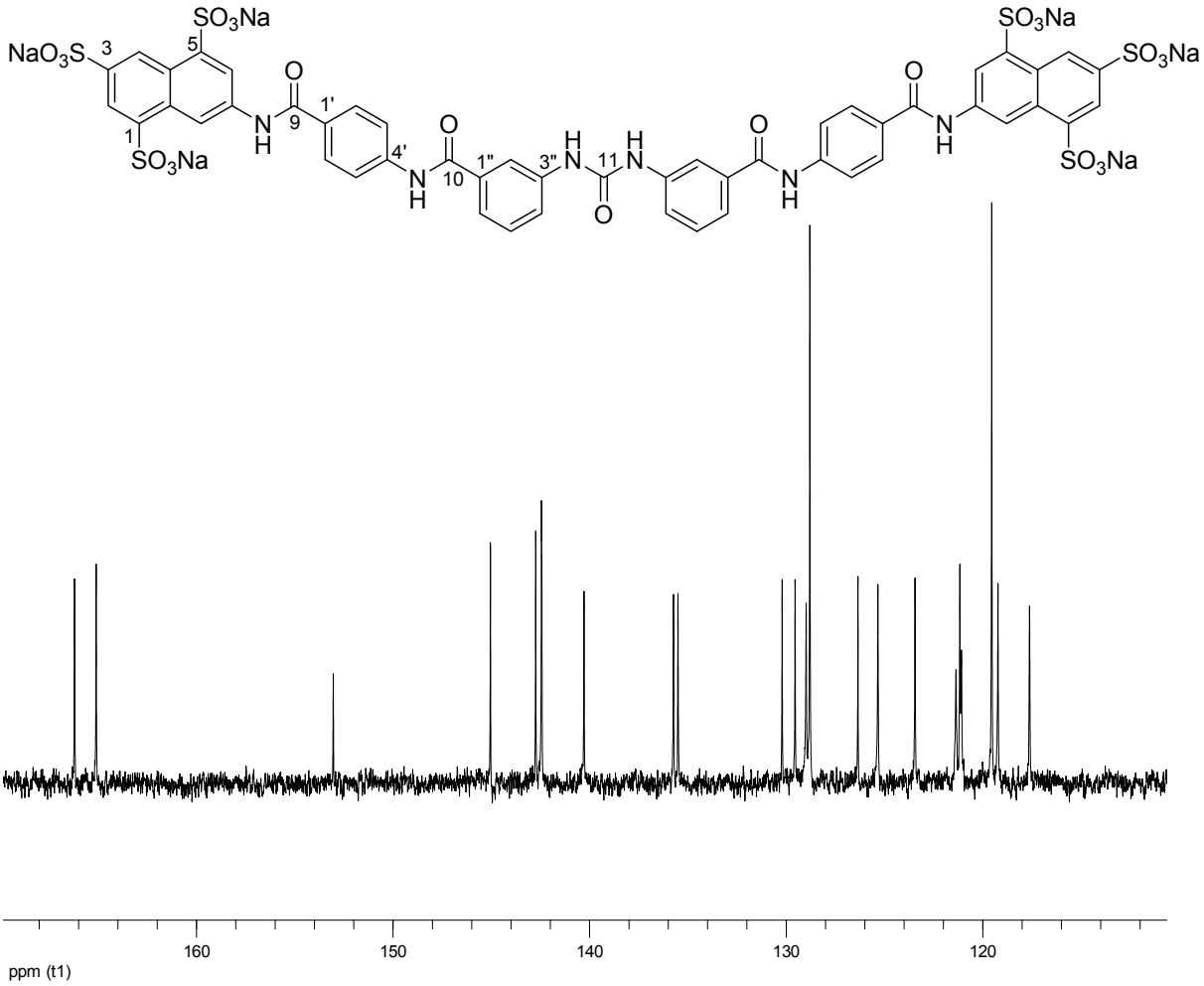

Figure 3.32 125 MHz ^{13}C NMR spectrum of compound 9c in DMSO-d_6.

The signal of the carbonyl urea appeared at 153.0 ppm. The carbonyl carbons of the amide groups appeared at 166.2 ppm and 165.1 ppm, respectively. The carbons of the naphthalene ring appeared in nearly the same positions as the

signals of naphthalene compounds 5a-5c. The interpretation of other signals was performed by comparison of the found signals with the estimated signals from the software ChemDraw Ultra 9.0 for compound 9a, 9b and 9c (Table 3.7).

Table 3.7 Comparison of the calculated and found ^{13}C NMR chemical shift of the carbons of compound 9a, 9b and 9c.

Carbon	Nitro-9a		Amino-9b		Urea-9c	
	δ (ppm)					
	Found	Calc	Found	Calc	Found	Calc
C1′	130.4	129.8	129.4	129.8	129.8	129.5
C2′-C6′	128.9	127.7	128.7	127.7	127.7	128.8
C3′-C5′	122.7	121.7	119.3	121.7	121.7	119.5
C4′	141.8	139.2	135.8	139.2	139.2	142.3
C1′′	135.4	135.1	135.4	135.0	134.4	135.5
C2′′	119.8	121.1	113.2	111.8	117.1	117.6
C3′′	147.9	148.0	148.9	148.5	135.9	135.7
C4′′	126.5	127.3	116.7	119.7	125.0	125.3
C5′′	130.2	129.8	128.9	129.7	129.1	128.9
C6′′	134.5	133.6	115.0	117.5	123.1	121.1

The signal of carbon C2′ and C6′ appeared as one signal with integration of two carbons at 128.8 ppm, 128.7 ppm, and 127.7 ppm for compound 9a, 9b and 9c, respectively. The signals were in agreement with the calculated signals. Signal carbons of C3′ and C5′ were appeared at 122.7 ppm, 119.3 ppm, and 121.7 ppm for compound 9a, 9b and 9c. The signals also appeared as AA′BB′ system and were equal with calculated signals. Due to the effect of a coupling to amide group, signal of C1’ and C6′ appeared at the lower field in comparison to the signals of carbons C2′, C6′, C3′, and C5′. Carbon C4′′ (126.5 ppm) of amino compound 9b was shifted to the higher field in comparison to the nitro compound 9a (116.7 ppm). This phenomenon was observed because of the $-M^+$ effect of the amino group. In general, the found signals are not significant difference compared to the calculated signals.

The ESI-MS spectrum was measured in the negative mode. The spectrum showed signals of $[M-Na]^-$ at 1379.2, $[M-2Na+H]^-$ at m/z 1357.1, and $[M-3Na-H]^-$ at m/z 1335.2 in comparison with calculated m/z of $[M-Na]^-$ at 1377.1, $[M-2Na+H]^-$ at 1355.1, and $[M-3Na+2H]^-$ at 1333.1

3.2. Synthesis of urea derivatives containing 4-fluoro-3,1-phenylene-linker at benzene or naphthalene sulfonates

The result from the pharmacological testing showed that the urea 5c with the 4-fluorobenzamido residue is the most potent antagonist activity at $P2Y_{11}$ receptors (see detail in 4.3). It was interesting to investigate other 5c derivatives with variations in the sulfonate part using naphthalene and benzene sulfonates as precursors. Naphthalene monosulfonates (15c-16c), disulfonates (17c-18c), and trisulfonate (19c) or benzene sulfonates (20c and 21c) were used for synthesis.
Figure 3.33 shows the synthesis pathway of urea derivatives with a 4-fluoro-3,1-phenylene-linker. The same method was used as explained for compounds 5a-5c.

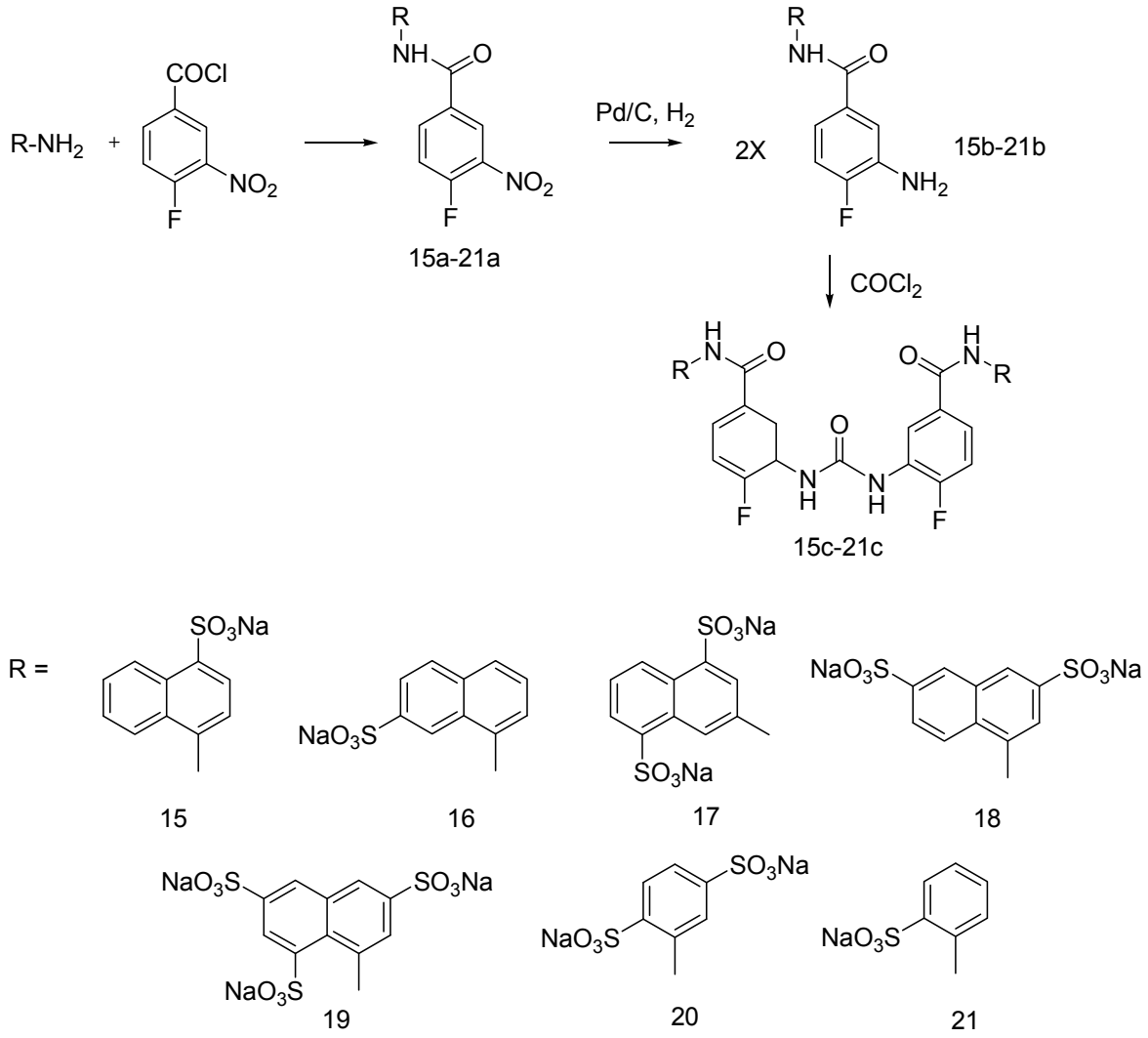

Figure 3.33 Synthesis pathway of urea derivatives with a 4-fluoro-3,1-phenylene-linker and various naphthalene and benzene sulfonates as precursors.

Here, the structure confirmation of compounds 20a, 20b, and 20c are explained as an example in this series.

3.2.1. Disodium 2-(4-fluoro-3-nitrobenzamido)benzene-1,4-disulfonate

Compound 20a was synthesized by acylation of 1,4 aniline disulfonate disodium salt (Figure 3.34). Compound 20a was obtained as a pale yellow powder with the yield of 60.3 %.

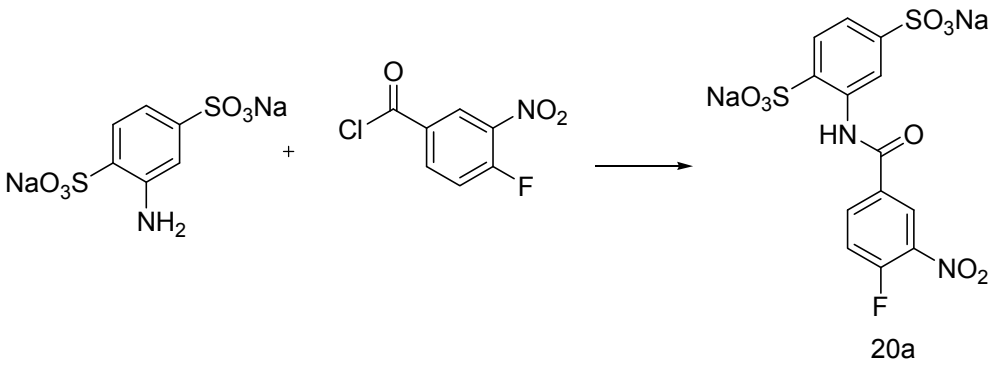

20a

Figure 3.34 Acylation of disodium aminobenzene-1,4-disulfonate with 4-fluoro-3-nitrobenzoylchloride.

Purity and structure confirmation

The TLC of compound 20a showed one spot. Further, purity check by HPLC showed a purity of 98.5 % at a retention time of 2.37 minutes. The UV spectrum showed a maximum absorption wavelength at 261 nm.

Figure 3.35 shows the ^{1}H NMR spectrum of compound 20a.

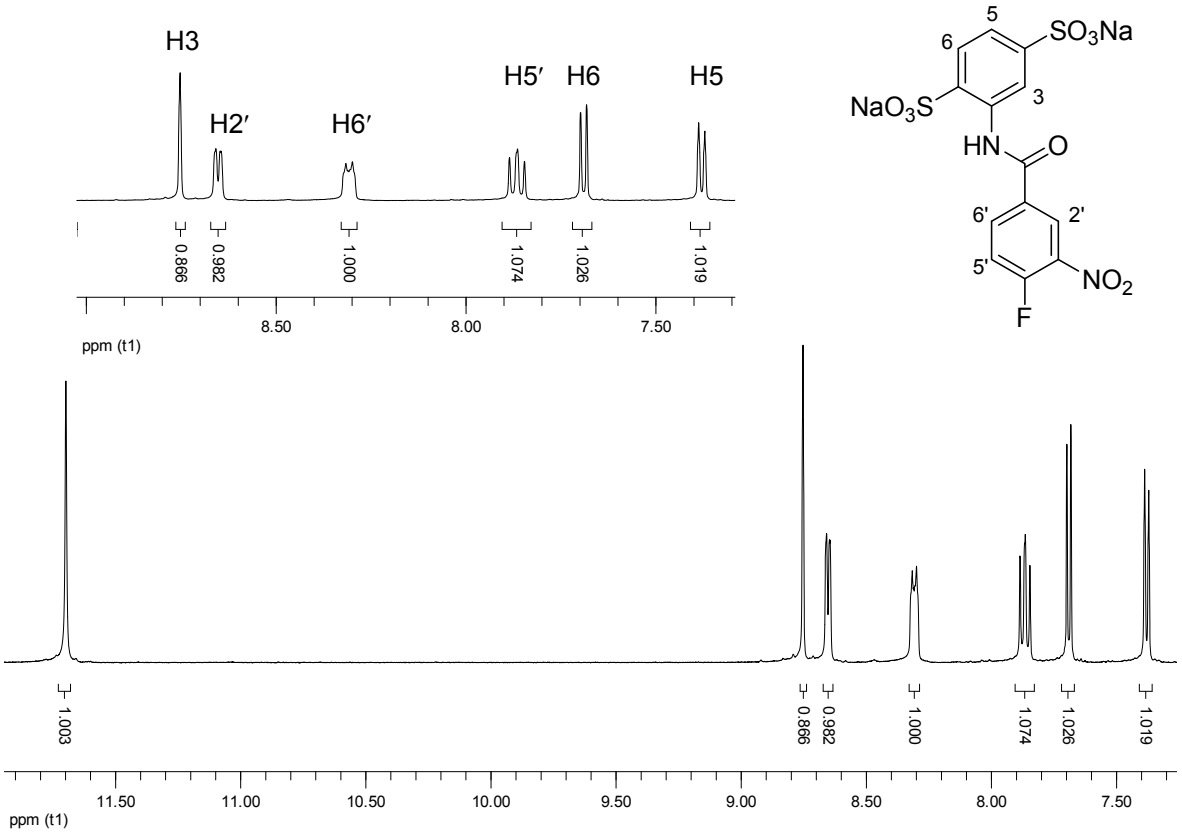

Figure 3.35 500 MHz ^{1}H NMR spectrum of compound 20a in DMSO-d_6.

It revealed the presence of seven signals with the integration of seven protons. The amide proton signal appeared at 11.70 ppm (singlet) with an integration of one proton. The signal disappeared upon the addition of D_2O. The signal of proton H3 appeared at 8.75 ppm. The splitting pattern of H3 was much better observed in compound 20b. The proton H6 appeared as doublet at 7.69 ppm and coupled to H5 (^3J = 8.0). The signal of proton H5 appeared as a doublet at 7.38 ppm with one ortho coupling (^3J = 8.0). The presence of the fluoro substituted phenylene-linker protons was confirmed by signals at 8.65 ppm, 8.31 ppm and 7.89 ppm. The doublet of doublet at 8.65 ppm was interpreted as the signal of H-2′. This proton coupled to H6′ (^4J = 2.0 Hz) and to the fluorine atom (^4J = 7.0 Hz). A multiplet signal at 8.31 ppm represented the proton H6′, which coupled to H5′, H2′ and fluorine. A doublet of doublet signal at 7.89 ppm was assigned to H5′, which coupled to H6′ and the fluorine atom (^3J = 9.0 Hz, ^3J = 11.0 Hz).

Figure 3.36 shows the ^{13}C NMR of compound 20a.

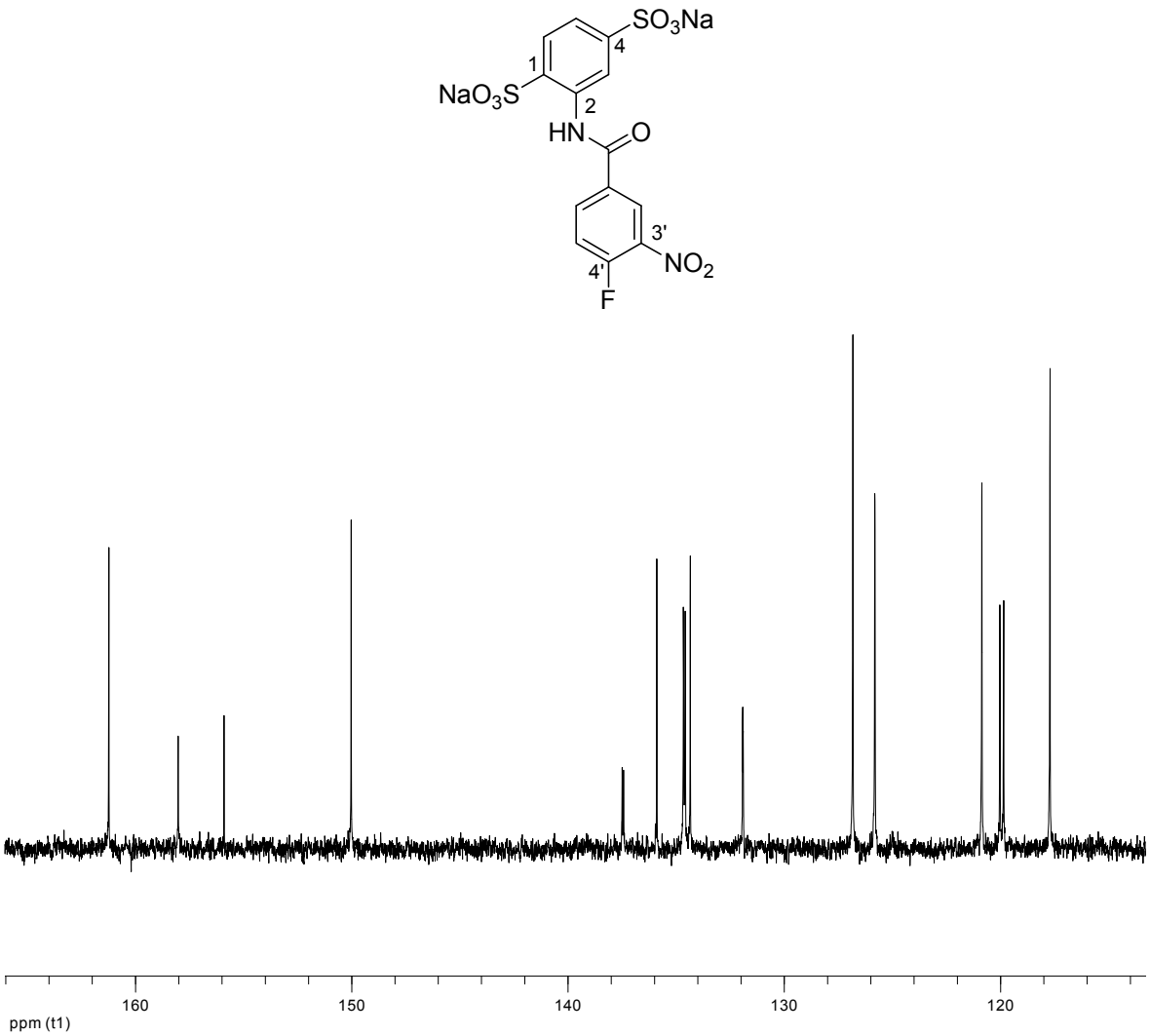

Figure 3.36 125 MHz ^{13}C NMR spectrum of compound 20a in DMSO-d_6

The signals at 126.8 ppm, 117.1 ppm and 135.9 ppm could be interpreted as C2′, C5′ and C6′, respectively. The signal of C4′ was detected at 156.9 ppm as doublet with ^{1}J = 265.3 Hz

Table 3.8 shows the ^{13}C NMR signals of the fluorobenzamido residue in comparison with calculated signals.

Table 3.8 Comparison of the calculated and found ^{13}C NMR chemical shift of the fluorinated phenylene-linker of compound 20a.

Position	δ (ppm)	
	calculated	found
C1′	130.7	131.9
C2′	122.7	125.8
C3′	137.0	137.5
C4′	158.9	156.9
C5′	116.5	117.7
C6′	135.2	135.9

Table 3.9 shows the chemical shifts of the carbons at the sulfonate substituted phenyl ring of compound 20a according to ^{13}C and HSQC correlation spectrum between ^{1}H and ^{13}C.

Table 3.9 Chemical shift of carbons at the sulfonate substituted phenyl ring of compound 20a according to ^{13}C and HSQC spectra.

Position	δ (ppm)		
	Found	Calculated	HSQC
C1	134.7	143.4	-
C2	134.3	129.6	-
C3	119.9	125.0	H3
C4	150.0	153.8	-
C5	120.9	121.9	H5
C6	126.8	137.2	H6

Figure 3.37 shows the HSQC spectrum of compound 20a.

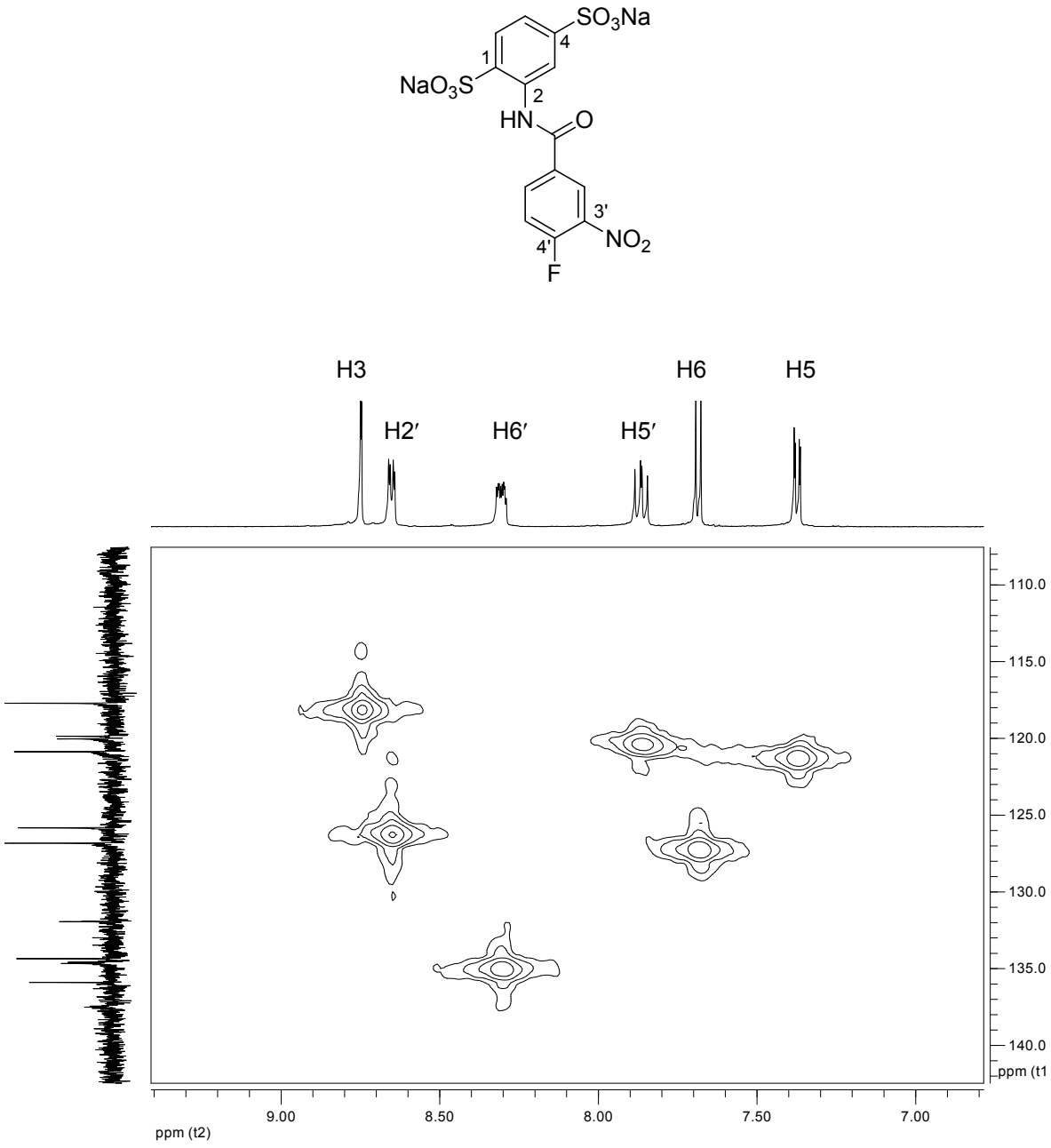

Figure 3.37 HSQC spectrum of compound 20a in DMSO-d_6. Only signals in the aromatic region are shown here. The one-dimensional 500 MHz ^{1}H NMR spectrum is shown at the top edge, while at the left-hand edge the one-dimensional 125 MHz ^{13}C NMR is shown.

The signal at 119.9 ppm was interpreted as C3, which coupled to H3. C6 and C5 appeared at 126.8 ppm and 120.9 ppm, respectively. C1 and C4 appeared at 134.7 ppm and 153.8 ppm. The coupling pattern of the fluorinated phenylene-linker carbons was observed in nearly similar pattern of compound 5a. C4′ coupled

to fluorine atom at 156.9 ppm. C5′ coupled to H5′ (doublet of doublet) at 117.7 ppm. C6′ coupled to H6′ (multiplet) and appeared at 135.9 ppm. C2′ coupled to H2′ and appeared at 125.8 ppm.

The IR spectrum confirmed the presence of the amide functional group with the characteristic band of the C=O stretching vibration at 1677 cm^{-1} and the N-H bending vibration at 1537 cm^{-1}.

3.2.2. Disodium 2-(3-amino-4-fluorobenzamido)benzene-1,4-disulfonate

Compound 20a was hydrogenated in water using palladium/carbon as catalyst (Figure 3.38). The product (20b) was obtained as beige powder with a yield of 88.5 %.

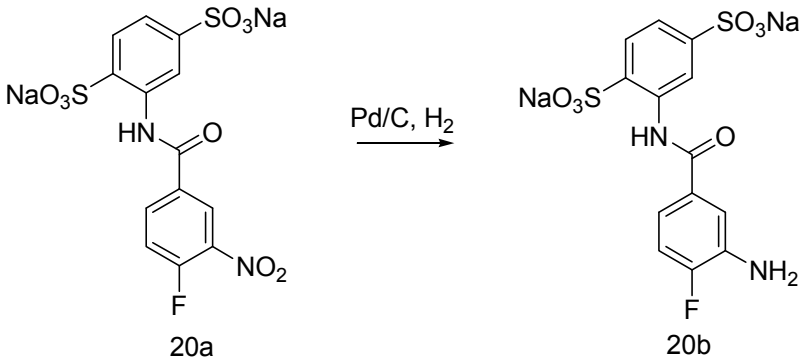

Figure 3.38 Hydrogenation of disodium 2-(4-fluoro-3-nitrobenzamido)benzene-1,4-disulfonate.

Purity and structure confirmation

The TLC of amine 20b showed one spot. The HPLC chromatogram showed a purity of 98.52 % peak area at a retention time of 1.54 minutes. The UV spectrum showed maximum absorption at a wavelength of 257 nm.

Figure 3.39 shows the ^{1}H NMR spectrum of compound 20b.

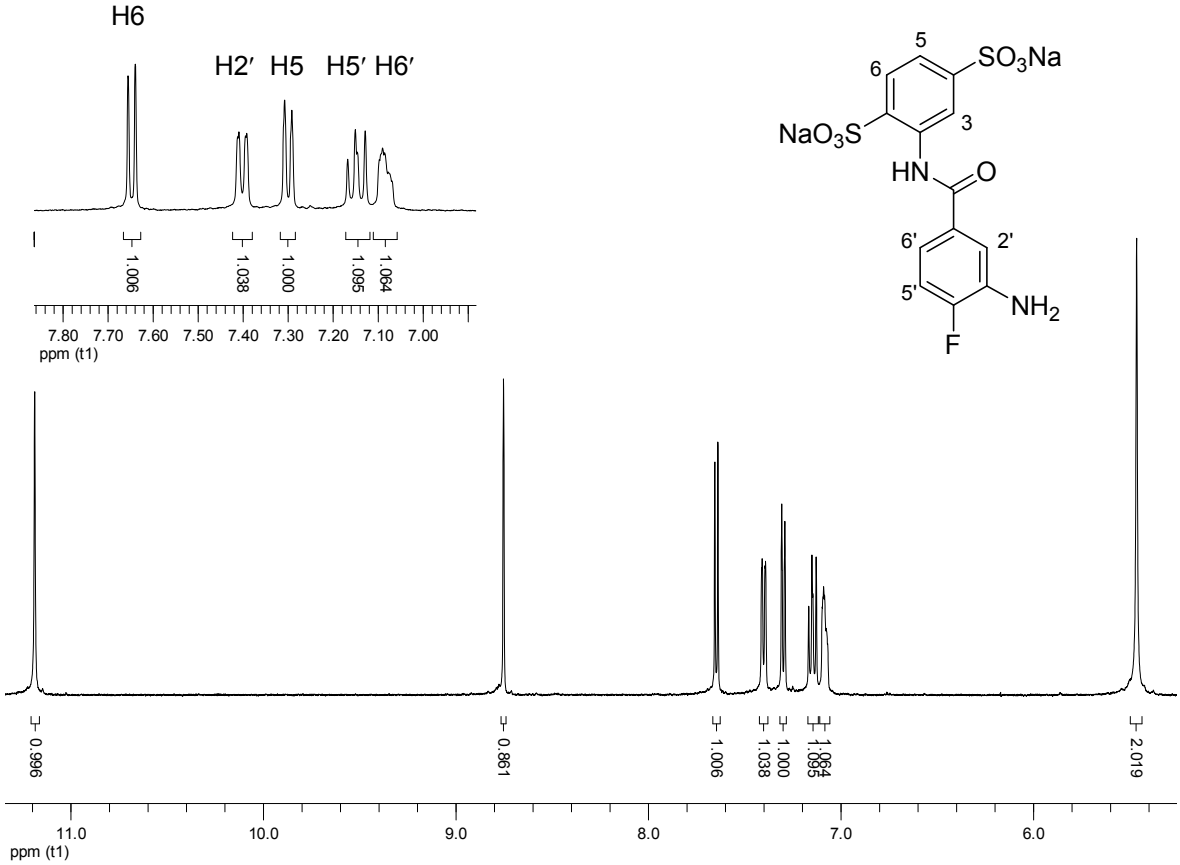

Figure 3.39 500 MHz ^{1}H NMR spectrum of compound 20b in DMSO-d_6.

The spectrum revealed eight signals with the integration of nine protons. The D_2O exchangeable singlet at 5.46 ppm with an integration of two protons was assigned to the -NH_2 protons. The amide proton appeared as a singlet at 11.20 ppm, which also disappeared in the D_2O exchange spectrum. Protons H3, H5 and H6 appeared in nearly the same positions as the signals of the nitro compound (20a). The proton signals of the benzamido residue of 20b were shifted to the upper field in comparison with the nitro precursor (20a) because of the +M effect of the amino group. The signal of proton H2′ appeared as a doublet of doublet at 7.40 ppm and

coupled to H5′ and the fluorine atom (^4J = 1.5 Hz, ^4J = 9.0 Hz). The signal of the multiplet H6′ was shifted to 7.08 ppm, whereas the signal of H5′ appeared as a doublet of doublet at 7.13 ppm. H5′ coupled to H6′ and the fluorine atom (^3J = 8.0 Hz, ^3J = 11.0 Hz). The proton H6 appeared as doublet at 7.65 ppm and coupled to H5 (^3J = 8.0 Hz). The signal of proton H5 appeared as a broad doublet at 7.30 ppm with one ortho coupling (^3J = 8.0 Hz). The proton H3 appeared as a broad doublet at 8.75 ppm because of poor resolution.

Figure 3.40 shows the ^{13}C NMR spectrum of compound 20b.

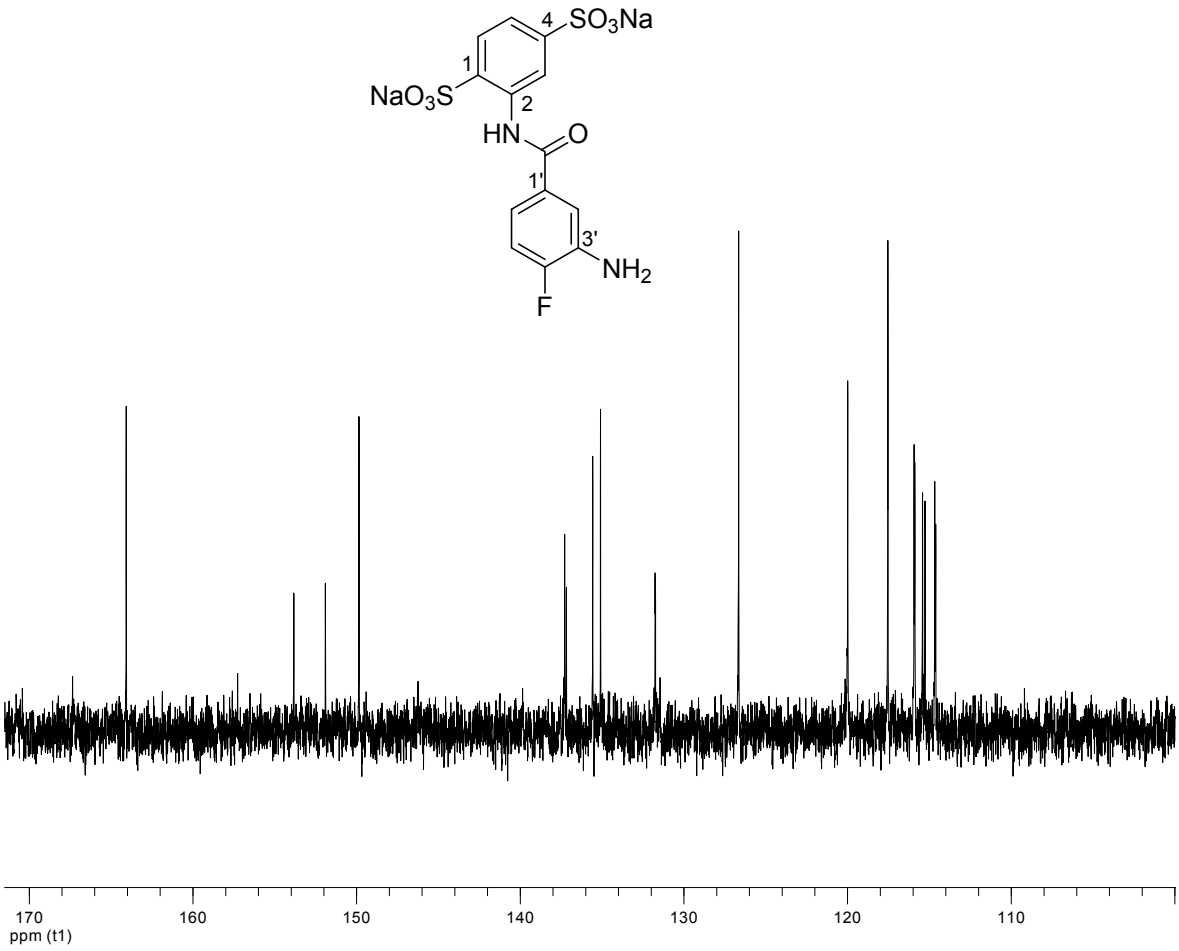

Figure 3.40 125 MHz ^{13}C NMR spectrum of compound 20b in DMSO-d_6

The signal of the carbonyl carbon appeared in the lowest field (164.0 ppm). The signals of the sulfonate substituted phenyl carbons appeared in the relatively same range as in the nitro derivative (compound 20a). The +M effect of the -NH_2 group caused a shift of the carbon signals of the fluorine substituted phenylene-linker to

the higher field. The amino-substituted carbon C3′ was detected as a signal at 137.3 ppm. Similar to compound 20a, the signal of C4′ was detected in the lower field at 152.9 ppm as doublet. The carbon C4′ coupled with the fluorine atom with ^1J = 241.3 Hz. The assignment of the carbon C2′ (115.9 ppm), C5′ (115.4 ppm), and C6′ (114.6 ppm) was confirmed by the HSQC spectrum (Figure 3.41) The coupling of C2′, C5′, and C6′ to H2′, H5′, and H6′ can be observed. Carbon C1′ and the remaining carbons from the sulfonate substituted phenyl ring were interpreted by the substitution increment calculation (Table 3.10 and Table 3.11).

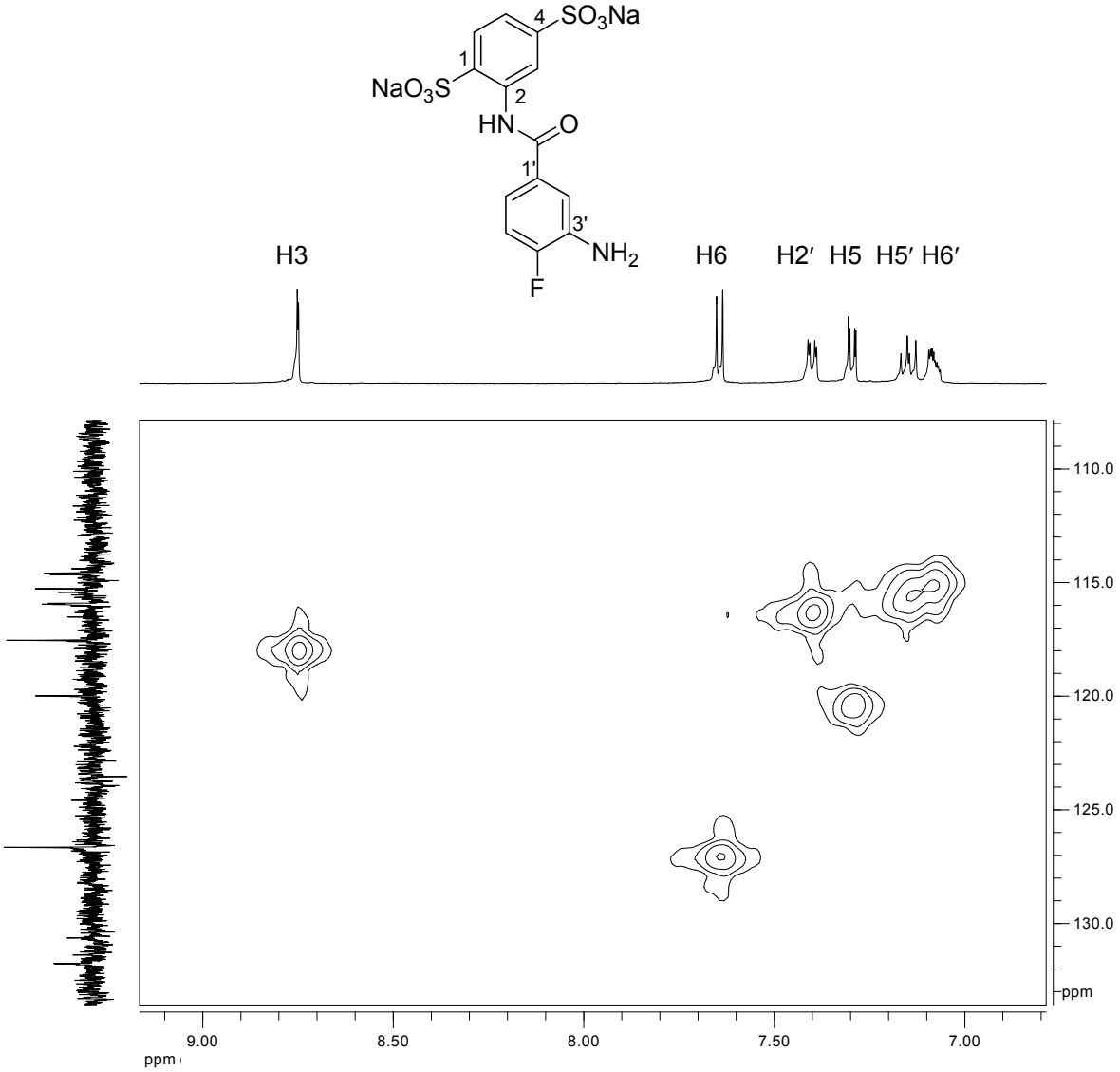

Figure 3.41 HSQC spectrum of compound 20b in DMSO-d_6. Only signals in the aromatic region are shown here. The one-dimensional 500 MHz ^{1}H NMR spectrum is shown at the top edge, while at the left-hand edge the one-dimensional 125 MHz ^{13}C NMR is shown.

Table 3.10 Chemical shifts of the carbons at the fluorine substituted phenylene-linker of compound 20b according to ^{13}C and HSQC spectra.

Position	^{13}C δ (ppm)		
	Found	Calculated	HSQC
C1′	131.8	130.6	-
C2′	115.9	113.4	H2′
C3′	137.1	136.4	-
C4′	152.5	161.1	-
C5′	115.4	116.4	H5′
C6′	114.6	119.1	H6′

Table 3.11 Chemical shift of carbons at the sulfonate substituted phenyl ring of compound 20b according to ^{13}C and HSQC spectra.

Position	^{13}C δ (ppm)		
	Found	Calculated	HSQC
C1	135.6	143.4	-
C2	135.1	129.6	-
C3	117.5	125.0	H3
C4	149.9	153.8	-
C5	119.9	121.9	H5
C6	126.7	137.2	H6

3.2.3. Tetrasodium 2,2'-{carbonylbis[azanediyl(4-fluoro-3,1-phenylene)carbonylazanediyl]}bis(benzene-1,4-disulfonate)

Phosgenation of compound 20b was performed in aqueous solution using a solution of phosgene in toluene (20 %) (Figure 3.42). Compound 20c was obtained as a beige powder with a yield of 76.5 %.

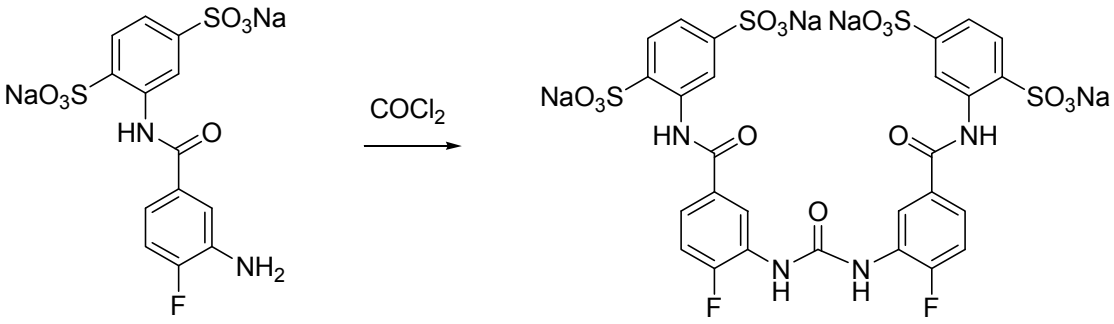

20b 20c

Figure 3.42 Phosgenation of 2-(3-amino-4-fluorobenzamido)benzene-1,4-disulfonate disodium salt.

Purity and structure confirmation

The TLC of compound 20c showed one spot. HPLC chromatogram showed a purity of 96.58 % at a retention time of 6.32 minutes. The UV spectrum showed maximum absorption at a wavelength of 261 nm.

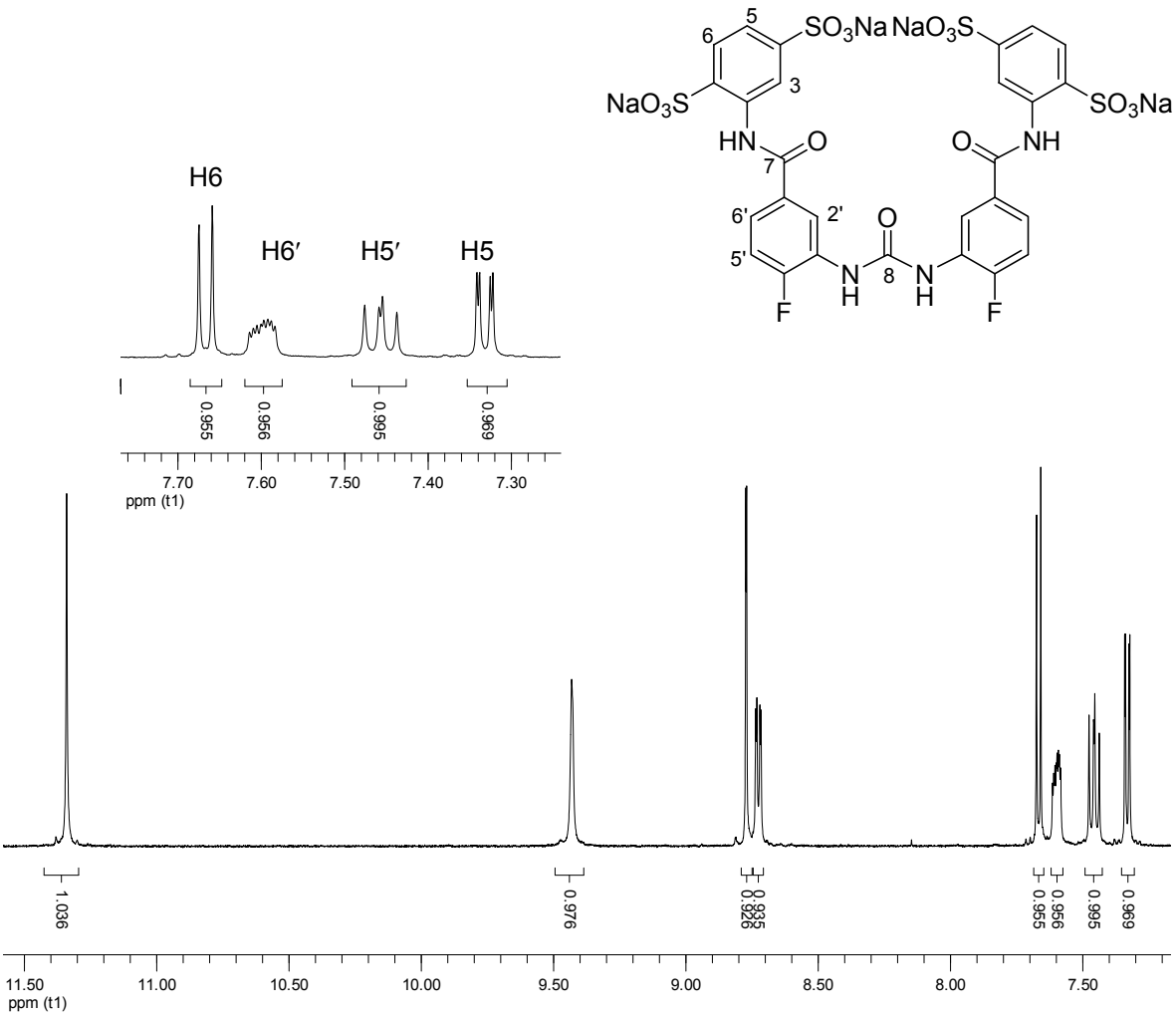

Figure 3.43 500 MHz ^{1}H NMR spectrum of compound 20c in DMSO-d_6.

Figure 3.43 shows the ^{1}H NMR of compound 20c. The spectrum revealed the presence of eight signals with an integration of 16 protons. The signals of the amide proton at 11.34 ppm and urea at 9.43 ppm disappeared by the addition of D_2O. The protons of the phenyl rings showed signals which are comparable to the amine derivative. At 8.77 ppm, proton H3 appeared as doublet with ^{4}J = 1.5 Hz. The signal at 7.67 was interpreted as H6 (^{3}J = 7.9 Hz) which coupled to H5. H5 coupled to H3 and H6 and appeared at 7.32 ppm (^{3}J = 7.9 Hz, ^{4}J = 1.5 Hz). The doublet of doublet signal at 8.72 ppm was assigned to H2′. H2′ coupled to H6′ and the fluorine atom with ^{4}J = 2.0 Hz and ^{4}J = 8.0 Hz, respectively. The protons H6′ and H5′ were assigned to signals at 7.60 ppm and 7.43 ppm, respectively. The

interpretation of the protons of compound 20c was supported by COSY spectrum (Figure 3.44). The cross peaks (dotted lines) in the spectrum showed the coupling of the protons H3 to H5. Furthermore, the coupling of phenylene-linker protons H2′, H5′ and H6′ can be observed.

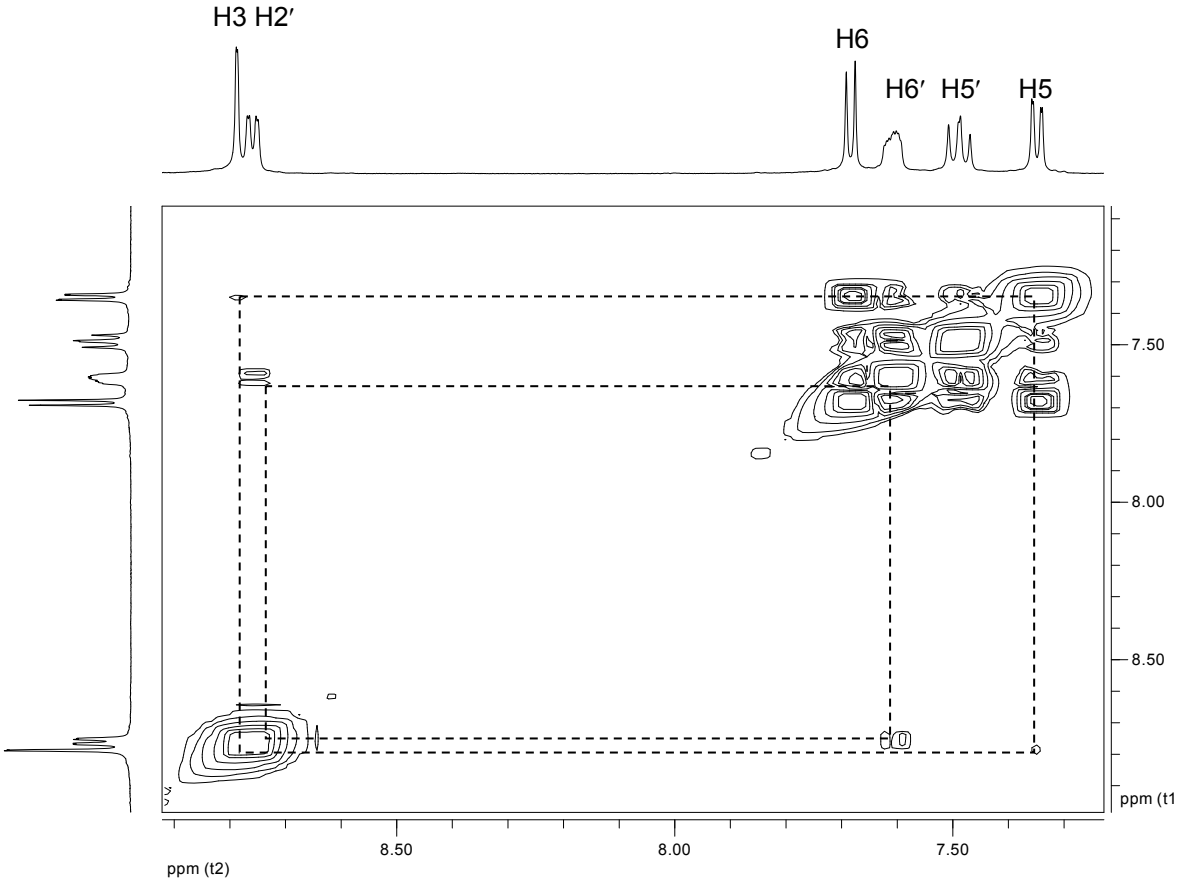

Figure 3.44 500 MHz-^{1}H COSY compound 20c shown as a contour plot. At the top and the left-hand edge is the one dimensional ^{1}H NMR spectrum with partial assignments.

Table 3.12 shows the comparison of δ values of the protons at the fluorine substituted phenylene ring between 20a-20c. The +M effect of the -NH_2 group caused the shifting of signals to the higher field.

Table 3.12 Comparison of ^{1}H NMR signals at the fluorine substituted phenylene residues between compounds 20a-20c.

Position	δ (ppm)		
	(20a)	**(20b)**	**(20c)**
	Nitro-derivative	**Amine-derivative**	**Urea**
H2′	8.65	7.40	8.72
H5′	7.89	7.13	7.43
H6′	8.31	7.08	7.60

Figure 3.45 shows the ^{13}C NMR of compound 20c.

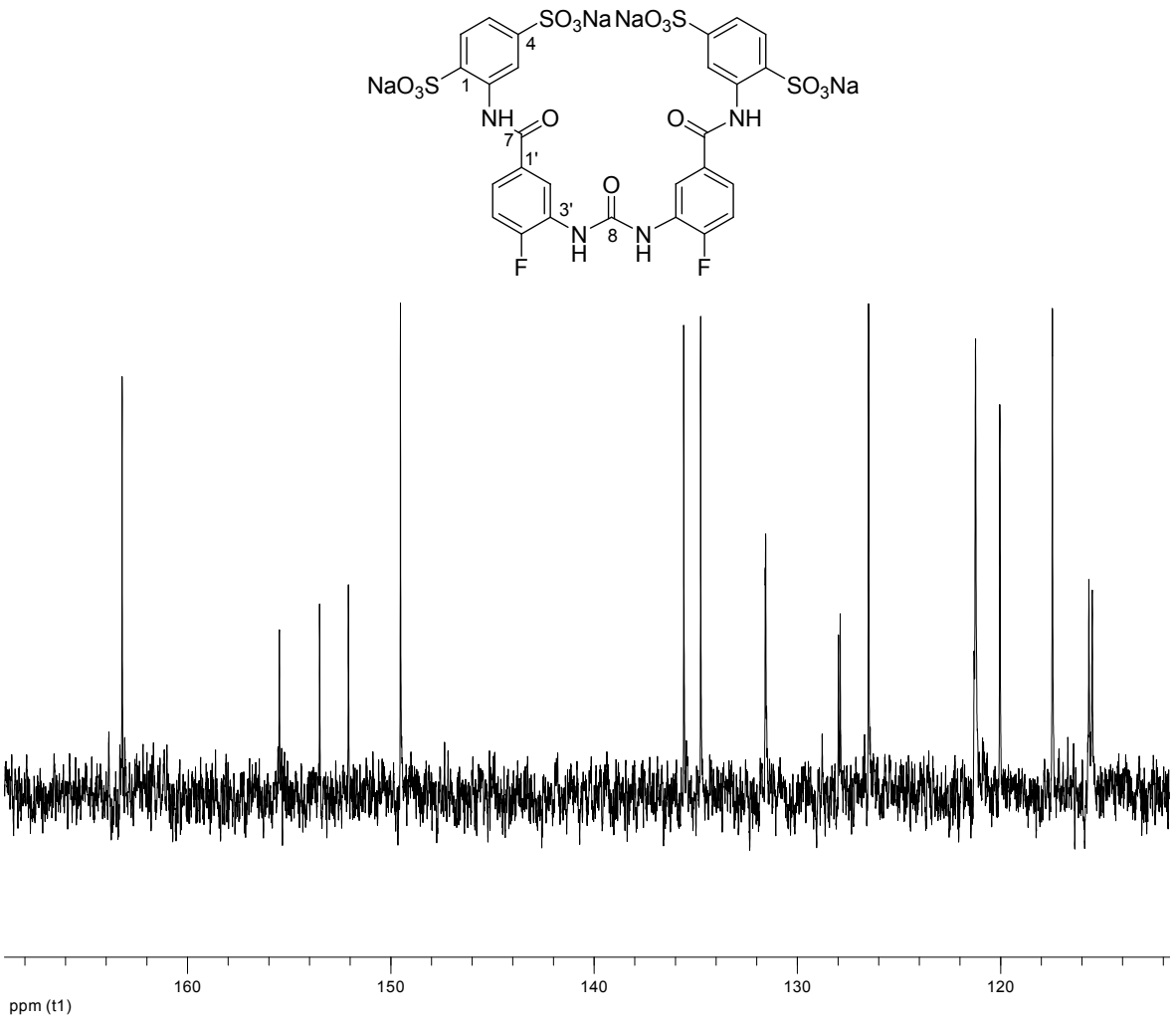

Figure 3.45 125 MHz ^{13}C NMR spectrum of compound 20c in DMSO-d_6.

The urea carbonyl carbon appeared at 152.1 ppm (C8) whereas the carbonyl carbon of the amide group (C7) appeared at 163.2 ppm. The signals of the phenyl ring carbons appeared in similar range of the precursor 20a. C3′ was detected at 137.3 ppm. As observed in compound 20a and 20b, signal of C4′ was also in similar range at 155.5 ppm. C4′ coupled to fluorine atom as doublet signal with ^{1}J = 247 Hz. The assignment of the carbon C2′ (121.1 ppm), C5′ (115.7 ppm), and C6′ (127.9 ppm) was confirmed by the HSQC spectrum (Figure 3.46). Comparison of the carbon signal of the fluorine substituted phenylene-linker compounds 20a-20c is presented in Table 3.13. Table 3.14 presents chemical shifts of carbons at the sulfonate substituted phenyl ring of compound 20c according to ^{13}C and HSQC spectra. Figure 3.45 shows the HSQC spectrum.

Table 3.13 Comparison of ^{13}C NMR signals (DMSO-d_6) and coupling patterns of carbons at fluorine substituted phenylene residues between compounds 20a-20c.

Position	Found , δ (ppm)		
	20a	**20b**	**20c**
C1′	131.9	131.8	131.6
C2′	126.8	115.9	121.1
C3′	137.5	137.1	137.3
C4′	158.0	152.5	155.5
C5′	117.7	115.4	115.7
C6′	135.9	114.6	127.9

Table 3.14 Chemical shift of the carbons at the sulfonate substituted phenyl ring of compound 20c according to ^{13}C and HSQC spectra.

Position	^{13}C δ (ppm)		
	Found	Calculated	HSQC
C1	135.6	143.4	-
C2	134.8	129.6	-
C3	117.5	125.0	H3
C4	149.5	153.8	-
C5	120.5	121.9	H5
C6	127.0	137.2	H6

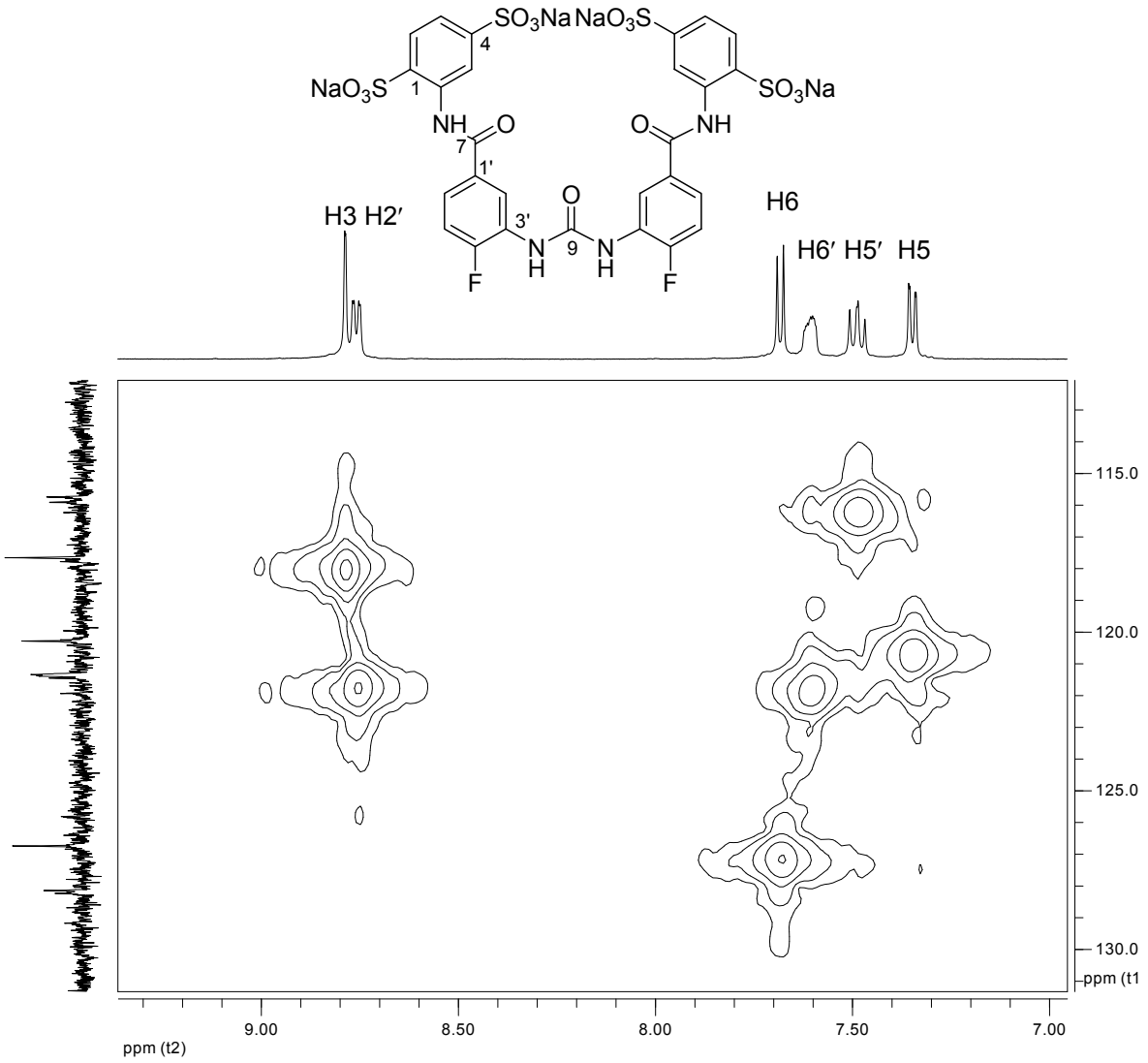

Figure 3.46 HSQC expanded signal in the aromatic region spectrum of compound 20c in DMSO, d_6. The one-dimensional 500 MHz ^{1}H NMR spectrum is shown at the top edge, while at the left-hand edge the one-dimensional 125 MHz ^{13}C NMR spectrum is shown.

The HSQC spectrum showed the coupling of C2′ (121.1 ppm) to H2’ (8.72 ppm) whereas C5′ (115.7 ppm) and C6′ (127.9 ppm) coupled to H5′ (7.43 ppm) and H6′ (7.60 ppm), respectively. Furthermore, C3 (117.5 ppm), C5 (120.5 ppm) and C6 (127.0 ppm) coupled to H3 (8.77 ppm), H5 (7.32 ppm), and H6 (7.67 ppm), respectively.

3.3. Synthesis of urea derivatives containing trisodium 3-(2,4-disulfonatophenylcarbamoyl)benzoate substituent

Two products were obtained during synthesis of nitro precursor of NF449 (see Figure 1.3) which are tetrasodium 4,4′-(5-nitro-1,3-phenylenedicarbamido)-bis(benzene-1,3-disulfonate) (“bisamide sulfonate”) and trisodium 3-(2,4-disulfonato phenycarbamoyl)-5-nitrobenzoate (“monoamide sulfonate”) as side product (Figure 3.47) (Ullmann, 2001). The urea compound of the “monosulfonate” was synthesized by Ullmann (Dissertation Ullmann, in process). A further extension of phenylene-linker of urea derivatives containing trisodium 3-(2,4-disulfonato phenycarbamoyl)benzoate were synthesized in this study.

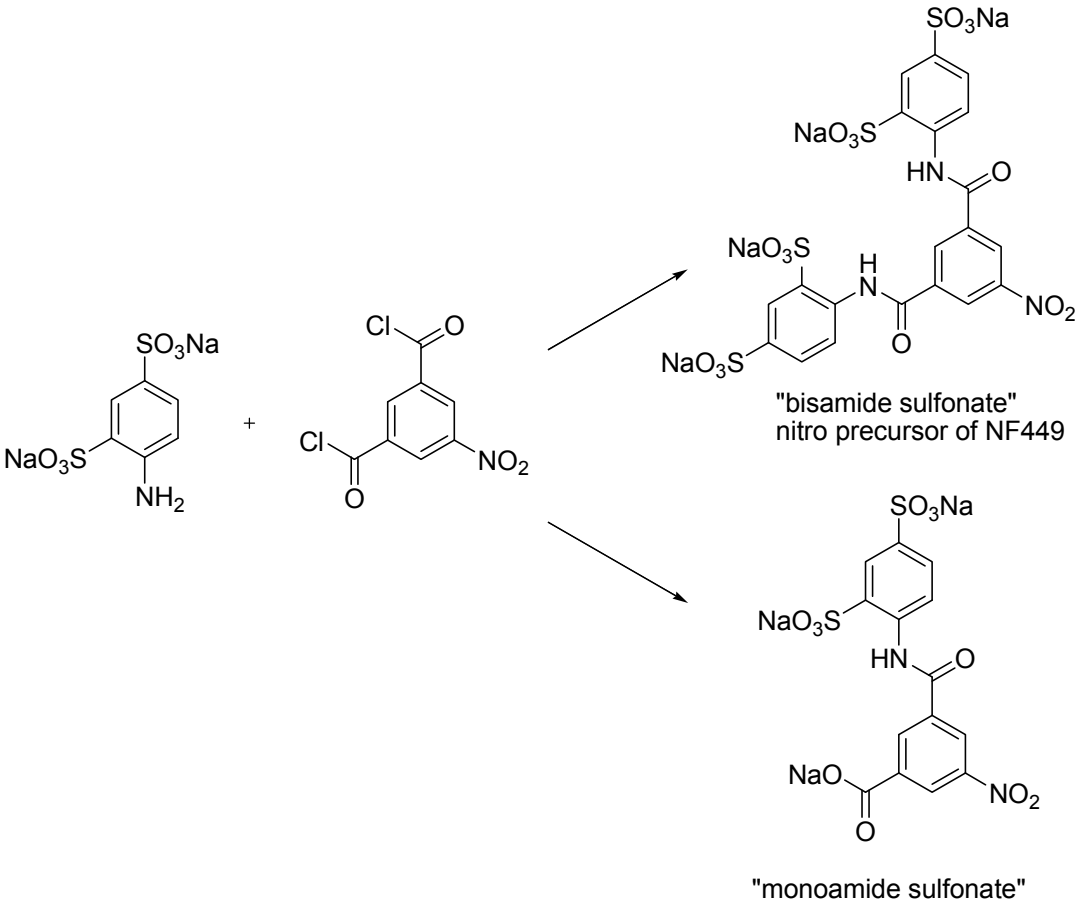

Figure 3.47 Synthesis of the nitro precursor of NF449 and its major side product.

Four ureas and their precursor were synthesized. Figure 3.48 shows the scheme of the synthesis of urea derivatives containing trisodium 3-(2,4-disulfonatophenylcarbamoyl)benzoate.

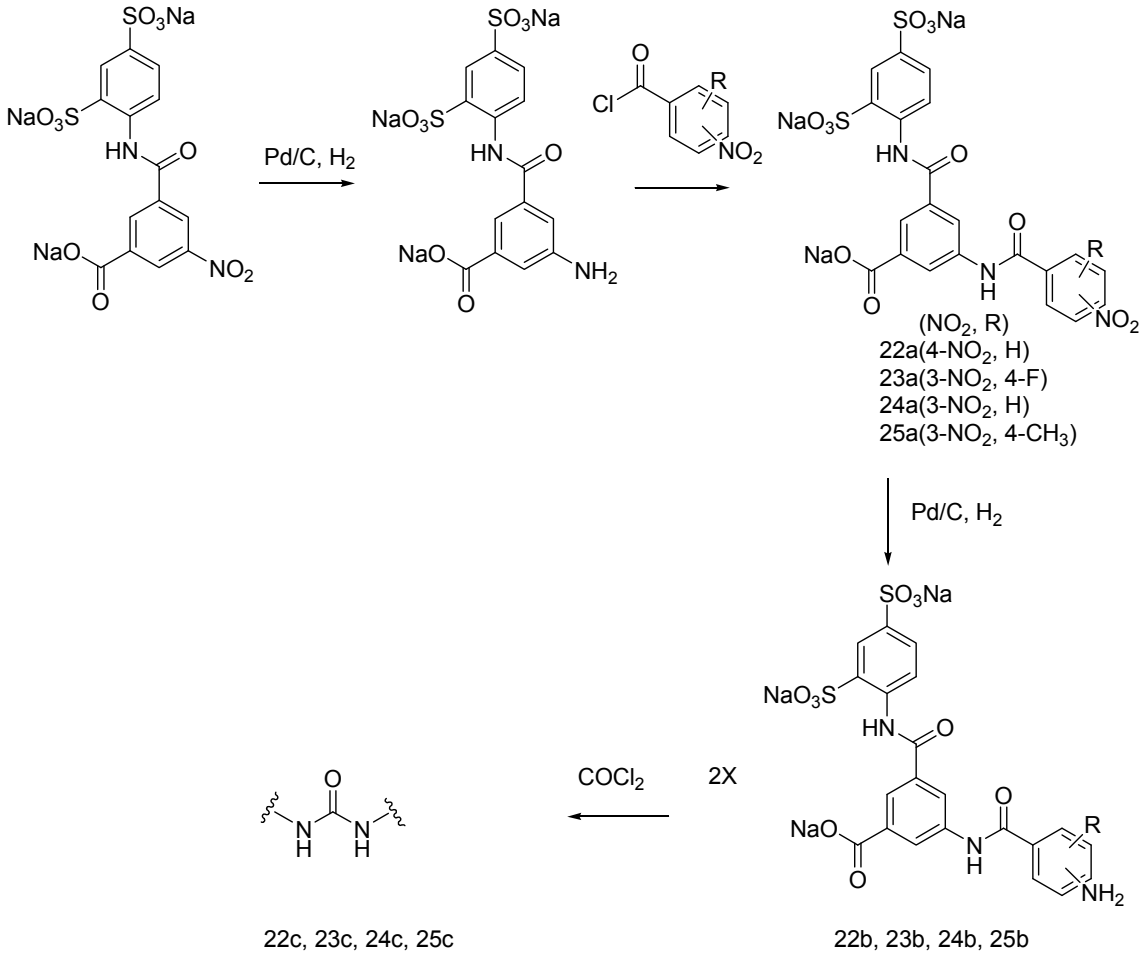

Figure 3.48 Synthesis pathway of urea derivatives of trisodium salt 3-(2,4-disulfonatophenylcarbamoyl)benzoate.

3.3.1. Trisodium 3-(2,4-disulfonatophenylcarbamoyl)-5-(4-nitrobenzamido)benzoate

Compound 22a was synthesized by acylation of the amine precursor. The same method as explained for the synthesis of compound 5a was used (Figure 3.49). Compound 22a was obtained as a yellow powder with a yield of 85.3 %.

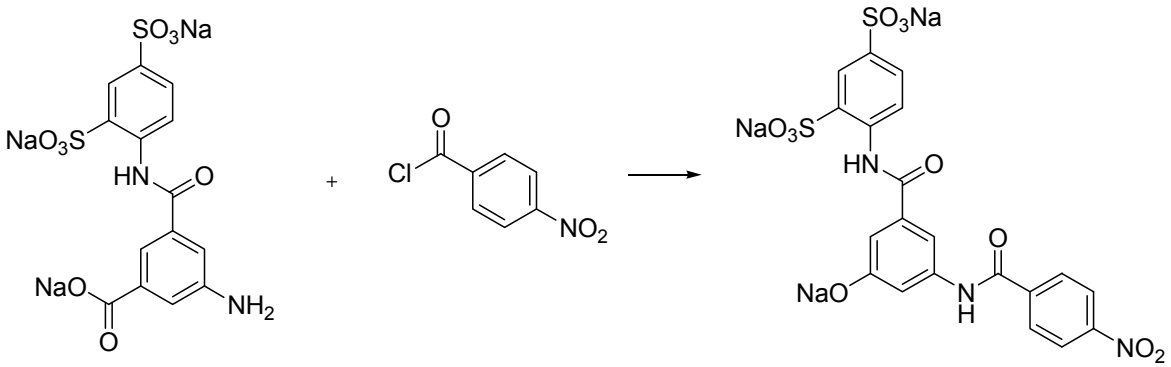

Figure 3.49 Acylation of trisodium 5-amino-3-(2,4-disulfonato phenylcarbamoyl) benzoate.

Purity and structure confirmation

The TLC of compound 22a showed one spot. The HPLC chromatogram showed a purity of 98.60 % at a retention time of 3.41 minutes. The UV spectrum showed maximum absorption at a wavelength of 277 nm.

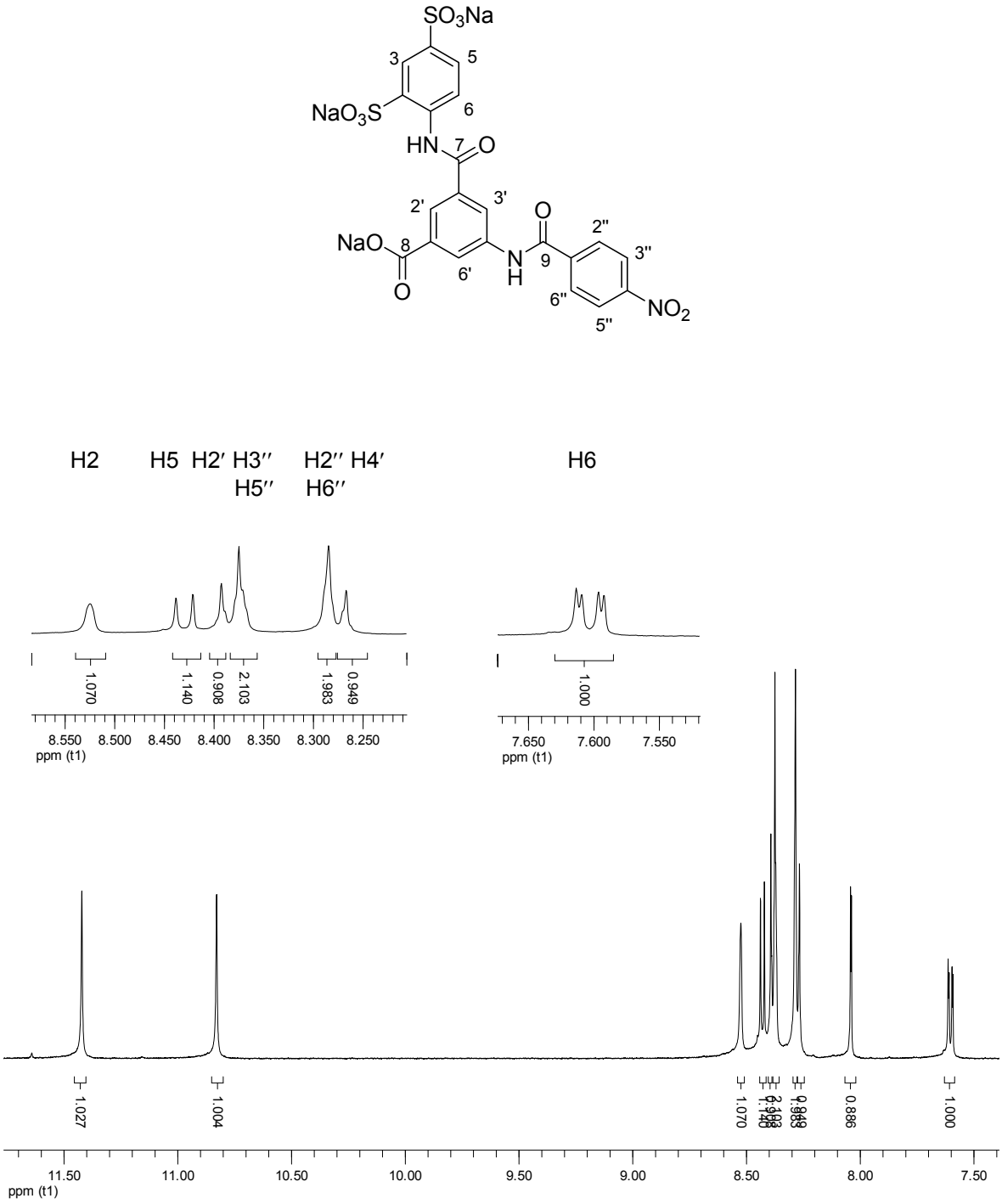

Figure 3.50 500 MHz ^{1}H NMR spectrum of compound 22a in DMSO-d_6.

Figure 3.50 shows the ^{1}H NMR spectrum of compound 22a. The spectrum revealed the presence of 12 protons. Signals of the two amide protons appeared at 11.42 ppm and 10.84 ppm. The phenylene ring formed a AA′BB′ system. Two signals were assigned to protons H3′′, H5′′ and H2′′, H6′′ at 8.38 ppm and 8.28 ppm, respectively. The signals were assigned by using the software

ChemDraw 9. Broad singlet signal at 8.52 ppm was interpreted as H2. Signal H5 appeared at 8.43 ppm and coupled to H6 with ortho coupling (^3J = 8.5 Hz). Signal H6 appeared as doublet of doublet at 7.60 ppm which coupled to H5 (^3J = 8.5 Hz) and H2 (^4J = 2.5 Hz). Signals of H2′, H4′ and H6′ (^4J = 2.5 Hz) appeared at 8.39 ppm, 8.26 ppm and 8.04 ppm respectively with a meta coupling. Coupling constant of H2′, H4′ could not be measured because of poor resolution.

Figure 3.51 shows the ^{13}C NMR spectrum of compound 22.

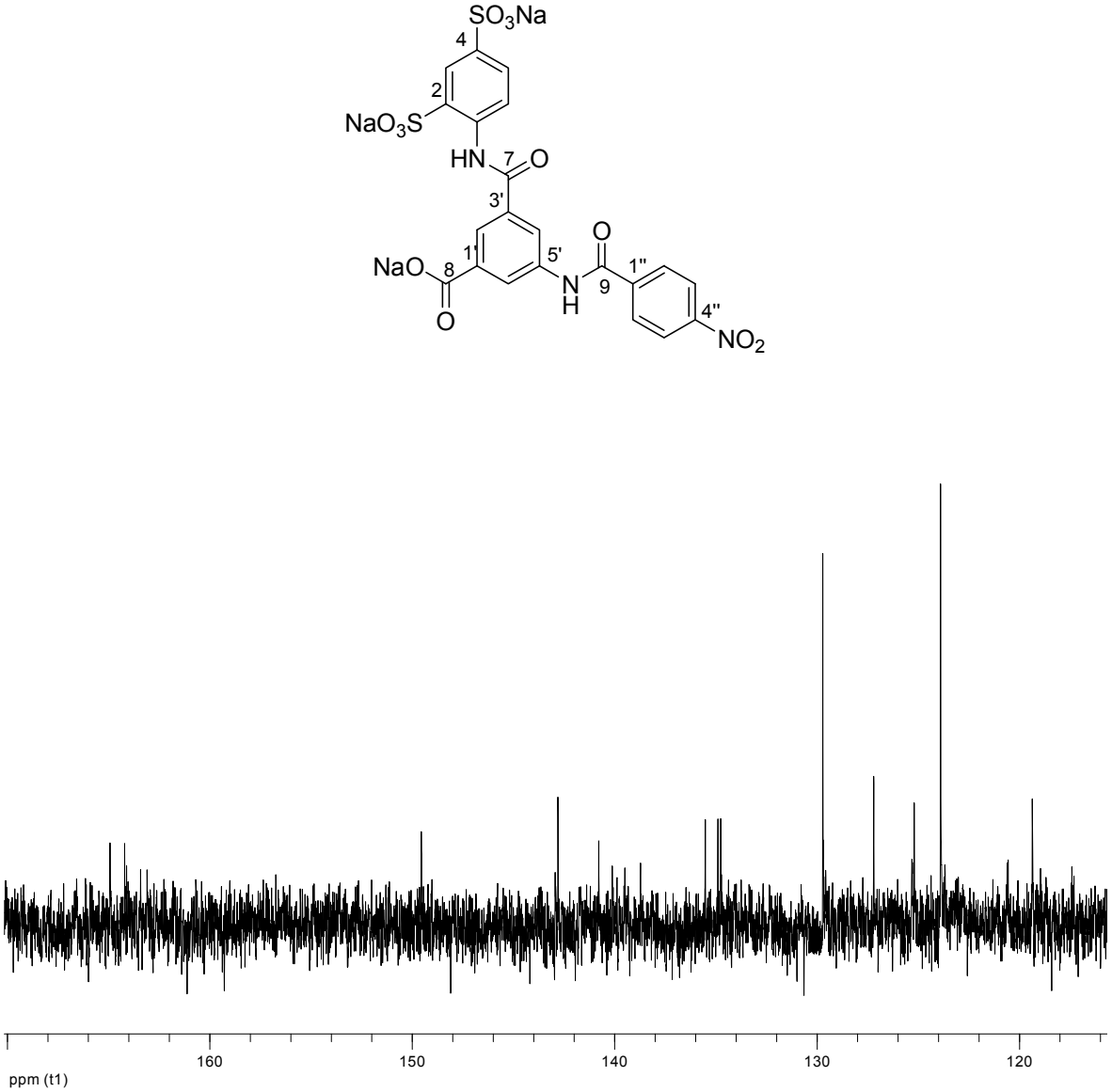

Figure 3.51 125 MHz ^{13}C NMR spectrum of compound 22a in DMSO-d_6

The ^{13}C spectrum of compound 22a shows the carbonyl carbons appeared in the lower field at 164.9 ppm and 164.2 ppm. Due to the poor resolution, the carboxylic

acid carbon which appeared at 169.1 ppm was not clearly shown. This carbon can be observed at amino compound 22b. The AA′BB′ system can be observed at signals of carbons C2′′, C6′′ (129.7 ppm) and carbons C3′′, C5′′ (123.9 ppm). The interpretation of other signals was performed by comparison of the found signals with the estimated signals from the software ChemDraw Ultra 9.0 which explained in Chapter 3.3.3

3.3.2. Trisodium 3-(2,4-disulfonatophenylcarbamoyl)-5-(4-aminobenzamido)benzoate

Compound 22b was hydrogenated in water using palladium/carbon as catalyst. The method was carried out similarly to the synthesis of compound 5b (Figure 3.52). The product (22b) was obtained as beige powder with a yield of 82.10 %.

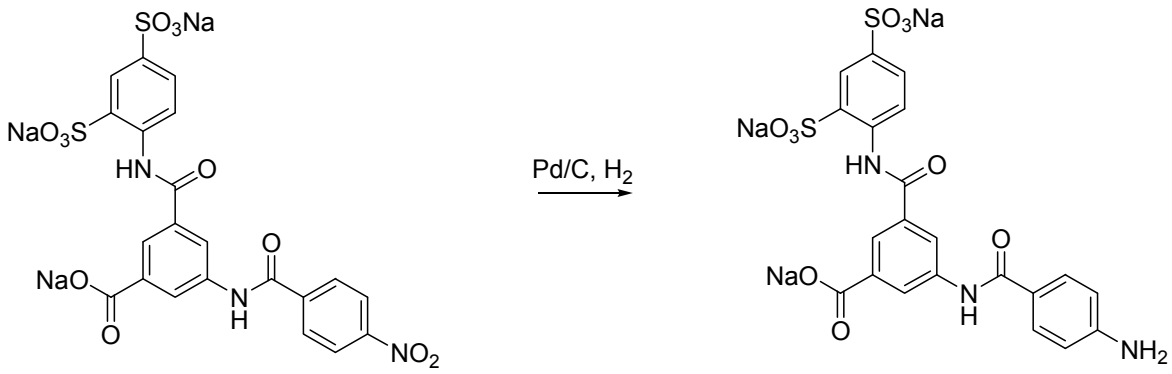

Figure 3.52 Hydrogenation of trisodium 3-(2,4-disulfonatophenylcarbamoyl)-5-(4-nitrobenzamido)

Purity and structure confirmation

The TLC of amine 22b showed one spot. The HPLC chromatogram showed a purity of 98.2 % at a retention time of 1.63 minutes. The UV spectrum showed maximum absorption at a wavelength of 295 nm.

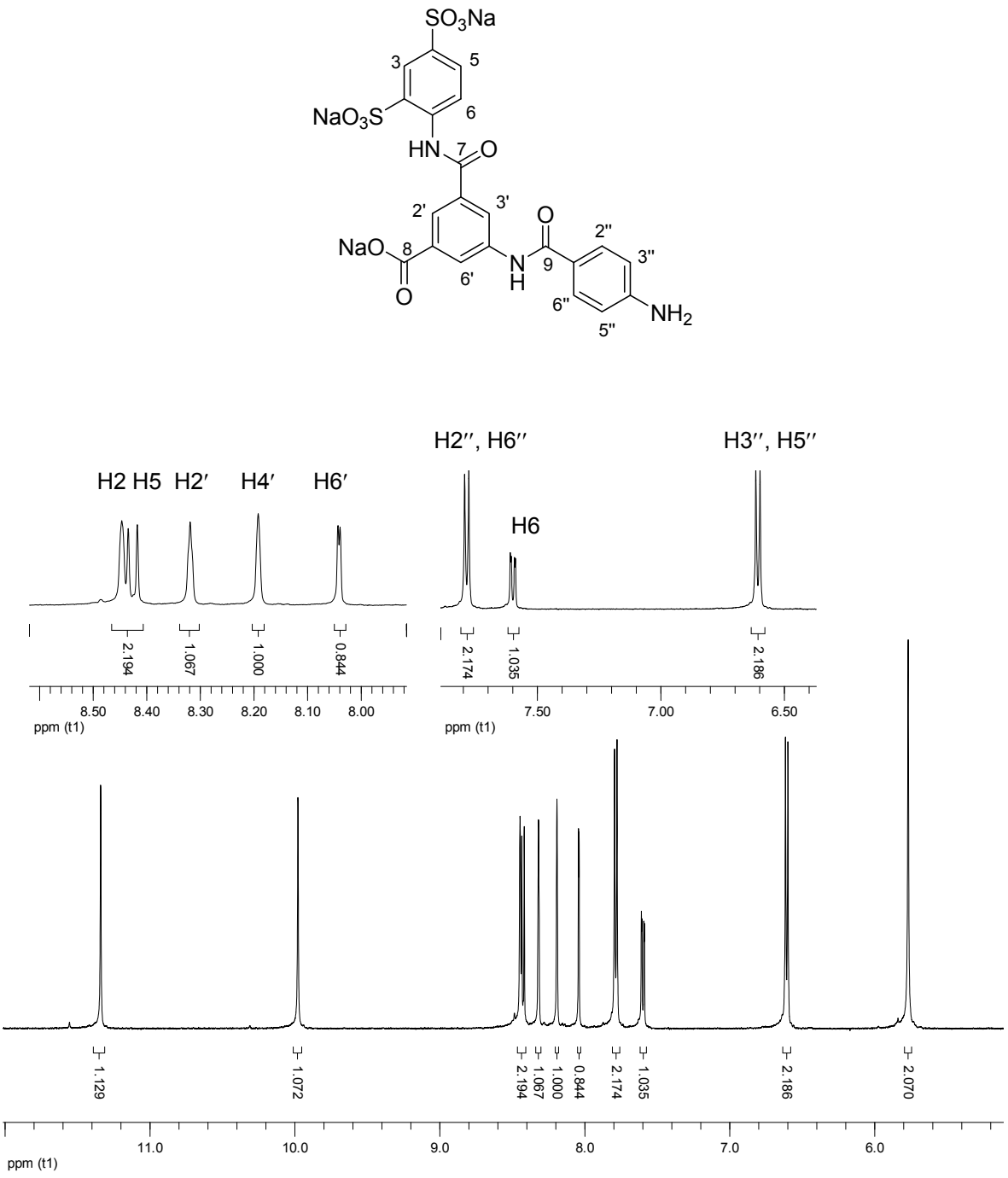

Figure 3.53 500 MHz ^{1}H NMR spectrum of compound 22b in DMSO-d_6.

Figure 3.53 shows the ^{1}H NMR spectrum of compound 22b. A characteristic signal of the amine protons appeared at 5.77 ppm with integration of 2 protons. The +M effect of the -NH_2 group caused the shifting of signals of the aminobenzamido residue to the higher field as seen for the protons H2″, H6″ and H3″, H5″ at

7.79 ppm and 6.62 ppm, respectively. The remaining protons appeared in nearly similar range with protons of compound 22a.

Figure 3.54 shows the ^{13}C spectrum of compound 22b.

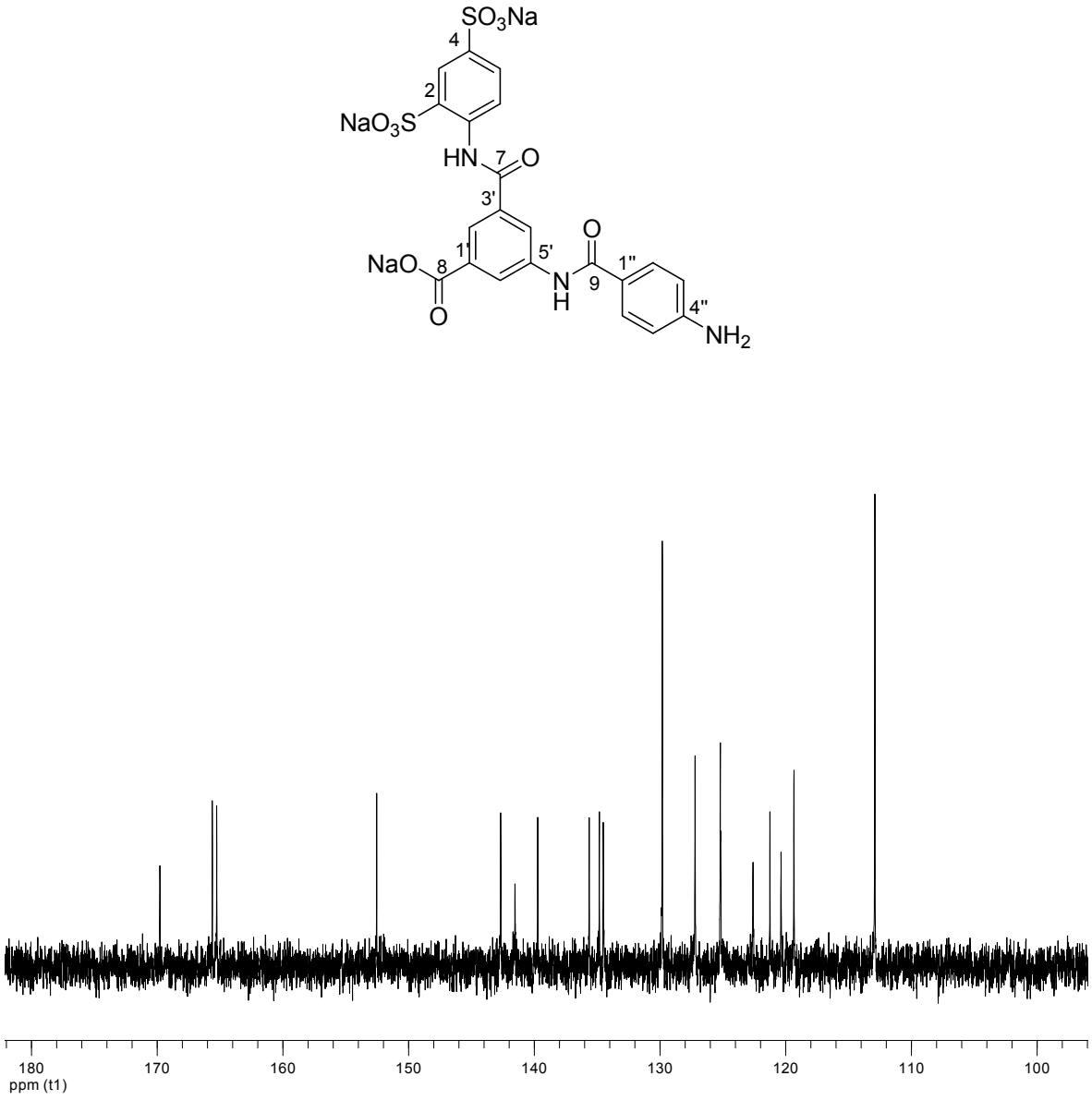

Figure 3.54 125 MHz ^{13}C NMR spectrum of compound 22b in DMSO-d_6.

The carbonyl carbons appeared in the lower field at 165.6 ppm and 165.3 ppm. The carboxylic acid carbon appeared at 169.8 ppm. The AA′BB′ system can also be observed at signals of carbons C2′′, C6′′ (129.8 ppm) and carbons C3′′, C5′′ (112.9 ppm). The interpretation of other signals was performed by comparison of the found signals with the estimated signals from the software ChemDraw Ultra 9.0 which explained in chapter 3.3.3

3.3.3. Hexasodium 5,5′-[carbonylbis(azanedyl-4,1-phenylenecarbonylazanediyl)]bis[3-(2,4-disulfonatophenylcarbamoyl)benzoat]

Phosgenation of compound 22b was performed in aqueous solution using phosgene solution (Figure 3.55). The synthesis was carried out with the similar method of synthesis of compound 5c. Compound 22c was obtained as a pale orange powder with a yield of 75.6 %.

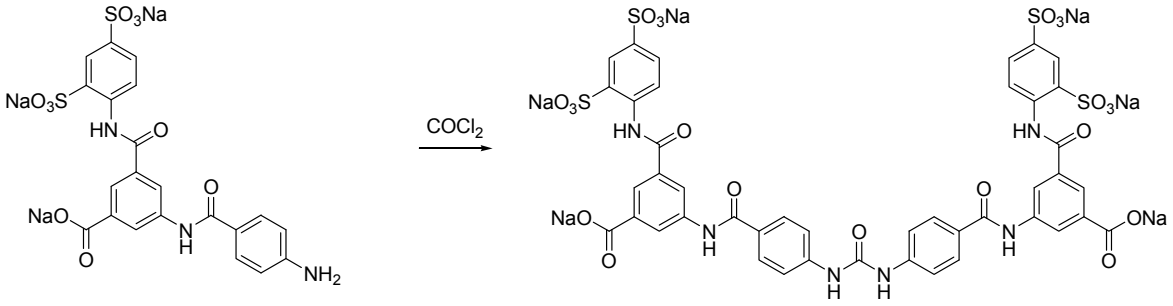

Figure 3.55 Phosgenation of trisodium 3-(2,4-disulfonatophenylcarbamoyl)-5-(4-aminobenzamido) benzoate.

Purity and structure confirmation

The TLC of compound 22c showed one spot. The HPLC chromatogram showed a purity of 99.51 % at a retention time of 5.87 minutes. The UV spectrum showed maximum absorption at a wavelength of 268 nm.

Figure 3.56 shows the ^{1}H NMR of compound 22c. The spectrum revealed 13 signals. Urea proton appeared at 10.45 ppm as singlet signal meanwhile the amide protons showed at 11.37 ppm and 11.30 ppm.

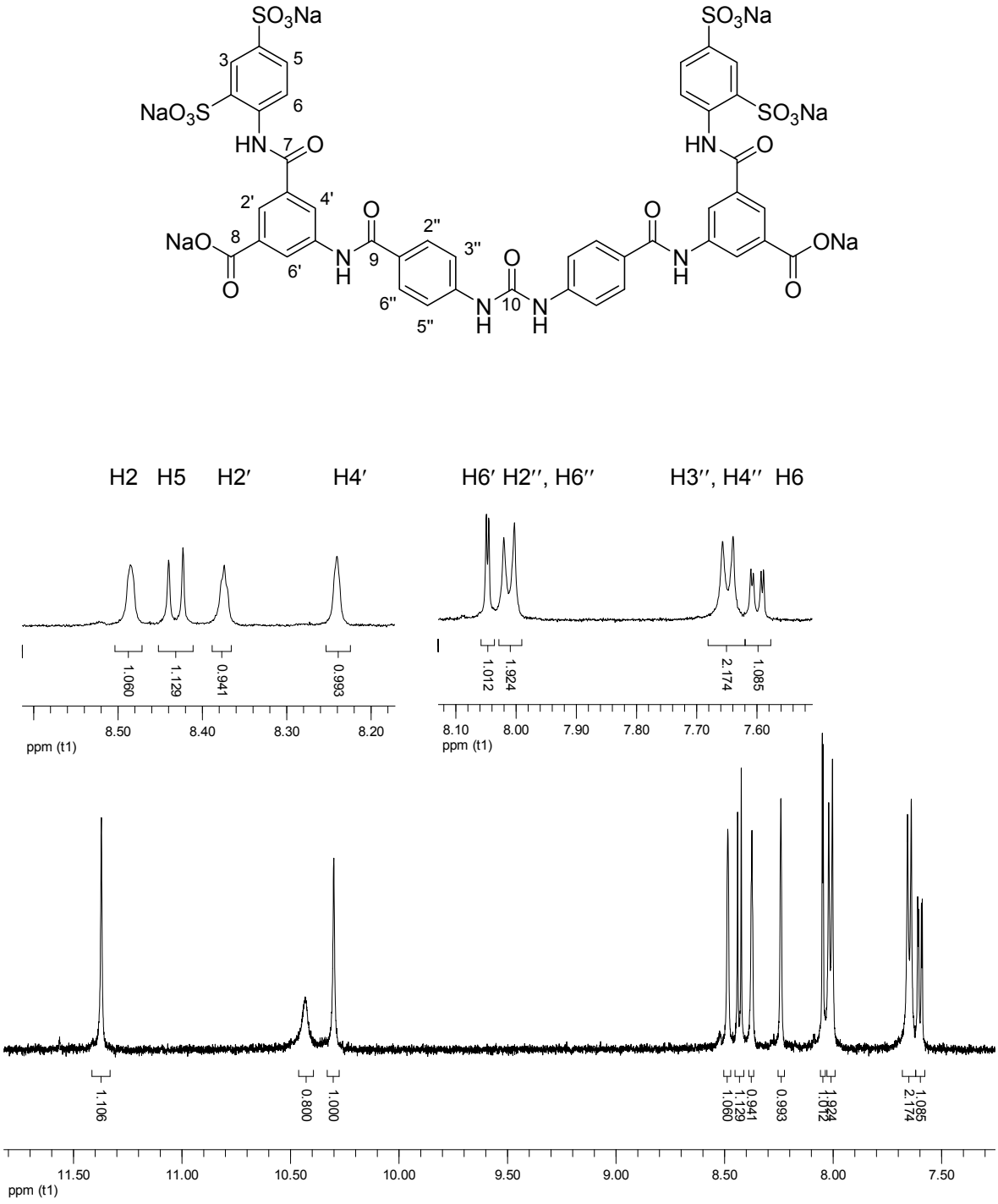

Figure 3.56 500 MHz ^{1}H NMR spectrum of compound 22c in DMSO-d_6.

Table 3.15 Comparison of ^{1}H NMR signals (DMSO-d_6) and coupling patterns of proton between compounds 22a-22c.

Proton	δ (ppm), *J* (Hz)		
	22a	**22b**	**22c**
H2	8.52	8.44	8.48
H5	8.43 (^{3}J = 8.5)	8.42 (^{3}J = 8.5)	8.43
H6	7.60 (^{3}J = 8.5, ^{4}J = 2.0)	7.60 (^{3}J = 8.5, ^{4}J = 2.0)	7.60 (^{3}J = 8.5, ^{4}J = 2.0)
H2′	8.39	8.32	8.37
H4′	8.26	8.19	8.24
H6′	8.04 (^{4}J = 2.0)	8.04 (^{4}J = 2.0)	8.04 (^{4}J = 2.0)
H3′′, H5′′	8.38 (^{3}J = 8.9)	6.62 (^{3}J = 8.5)	8.01 (^{3}J = 8.5)
H2′′, H6′′	8.28 (^{3}J = 8.9)	7.79 (^{3}J = 8.5)	7.70 (^{3}J = 8.5)

Table 3.15 shows the chemical shifts of the protons of compounds 22a, 22b, and 22c. The AA′BB′ system was observed at 8.38 ppm, 6.62 ppm and 8.01 ppm as H3′′ and H5′′ in nitro, amine and urea compound, respectively, whereas signals H2′′ and H6′′ appeared at 8.28, 7.79 and 7.70 ppm. Due to the poor resolution, coupling of H2 was not observed. Coupling between H5 and H6 can be observed by *J* coupling of 8.5 Hz.

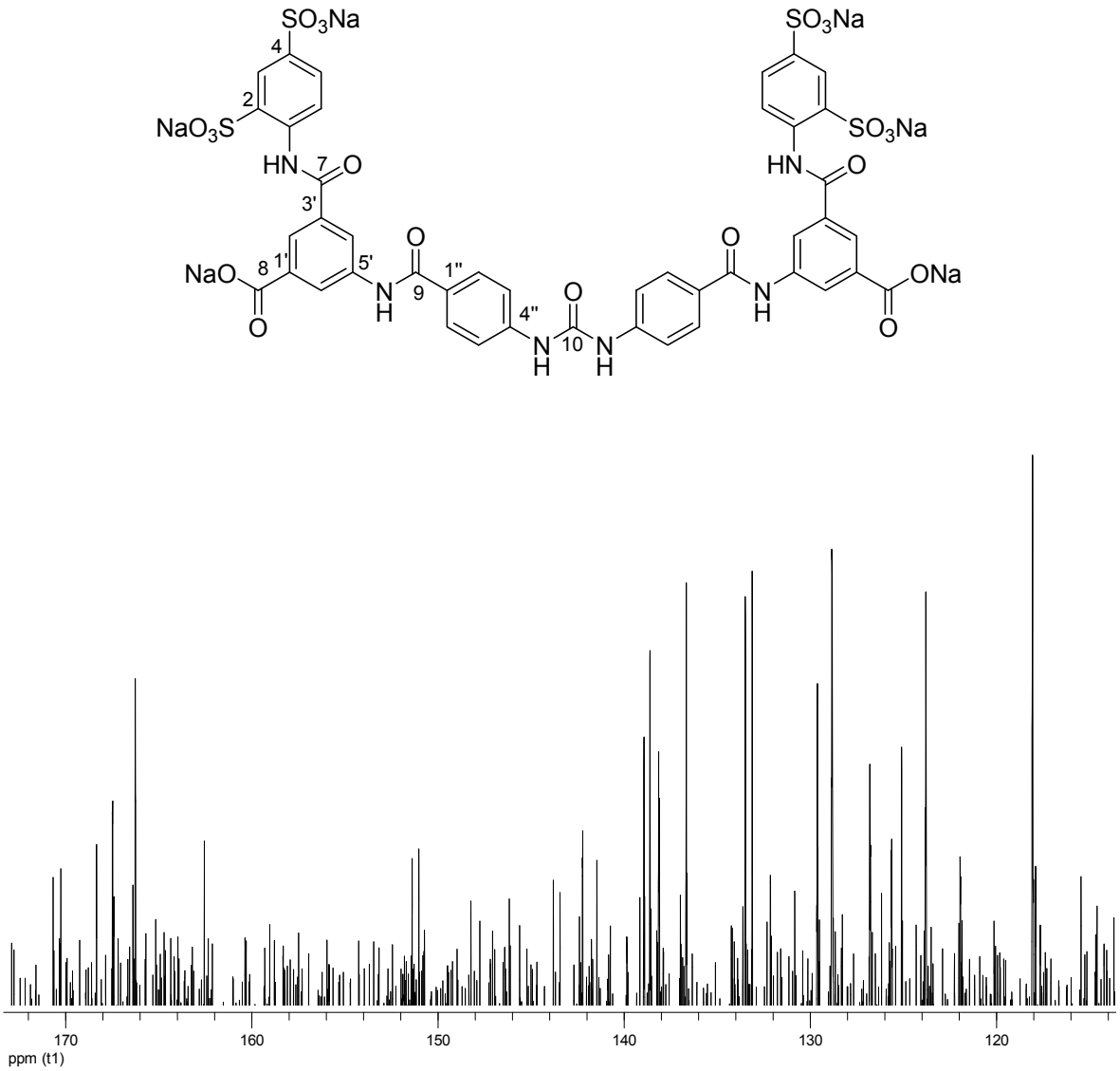

Figure 3.57 125 MHz ^{13}C NMR spectrum of compound 22c in DMSO-d_6

Figure 3.57 shows the ^{13}C NMR spectrum of compound 22c. The specific urea carbonyl carbon at compound 22c appeared at 151.0 ppm. Table 3.16 shows the comparison of the chemical shifts of the carbons from compounds 22a, 22b, and 22c.

Table 3.16 Comparison of the calculated and found ^{13}C NMR chemical shift of carbons of compounds 22a-22c.

Carbon	22a		22b		22c	
	δ (ppm)					
	Found	Calc	Found	Calc	Found	Calc
C1	142.8	146.7	142.7	146.7	142.2	146.7
C2	123.6	123.7	120.4	123.7	123.8	123.7
C3	140.8	140.9	141.5	140.9	141.5	140.9
C4	139.5	139.7	139.7	139.7	138.9	139.7
C5	120.6	124.2	121.5	124.2	125.1	124.2
C6	134.7	132.1	125.2	132.1	133.1	132.1
C1′	138.7	138.1	134.8	138.1	138.1	138.1
C2′	127.2	126.4	125.1	126.4	128.8	126.4
C3′	134.9	136.6	135.6	136.6	133.5	136.6
C4′	119.4	121.7	119.3	121.7	121.9	121.7
C5′	135.2	138.1	134.5	138.1	136.6	138.1
C6′	125.2	126.3	127.2	126.3	126.8	126.3
C1′′	140.1	140.3	122.6	124.2	129.8	129.8
C2′′, C6′′	129.7	128.4	129.8	128.3	129.6	127.7
C3′′, C5′′	123.9	124.0	112.9	116.4	118.1	121.7
C4′′	149.5	151.3	152.5	151.8	138.2	139.2

The carbonyl carbons of the amide groups (C7 and C9) compound 22a appeared at 164.9 ppm and 164.2 ppm; of 22b at 165.6 ppm and 165.3 ppm; and of 22c at 166.3 ppm and 162.5 ppm. The signals of the carboxylic acid carbons of compounds 22a, 22b, and 22c appeared at 169.1 ppm, 169.8 ppm, and 169.1 ppm, respectively. Carbons C2′′, C6′′ and carbons C3′′ and C5′′ performed AA′BB′ system and appeared as one signal with two integrations, respectively. Due to the effect of $-M^+$, the carbons C3′′, C5′′ shifted to the higher field in comparison to the nitro 22a. The measurement of ESI-MS of compound 22c showed a m/z signal of $[M-Na]^-$ at 1205.3 in comparison with calculated $[M-Na]^-$ at m/z 1204.9 from the calculation.

4. Pharmacology

4.1. Evaluation of the test system

The Ca^{2+} signal is an essential part of a variety of biological processes (Carafoli, 2004; Monteith and Bird, 2005). The change of fluorescence intensity before and after injection control (buffer) or compounds can be visualized with calcium sensitive fluorescence indicators such as Oregon Green® BAPTA-1AM. To study the response of a G_q coupled receptor to the respective standard agonist, the cells were incubated with Oregon Green® BAPTA-1AM and the ligand-induced dynamic changes in the intracellular calcium concentration ($[Ca^{2+}]$) were monitored as mentioned in the chapter Materials and Methods. The EC_{50} values of the standard agonists in this study were compared with the EC_{50} values reported in the literature (Table 4.1).

Table 4.1 Comparison of the EC_{50} values estimated in this study and reported EC_{50} values from literature.

Receptors subtype	Standard agonist	EC_{50} (nM)	
		this study	literature
$P2Y_1$	2-MeSADP	3.0	6.0 (Chhatriwala, 2004)
			3.5 (Meis, 2008)
$P2Y_2$	UTP	94.2	140 (Jacobson *et al.*,2000)
$P2Y_4$	UTP	12.8	20.0 (Meis, 2008)
$P2Y_{11}$	ATP	249	214 (Meis, 2008)

The results demonstrated that the agonistic activity of all standard agonists in the chosen test system were in the range of the literature data. It showed that the evaluation system was suitable. Therefore, ATP, 2-MeSADP and UTP were used as standard agonist for the respective receptor subtypes.

ATP was used as standard agonist and NF157 was used as standard antagonist at $P2Y_{11}$ receptors. The effect of NF157 was tested by measuring its ability to inhibit the calcium response elicited by the injection of 1 µM ATP to $P2Y_{11}$

receptors recombinantly expressed in 1321N1 astrocytoma cells. The concentration-response curve of the standard agonist ATP and the concentration-inhibition curve of the standard antagonist NF157 are shown in Figure 4.1.

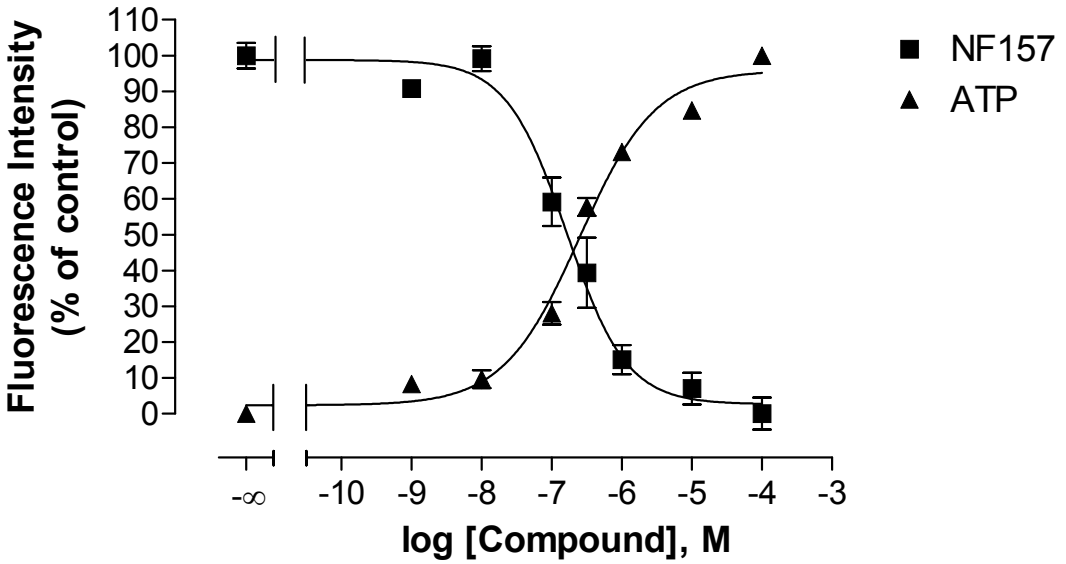

Figure 4.1 Functional characterization of $P2Y_{11}$ receptors measuring intracellular calcium concentration. The concentration-response curve of ATP and concentration inhibition curve of NF157 were determined. Buffer (= 0 %) and 1 µM ATP (= 100 %) were used as controls for the concentration-inhibition curve of NF157. Data shown are mean ± SEM of the pooled data (n = 4, each experiment was performed with three replicates). Slopes were not significant different from unity. NF157: IC_{50} 163 nM / app. pKi: 7.34 ± 0.08; ATP: EC_{50}: 249 nM / pEC_{50}: 6.61 ± 0.05.

ATP at $P2Y_{11}$ receptors gained pEC_{50} of 6.61 ± 0.05 and EC_{50} of 249 nM. The result was in approximate agreement with the EC_{50} found by Meis (214 nM) (Meis, 2008). 1 µM ATP was used as the standard agonist concentration for $P2Y_{11}$ receptors. The app. pK_i value of NF157 was calculated as 7.34 ± 0.08 which was equal to the app. pK_i value of 7.35 reported in the literature (Ullmann *et al.*, 2005).

4.2. Agonist screening of compounds at $P2Y_{11}$ receptors

4.2.1. Primary agonist screening of compounds at $P2Y_{11}$ receptors

At $P2Y_{11}$ receptors, ATP and nucleotide derivatives such as ATPγS are known and used as agonists. Nucleotide and nucleotide derivatives agonists at $P2Y_{11}$ receptors have been summarized in the literature (Abbrachio *et al.*, 2006). Meis reported the finding of non-nucleotide agonists. NF546 and NF709 showed agonistic activity at $P2Y_{11}$ receptors (Meis, 2008). In this study, 75 compounds consisting of ureas and their precursors were screened at $P2Y_{11}$ receptors using the functional calcium assay. Table 4.2 lists the results for all tested compounds as % of response of 1 µM ATP. The results for urea compounds are shown in Figure 4.2.

Table 4.2 Agonist activities of the synthesized nitro (xa)-, amino (xb)-, and urea (xc) derivatives at concentrations of 10 µM and 100 µM are shown as percent response of 1 µM ATP at $P2Y_{11}$ receptors. Data shown are mean ± SEM of the pooled data ($n \geq 2$, each experiment was performed with three replicates).

Comp.	10 µM	100 µM	Comp.	10 µM	100 µM
1c	12.3 ± 1.8	28.1 ± 5.5	14a	9.7 ± 9.0	17.6 ± 2.4
2a	0.0 ± 16.3	8.4 ± 1.3	14b	17.6 ± 3.7	15.7 ± 5.0
2b	7.6 ± 9.7	12.4 ± 4.3	14c	1.4 ± 2.4	37.3 ± 4.4
2c	5.1 ± 1.1	5.3 ± 10.9	15a	1.0 ± 4.0	0 ± 5.2
3a	0 ± 5.6	0 ± 3.5	15b	0 ± 3.2	0 ± 4.8
3b	0 ± 9.8	14.7 ± 2.2	15c	1.6 ± 1.6	7.2 ± 1.9
3c	4.9 ± 2.5	9.9 ± 9.8	16a	0 ± 5.9	0 ± 6.6
4a	0 ±12.9	17.5 ± 2.4	16b	0.7 ± 9.2	0 ± 3.1
4b	12.8 ± 4.9	23.6 ± 3.8	16c	0 ± 6.7	9.3 ± 7.9
4c	7.6 ± 6.5	11.2 ± 6.1	17a	10.5 ± 3.4	2.2 ± 8.7
5a	0 ± 4.4	6.0 ± 3.4	17b	0 ± 2.9	0 ± 1.6
5b	0 ± 8.8	13.0 ± 2.7	17c	0 ± 1.9	0 ± 7.9
5c	3.3 ± 1.7	7.4 ± 14.4	18a	5.0 ± 11.0	4.3 ± 6.7
6a	0 ± 7.8	0 ± 3.7	18b	2.3 ± 4.8	0 ± 9.8
6b	14.9 ± 7.3	6.3 ± 6.3	18c	6.4 ± 2.3	17.5 ± 2.0
6c	4.4 ± 6.9	3.2 ± 2.6	19a	9.9 ± 2.9	0 ± 10.0
7a	5.7 ± 16.2	0 ± 2.5	19b	8.1 ± 12.7	0 ± 0.5
7b	1.4 ± 4.8	0.5 ± 3.3	19c	6.8 ± 2.0	3.4 ± 8.8
7c	0 ± 1.9	0 ± 4.4	20a	0 ± 2.1	0 ± 8.2
8a	0 ± 11.3	6.9 ± 11.9	20b	1.2 ± 2.8	8.7 ± 8.5
8b	0 ± 5.3	6.1 ± 2.7	20c	0.0 ± 4.1	2.6 ± 1.6
8c	24.9 ± 9.6	39.1 ± 15.4	21a	3.4 ± 6.5	0 ± 2.1
9a	10.0 ± 2.7	14.0 ± 4.1	21b	13.9 ± 15.6	0 ± 5.8
9b	6.9 ± 2.4	24.2 ± 5.7	21c	2.6 ± 10.2	2.6 ± 7.7
9c	67.2 ± 11.2	80.8 ± 15.9	22a	10.0 ± 1.9	0 ± 4.8
10a	11.8 ± 8.4	4.7 ± 13.8	22b	0 ± 2.1	0 ± 10.3
10b	2.2 ± 10.8	31.8 ± 4.2	22c	0 ± 3.3	0 ± 2.9
10c	0 ± 9.6	11.1 ± 1.2	23a	5.2 ± 2.2	0 ± 2.5
11a	0 ± 6.0	3.9 ± 7.5	23b	0 ± 2.5	40.4 ± 2.5
11b	7.7 ± 2.9	2.4 ± 4.7	23c	0 ± 1.1	32.6 ± 2.3
11c	0 ± 5.9	0 ± 1.6	24a	0 ± 8.8	0 ± 3.8
12a	1.8 ± 7.4	7.8 ± 5.9	24b	2.1 ± 2.2	16.8 ± 1.9
12b	17.0 ± 4.2	16.8 ± 4.5	24c	0 ± 3.2	4.3 ± 8.9
12c	10.6 ± 7.8	0.5 ± 14.2	25a	0 ± 3.6	0 ± 13.1
13a	18.0 ± 8.4	8.2 ± 5.4	25b	4.4 ± 5.4	0 ± 18.7
13b	6.1 ± 4.8	3.4 ± 6.6	25c	0 ± 5.8	0 ± 9.7
13c	8.5 ± 2.3	0 ± 8.7			

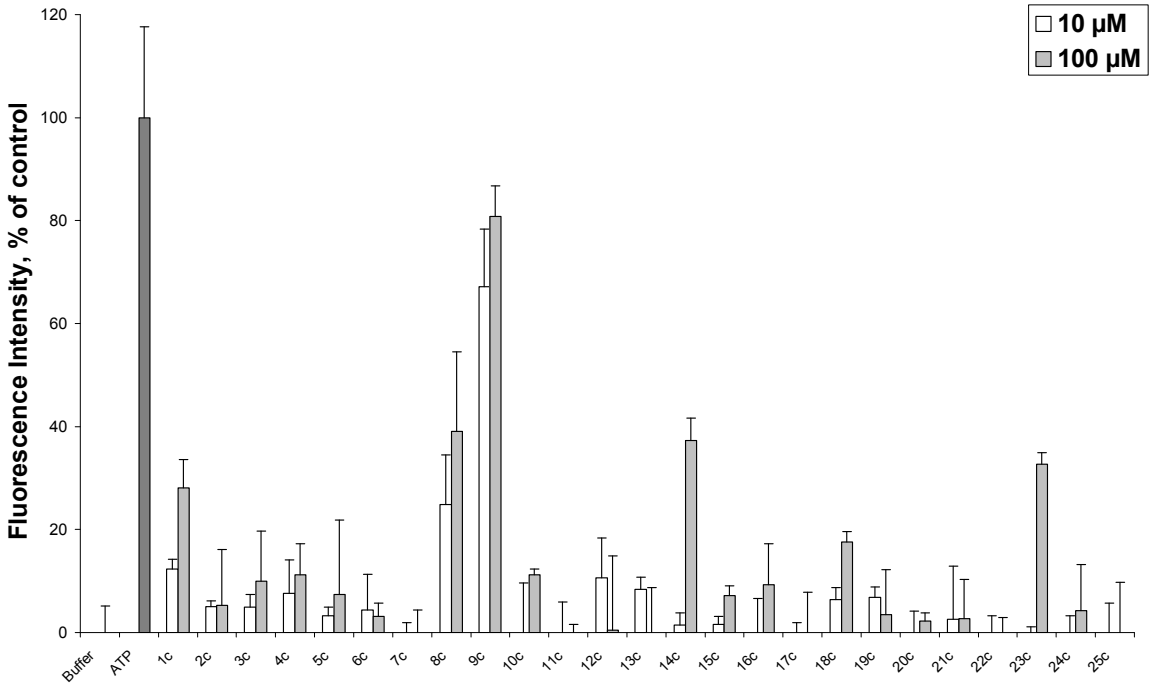

Figure 4.2 Agonist screening of urea compounds at $P2Y_{11}$ receptors are shown as response at concentrations of 10 µM and 100 µM as % of 1 µM ATP control (100 %). Buffer was set as 0 %. Data shown are mean ± SEM of the pooled data ($n \geq 2$).

At concentrations of 10 µM and 100 µM, most of the compounds showed agonistic activity of less than 20 % of the ATP response except compounds 1c, 4b, 8c, 9b, 9c, 10b, 14c, 23b and 23c which showed an activity of more than 20 % at 100 µM. Moreover, compound 8c and 9c showed agonistic activity more than 20 % at both concentrations. The urea compounds 1c, 8c, and 9c showed agonistic activity at 10 µM and 100 µM concentrations whereas 14c and 23c at 100 µM. Urea 18c was added as the test compound because of their agonistic activity at 100 µM (17.52 %). Based on the results, further tests were carried out only for urea 1c, 8c, 9c, 14c, 18c, and 23c as target compounds to determine their efficacy.

4.2.2. Efficacy and potency testing

Different concentrations of compounds 1c, 8c, 9c, 14c, 18c, and 23c were further tested to analyze their potency and efficacy at $P2Y_{11}$ receptors. The assay was carried out using the agonist mode. The results were compared to the effect of injection of 1 µM ATP (Figure 4.3).

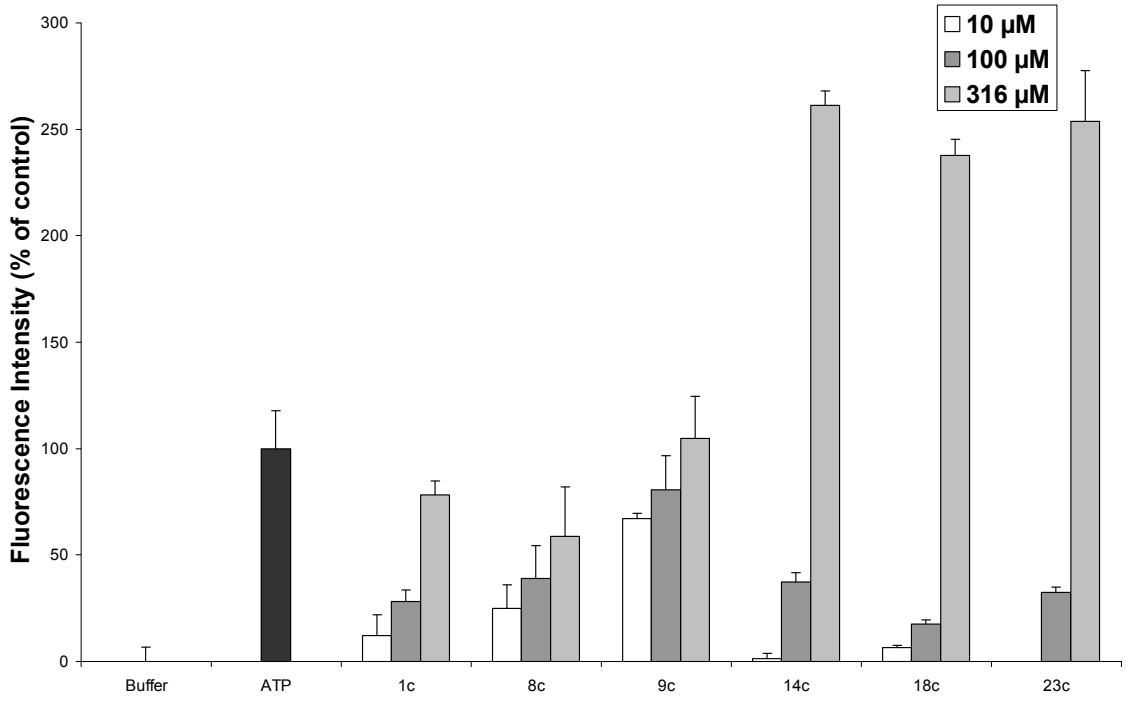

Figure 4.3 Agonistic activities of compounds 1c, 8c, 9c,14c,18c, and 23c are shown as % of 1 µM ATP control (100 %). Buffer response was set as 0 %. Data shown are mean ± SEM of the pooled data (n = 2, each experiment was performed in three replicates).

Compounds 14c, 18c, and 23c showed fluorescence signals at a concentration of 316 µM, exceeding 200 % of the signal caused by 1 µM ATP. It might be presumed as a toxic effect of the compounds. Compound 1c showed an exceptional signal at 316 µM compared to its signal at 10 µM and 100 µM. The full nature of 1c needs to be further determined. Therefore, further test was carried out only to compounds 8c and 9c. To identify $P2Y_{11}$ receptors as mediator of the stimulatory effect of compounds 8c and 9c, further test was performed. $P2Y_{11}$ receptors expressed in 1321N1 cells were preincubated with 10 µM NF157 for

30 minutes prior to the injection of compounds 8c and 9c at concentrations of 10 µM and 100 µM to the cell suspension (Figure 4.4).

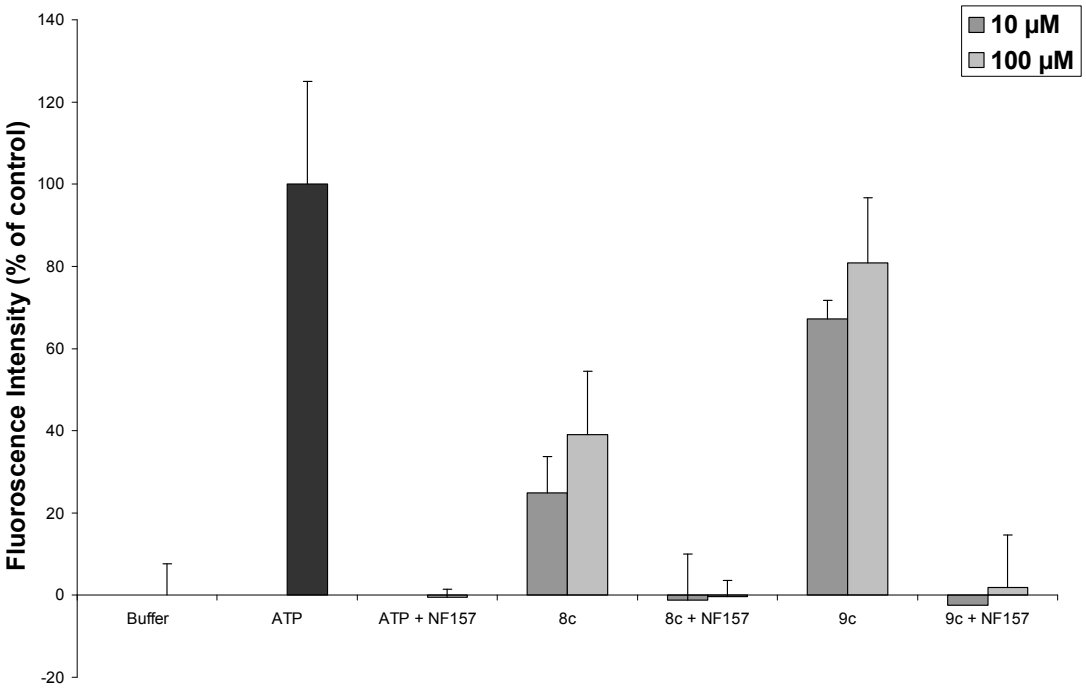

Figure 4.4 Effect on calcium mobilization after injection of compounds 8c [10 or 100 µM], 9c [10 or 100 µM] and 1 µM ATP to $P2Y_{11}$ receptors. The result is expressed as % of control (ATP 1 µM) and buffer response was set as 0 %. The effect was tested with or without preincubation of 10 µM NF157. Data shown are mean ± SEM of the pooled data (n = 2, each experiment was performed in three replicates).

The signal of compounds 8c and 9c could be completely blocked by NF157. This result confirmed that the compound effects were mediated through $P2Y_{11}$ receptors.

4.2.3. Concentration-response curves of compounds 8c and 9c

Concentration-response curves of 8c and 9c in comparison to ATP were determined at $P2Y_{11}$ receptors (Figure 4.5).

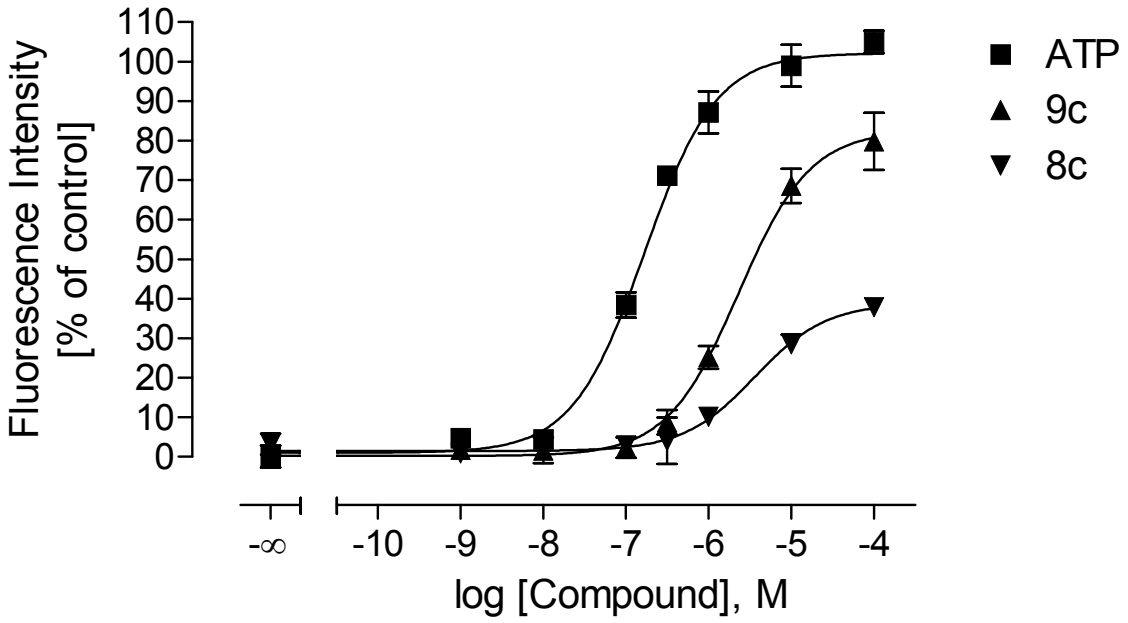

Figure 4.5 Concentration response curves of compounds 8c and 9c at $P2Y_{11}$ receptors. Data shown are mean ± SEM of the pooled data. (n = 3, each experiment with three replicates). EC_{50} of ATP = 170 µM, pEC_{50} = 6.77 ± 0.08; EC_{50} of 8c = 3.73 µM, pEC_{50} = 5.43 ± 0.18; EC_{50} of 9c = 2.10 µM, pEC_{50} = 5.68 ± 0.10.

As mentioned, NF546 and NF709 were reported as agonists at $P2Y_{11}$ receptors (Meis, 2008). The EC_{50} values of 8c and 9c in comparison to NF546, NF709, and ATP are summarized in Table 4.3.

Table 4.3 EC_{50} and pEC_{50} values of ATP and compounds 8c-9c. Data shown of ATP, compound 8c, and compound 9c are mean ± SEM of the pooled data. (n = 3, each experiment with three replicates).

	EC_{50} (nM)	**pEC_{50}**	**Intrinsic activity in comparison to ATP (%)**	**Slopes**
ATP	170	6.77 ± 0.08	100 ± 4.29	0.93 ± 0.15
8c	3730	5.43 ± 0.18	38.9 ± 2.86	0.95 ± 0.26
9c	2100	5.68 ± 0.10	83.7 ± 4.90	1.13 ± 0.21
NF546 *)	542	6.27 ± 0.07	99.6 ± 3.04	0.93 ± 0.09
NF709 *)	84.8	7.07 ± 0.06	52.7 ± 2.20	1.20 ± 0.31

*) Meis, 2008, in comparison to ATPγS

Compound 8c showed 7-fold and 44-fold lower agonistic activity, compared to NF546 and NF709, respectively. Compound 9c is 4 fold and 25 fold less potent than NF546 and NF709, respectively. The EC_{50} of 8c (3.73 µM) and 9c (2.10 µM) are higher than the EC_{50} value of ATP. Nevertheless, the EC_{50} values were in the low micromolar range. The intrinsic activities of compounds 8c and 9c are lower compared to ATP (100 %). These results implied that compounds 8c and 9c have possibly partial agonistic activity.

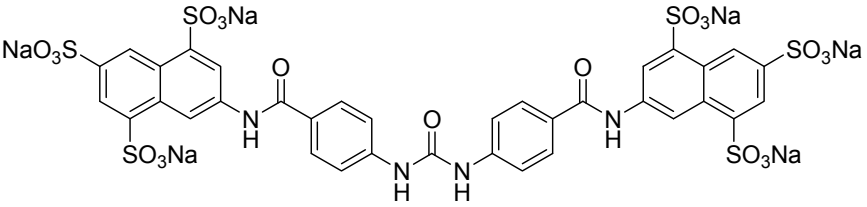

Compound 8c

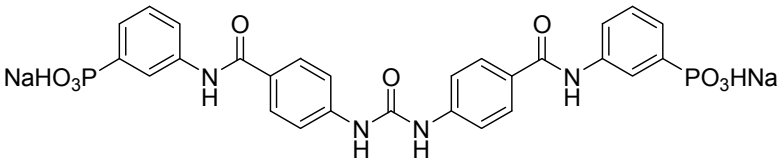

NF709

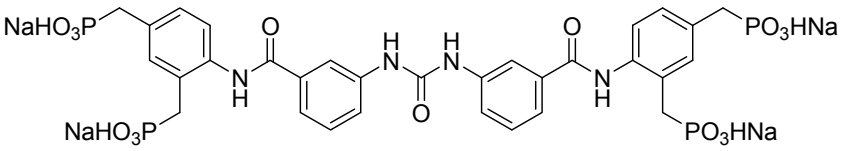

NF546

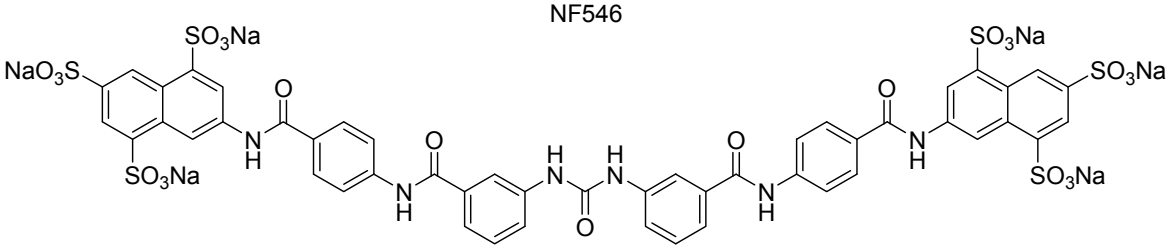

Compound 9c

Figure 4.6 Structure formulas of compounds 8c, 9c, NF709, and NF546

Figure 4.6 shows the structures of compounds 8c, 9c, NF709 and NF546. The structure comparison of compound 8c with NF709 shows that both compounds have a para-phenylene-linker.

4.2.4. Schild analysis of compound 9c

Compound 9c showed more potent agonistic activity than compound 8c. Therefore, further test was carried out for compound 9c. To investigate if 9c uses the same binding site as ATP, concentration-response curves of compound 9c in the absence and the presence of increasing concentrations of NF157, a competitive antagonist at $P2Y_{11}$ receptors, were monitored. The decrease of intrinsic activity of compound 9c can be clearly detected with the increase in the concentration of NF157. The upper plateau showed significant decrease compared to upper plateau of control. This phenomenon was similar to NF709 schild plot analyses which was reported by Meis (Meis, 2008). Furthermore, the results showed significantly rightward-shift when comparing the EC_{50} of compound 9c with the presence of 316 nM NF157 (Figure 4.7). Then, an analysis according to Schild was performed (Arunlakshana and Schild, 1957).

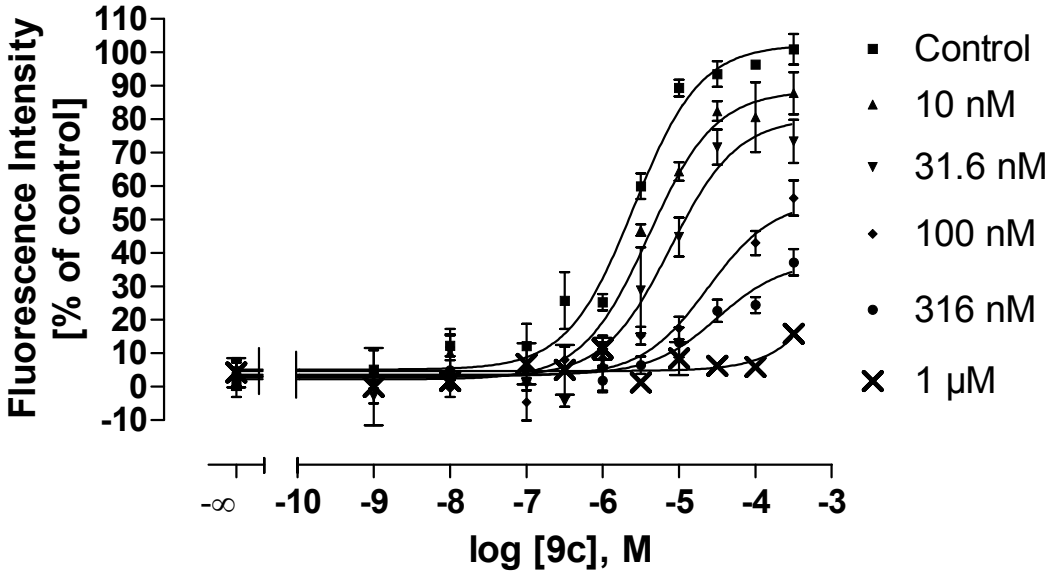

Figure 4.7 Concentration-response curves of 9c at $P2Y_{11}$ receptors using the calcium assay. 9c was tested in the absence and presence of increasing concentrations of NF157 ($n \geq 2$, each experiment was performed with 3 replicates).

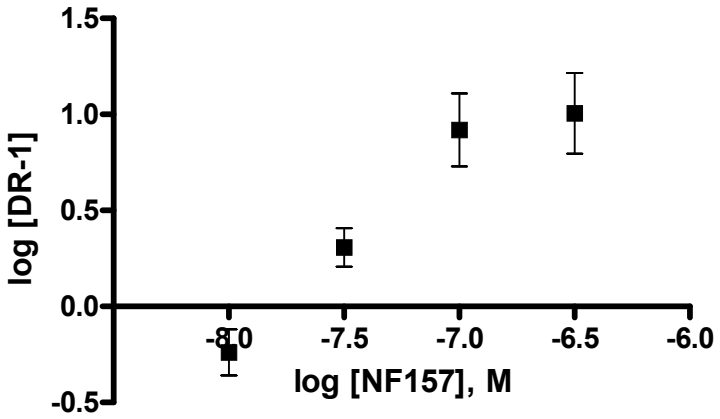

Figure 4.8 Schild plot of compound 9c (n ≥ 2, each experiment was performed with 3 replicates).

Figure 4.8 shows the Schild plot of compound 9c. The Schild plot analysis showed a non linier fit. The results implied that a competitive mechanism of NF157 and 9c was unlikely. The maximum activity was then put in relation to the concentrations of the antagonist. Concentrations 10 nM, 31.6 nM, 100 nM, and 316 nM were used. EC_{50} and maximum activity at concentration of 1 µM could not be estimated because NF157 at this concentration blocked the signals of 9c almost completely. Table 4.4 shows the effect of NF157 at concentration response curves of 9c at $P2Y_{11}$ receptors.

Table 4.4 Effect of NF157 at concentration response curves of compound 9c at $P2Y_{11}$ receptors. (n ≥ 2, each experiment was performed with 3 replicates).

Comp. 9c	**+ buffer (control)**	**+ NF157 10 nM**	**+ NF157 31.6 nM**	**+ NF157 100 nM**	**+ NF157 316 nM**	**+ NF157 1 µM**
pEC_{50}	5.54 ± 0.07	5.39 ± 0.12	5.11 ± 0.16	4.62 ± 0.19	4.50 ± 0.21	-
E_{max}	100 ± 2.49	92.5 ± 4.90	67.6 ± 5.22	47.6 ± 4.66	37.5 ± 4.33	-
n	4	2	2	2	4	4

Figure 4.9 shows the influence of increase concentration of NF157 to maximum of intrinsic activity (E_{max}) of 9c.

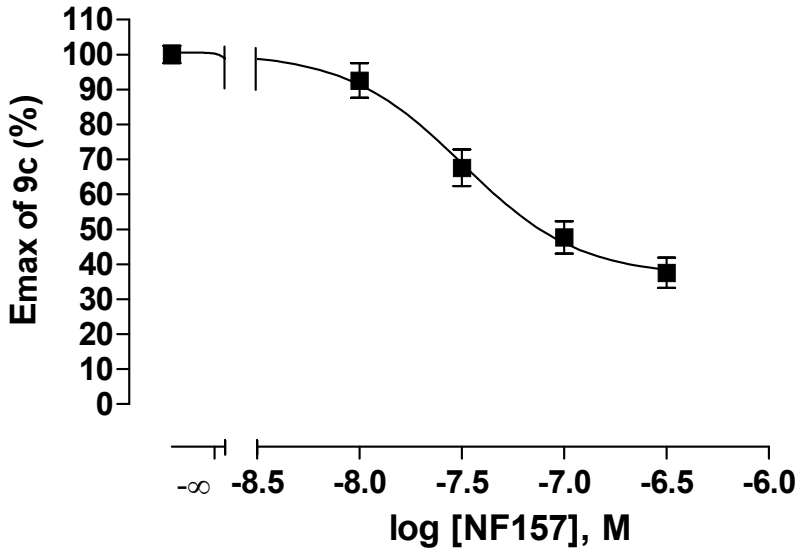

Figure 4.9 The influence of increase concentration of NF157 to maximum of intrinsic activity (E_{max}) of compound 9c at $P2Y_{11}$ receptors using the calcium assay. ($n \geq 2$, each experiment was performed with 3 replicates).

The pIC_{50} value was 7.49 ± 0.06 which in pK_i range of NF157. Based on the result of Schild plot analysis, it can be concluded that compound 9c showed a partial agonistic activity.

4.3. Antagonist screening at $P2Y_{11}$ receptors

A screening for antagonistic activity at $P2Y_{11}$ receptors was carried out with all precursors (xa, xb) and urea compounds (xc) at concentrations of 10 µM and 100 µM. The urea compounds were further examined to determine their app. pK_i values. Antagonist screening of compounds showed significant antagonistic activities at $P2Y_{11}$ receptors. The results are shown in Table 4.5 and Figure 4.10.

Table 4.5 Percent inhibition of the ATP-induced calcium signal by compounds in concentrations of 10 µM and 100 µM at $P2Y_{11}$ receptors. 1 µM ATP was used as standard agonist. Data shown are mean ± SEM of the pooled data ($n \geq 2$, each experiment was performed with three replicates).

Comp.	10 µM	100 µM	Comp.	10 µM	100 µM
1c	0 ± 14.4	20.2 ± 6.6	14b	22.0 ± 7.2	67.2 ± 2.6
2a	0 ± 10.5	58.0 ± 4.1	14c	80.3 ± 17.5	95.2 ± 7.3
2b	0 ± 9.5	79.4 ± 5.2	15a	3.7 ± 14.7	0 ± 3.4
2c	92.1 ± 4.7	99.3 ± 2.5	15b	0 ± 10.3	0.5 ± 9.9
3a	0 ± 12.0	70.8 ± 0.5	15c	30.2 ± 17.5	66.4 ± 7.5
3b	0 ± 12.9	81.5 ± 12.2	16a	0 ± 13.4	42.9 ± 17.4
3c	98.9 ± 3.8	94.6 ± 4.1	16b	0 ± 11.6	52.5 ± 10.6
4a	0 ± 13.1	38.2 ± 4.9	16c	34.5 ± 9.6	66.4 ± 4.0
4b	0 ± 8.2	90.2 ± 2.6	17a	18.0 ± 3.3	57.1 ± 4.9
4c	97.9 ± 2.2	95.8 ± 6.2	17b	32.6 ± 4.9	80.5 ± 4.4
5a	0 ± 5.1	42.7 ± 10.8	17c	34.5 ± 4.2	81.6 ± 6.9
5b	7.2 ± 7.9	74.4 ± 0.5	18a	12.8 ± 18.5	19.4 ± 0.2
5c	100 ± 4.9	108 ± 6.4	18b	5.2 ± 5.4	28.2 ± 9.2
6a	0 ± 10.6	74.4 ± 9.4	18c	18.5 ± 11.4	105 ± 3.6
6b	0 ± 4.9	59.0 ± 10.0	19a	12.2 ± 5.7	37.3 ± 3.4
6c	98.7 ± 2.1	96.9 ± 2.7	19b	15.5 ± 0.3	45.0 ± 12.5
7a	13.8 ± 4.5	75.8 ± 1.0	19c	51.3 ± 8.3	100 ± 3.8
7b	50.9 ± 15.1	71.9 ± 13.4	20a	18.5 ± 12.5	27.9 ± 5.1
7c	80.7 ± 7.6	103 ± 2.6	20b	18.1 ± 9.7	51.9 ± 13.7
8a	14.5 ± 9.2	13.5 ± 11.2	20c	64.1 ± 10.6	106 ± 3.6
8b	2.8 ± 1.6	61.9 ± 13.0	21a	5.9 ± 0.6	24.4 ± 15.5
9a	0 ± 6.6	8.4 ± 6.7	21b	0 ± 6.4	29.8 ± 11.5
9b	0 ± 6.8	17.6 ± 1.0	21c	19.2 ± 4.3	46.4 ± 3.2
10a	0 ± 19.9	5.0 ± 3.0	22a	2.5 ± 1.4	52.9 ± 9.4
10b	0 ± 12.7	4.0 ± 4.4	22b	16.1 ± 6.5	42.9 ± 13.1
10c	4.9 ± 28.1	108 ± 6.0	22c	22.9 ± 4.2	37.8 ± 1.6
11a	0 ± 15.0	47.5 ± 13.4	23a	3.3 ± 1.6	37.8 ± 9.8
11b	33.7 ± 13.9	67.9 ± 8.7	23b	16.3 ± 13.6	51.6 ± 14.8
11c	31.7 ± 5.6	88.2 ± 12.9	23c	13.7 ± 10.3	71.2 ± 3.8
12a	0 ± 13.4	61.1 ± 11.0	24a	30.1 ± 2.2	42.8 ± 5.6
12b	0 ± 5.7	42.7 ± 5.0	24b	6.5 ± 6.6	32.6 ± 8.6
12c	12.3 ± 11.0	117 ± 11.8	24c	49.3 ± 6.0	118 ± 2.2
13a	4.7 ± 2.7	52.1 ± 4.8	25a	4.8 ± 6.1	44.8 ± 6.4
13b	0 ± 9.4	71.40 ± 7.1	25b	7.6 ± 4.6	51.7 ± 2.4
13c	94.4 ± 2.2	119 ± 4.5	25c	43.6 ± 9.7	84.3 ± 17.2
14a	0.0 ± 7.8	37.9 ± 4.0			

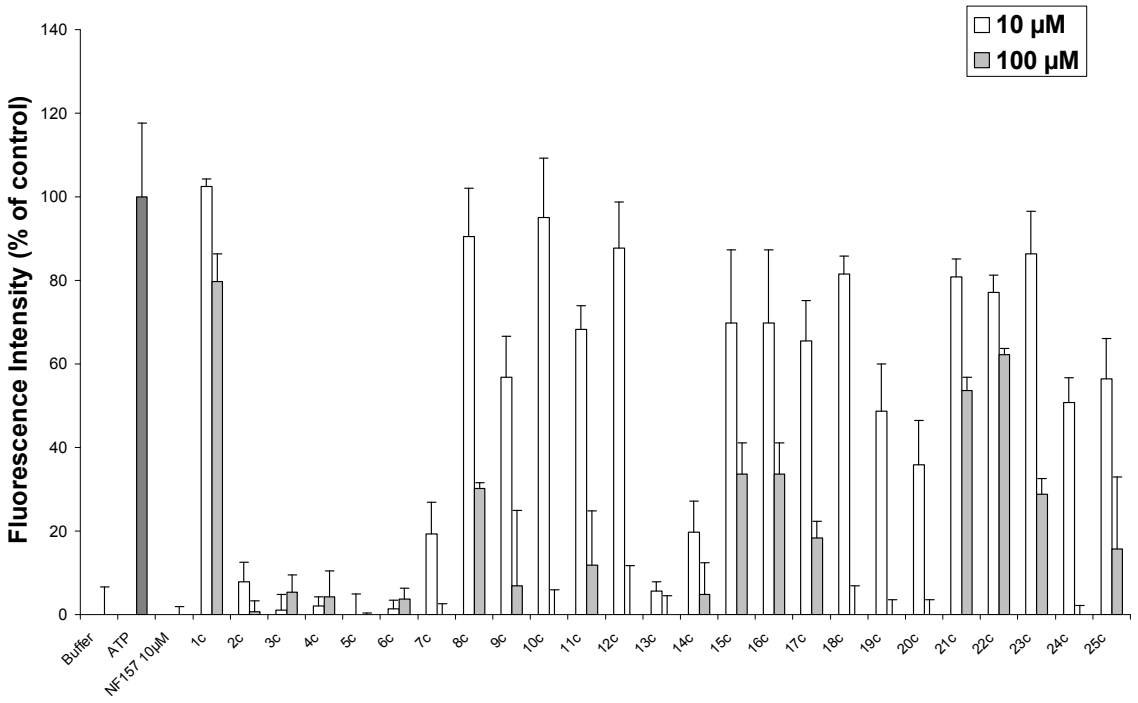

Figure 4.10 Antagonist screening of urea compounds (1c-25c) at $P2Y_{11}$ receptors shown as response of 1 µM ATP induced calcium mobilization at concentrations of 10 µM and 100 µM. Data shown are mean ± SEM of the pooled data ($n \geq 2$).

The primary screening of precursors and urea compounds showed interesting results (Table 4.5 and Figure 4.10). Concentration-inhibition curves of 25 urea compounds were estimated. The experiment was repeated three times with three replicates each experiment. The IC_{50} value each compound was estimated from concentration-inhibition curve. In each experiment, a concentration-response curve of ATP was monitored to obtain the EC_{50} value the agonist. Results of the estimated IC_{50} and EC_{50} were used for calculating the K_i value of the antagonistic compound. Data shown are mean ± SEM of the pooled data. Concentration inhibition curves of 25 urea compounds were estimated. Table 4.6 shows the summary of app. pK_i values and K_i values of all urea compounds.

Table 4.6 App. pK_i values of urea compounds (1c-25c) at $P2Y_{11}$ receptors. The pK_i values shown are mean ± SEM of the pooled data (n = 3, each experiment was performed with three replicates).

Compound	App. pK_i	App. K_i (μM)
1c	< 4	> 100
2c	7.34 ± 0.05	0.046
3c	7.16 ± 0.16	0.069
4c	6.92 ± 0.07	0.120
5c	7.55 ± 0.07	0.028
6c	7.35 ± 0.10	0.045
7c	5.88 ± 0.08	1.32
8c	pEC_{50} 5.43 ± 0.18	EC_{50} 3.73
9c	pEC_{50} 5.68 ± 0.10	EC_{50} 2.10
10c	4.46 ± 0.15	34.7
11c	< 4	> 100
12c	4.75 ± 0.09	17.8
13c	5.77 ± 0.07	1.70
14c	5.26 ± 0.07	5.49
15c	4.89 ± 0.08	12.9
16c	< 4	> 100
17c	5.67 ± 0.09	2.14
18c	4.54 ± 0.10	28.8
19c	5.27 ± 0.32	5.37
20c	5.02 ± 0.04	9.54
21c	< 4	> 100
22c	4.20 ± 0.16	63.1
23c	4.40 ± 0.16	39.8
24c	5.29 ± 0.20	5.13
25c	4.48 ± 0.13	33.1

Compounds 8c and 9c were found as novel agonists at $P2Y_{11}$ receptors whereas compounds 1c needs to be further investigated their full nature (see Chapter 4.2.2). Detail of app. pK_i of each compound is discussed in Chapter 4.4. App. pK_i of the nitro- and amino- precursors of compounds 2c, 3c, 4c, 5c and 6c were further estimated. Table 4.7 shows the structure of nitro precursors (2a, 3a, 4a, 5a, and 6a), amino precursors (2b, 3b, 4b, 5b, and 6b), and urea compounds (2c, 3c, 4c, 5c, and 6c).

Table 4.7 Structure formulas and app. pK_i values (mean ± SEM) and K_i values (μM) of nitro (xa)-, amino (xb)- precursor and urea (xc) compound (n = 2, each experiment was performed in three replicates).

R	Comp. No	RNO_2 (xa)	RNH_2 (xb)	RNH-CO-NHR (xc)
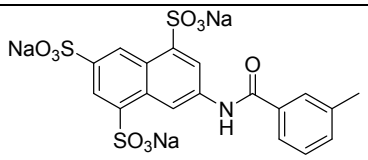	2	4.82 ± 0.08 15.2	5.25 ± 0.18 5.62	7.34 ± 0.05 0.046
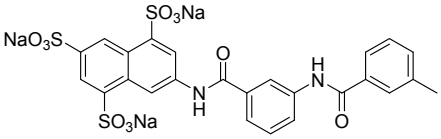	3	5.13 ± 0.30 7.41	5.48 ± 0.12 3.31	7.16 ± 0.16 0.069
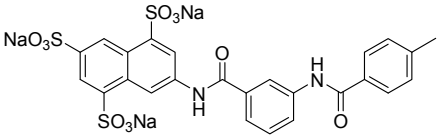	4	< 4 > 100	5.28 ± 0.18 5.25	6.92 ± 0.07 0.120
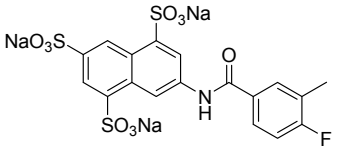	5	5.05 ± 0.20 8.91	4.67 ± 0.10 21.4	7.55 ± 0.07 0.028
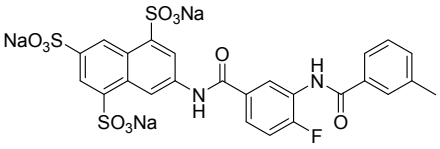	6	5.56 ± 0.40 2.75	4.94 ± 0.09 11.5	7.35 ± 0.10 0.045

The nitro- and amino- precursors showed antagonistic activity at $P2Y_{11}$ receptors. App. pK_i values of five nitro- and five amino-derivatives were estimated. Amino precursors of urea 2c, 3c and 4c showed higher potency than the nitro precursor whereas the nitro precursors of urea 5c and 6c showed the opposite effect. This study indicated that the symmetrical structure may not be required for antagonistic activity. This result was in agreement with the result of asymmetrical compounds reported by Bültmann and Hongwiset (Bültmann *et al.*, 1996, Hongwiset; 2008). Bültmann *et al.* concluded that symmetrical structure of suramin was not a requirement for antagonistic activity (Bültmann, 1996). However, the nitro- and amino precursor derivatives in this study were much less potent than their urea

compound. Hongwiset reported that the asymmetric carboxylic acid derivative MK071 (Figure 4.11) showed a higher potency (app. pK_i 6.79 ± 0.29) than suramin with an app. pK_i of 6.52 ± 0.13 (Ullman *et al.,* 2005; Hongwiset, 2008). It can be concluded that negatively charged groups at both ends of naphthalene structures seem to be important for antagonistic activity (Hongwiset, 2008).

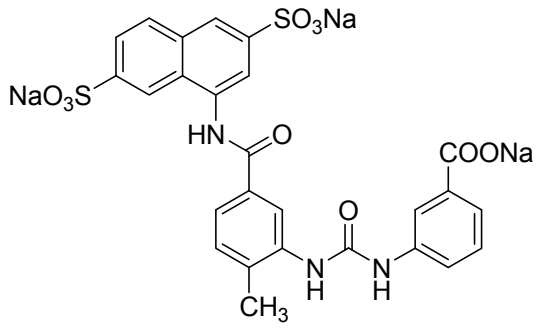

Figure 4.11 MK071, an asymmetrical derivative.

75 compounds consisting of ureas and their precursors were investigated for their antagonistic activity. The test compounds included:

- Compounds 1c-14c, which are urea derivatives containing trisodium 7-naphthalene-1,3,5- trisulfonate substituent.
- Compounds 15c-21c, which are urea derivatives containing 4-fluoro-3,1-phenylene-linker at benzene or naphthalene sulfonate.
- Compounds 22c-25c, which are urea derivatives containing trisodium 3(2,4-disulfonatophenylcarbamoyl)benzoate substituent.

4.4. Urea derivatives containing trisodium 7-naphthalene-1,3,5-trisulfonate substituent

4.4.1. Apparent pK_i value of urea 1c -14c

Meis found that NF340 and NF294 as disulfonate derivatives containing a meta-position between sulfonate and amido-linkage group gave a high potency with an app. pK_i value of 7.71 ± 0.04 and 7.42 ± 0.11, respectively. Suramin and NF157 as trisulfonate derivatives containing para position between sulfonate and the amido-linkage group, showed less potency with an app. pK_i value of 6.52 ± 0.13 (Ullman *et al.*; 2005) and 7.34 ± 0.08, respectively. Therefore, a trisulfonate precursor containing a meta-position between sulfonate and amido-linkage group was used in this study. Figure 4.12 shows the structure formulas of precursors of NF157, suramin, and compounds in this study.

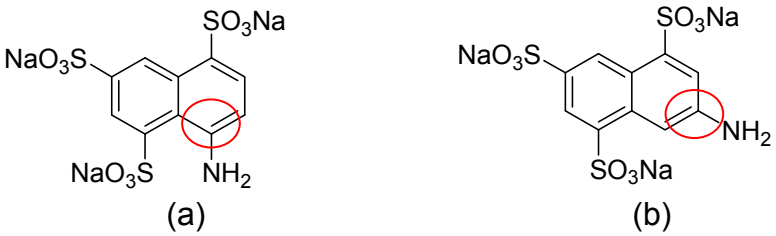

Figure 4.12 Precursor template of NF157 and suramin (a), and of compounds in this study (b).

1c, the urea of 7-amino-1,3,5-naphthalene trisulfonate (Figure 4.13) showed neither significant agonistic nor antagonistic activity at $P2Y_{11}$ receptors (See Table 4.2 and Table 4.5).

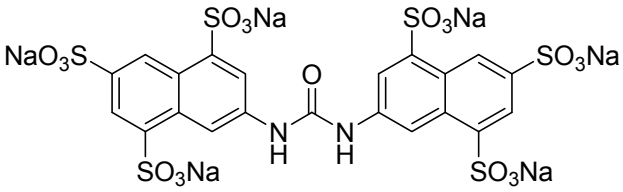

Figure 4.13 Structure of compound 1c.

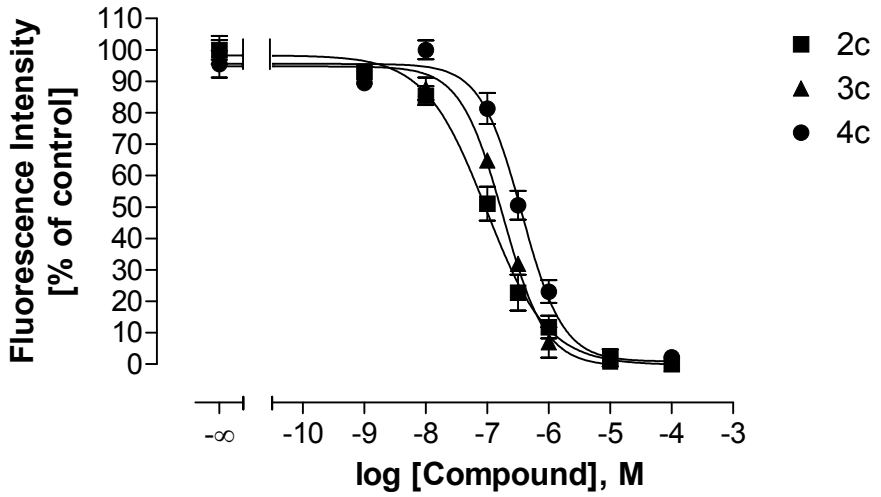

Figure 4.14 Concentration-inhibition curves of 2c, 3c and 4c at $P2Y_{11}$ receptors. 1 µM ATP was used as standard agonist.

Figure 4.14 shows the concentration-inhibition curves of compounds 2c, 3c and 4c. The obtained app. pK_i values and structure formulas of the compounds are presented in Table 4.8.

Table 4.8 Comparison of app. pK_i values and corresponding K_i values of compounds 2c, 3c and 4c at $P2Y_{11}$ receptors. 1 µM ATP was used as standard agonist.

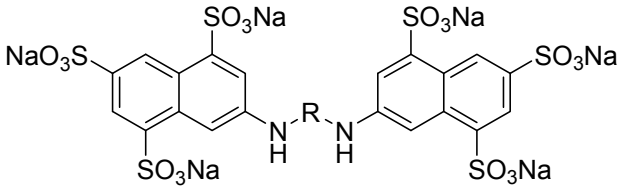

Comp.	R	App. pK_i	K_i (µM)
2c	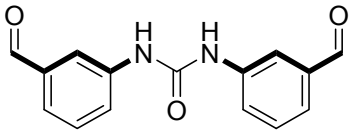	7.34 ± 0.05	0.046
3c	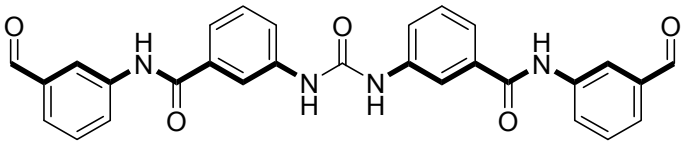	7.16 ± 0.16	0.069
4c	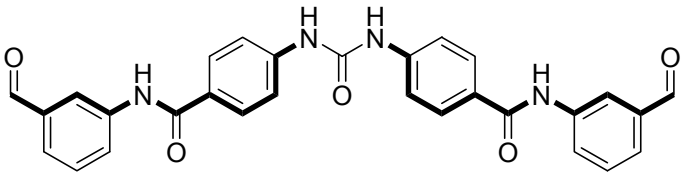	6.92 ± 0.07	0.120

2c containing a meta phenylene-linker showed an app. pK_i value of 7.34 ± 0.05 and no significant difference in comparison with the first potent antagonist NF157 with an apparent pK_i value of 7.34 ± 0.08. An extended structure of 2c with a second meta-phenylene-linker to obtain a larger structure such as NF157 was synthesized (3c) and showed a 1-5 fold slight decrease in potency. 2c, 3c and NF157 showed no significant difference in activity. Exchange of the second meta- to a para phenylene-linker was further investigated (compound 4c). The potency was reduced by 2.6 fold compared to NF157.

These results showed that a significant reduction of the app. pK_i occurred if the second meta phenylene-linker was exchanged against a para phenylene-linker. Based on the comparison of the activities of 2c-4c with compound 1c, it became evident that at least one phenylene-linker is required to obtain activity. Ullmann *et al.* reported that an electron-withdrawing residue such as fluorine has a positive

influence on the inhibitory potency. NF 157, the fluorine analogue of suramin turned out as the most potent $P2Y_{11}$ antagonist in their study (Ullmann *et al.*, 2005). Thus, a series of fluorine analogue derivatives of 2c were synthesized.

Figure 4.15 shows the concentration-inhibition curves of compounds 5c, 6c and 7c. The obtained pK_i values and structure formulas of the compounds are presented in Table 4.9.

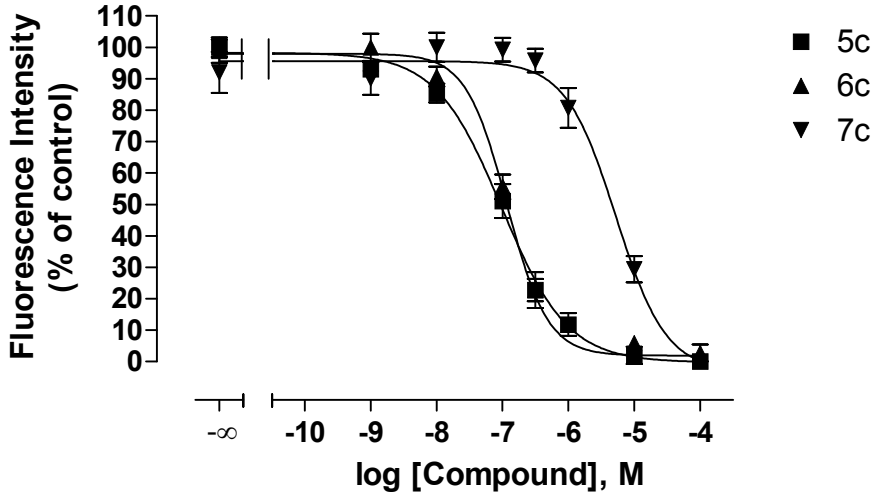

Figure 4.15 Concentration-inhibition curves of 5c, 6c and 7c at $P2Y_{11}$ receptors. 1µM ATP was used as standard agonist.

Table 4.9 Comparison of structure formulas, app. pK_i values, and corresponding K_i values of compounds 5c, 6c and 7c at $P2Y_{11}$ receptors. 1 µM ATP was used as standard agonist.

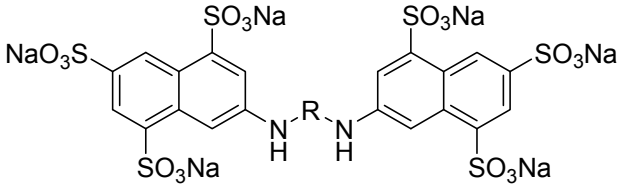

Comp.	Structure	App. pK_i	K_i (µM)
5c	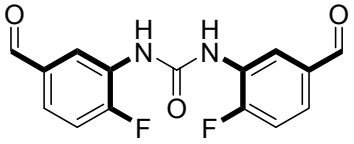	7.55 ± 0.07	0.028
6c	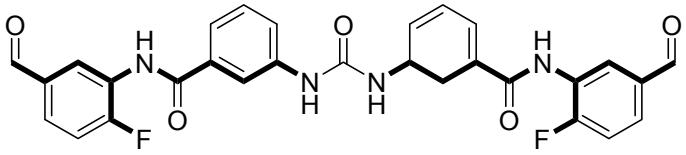	7.35 ± 0.10	0.045
7c	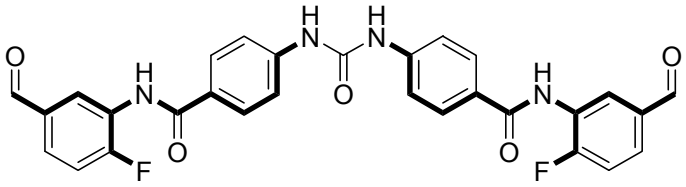	5.88 ± 0.08	1.32

Compound 5c is the fluorine analogue of 2c with an app. pK_i value of 7.55 ± 0.07. 5c showed a 1.6-fold increase in potency in comparison to NF157. Extended structures of 5c with a meta- and para phenylene-linker were also synthesized. The similar tendency was found in this variation. The results showed that an extension of the phenylene-linker of compound 5c exhibited a lower potency. App. pK_i values of 6c and 7c were 7.35 $\pm$ 0.10 (6c) and 5.88 $\pm$ 0.08 (7c), respectively. It was concluded that antagonistic activity of an extended structure of compounds 2c and 5c decreased when there is an exchange of the meta-phenylene-linker to para-phenylene-linker.

NF 340 is a small urea whereas NF157 is a large urea. Hongwiset found that large urea was not necessary for antagonistic activity. To confirm whether large urea was required for $P2Y_{11}$ receptors antagonistic activity in this study, a comparison between NF156, NF157, 5c, and 6c was made (Table 4.10).

Table 4.10 Comparison of app. pK_i values and corresponding K_i values of compounds 5c, 6c, NF156, and NF157 at $P2Y_{11}$ receptors.

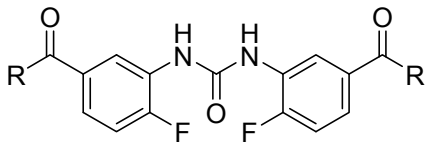

"small urea"

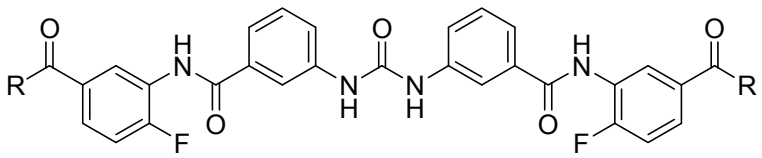

"large urea"

	R =					
	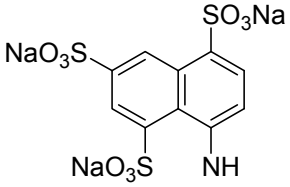			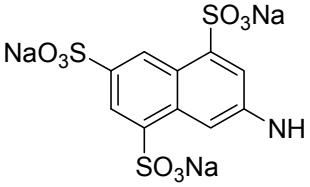		
	Comp	**App.pK$_i$**	**K$_i$ (µM)**	**Comp**	**App. pK$_i$**	**K$_i$ (µM)**
Small urea	NF156	5.63 ± 0.18 *)	2.36	5c	7.55 ± 0.07	0.028
Large urea	NF157	7.34 ± 0.08	0.047	6c	7.35 ± 0.10	0.045

*) Meis, 2008

An exchange of small urea NF156 to large urea NF157 increased the activity. NF157 with pK_i value of 7.34 ± 0.08 was 52-fold more potent than NF156 (5.63 ± 0.18). An interesting result was observed in comparison of small urea 5c and large urea 6c. App. pKi value of small urea 5c (7.55 ± 0.07) is slightly higher than 6c

(7.35 ± 0.10). The result showed that a large urea is not necessary for a high activity. This phenomenon was in agreement with the result found by Hongwiset (Hongwiset, 2008). Moreover, NF156 and NF157 contain trisulfonate derivatives with the sulfonate substitution in para position to the amido-linkage group. The extended structure (NF157) showed higher potency than NF156 whereas compound 5c and its extended structure (6c) which contain the sulfonate substitution in meta position to the amido-linkage group showed the opposite effect. It can be concluded that the sulfonate substitution in meta position to the amido-linkage group is important for the antagonist activity of small urea.

To obtain a complete picture of structure activity relationship, synthetic variation was continued using a para-phenylene-linker position in small ureas instead of a meta phenylene-linker. Table 4.11 shows the structure formulas, app. pK_i values and corresponding K_i values of compounds 5c, 8c, 9c, and 10c.

Table 4.11 Comparison of structure formulas, app. pKi values and corresponding K_i values of compounds 5c, 8c, 9c and 10c. 1 µM ATP was used as standard agonist.

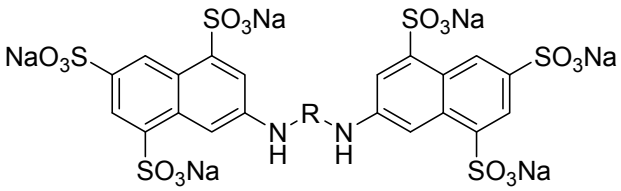

Comp.	R	Values	Values
5c	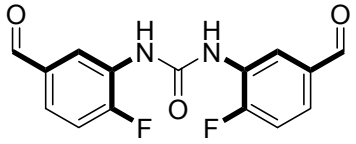	7.55 ± 0.07	0.028
8c	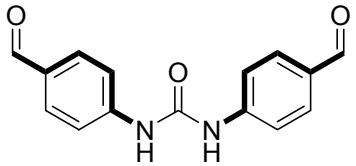	**pEC_{50}** 5.43 ± 0.18	**EC_{50}** 3.73
9c	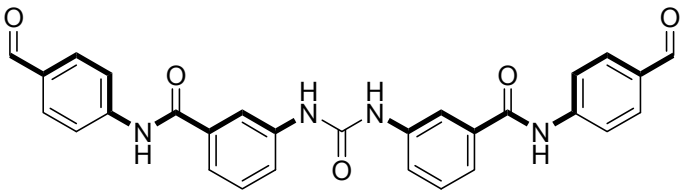	**pEC_{50}** 5.68 ± 0.10	**EC_{50}** 2.10
10c	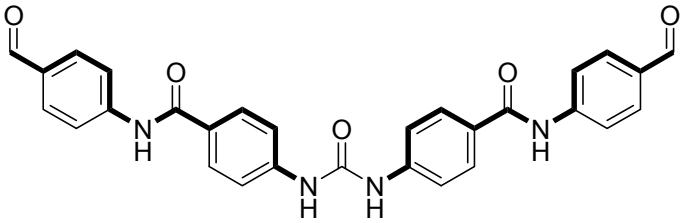	pK_i 4.46 ± 0.15	K_i 34.7

A small urea containing a para phenylene-linker instead of a meta phenylene-linker turned the antagonist 5c into an agonist 8c with a pEC_{50} value of 5.43 ± 0.18 (EC_{50} = 3.73 µM). An extension of the structure of this agonist containing a second meta phenylene-linker (9c) increased the agonistic activity slightly. 9c showed 1.8-fold higher potency than 8c (pEC_{50} = 5.68 ± 0.10, EC_{50} = 2.10 µM) (Chapter 4.2.3). An extension with a para phenylene-linker (10c) showed antagonist activity. MK094 a methyl analogue of 5c, as reported by Hongwiset, showed a potent antagonistic activity with an app. pK_i value of 7.14 ± 0.06 (Hongwiset, 2008). To study which position of the methylene at the phenylene-linker are more relevant for antagonist activity, compounds 11c and 12c were synthesized and investigated for

inhibitory effect. Table 4.12 shows the comparison of the antagonistic activity of compound 11c, 12c, and MK094 with variation of methyl and amide position.

Table 4.12 Comparison of structure formulas, app. pK_i values and corresponding K_i values of compounds 11c, 12c and MK094*) with variations of methyl and amide position. 1 µM ATP was used as standard agonist.

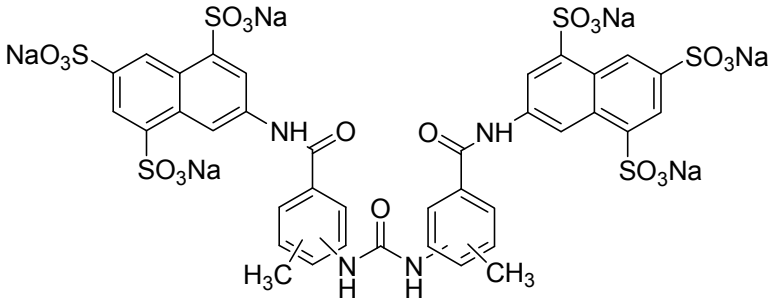

Compound	Position		App.pK_i	K_i (µM)
	-CH_3	-NH		
11c	3	4	< 4	> 100
12c	2	3	4.75 ± 0.09	17.8
MK094	4	3	7.14 ± 0.06 *)	0.072

*) Hongwiset, 2008

App. pK_i values of 11c and 12 c were < 4 and 4.75 ± 0.09, respectively. Methyl group at 4 position and amide at 3 position obtained a higher activity (app. pK_i 7.14 ± 0.06) compared to compound 11c and 12c. These results implied that the position of methyl group is important for the activity.

The exchange of the 4-methyl group (MK094) by methoxy turned out to reduce the app. pK_i value to 5.77 ± 0.07. Table 4.13 shows the comparison of app. pKi values of compounds 2c, 5c, 13c, and MK094 at $P2Y_{11}$ receptors. Compound 5c with the fluorine residue showed the highest app. pK_i among -H, methoxy and methyl residues (Table 4.13).

Table 4.13 Comparison of app. pK_i values and corresponding K_i values of compounds 2c, 5c, 13c and MK094 at $P2Y_{11}$ receptors. 1 µM ATP was used as standard agonist.

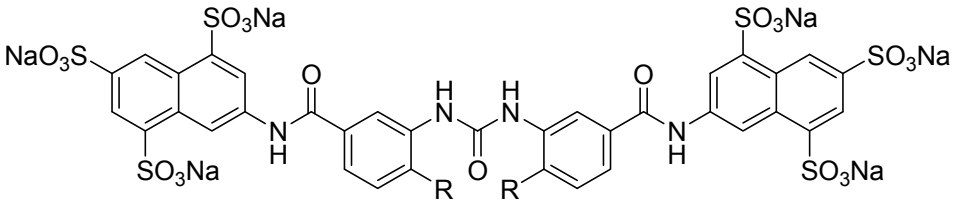

	R			
	-H	**-F**	**-OCH_3**	**-CH_3**
Compound	2c	5c	13c	MK094 *)
App. pK_i	7.34 ± 0.05	7.55 ± 0.07	5.77 ± 0.07	7.14 ± 0.06
K_i (nM)	46	28	1700	72.4

*) Hongwiset, 2008

Table 4.14 shows the comparison of app. pK_i values and corresponding K_i values of compounds 8c and 14c at $P2Y_{11}$ receptors. An exchange of the phenylene-linker of compound 8c to phenylene methylene turned the functional compound behaviour to an antagonist with an app. pK_i value of 5.26 ± 0.07 (14c).

Table 4.14 Comparison of app. pK_i values and corresponding K_i values of compounds 8c and 14c at $P2Y_{11}$ receptors. 1 µM ATP was used as standard agonist.

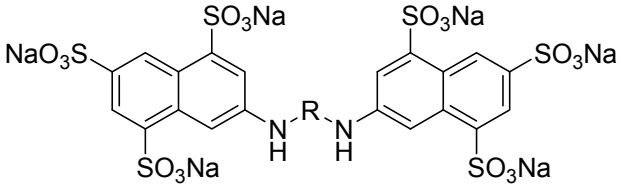

	R	
	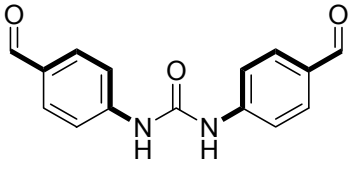	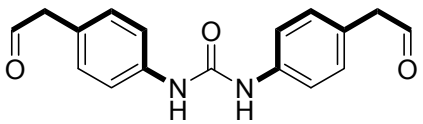
Compound	8c	14c
Values	pEC_{50} : 5.43 ± 0.18	pK_i: 5.26 ± 0.07
	EC_{50} : 3.73 µM	K_i: 5.49 µM

4.4.2. Schild analysis of compound 5c

Compound 5c was the most potent compound in this study and showed slightly higher activity than NF157. Therefore, the antagonistic character was further investigated. The concentration-response curves of the standard agonist ATP in the absence and the presence of increasing concentrations of compound 5c showed a rightward-shift with the same maximum effects (Figure 4.16).

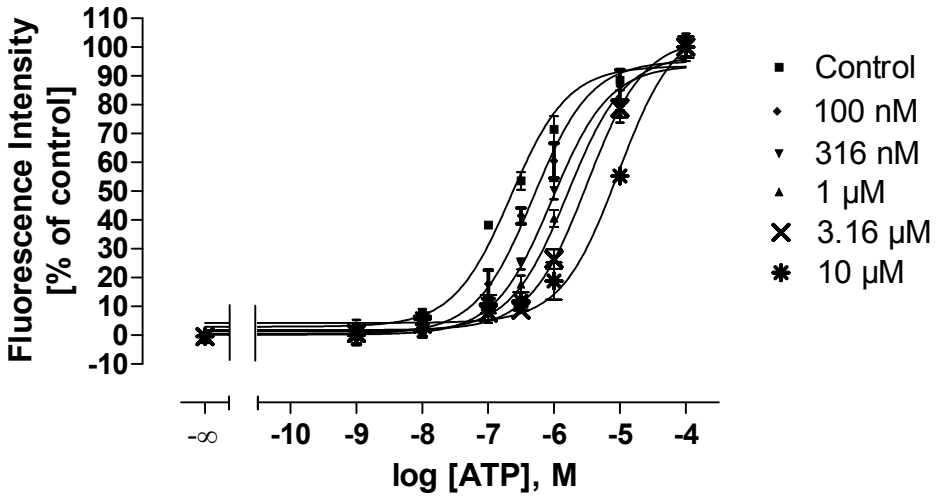

Figure 4.16 Concentration-response curves of ATP at $P2Y_{11}$ receptors using the calcium assay. ATP was tested in the absence and presence of increasing concentrations of compound 5c ($n \geq 2$, each experiment was performed in three replicates). Slopes were not significant different from unity.

The nature of the antagonism of compound 5c was investigated using a Schild analysis. The Schild plot of 5c is shown in Figure 4.17

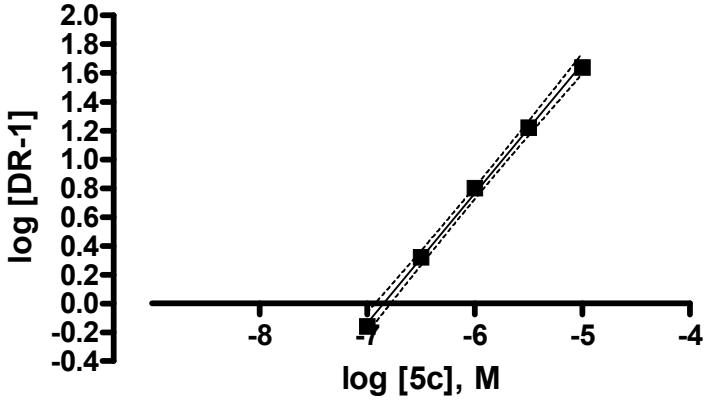

Figure 4.17 Schild plot of compound 5c. X intercept = 6.85, slope = 0.9000 ± 0.02. (n ≥ 2, each experiment was performed with 3 replicates).

The Schild plot showed a slope 0.9000 ± 0.02 which is within range of 0.8417 to 0.9583 (95 % confidence interval). The slope was close to 1. Therefore, it could be concluded that compound 5c is possibly a competitive antagonist at $P2Y_{11}$ receptors. The pA_2 value of compound 5c was estimated with value of 6.85 which was lower than the app. pK_i (7.55 $\pm$ 0.07). Nevertheless, the pA_2 value was in approximate agreement with pIC_{50} value (6.99 $\pm$ 0.07).

4.5. Urea derivatives containing 4-fluoro-3,1-phenylene-linker.

As mentioned in chapter 4.4, the fluorine derivative (5c) showed the most potent antagonistic activity at $P2Y_{11}$ receptors among 1c-14c. Therefore, it was interesting to further investigate the structural modification of other derivatives containing 4-fluoro-3,1-phenylene-linker. In this series, 7 urea compounds with different naphthalene or benzene sulfonate precursors were synthesized. Tuluc *et al.* found out that the exchange of sulfonate residue position in RB2 from meta or para position to ortho position had impact on ligand binding at P2 receptors (Tuluc *et al.*, 1998). Structure-activity relationship of RB2 analogues was further done by Glaenzel *et al*. They also found that the moieties of anionic sulfonate groups are important for the blockade of the $P2X_1$ and $P2Y_1$ receptors (Glaenzel *et al.*, 2005). An overview on the variations of naphthalene precursors is given in Table 4.15.

.

Table 4.15 Structure formulas and functional activities of compounds 15c-19c, NF156 and 5c with variations of the naphthalene precursor at $P2Y_{11}$ receptors. 1 µM ATP was used as standard agonist.

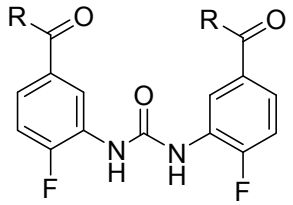

	R						
	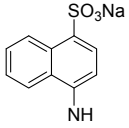	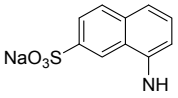	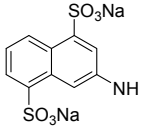	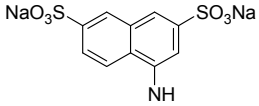	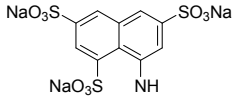	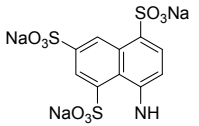	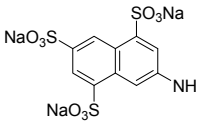
Compound	15c	16c	17c	18c	19c	NF156	5c
App. pK_i	4.89 ± 0.08	< 4	5.67 ± 0.09	4.54 ± 0.10	5.27 ± 0.32	5.63 ± 0.18	7.55 ± 0.07
K_i (µM)	12.9	> 100	2.14	28.8	5.37	2.36	0.028

To study which position of the sulfonate group are more relevant for antagonistic activity, the monosulfonate derivatives 15c and 16c were synthesized (Figure 4.18).

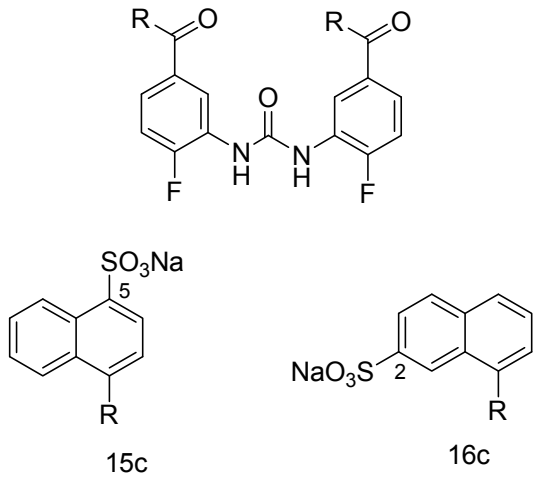

Figure 4.18 Structure formulas of compound 15c and 16c

15c with sulfonate residue in position 5 showed an app. pK_i of 4.89 ± 0.08 whereas compound 16c with sulfonate residue in position 2 showed an app. pK_i value less than 4. Although compound 15c showed antagonistic activity, it was much less than the trisulfonate compound 5c (pK_i 7.55 ± 0.07) and disulfonate compound 17c (pK_i 5.67 ± 0.09). Therefore, it was concluded that more than one sulfonate group is needed to obtain a better antagonistic activity. Compound 18c with disulfonate showed an exceptional result, the antagonistic activity was lower than monosulfonate 15c. It was further concluded that not only the moieties of sulfonate is important for antagonistic activity, moreover the position of sulfonate is interesting to investigate. Urea with sulfonate residues in 1, 3, and 6 position showed an app. pK_i value of 5.27 ± 0.32 (19c) which is 2.3-fold less potent than NF156 (5.63 ± 0.18) with sulfonate residues in positions 1, 3 and 5. Shift of the amido linker to position 7 led to the most potent antagonist in this study (5c).

It was noticed that the most potent antagonist (5c) in this study had a sulfonate substitution in meta position to the amido-linkage group, trisulfonate of naphthalene and a fluorinated phenylene-linker. Exchange of the fluorine atom against methyl group was studied (Table 4.16).

Table 4.16 Structure formulas and functional activities of naphthalene sulfonate substituted compounds 5c, 17c, 18c, 19c, NF294, MK082, NF340, NF248 and MK094 at $P2Y_{11}$ receptors.

R	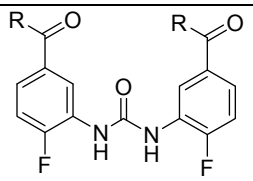		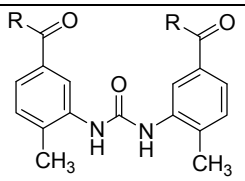	
	App. pK_i	**K_i (μM)**	**App. pK_i**	**K_i (μM)**
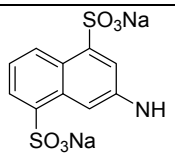	5.67 ± 0.09	2.14	7.42 ± 0.11	0.038
Compound	17c		NF294 *)	
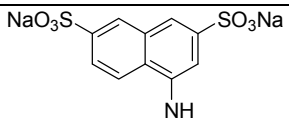	4.54 ± 0.10	28.8	6.09 ± 0.08	0.812
Compound	18c		MK082 **)	
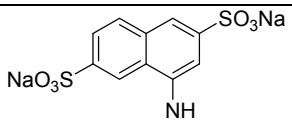	6.43 ± 0.16	0.371	7.71 ± 0.04	0.019
	MK196 **)		NF340 *)	
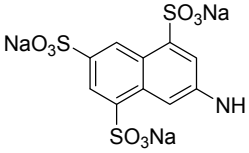	7.55 ± 0.07	0.028	7.14 ± 0.06	0.072
Compound	5c		MK094 **)	
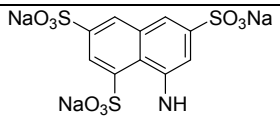	5.27 ± 0.32	5.37	6.47 ± 0.08	0.339
Compound	19c		NF248 *)	

*) Meis, 2008; **) Hongwiset, 2008

The fluorinated derivatives of disulfonate urea were less potent than methyl derivatives. Urea 17c was found to have a low antagonistic activity with 56-fold lower potency than NF294. The similar tendency was found for urea 18c which was 35-fold less potent than MK082 as well as for NF340 which was 19-fold higher potency than its fluorine derivative (MK196) (Meis 2008, Hongwiset, 2008). The

opposite phenomenon was found for compound 5c which showed 2.6-fold higher potency than its methyl derivative (MK094). Surprisingly, trisulfonate derivative 19c was less potent than the methyl derivative NF284. Therefore it could be concluded that the exchange of fluorine by methyl group provides a lower potency at $P2Y_{11}$ receptors in the trisulfonate derivative but not in the disulfonate derivative. Furthermore, the position of sulfonate group is important for antagonistic activity.

The next aim of this work was to confirm whether the naphthalene ring is important for $P2Y_{11}$ receptor antagonistic activity. Therefore, exchange of naphthalene by a benzene precursor was performed. NF251 with a methyl substituted phenylene-linker and disulfonate residues showed a 52.5-fold higher potency than disulfonate residues containing fluoro-3,1-phenylene linker (20c) whereas the monosulfonate derivative (21c) showed no activity which was equal to its methyl derivative (MK104) (Table 4.17).

Table 4.17 Structure formulas and functional activities of urea compounds containing benzene sulfonate compounds 20c, 21c, NF251 and MK104 containing methyl phenylene-linker at $P2Y_{11}$ receptors. 1 µM ATP was used as standard agonist.

	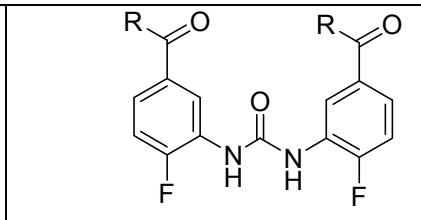		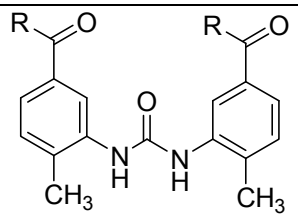	
R	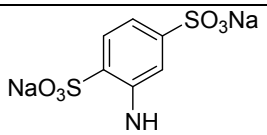	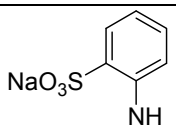	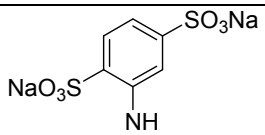	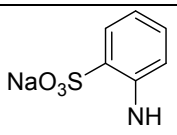
Comp	20c	21 c	NF251*	MK104*
App. pK_i	5.02 ± 0.16	<4	6.74 ± 0.11	<4
K_i	9.54	> 100	182	> 100

*) Hongwiset 2008

From this result, it might be presumed that urea derivatives containing naphthalene with specific position of sulfonate residue showed high potency as shown for compound 5c, NF157, NF294 and NF340.

4.6. Urea derivatives containing trisodium 3(2,4-disulfonatophenylcarbamoyl)benzoate substituent

Out of the series above, synthesis of urea derivatives containing trisodium 3(2,4-disulfonatophenylcarbamoyl)benzoate substituent with a variation of phenylene linker was carried out. Ullmann reported that urea derivative containing trisodium 3(2,4-disulfonatophenylcarbamoyl)benzoate substituent showed no antagonistic activity at $P2Y_{11}$ receptors (Figure 4.19). It is interesting that in this study, an extended structure of MK006 with a second phenylene-linker, showed antagonistic activity.

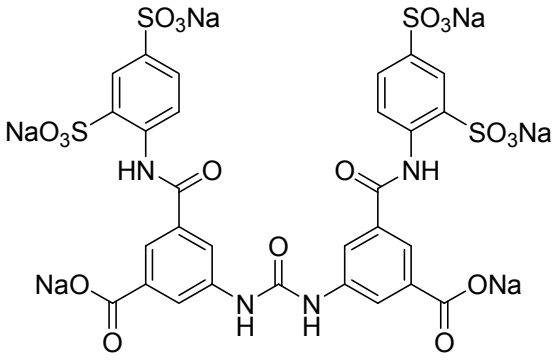

Figure 4.19 Structure formula of MK006 (Ullmann, Dissertation in process).

First variation contained a para phenylene-linker (22c) that showed an app. pK_i value of 4.20 ± 0.16 (Table 4.18). Exchange of para-phenylene urea linker by meta phenylene-linker led to a 12.3-fold higher potency than compound 22c. 24c showed an app. pK_i value of 5.29 ± 0.20 (24c).

The results of the first series (Chapter 4.4) showed that fluorine substitution in the phenylene-linker was found to increase potency. Surprisingly, in this series, the biological activity of the fluorinated compound showed a 7.6-fold reduction of potency compared to compound 24c. Compound 23c showed an app. pK_i value of 4.40 ± 0.16. The exchange of fluorine against a methyl residue did not change the potency (25c, app. pK_i value of 4.48 ± 0.13). In conclusion, the unsubstituted meta phenylene-linker containing 24c showed the highest potency among this series. However, compound 5c was still more than 100-fold more potent.

Table 4.18 Structure formulas and functional activities of compounds 22c-25c at $P2Y_{11}$ receptors. 1 μM ATP was used as standard agonist.

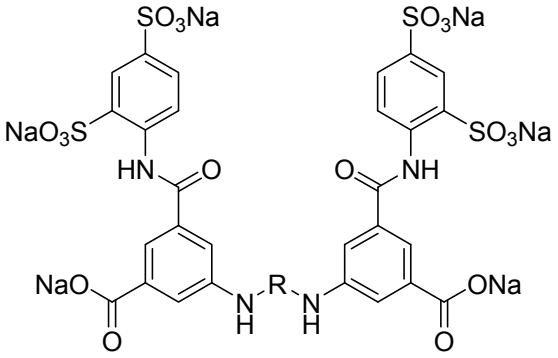

Compound	R	App. pK_i	Ki (μM)
22c	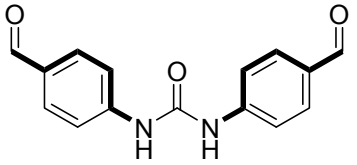	4.20 ± 0.16	63.1
23c	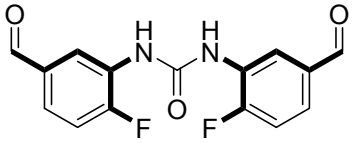	4.40 ± 0.16	39.8
24c	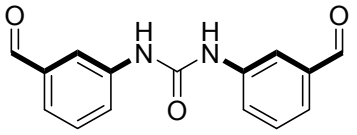	5.29 ± 0.20	5.13
25c	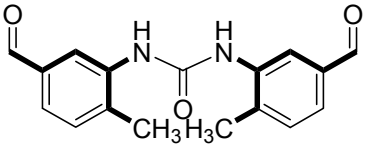	4.48 ± 0.13	33.1

4.7. Selectivity of the test compound

4.7.1. Selectivity test at $P2Y_1$ receptors

$P2Y_1$ receptors share 33 % identity with $P2Y_{11}$ receptors (Communi, 1999). Therefore, a counter screen at these receptors was needed for the evaluation of receptor selectivity. At $P2Y_1$ receptors, 2-MeSADP was used as agonist with an EC_{50} of 3.0 nM (pEC_{50} = 8.53 ± 0.10) as shown in Figure 4.20. The determined EC_{50} of 2-MeSADP in the used test system was in the same range as literature data (6 nM) (Chhatriwala *et al.*, 2004). Synthesized compounds were screened at $P2Y_1$ receptors recombinantly expressed in 1321N1 astrocytoma cells.

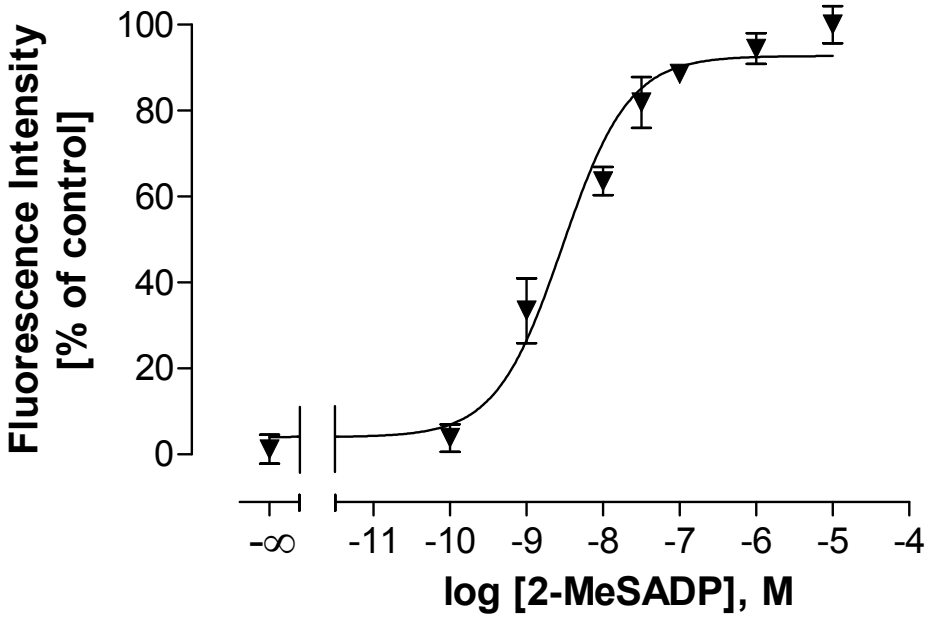

Figure 4.20 Concentration-response curve of 2-MeSADP at $P2Y_1$ receptors. Data shown are mean ± SEM of the pooled data (n = 3, each experiment was performed in three replicates). Slopes were not significant different from unity. EC_{50} = 3.0 nM, pEC_{50} = 8.53 ± 0.10.

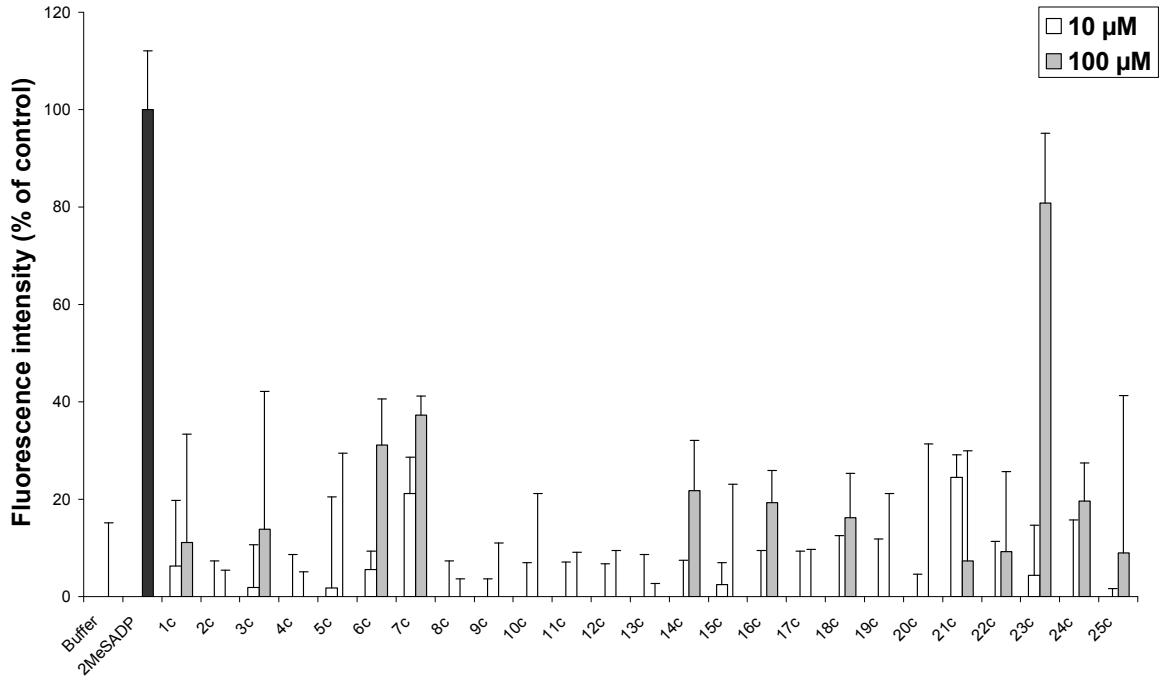

Figure 4.21 Agonist screening of urea compounds at $P2Y_1$ receptors at concentrations of 10 µM and 100 µM as % of 31.6 nM 2-MeSADP control. Buffer was set as 0 %. Data shown are mean ± SEM of the pooled data ($n \geq 2$, each experiment was performed in three replicates)

All urea compounds showed no significant agonistic activity at $P2Y_1$ receptors, except compound 23c, which showed 80.8 % response in comparison with the standard agonist at a concentration of 100 µM (Figure 4.21). Nitro- and amino precursors showed also no significant response at a concentration of 100 µM except compounds 15a and compound 23b, which showed 50.3 and 70.1 % response, respectively. However, there were no significant responses for both precursors and urea compounds at a concentration of 10 µM (Appendix A1).

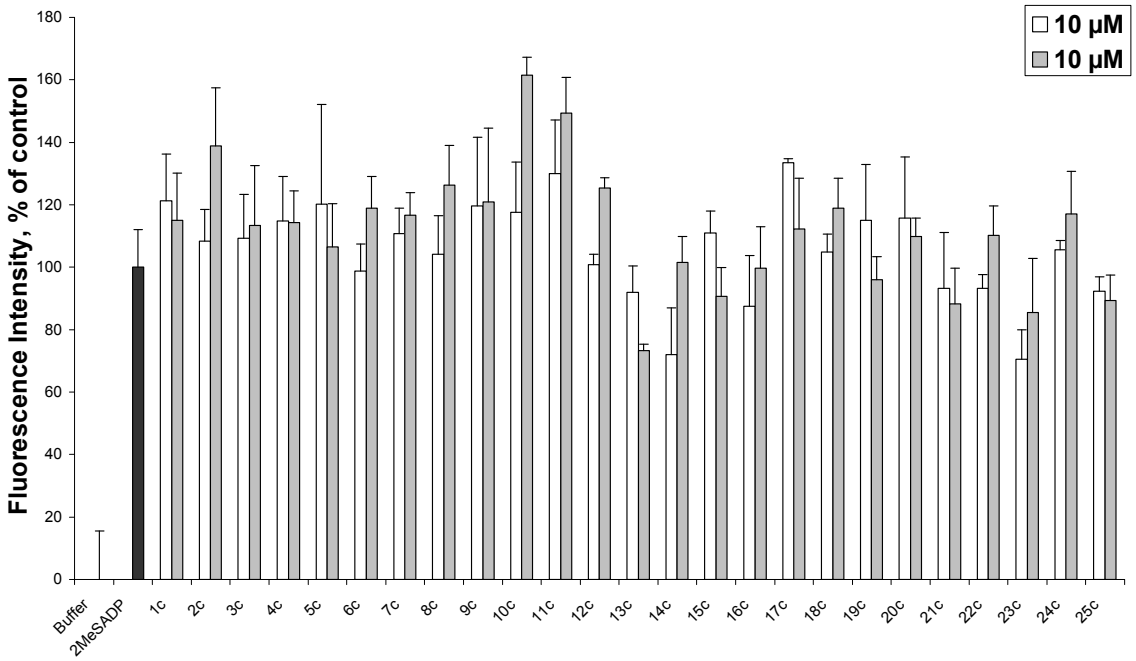

Figure 4.22 Antagonist screening of urea compounds at $P2Y_1$ receptors. Response of 31.6 µM 2-MeSADP induced calcium mobilization as standard agonist with preincubated compounds (1c-25c) at concentrations of 10 µM and 100 µM at $P2Y_1$ receptors. Data shown are mean ± SEM of the pooled data ($n \geq 2$, each experiment was performed in three replicates).

None of the urea compounds showed more than 30 % inhibition in antagonist screening at $P2Y_1$ receptors (Figure 4.22). The same results were obtained for nitro- and amino precursors (see Appendix A2). It could be concluded that there is no interesting compound as candidate for antagonistic activity at $P2Y_1$ receptors. This result showed the selectivity of compounds as antagonists at $P2Y_{11}$ receptors over $P2Y_1$ receptors.

4.7.2. Selectivity test at $P2Y_2$ receptors

UTP was used as standard agonist at $P2Y_2$ receptors recombinantly expressed in 1321N1 astrocytoma cells with EC_{50} = 94.2 nM, pEC_{50} = 7.02 ± 0.13 (Figure 4.23). Jacobson *et al.* found an EC_{50} value of 140 nM (Jacobson *et al.*, 2000). The results are shown for urea compounds in Figure 4.24 and Figure 4.25. Detail results in % response and % inhibition for nitro-, amino-, and urea derivatives are given in Appendix A3 and A4.

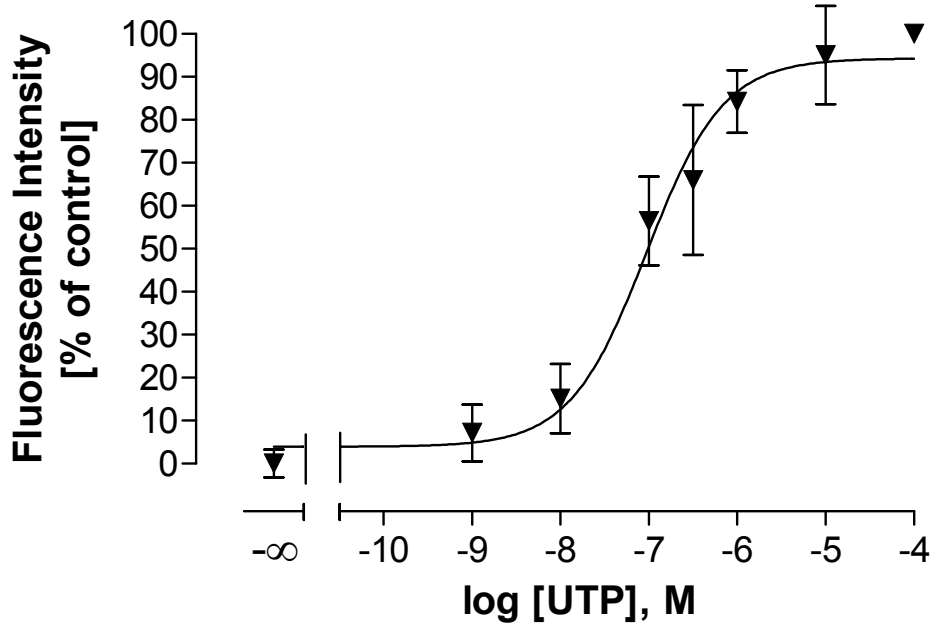

Figure 4.23 Concentration-response curve of UTP at $P2Y_2$ receptors. Data shown are mean ± SEM of the pooled data (n = 2, each experiment was performed in three replicates). Slopes were not significant different from unity. EC_{50} = 94.2 nM, pEC_{50} = 7.02 ± 0.13.

Agonist screening of urea compounds at $P2Y_2$ receptors showed that all responses were not more than 30 % of UTP signal at concentrations 10 µM and 100 µM, respectively (Figure 4.24). Nitro- and amino- precursor of the synthesized compounds of this study showed no more than 30 % responses (see Appendix A3).

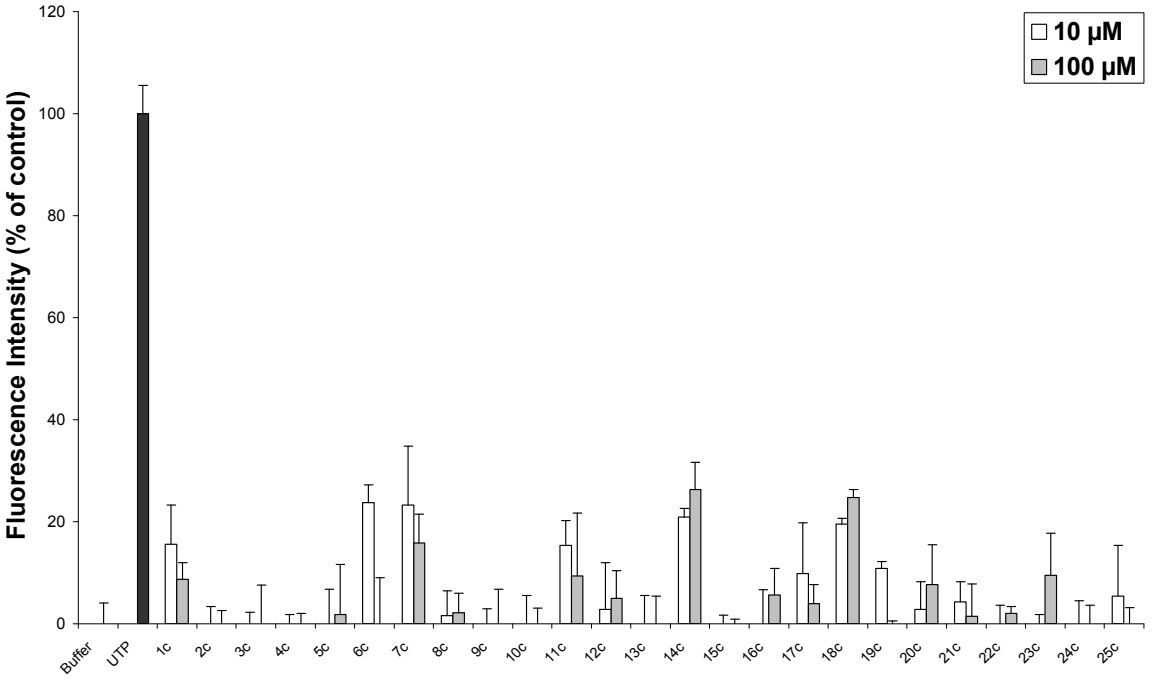

Figure 4.24 Agonist screening of urea compounds at $P2Y_2$ receptors at concentrations of 10 µM and 100 µM as % of 1 µM UTP control (100 %). Buffer was set as = %. Data shown are mean ± SEM of the pooled data ($n \geq 2$, each experiment was performed in three replicates).

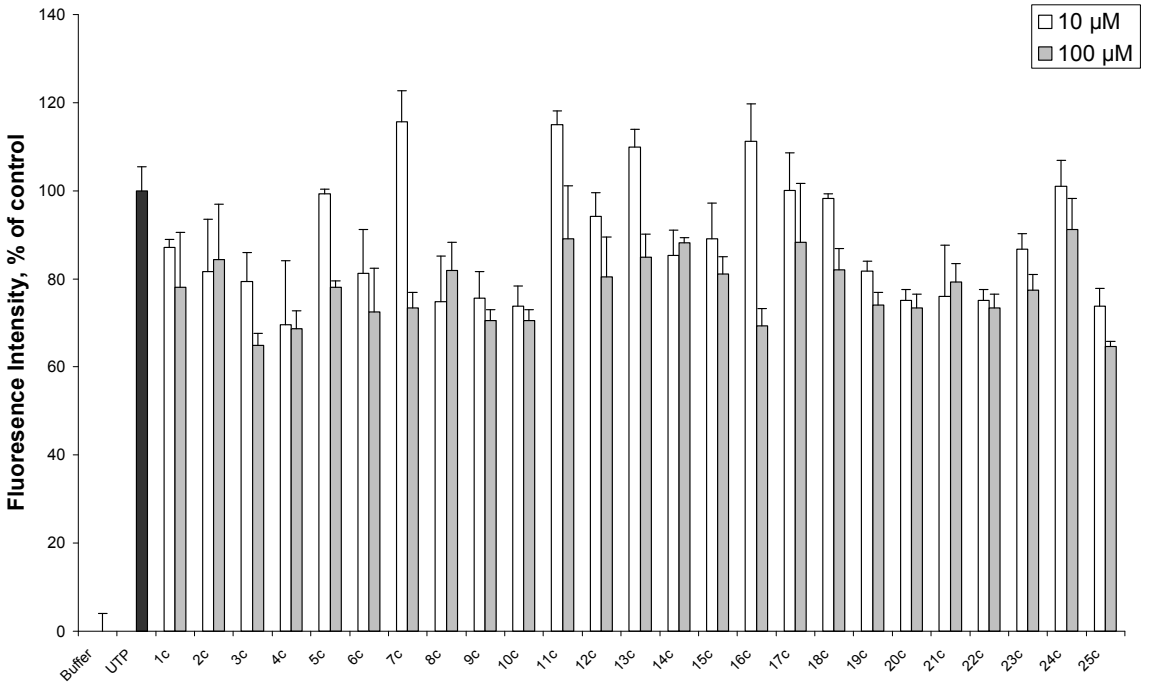

Figure 4.25 Antagonist screening of urea compounds at $P2Y_2$ receptors. Response of 1 µM UTP induced calcium mobilization as standard agonist with preincubated compounds (1c-25c) at concentrations of 10 µM and 100 µM. Data shown are mean ± SEM of the pooled data ($n \geq 2$, each experiment was performed in three replicates).

Antagonist screening of the urea compounds at $P2Y_2$ receptors showed no significant antagonistic activity (Figure 4.25). This result was also found for nitro- and amino precursors (see Appendix A4).

4.7.3. Selectivity test at $P2Y_4$ receptors

UTP was used as standard agonist with an EC_{50} of 12.8 nM, pEC_{50} 7.89 ± 0.16 (Figure 4.26). The result was in approximate agreement with the EC_{50} value found by Meis using the functional Ca^{2+}-assay (20 nM) (Meis, 2008).

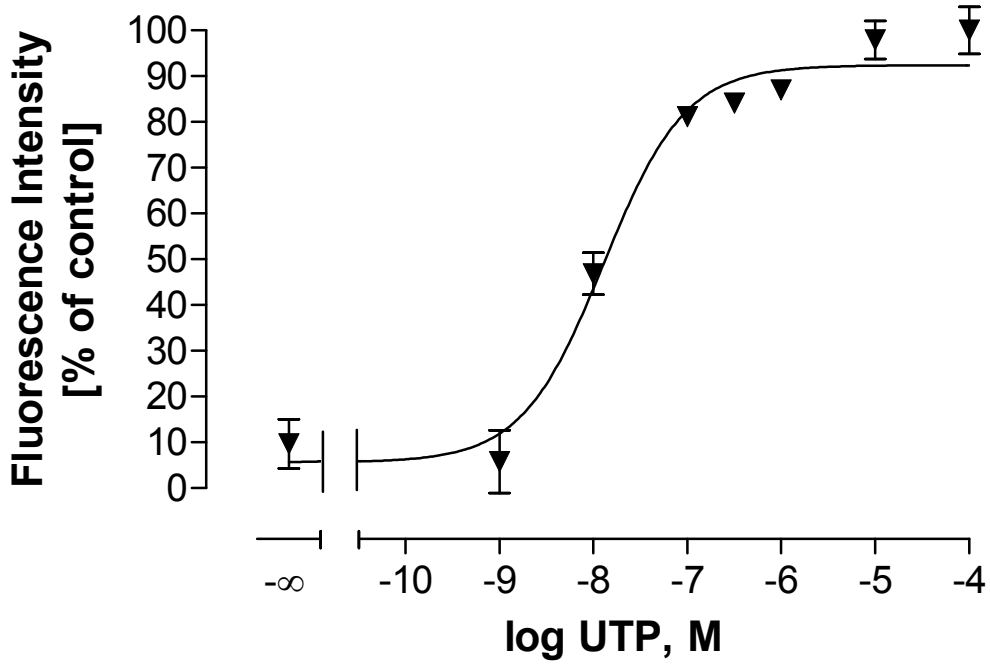

Figure 4.26 Concentration-response curve of UTP at $P2Y_4$ receptors. Data shown are mean ± SEM of the pooled data (n = 3, each experiment was performed in three replicates). Slopes were not significant different from unity. EC_{50} = 12.8 nM, pEC_{50} 7.89 ± 0.16.

Synthesized compounds were screened at $P2Y_4$ receptors recombinantly expressed in 1321N1 astrocytoma cells. The results for urea compounds are shown in Figure 4.27 and Figure 4.28. Detailed results in % response and % inhibition for nitro-, amine-, and urea derivative are shown in Appendix A5 and A6. None of the compounds showed more than 25 % response of 1 µM UTP-induced signal (Figure 4.27, Appendix 5).

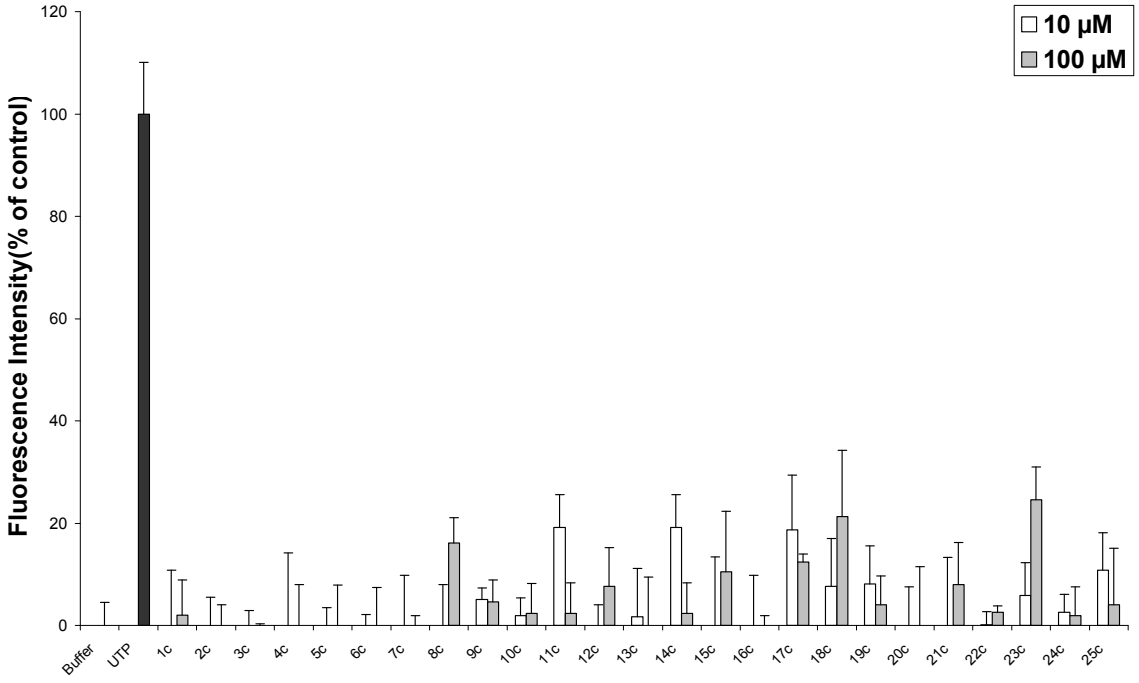

Figure 4.27 Agonist screening of urea compounds at $P2Y_4$ receptors at concentrations of 10 µM and 100 µM shown as % of 1 µM UTP control (100 %). Buffer was set as 0 %. Data shown are mean ± SEM of the pooled data ($n \geq 2$, each experiment was performed in three replicates).

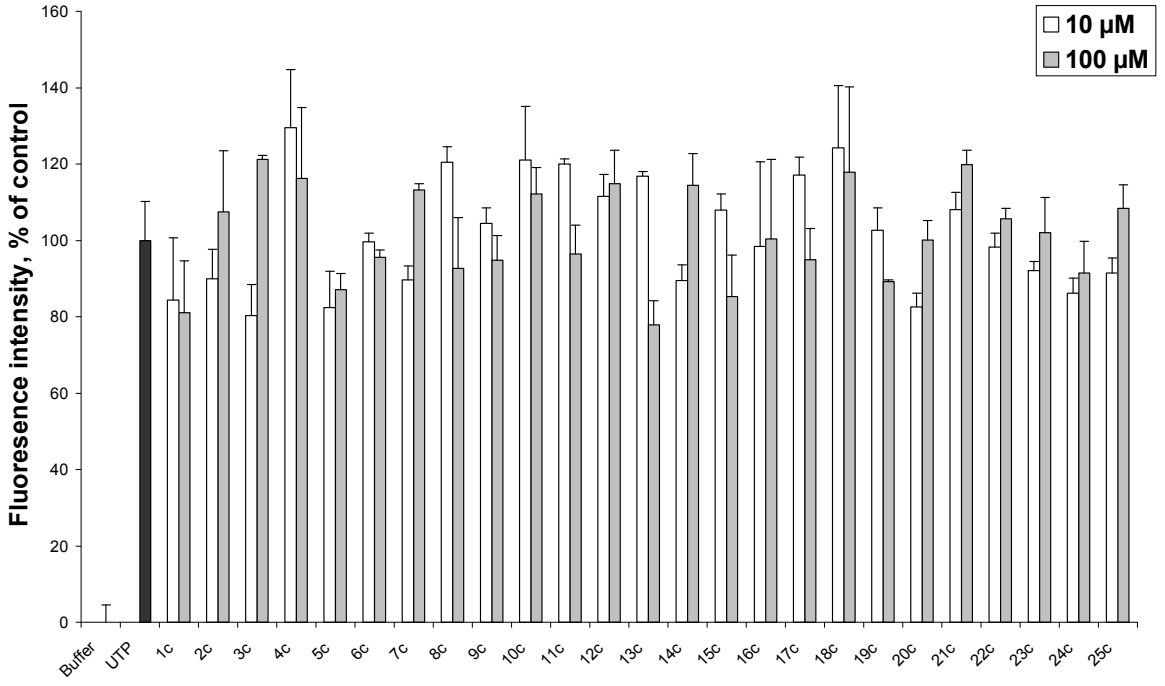

Figure 4.28 Antagonist screening of urea compounds at $P2Y_4$ receptors. Response of 1 µM UTP induced calcium mobilization as standard agonist with preincubated compounds (1c-25c) at concentration of 10 µM and 100 µM. Data shown are mean ± SEM of the pooled data ($n \geq 2$, each experiment was performed in three replicates).

None of the compounds showed more than 25 % inhibition at concentrations of 10 μM and 100 μM, except compound 23b with an inhibition of 31.5 % (Figure 4.28, Appendix 6).

5. Conclusion

$P2Y_{11}$ receptors are G protein-coupled receptors with unique features among other purinergic receptors. They are coupled to both phospholipase C and adenylyl cyclase pathways and their gene is the only one of the purinergic receptors containing an intron in the coding sequence (Qi *et al.,* 2001; Communi *et al.*, 2001). $P2Y_{11}$ receptors were reported to have a role in maturation of dendritic cells, inhibition of TNF-α release, and in myocardial contractility (Schnurr *et al.*, 2000; Wilkin *et al.*, 2001, Balogh *et al.*, 2005, Swennen, 2006). However, $P2Y_{11}$ receptors are less investigated than other P2Y receptors (Zyberg *et al.*, 2007). So far, NF157 and NF340 are interesting new compounds with high potency and selectivity at $P2Y_{11}$ receptors (Ullmann *et al.*, 2005; Meis 2008). NF294 and MK094 were reported to have a high potency (Hongwiset 2008; Meis 2008). Moreover, Meis reported the finding of non-nucleotide agonists (NF546 and NF709) (Meis, 2008). In this work, 25 ureas and their precursors were synthesized and their biologically activity were tested at $P2Y_{11}$ receptors recombinantly expressed in 1321N1 astrocytoma cells with a functional fluorescence-based calcium assay. The results led to the discovery of new agonists and new potent antagonists. Two new agonists are introduced in this study (Figure 5.1)

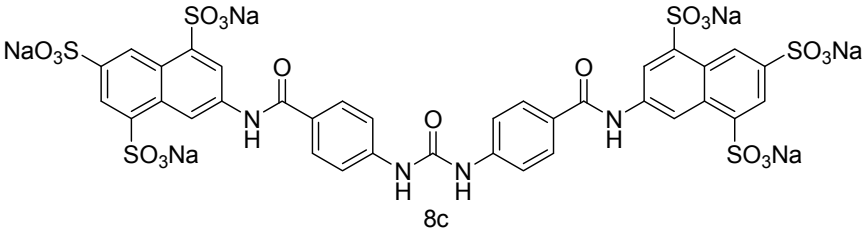

8c

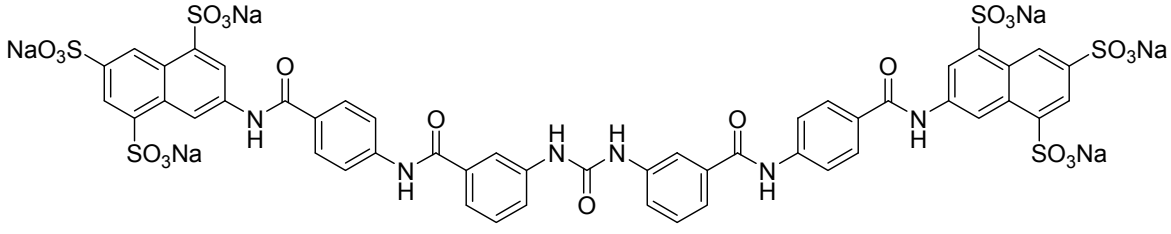

9c

Figure 5.1 Structure formulas of compounds 8c and 9c, new agonists at $P2Y_{11}$ receptors.

Compounds 8c and 9c activate $P2Y_{11}$ receptors with 22 and 12-fold lower potency than ATP, respectively. Compound 8c and 9c showed a partial agonistic activity. Nevertheless, the EC_{50} values of both compounds (3.73 µM and 2.10 µM) were in the lower micro molar range. Compounds 8c and 9c showed no agonistic or antagonistic activity at $P2Y_1$, $P2Y_2$ and $P2Y_4$ receptors.

Compound 5c (Figure 5.2) is the most potent antagonist found in this study with an app. pK_i value of 7.55 $\pm$ 0.07 corresponding to a K_i value of 28.0 nM. The antagonistic activity of compound 5c is between NF157 (44.3 nM) and NF340 (19.5 nM). Compound 5c is a possibly competitive antagonist as found in a Schild analysis. The pA_2 value of compound 5c was estimated as of 6.85. The pA_2 value was lower than the estimated app. pK_i of compound 5c. Moreover, compound 5c shows no agonistic and antagonistic activity at $P2Y_1$, $P2Y_2$ and $P2Y_4$ receptors.

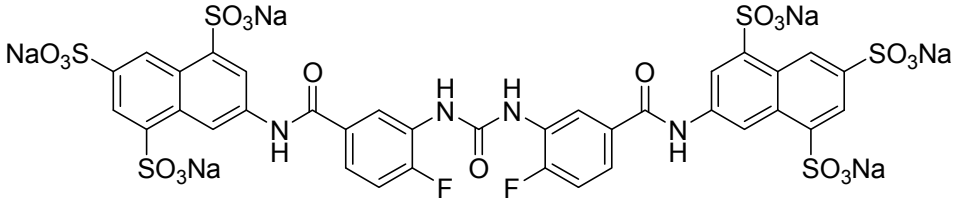

Figure 5.2 Structure formula of 5c, the most potent naphthalene sulfonate derivative in this study. App pKi value: 7.55 $\pm$ 0.07, K_i : 28 nM.

Structure activity relationships are summarized in Figure 5.3.

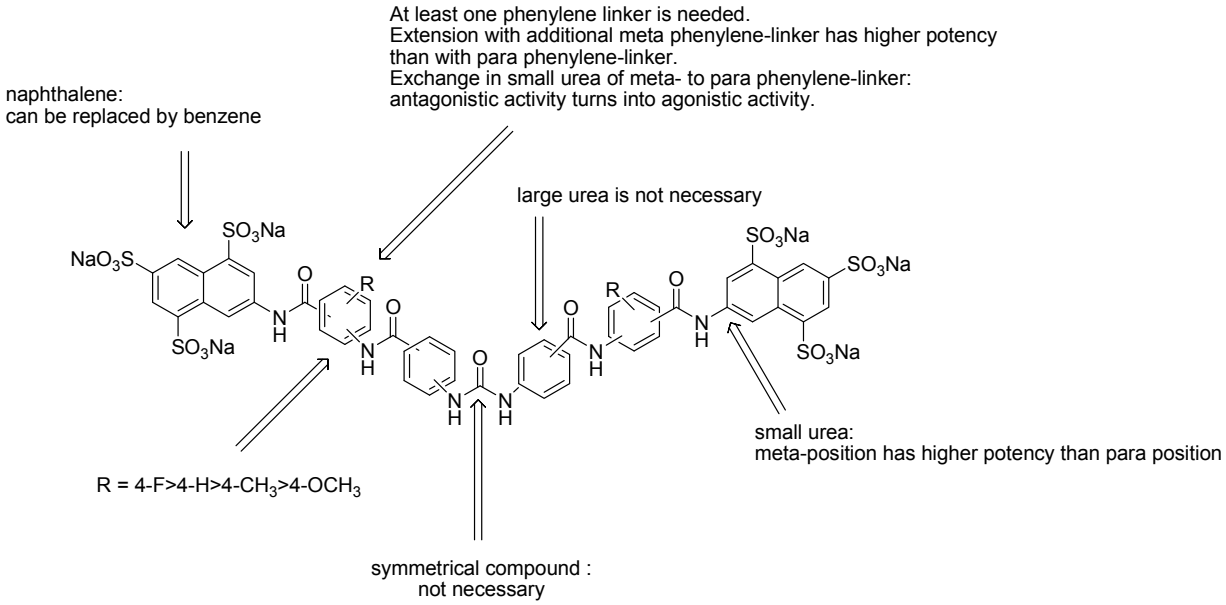

Figure 5.3 Summary scheme of structure activity relationship of sulfonate urea derivatives.

The conclusion for structure activity relationships of the compounds synthesized in this work are explained as follows:

- When comparing the activity of 2c-4c with the shortest urea compound 1c, it became evident that at least one phenylene-linker is required to obtain activity. Extension of the structures of 2c and 5c containing additional phenylene linker (large ureas) showed lower antagonistic activity than the small ureas. Therefore, it can be concluded that in this series a large urea is not necessary. This conclusion was in agreement with results reported by Hongwiset (Hongwiset, 2008). Ureas derivatives of 5c containing an additional meta phenylene-linker showed higher potency than containing an additional para phenylene-linker. A small urea containing a para phenylene-linker instead of a meta phenylene-linker turned the antagonist 5c into an agonist 8c. An extension of the structure of this agonist containing a second meta phenylene-linker (9c) increased the agonistic activity slightly.
- Small ureas containing a sulfonate moiety in meta position to the amido-linkage showed higher antagonistic potency (5c, NF294, NF340, MK094) than compounds with a para position.

- Small urea derivatives of 5c containing hydrogen, a methyl group or methoxy group at the 4 position of the phenylene linker are less potent than the fluorine substitution (5c).
- The app. pK_i values of the nitro- and amino-precursors of compound 2c-6c were estimated. Nitro and amino-derivatives showed K_i values in the range of 2.75 and 21.4 µM. This result indicated that the symmetry of the urea molecule is not required. Ullman *et al.* found that nitro and amine precursors of the urea compounds showed no activity (Ullmann *et al*., 2005), which is in contrast to the moderate or low potency of the precursors in this study.
- The naphthalene ring could be substituted by a benzene ring. Although in this study the benzene sulfonate ureas showed lower activity than naphthalene derivatives, the antagonistic activity of the benzene sulfonate ureas is in the low micro molar range (20c, IC_{50} = 9.54 µM)

In conclusion, this work introduces a potent antagonist (5c, K_i = 28.0 nM) at $P2Y_{11}$ receptors which is selective over $P2Y_1$, $P2Y_2$ and $P2Y_4$ receptors, as well as two new partial agonists (8c, 9c). This result might be helpful in the design of further improved ligands.

6. Abstract

Their roles in maturation of dendritic cells, inhibition of TNF-α release, and in myocardial contractility are reasons for investigating $P2Y_{11}$ receptors. NF157 and NF340 are known nanomolar potency $P2Y_{11}$ antagonists containing naphthalene sulfonate groups. Further, non-nucleotide agonists were recently found for $P2Y_{11}$ receptors. However, the structure-activity relationships of naphthalene sulfonate urea derivatives are not fully understood. This prompted us to synthesize variations of known $P2Y_{11}$ ligands to understand structure-activity relationships. 25 New symmetrical ureas and their precursors were synthesized. Compounds were biologically tested at $P2Y_{11}$ receptors recombinantly expressed in 1321N1 astrocytoma cells by a fluorescence calcium assay. Results led to the discovery of new agonists and antagonists. The naphthalene trisulfonate urea derivatives 8c and 9c activate $P2Y_{11}$ receptors. The EC_{50} values were 3.73 µM and 2.10 µM, respectively. Hexasodium 7,7′- {carbonylbis[azanediyl(4-fluoro-3,1-phenylene) carbonylazanediyl]}bis(naphthalene-1,3,5-trisulfonate) (5c) was the most potent competitive antagonist in this study with an app. pK_i value of 7.55 $\pm$ 0.07 (K_i = 28.0 nM) and almost as potent as NF340 (app. pK_i 7.71 $\pm$ 0.04, K_i = 19.5 nM). Structure-activity relationships were further analysed. At least one phenylene-linker is needed in the naphthalene sulfonate ureas for activity at $P2Y_{11}$ receptors. Exchange of a meta against a para phenylene-linker turned the antagonist 5c into the agonist 8c. Extension of the agonist 8c with a second meta phenylene-linker increased the agonistic activity slightly (9c). Ureas like 5c with a meta position between a sulfonate group and the amido phenylene-linker showed the highest potency. Substitution of the 4-position in the phenylene-linker of 5c resulted in the following rank order of potency -F(5c) >-H >-CH_3 >-OCH_3. A symmetrical urea is not required for activity as some precursors showed which is in accordance with previous studies. The new non-nucleotide ligands 5c, 8c, and 9c are selective for $P2Y_{11}$ over $P2Y_1$, $P2Y_2$, and $P2Y_4$ receptors. In conclusion, structure-activity relationships of naphthalene sulfonate urea derivatives are better understood and will assist in the design of improved $P2Y_{11}$ ligands.

7. Zusammenfassung

$P2Y_{11}$-Rezeptoren spielen eine wichtige Rolle bei der Modulierung der TNF-α-Freisetzung, der Reifung von dendritischen Zellen sowie der Myokardkontraktilität. NF157 und NF340 sind bekannte nanomolare $P2Y_{11}$ Rezeptorantagonisten, die beide eine Naphthalin-Sulfonat-Gruppe aufweisen. Weiterhin wurden kürzlich nicht-nukleotidische $P2Y_{11}$-Agonisten gefunden. Allerdings sind die Struktur-Wirkungs-Beziehungen von Naphthalinsulfonat-Harnstoffderivaten noch nicht vollständig geklärt. Ziel dieser Arbeit war daher, Variationen bekannter $P2Y_{11}$-Liganden zu synthetisieren. 25 Neue symmetrische Harnstoffe und deren Vorstufen wurden synthetisiert. Diese Verbindungen wurden an rekombinant in 1321N1 Astrozytoma Zellen exprimierten $P2Y_{11}$-Rezeptoren mit Hilfe eines Fluoreszenz-basierten funktionellen Calciumassay untersucht. Die Ergebnisse der biologischen Testung führten zur Identifizierung neuer Agonisten und Antagonisten. Die Naphthalin-Trisulfonat-Harnstoff-Derivate 8c und 9c aktivieren $P2Y_{11}$-Rezeptoren und weisen EC_{50}-Werte von 3,73 µM bzw. 2,10 µM auf. Hexanatrium 7,7′ {carbonylbis[azandiyl(4-fluor-3,1-phenylen)carbonylazandiyl]} bis(naphthalin-1,3,5-trisulfonat) (5c) wurde in dieser Studie als der potenteste kompetitive Antagonist mit einem pK_i-Wert von 7,55 $\pm$ 0,07 (K_i = 28,0 nM) identifiziert und weist damit eine ähnliche Potenz wie NF340 (pK_i 7,71 $\pm$ 0,04; K_i = 19,5 nM) auf. Eine Analyse der Struktur-Wirkungs-Beziehungen ergab, dass mindestens ein Phenylen-Linker für die Aktivität an $P2Y_{11}$-Rezeptoren erforderlich ist. Der Austausch eines meta- gegen einen para-Phenylen-Linker verursachte einen Wechsel der funktionellen Aktivität von antagonistisch (5c) zu agonistisch (8c). Die Verlängerung des Agonisten 8c mit einem zweiten meta-Phenylen-Linker erhöhte geringfügig die agonistische Aktivität (9c). Harnstoffe wie 5c mit einer meta-Position zwischen einer Sulfonat-Gruppe und dem Amido-Phenylen-Linker zeigten die höchste antagonistische Aktivität. Eine Variation der 4-Position des Phenylen-Linkers von 5c führte zu folgender Rangfolge der Aktivität: -F(5c) >-H >-CH_3 >-OCH_3. Ein symmetrischer Harnstoff ist für eine $P2Y_{11}$-Aktivität nicht erforderlich, wie die Ergebnisse mit Vorstufen ergaben, und steht im Einklang mit früheren Studien. Die neuen nicht-nukleotidischen Liganden

5c, 8c, und 9c sind selektiv für $P2Y_{11}$- gegenüber $P2Y_1$-, $P2Y_2$- und $P2Y_4$-Rezeptoren. Durch diese Arbeit werden die Struktur-Wirkungs-Beziehungen von Naphthalin-Sulfonat-Harnstoff-Derivaten besser verstanden und können zur Entwicklung verbesserter $P2Y_{11}$-Liganden beitragen.

8. Materials and methods

8.1. Chemistry

8.1.1. Instruments and analytical methods

8.1.1.1. pH stat

The synthesis of the nitro derivatives and urea compounds of sulfonate analogues were carried out using a pH stat instrument produced by Metrohm AG, Herisau, Switzerland.

Instrument:

- Titrator E-256
- Integrated pH-glass electrode Metrohm (6.0202.020)
- Metrohm turning unit 535-138 (6.1518.153)
- Metrohm dosimeter 655

During the reaction, pH was maintained by automatic addition of 2 M Na_2CO_3 to the solution.

8.1.1.2. Thin layer chromatography

TLC-plate: Silica gel 60 F_{254}, 0.2 mm thick, 20 x 20 cm. Merck, No. 1.05554.

Mobile phase:

- MP1: 2-propanol + NH_3 (25 %) (7 + 3)
- MP2: 2-propanol + NH_3 (25 %) + water (7 + 3 + 0.5)

Detection:

- UV light at 254 nm and 366 nm (UV-Cabinet II, CAMAG Berlin)
- Ehrlich reagent modification (2.0 g of 4-dimethylamino-benzaldehyde in 25 ml of glacial acetic acid and 75 ml of methanol)

Analysis: R_f value :

$$R_f = \frac{a}{b} \qquad \textbf{E.6.1}$$

a = distance reached by substance

b = distance reached by mobile phase

8.1.1.3. High performance liquid chromatography

Instrument:

- Pump: HP series 1050 with 4 solvent flasks degassing with helium
- Software: Chemstation HP 79994 A
- Manual syringe: Rheodyne 7125 (20 µl)
- Syringe: 10 µl Hamilton 701 NR Rheodyne
- Diode array detector (DAD) HP1040 A
- Flexible steel capillary with inner diameter of 0.12 mm
- Magnetic stirrer Heidolph MR 2002
- HP Think Jet Printer

Column: RP-8, MOS-Hypersil, 5 µm, 100 x 2.1 mm with pre column RP-8, MOS-Hypersil, 5 µm, 20 x 2.1 mm

Injection volume: 10 µl

Detection: UV at 220 nm, 254 nm and 299 nm

Flowrate: 0.6 ml/min

Mobile phase (Kassack and Nickel, 1996):

- A: Phosphate buffer (0.02 M), pH 6.5. 931 mg NaH_2PO_4 (7.76 mM), 1737.6 mg Na_2HPO_4 (12.24 mM) and 2122 mg tetrabutylammonium hydrogensulfate (TBAHS) (6.25 mM) in 1000 ml distilled water)
- B: Methanol (HPLC grade)

Gradient system:

Time (min)	A(%v/v)	B (%v/v)
0	80	20
0-8	46	54
8-9	20	80
9-11	80	20

8.1.1.4. UV-visible spectrophotometry

Ultraviolet spectra of compounds were obtained from HPLC-DAD. The spectra were measured at wavelengths from 210-400 nm. The wavelength of maximum absorption was further determined.

8.1.1.5. Titration method: NaCl determination

NaCl determination was carried out using an instrument produced by Metrohm AG, Herisau-Switzerland.

Instrument:

- Titrator 672
- Electrode : Micro-silver-titrode (6.0433.100)
- Metrohm turning unit 535-138 (6.1518.153)
- Metrohm dosimeter 655
- Vessel EA 875-5

Approximately 15 mg sample were diluted in 8 ml bidistilled water and 2 ml acetic acid were added and were titrated with 0.1 N silver nitrate solution. NaCl was estimated by potentiometric titration method.

$$NaCl\ (\%) = \frac{58.44\ x\ V\ x\ N\ x\ 100}{m} \qquad \textbf{E.6.2}$$

V = volume of 0.1 N silver nitrate (ml)
N = normality of silver nitrate
m = weight of test compound (mg)

8.1.1.6. Elemental analysis

Instrument **:**

- Vario EL, Firma Elemental Analysensysteme GmbH (University of Bonn)
- PerkinElmer PE 2400 CHN elemental analyzer (University of Düsseldorf)

CHN analyse and C/N ratio confirmed the purity by comparison with theoretical values. Most of % C and % H results showed a great deviation from calculation because of crystal water, sodium chloride and other impurities. Thus, calculation

including water contents and sodium chloride was performed and then values were compared to the found results (Ullmann *et al.*, 2005).

8.1.1.7. Infrared spectroscopy

Instrument: PerkinElmer FT IR-spectralphotometer

Sample: Compounds were prepared as a KBr pellet

Characterization (% transmission, cm^{-1}):

- br: broad
- vs: very strong 10-0
- s: strong 30-10
- m: medium 50-30
- w: weak 70-50
- vw: very weak 90-70

8.1.1.8. Nuclear magnetic resonance spectroscopy

Instrument: ^{13}C NMR 125 MHz Bruker AC-200
^{1}H NMR 500 MHz Bruker Avance DRX 500

Spectra: ^{1}H, D_2O exchangeable, ^{13}C, H-H COSY (Correlation Spectroscopy) and HSQC (Heteronuclear single quantum correlation)

Analysis: Compounds were diluted in DMSO-d_6 or D_2O. The chemical shift was presented in δ = ppm. Tetramethylsilane (TMS) was used as internal standard.

The NMR spectra were measured at the Institute of Pharmaceutical Chemistry University of Bonn or the Institute of Inorganic Chemistry, University of Düesseldorf (Dr. Peters and colleagues).

8.1.1.9. ESI-Mass spectrometry

Instrument: ESI-Finnigan MAT 4000 and ESI-Finnigan MAT 8200

The mass spectra were measured at the Institute of Pharmaceutical Biology (Dr. Ebel and Ms. Julia Kjer) or the Institute of Inorganic Chemistry, University of Düsseldorf (Dr. Keck and Dr. Tommes).

8.1.2. Chemical

Ammonia solution 25 % (05003)	Riedel-deHäen
4-Dimethylaminobenzaldehyd (59143)	Merck
N,N-Dimethylformamide (2937)	Merck
Diethylether (923)	Merck
Disodium aminobenzene-1,4-disulfonate *)	Bayer AG
Disodium aminobenzene-2,4-disulfonate (328-43135)	Wako Lab
Disodium 7-aminonaphthalene-1,5-disulfonate (326-20671)	Wako Lab
Disodium 8-aminonaphthalene-4,6-disulfonate (N60-5)	Aldrich
4-Fluorobenzoic acid (156161000)	Merck
Hydrochloric acid 30 % (59415)	Merck
Methanol, HPLC grade (6009)	Merck
2-Methyl-3-nitrobenzoic acid (818485)	Merck
2-Methyl-5-nitrobenzoic acid (841114)	Merck
4-Methyl-3-nitrobenzoic acid (15.140-0)	Aldrich
4-Methoxy-3-nitrobenzoic acid (187830250)	Fluka
4-Nitrophenyl acetic acid (800599)	Merck
3-Nitrobenzoylchloride (73110)	Fluka
4-Nitrobenzoylchloride (806772)	Merck
5-Nitroisophthalic acid (N1, 800-5)	Aldrich
Palladium/active carbon (10 % Pd) (807104)	Merck
Phosgene (20 % in toluene) (79380)	Fluka
Sodium carbonate (0274)	Baker
Sodium dihydrogen phosphate p.a. (7496)	Fluka
di-Sodium hydrogen phosphate (71640)	Fluka
Sodium aminobenzene-2-sulfonate *)	Bayer AG
Sodium 8-Aminonaphthalene-5- sulfonate *)	Bayer AG
Sodium 8-Aminonaphthalene-2- sulfonate *)	Bayer AG
Silver nitrate solution 0.1 M (35375)	Riedel-deHäen
Tetrabutylammonium hydrogensulfate (TBAHS) (86868)	Fluka
Thionylchloride (88952)	Fluka

Toluene (34866)	Riedel-deHäen
Trisodium 7-aminonaphthalene-1,3,5-trisulfonate (328-200712)	Wako Lab
Trisodium 8-aminonaphthalene-1,3,5-trisulfonate *)	Bayer AG

*) *Gift from Bayer AG. Leverkusen.*

8.1.3. General reaction procedures (GRP)

8.1.3.1. GRP 1: Preparation of acylchloride

To a suspension of approximately 25 mmol nitrobenzoic acid derivative in 50 ml toluene and DMF (0.5 ml), an excess of thionylchloride (approximately 75 mmol) was added and stirred under reflux for approximately two hours until the reaction mixture turned into a clear solution. Excessive thionylchloride and toluene were removed under vacuum. The obtained products were dissolved in 25 ml toluene and immediately used for the acylation reaction.

8.1.3.2. GRP 2: Synthesis of nitro derivative

Approximately 7.5 mmol of the nitro benzoic acid chloride derivative dissolved in toluen were slowly dropped to the stirred solution of approximately 5 mmol amine derivative in water. During the acylation process, for sulfonate analogues, the reaction mixture was kept at constant pH of 3.8 by automatic addition of 2 M Na_2CO_3 solution. The reaction was controlled by TLC. After separating the water phase from the toluene phase, pH was adjusted to 2.0 and the aqueous phase was extracted three times with diethylether. The aqueous phase was then adjusted to pH 7.0 and the solvent was removed under vacuum. NaCl was removed by stirring the crude product in methanol and controlled by NaCl determination.

8.1.3.3. GRP 3: Synthesis of amine derivative

20 mg of Palladium (10 %) on charcoal were added as catalyst to a solution of approximately 5 mmol nitro derivative in 50 ml water, at pH 7. Under heavy stirring, the reaction mixture was hydrogenated under pressure (4.0 bar) in a Parr

apparatus for approximately 12 hours. The reaction was controlled by TLC. Pd/C was then filtrated and the solvent was removed under vacuum.

8.1.3.4. GRP 4: Synthesis of urea compound

Preparation of ureas of sulfonate analogues was carried out as follows: approximately 10 mmol phosgene (20 % in toluene) were slowly added to a solution of approximately 5 mmol amine derivative in water under heavy stirring at room temperature. The reaction mixture was kept constant at pH 4 by automatic addition of 2 M Na_2CO_3 solution. The reaction was controlled by TLC. The aqueous phase was adjusted to pH 7.0 and the solvent was removed under vacuum. NaCl was removed by stirring the crude product in methanol and controlled by NaCl determination.

8.2. Biological testing

8.2.1. Instruments and materials

NOVOstar® Microplate reader with injector	BMG Lab Tech
Accujet pipette	Brand
Autoclave (V-65)	Systec
Centrifuge: Micro 200 R (2405)	Hettich
Centrifuge: Rotina 420 R (4708)	Hettich
Cell counter clicker (1-7510)	IVO
Neubauer cell counter chamber	Optic Lab
Cryo vial: cryo pure, 2 ml with quick seal top	Sarstedt
Culture flask (T175, T75)	Sarstedt
Microtube: 1.5 ml	Sarstedt
PP-tube: 15 ml and 50 ml	Sarstedt
Incubator: Heraeus (BB15)	Thermo
Microbiological safety bench advantage series	Thermo
Multichannel pipette: 20-200 µl	Capp
Measurement plate: flat-bottom, 96 wells	Sarstedt
Microscope (AE 21)	Motic
Reagent plate: U-bottom, 96 wells	Sarstedt
Rotation vortex	IKA
Water bath	Julabo

8.2.2. Chemicals

Adenosine-5'-triphosphate (ATP) (A-7699)	Sigma-Aldrich
Calcium chloride x 2 H_2O, p.A. (08-307.1000)	KMF-Optichem
Dimethylsulfoxide (DMSO) (167852500)	Riedel-de Häen
D-Glucose x 1 H_2O for microbiology (16325)	Riedel-de Häen
Dulbecco's modified Eagle's medium (DMEM) (D 6546)	Sigma-Aldrich
Fetal bovine serum (F7524)	Sigma-Aldrich
Geneticindisulfate (G418) (345810)	Calbiochem
4-(2-hydroxyethyl)-1-piperazineethanesulfonic acid (HEPES) (79694)	ICN Biomedical

L-glutamine (G 7513)	Sigma-Aldrich
Sodium chloride, p.A. (0525901026)	J.T Baker
Sodium bicarbonate, p.A. (31431)	BDH Prolabo
2-Methylthioadenosin-5'-diphosphate (2-MeSADP) (M-152)	Sigma-Aldrich
Magnesium sulfate x 7 H_2O, p.A. (63140)	Fluka
Oregon Green® 488 BAPTA-1/AM (OG 807)	Invitrogen
Pluronic F-127 (P-2443)	Sigma-Aldrich
Penicillin/streptomycin (P-0781)	Sigma-Aldrich
Potassium chloride, p.A. (26764.298)	Roth
Potassium dihydrogenphosphate, p.A. (3904.1)	Roth
Disodium hydrogenphosphate, p.A. (28029292)	BDH Prolabo
Trypsin-EDTA solution (1x) (T-3924)	Sigma-Aldrich
Uridin-5'-triphosphate (UTP) (U-6625)	Sigma-Aldrich

8.2.3. Buffers and solutions

Adenosinetriphosphate (ATP) solution 10 mM

55.11 mg ATP were dissolved in 10 ml bidistilled water and diluted in 1x KHB. The solution was stored at -20 °C.

Geneticindisulfate (G418)-solution 100 mg/ml

About 5 g of G418 powder were weighed. Under consideration of the value of the specific activity (µg/mg), G418 was dissolved in a certain amount of bidistilled water using the following equation:

$$\text{Water amount}\,(\mu l) = \frac{Activity(\mu g / mg)\; x\; \text{G418}\,(\text{mg})}{100(mg / ml)} \qquad \textbf{E.6.3}$$

The solution was sterile filtrated and was divided into 1 ml aliquots under aseptic conditions. Aliquots were stored at -20 °C. 2 ml solution were added to 500 ml growth medium (400 µg/ml).

Krebs-HEPES-Buffer 5x (KHB 5X)

- 17.33 g NaCl (590 mM)
- 0.876 g KCl (23.5 mM)
- 0.408 g KH_2PO_4 (6 mM)
- 0.882 g $NaHCO_3$ (21 mM)
- 5.79 g D-Glucose x 1 H_2O (21 mM)
- 5.69 g HEPES (50 mM)
- 500 ml bidistilled water

Reagents were dissolved in bidistilled water and were adjusted to pH 7.4. The solution was divided into 100 ml aliquots. The aliquots were stored at -20 ^oC.

Calcium chloride solution (1 M)

1.47 g $CaCl_2$ x 2 H_2O were dissolved in 10 ml bidistilled water and were stored at 4 ^oC.

Magnesium sulfate solution (1 M)

2.465 g $MgSO_4$ x 7 H_2O were dissolved in 10 ml bidistilled water and were stored at 4 ^oC.

Krebs-HEPES-Buffer 1x (KHB 1X)

- 100 ml KHB 5 X
- 650 µl 1M $CaCl_2$ solution (1.3 mM)
- 600 µl 1M $MgSO_4$ solution (1.2 mM)

One aliquot of KHB 5 X (100 ml) was dissolved in 500 ml bidistilled water. 650 µl of 1M $CaCl_2$ and 600 µl 1M $MgSO_4$ solution were added.

Oregon Green® 488 BAPTA-1/AM solution 1 mM

A 50 µg aliquot of Oregon Green® BAPTA-1 AM was diluted in 39.7 µl DMSO and was divided into 3 µl aliquots in 1.5 ml Eppendorf caps. The aliquots were stored at -20 ^oC and protected from light.

Phosphate-Buffered-Saline 1x (PBS)

- 8.0 g NaCl (140 mM)
- 0.2 g KCl (3 mM)
- 1.44 g Na_2HPO_4 x 2 H_2O (8 mM)
- 0.24 g KH_2PO_4 (1.5 mM)
- 1000 ml bidistilled water

All reagents were dissolved in 1000 ml bidistilled water and pH was adjusted to 7.4. The solution was then autoclaved and stored at 4°C.

Pluronic F-127 solution 20 %

0.2 g Pluronic F-127 were diluted in 1 ml DMSO.

8.2.4. Cell culture method

8.2.4.1. General aspects

All cell culture techniques were carried out under aseptic conditions by using a workbench with sterile laminar airflow. Cells were cultivated in an incubator at 37 ^{o}C, under 5 % CO_2 atmosphere, and 96 % humidity. Within this study, $P2Y_1$, $P2Y_2$, $P2Y_4$, and $P2Y_{11}$ receptors were used for biological testing. The receptors are recombinantly expressed in 1321N1 astrocytoma cells. The $P2Y_1$, $P2Y_2$, and $P2Y_{11}$ cell lines were established by S. Meis using cDNA clone from the UMR cDNA resource center (Meis, 2008). 1321N1 $P2Y_4$ receptor expressing cells were kindly provided by Prof. Gachet, University of Strassbourg.

8.2.4.2. Growth medium

Dulbecco's Modified Eagle's Medium (DMEM) was used as growth medium for 1321N1 $P2Y_1$, $P2Y_2$, $P2Y_4$, and $P2Y_{11}$ receptors. 500 ml DMEM was supplemented under aseptic conditions with:

- 10 % fetal bovine serum
- 5 mM L-glutamin
- 100 U/ml penicillin G

- 100 µg/ml streptomycin (6 ml of the mixture)
- 400 µg/ml G418

Complete growth medium was stored at 4 °C. Growth medium was first warmed at 37 °C for 15 minutes in a water bath. Medium must be changed one day after cells thawing from cryoconservation. The next change of medium depends on the cell vitality that was observed under microscope and the color of medium.

8.2.4.3. Detaching process

The cell lines were collected from T-175 culture flask. The cells were detached with the following method: medium was first aspirated with pipette helper. 3 ml of PBS were added and aspirated. 3 ml trypsin EDTA were added. After all the cells were detached, 7 ml growth medium were added and the suspension was centrifuged in a sterile 50 mm PP-tube (266 x g, 4 °C for 4 minutes). The supernatant was aspirated and the cell pellet was used as needed.

8.2.4.4. Cryoconservation

Cells were detached using method at 8.2.4.3. The cell pellet was suspended in FBS containing 10 % DMSO and was divided into cryo caps in an amount of 1 ml. The caps were stored in 80 °C freezer for one day and were then moved into liquid nitrogen environment (-196 °C).

8.2.4.5. Passaging cells

Cell lines from cryoconservation were thawed in the water bath at 37 °C. The suspension was added to T75 culture flask filled with 20 ml medium. After cultivation, confluent cells (80-90 %) were split to another passage. The cells were detached first (s. 8.2.4.3). The cell pellet was resuspended in 10 ml medium and 1 ml of cells was transferred to T-75 or T-175 flask. 20 ml and 30 ml medium were added to T-75 and T-175 flask, respectively. The cells had to be passaged two times after thawing before was used for the first assay.

8.2.5. Biological testing technique

8.2.5.1. Preparation of the dilution series

Stock solutions of standard agonists (ATP, 2-MeSADP, UTP), antagonist (NF157) and compounds were prepared in concentration of 10 mM in bidistilled water and the dilution series in KHB. The solutions were then stored at -20 ^{o}C.

8.2.5.2. Assay preparation

The assay was carried out using methods established by Lin *et al.* and Kassack *et al.* (Lin *et al.*, 1999; Kassack *et al*, 2002). The methods are explained as follows:

Cell harvesting

90 % confluent cells were detached (s. 8.2.4.3) and harvested from the T-175 flask. After centrifugation, pelleted cells were resuspended in new medium and incubated at 37 ^{o}C, under 5 % CO_2 atmosphere and 96 % humidity for 15 minutes. After 15 minutes, the cells were centrifuged and the supernatant was aspirated.

Cell incubation with fluorescence dye

The cell pellet was resuspended with 800 µL 1x KHB in an Eppendorf cap and then centrifuged with fast impulse up to 8000 rpm. The process was repeated for a total of three washes. The pellet was resuspended in 500 µL 1x KHB solution and then added to 3 µL Oregon Green® BAPTA-1/AM and 3 µL Pluronic F-127. The mixture was incubated at room temperature in a Vortex at 600 rpm for 60 minutes. Calcium-sensitive fluorescence indicator BAPTA is a polycarboxylate compound derived from EGTA (ethylene glycol-bis-(β-amino-ethyl ether) N, N, N′, N′-tetra-acetic acid) (Monteith and Bird, 2005; Rudolf *et al.*, 2003; Takahashi *et al.* 1999).

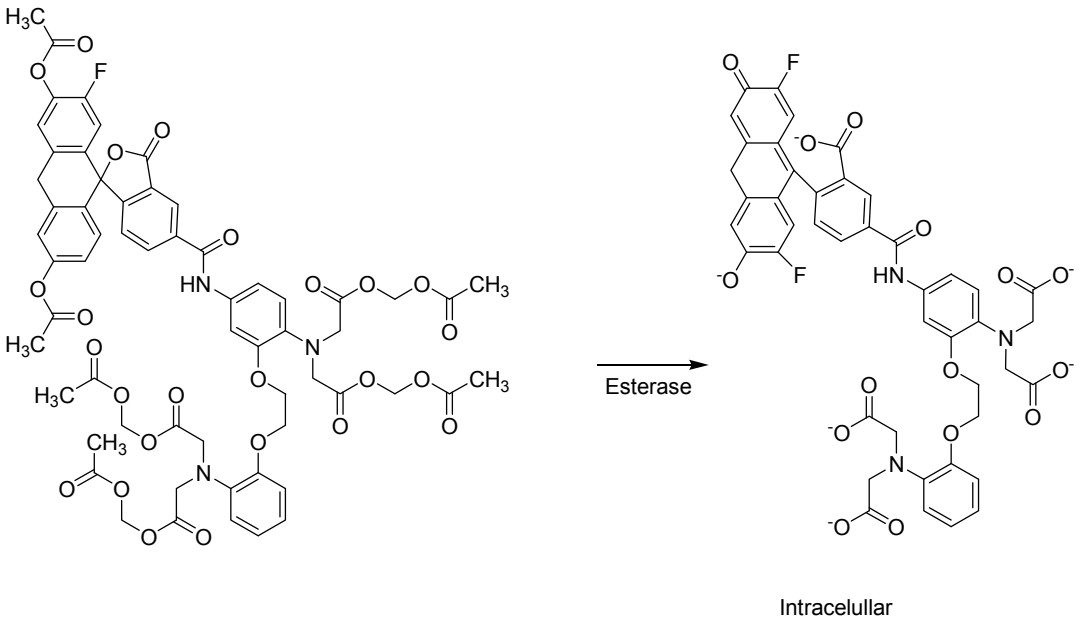

Figure 8.1 Oregon Green® 488 BAPTA-1/AM
Unspecific esterase hydrolyzes ester groups. The product binds Ca^{2+} to build a chelate complex.

In this study, Oregon Green® 488 BAPTA-1AM (OG) was used as a single excitation wavelength dye. This dye is a compound combining the fluorescent dye Oregon Green® 488 and BAPTA (1,2-bis(o-aminophenoxy) ethane-N,N,N',N',-tetraacetic acid) as a calcium-specific chelator. Liphophil and calcium insensitive compound could pass the cell membrane by passive diffusion. Unspecific endogenous esterases hydrolyze the ester to a polyanion calcium sensitive dye. After calcium binding, the fluorescence intensity would raise (Haughland, 2006).

Cell transfer

After 60 minutes, the mixture was centrifuged and the supernatant was aspirated. Cells were resuspended with 800 µl KHB and then centrifuged with short spin up to 8000 rpm. The process was repeated two times. In the last step, the cells were resuspended in 1 ml KHB and placed in a cell reservoir. KHB were added to the reservoir according to Table 8.1. With the multichannel pipette, the cells were transferred to the 96 well measurement plate at a density of 50,000 -100,000 cells/well.

Table 8.1 Volume of cell suspension and compounds per well each screening.

Screening	Cell suspension per well	Test compound per well	Standard agonist per well
Agonist	180 µl	20 µl	-
Antagonist	160 µl	20 µl	20 µl
Agonist followed by antagonist	160 µl	20 µl	20 µl

End incubation

Cells were incubated at 37 ^{o}C for 30 minutes before the assay began.

8.2.5.3. Screening of compounds

Screenings for agonistic and antagonistic behaviour of compounds was performed. For agonist screening, 180 µl cell suspension in KHB were placed in measurement plate and 20 µl test compounds with concentration of 10 µM and 100 µM, respectively were injected from the reagent plate into the measurement plate. Responses were compared with the response of 1 µM ATP as 100 % of control at $P2Y_{11}$ receptors. For antagonist screening, 160 µl cell suspension were placed in measurement plate, then 20 µl of 10 µM or 100 µM compounds were added, respectively and incubated at 37 ^{o}C for 30 minutes. 20 µl of 1 µM ATP were then injected from the prepared reagent plate to the measurement plate using the NOVOstar® injector. The final volume per well was 200 µl.

Compounds were further screened at $P2Y_1$, $P2Y_2$ and $P2Y_4$ receptors. Agonist and antagonist screening at those receptors were carried out using the same method. 1 µM UTP was used as standard of agonist at $P2Y_2$ and $P2Y_4$ receptors and 31.6 nM 2-MeSADP were used as standard of agonist at $P2Y_1$ receptors.

8.2.5.4. Assay condition

Using NOVOstar® software, Ca^{2+}-assay was carried out with the following setting:

1. Basic parameters:
   - Excitation filter: 485 nm
   - Emission filter: 520 nm
   - Positioning delay: 0.5 s
   - Measurement temperature: 37 ^{o}C
   - Reading direction: horizontal
2. Kinetic windows:
   - Interval of measuring fluorescence intensity: 0.4 s
   - Duration of measurement: 33.6 s per well
   - Total measuring time: 57 min, 16 s (for 96 wells)
3. Injection setting:
   - Injection volume: 20 µl of solution
   - Injection speed: 33 µl/s
   - Wash cycles: 1
   - Rinse cycles: 3
4. Gain adjustment:
   - Required value: 50 % (gain value was calculated from the mean of 5 wells)

8.2.5.5. EC_{50} and IC_{50}

IC_{50} is the molar concentration of an antagonist that reduces the response of an agonist by 50 % whereas EC_{50} is the molar effective concentration of an agonist that produces 50 % of the maximal possible effect in the chosen test system. Compounds with a significant agonist activity in a first primary screening were further investigated to determine their EC_{50} values. A series of dilution concentrations was made to monitor the concentration response curve (CRC) using agonist mode. For potent antagonists a series of dilution concentrations was made to build concentration inhibition curves (CIC) in the antagonist mode (s.8.2.5.3). CICs were used to determine IC_{50} values.

8.2.5.6. Data analysis

All data were analyzed using NOVOstar® software, supported by Microsoft® Excel Program. At the point of injection, fluorescence intensity has the lowest value and was marked as „minimum“. The highest fluorescence intensity evoked by injection of agonist was marked as „maximum“. Minimum was subtracted from maximum and the difference was used as a measure for the response (E 6.4).

$$F = F\max - F\min \qquad \textbf{E.6.4}$$

F: Fluorescence signal produced by an agonistic compound
F_{Max}: maximum intensity after the injection of a compound (between 11.6 - 30 s)
F_{Min}: minimal intensity before injection of the substance (between 0 - 11.5 s)

Data were then normalized compared to the respective standard agonist. For agonist screening the result was reported as % of control and calculated from the comparison of the fluorescence intensity of the test compound, of buffer, and of the standard agonist. The fluorescence intensity evoked by standard agonists was set as maximal stimulation (100 %), whereas the fluorescence intensity of buffer was set as 0 % control. For antagonist screening the result was reported as % inhibition as a result of subtraction of % of control from 100%. A concentration-response curve or concentration-inhibition curve was constructed by plotting the fluorescence intensities (F) against log concentrations of test compound. An EC_{50} or IC_{50} was estimated, using nonlinear regression analysis by the software GraphPad Prism 4.00®.
The apparent inhibition constant was estimated according to equation E.6.5. The EC_{50} value of standard agonist at $P2Y_{11}$ receptors was measured from series of ATP dilutions in the same measurement plate as the test compound. The apparent pK_i was estimated according to a modified Cheng and Prusoff equation (Cheng and Prusoff, 1973).

$$K_i = \frac{IC_{50}}{1 + \frac{C(agonist)}{(EC_{50})agonist}} \qquad \textbf{E.6.5}$$

K_i = constant of inhibition

C = concentration of standard agonist (M)

$$App.pK_i = -\log Ki \qquad \textbf{E.6.6}$$

8.2.5.7. Schild-analyse

Analysis of competitive character of compound 5c and 9c were carried out using Schild-analyse experiments. For agonist 9c, concentration-response curves of each compound in the absence and in the presence of 10 nM, 31.6 nM, 100 nM, and 316 nM of NF157 were monitored and an EC_{50} of each concentration was calculated. Meanwhile, for antagonist compound 5c, concentration-response curves of ATP in the absence and in the presence of 31.6 nM, 100 nM, 316 nM, 1 µM, and 3.16 µM of compound 5c were monitored and an EC_{50} of each concentration was estimated. The obtained EC_{50} values were further used for analysis by linear regression method (Arunlakshana and Schild, 1957). Schild analysis DR (Dose ratio) was calculated according to the equation E.6.7

$$DR = EC_{50}{}^{¤}/EC_{50} \qquad \textbf{E.6.7}$$

$EC_{50}{}^{¤}$: The EC_{50} of agonist obtained in the presence of antagonist.

EC_{50}: The EC_{50} of agonist obtained in the absence of antagonist.

A plot of (DR-1) against log concentration of each compound was performed and analysed by linear regression, using the software GraphPad Prism 4.00®. A pA_2 was calculated from an X-intercept of the plot. If the slope was not significantly different from unity, a competitive character could be assumed.

9. Monographs

Trisodium 7,7′-(carbonylbisazanediyl)bis(naphthalene-1,3,5-trisulfonate) 1c

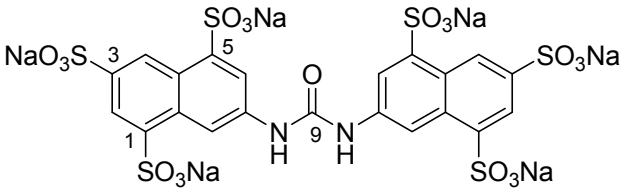

$C_{21}H_{10}N_2Na_6O_{19}S_6$ (924.6)

A solution of 1.6 mmol phosgene (20 % in toluene) was slowly added to a solution of 400 mg (0.8 mmol) trisodium 7-aminonaphthalene-1,3,5-trisulfonate in 20 ml water, under heavy stirring at room temperature. The reaction was carried out according to GRP 4.

Yield: white powder, 60.5 % (242 mg)
TLC: R_f = 0.48 (MP2)
HPLC: 96.9 % (t_R = 3.35 min)
UV spectrum (phosphate buffer pH of 6.5): λ_{max} = 264.5 nm
NaCl: 67.9 %

Elemental analysis (%):

	C	H	N	C/N
Calculation:	27.3	1.09	3.03	9.00
Calculation with H_2O and NaCl:	8.35	0.50	0.93	9.00
Found:	8.63	0.89	1.05	8.22

Water content: 2 mol/mol

ESI-MS negative mode: m/z
$[M-Na]^-$: 901.4

IR spectrum (cm^{-1}):

3457 (br, s)	2361 (w)	1616 (m)	1551 (w)
1474 (m)	1406 (w)	1219 (br, s)	1118 (w)
1077 (w)	1043 (s)	798 (w)	668 (m)
614 (m)	532 (w)		

500 MHz ^{1}H NMR spectrum (DMSO-d_6): δ (ppm), *J* (Hz)

9.32	-NH-CO-NH-	s	1H (exchangeable)
9.10	H8	dd (^5J = 0.6, ^4J = 1.9)	1H
8.79	H4	dd (^5J = 0.6, ^4J = 2.2)	1H
8.43	H2	d (^4J = 2.2)	1H
8.25	H6	d (^4J = 1.9)	1H

125 MHz ^{13}C NMR spectrum (DMSO-d_6): δ/ppm

152.9	C9	136.2	C3	123.5	C6
145.4	C7	130.4	C8a	118.5	C2
142.0	C5	125.4	C4a	115.2	C4
141.7	C1	125.2	C8		

Trisodium 7-(3-nitrobenzamido)-naphthalene-1,3,5-trisulfonate
2a

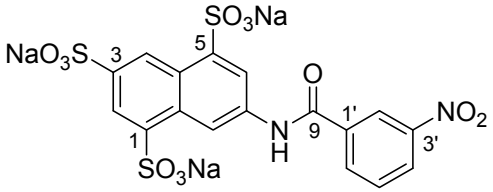

$C_{17}H_9N_2Na_3O_{12}S_3$ (598.4)

916.7 mg (4.94 mmol) 3-Nitrobenzoylchloride dissolved in 10 ml toluene were slowly added to the stirred solution of 1.0 g (2.22 mmol) trisodium 7-aminonaphthalene-1,3,5-trisulfonate in 50 ml water, until there was no precursor left. The reaction was carried out according to GRP 2.

Yield: white powder, 92.0 % (1.4 g)
TLC: R_f = 0.77 (MP 1)
HPLC: 96.8 % (t_R = 3.34 min)
UV spectrum (phosphate buffer pH of 6.5): λ_{max} = 258.5 nm
NaCl: 4.70 %

Elemental analysis (%):

	C	H	N	C/N
Calculation:	34.1	1.5	4.7	7.3
Calculation with H_2O and NaCl:	28.3	2.7	3.9	7.3
Found:	28.2	2.5	4.0	7.1

Water content: 5 mol/mol

IR spectrum (cm^{-1}):

3463 (br, s)	1677 (s)	1616 (m)	1577 (m)
1551 (s)	1530 (s)	1467 (w)	1438 (w)
1329 (s)	1356 (m)	1195 (b.s)	1117 (s)
1079 (m)	1043 (vs)	918 (vw)	795 (m)
770 (vw)	714 (m)	671 (s)	615 (vs)
529 (m)			

500 MHz ^{1}H NMR spectrum (DMSO-d_6): δ (ppm), J (Hz)

10.92	NH-CO	s	1H exchangeable
9.14	H8	dd (^5J = 0.6, ^4J = 1.6)	1H
9.08	H4	d (^4J = 1.9)	1H
8.89	H2′	t (^4J = 2.2)	1H
8.49	H6′	d (^3J = 7.9)	1H
8.47	H2	d (^4J = 1.9)	1H
8.43	H4′	dd (^5J = 0.9, ^4J = 2.2)	1H
8.29	H6	d (^4J = 1.6)	1H
7.85-7.82	H5′	t (^3J = 7.9)	1H

125 MHz ^{13}C NMR spectrum (DMSO-d_6): δ (ppm)

163.5	C9	134.8	C6′	125.2	C8
147.9	C3′	134.5	C3	123.5	C6
145.3	C7	130.2	C5′	122.8	C2′
143.0	C5	130.1	C8a	120.9	C2
142.8	C1	126.6	C4′	119.5	C4
136.4	C1′	126.2	C4a		

Trisodium 7-(3-aminobenzamido)-naphthalene-1,3,5-trisulfonate
2b

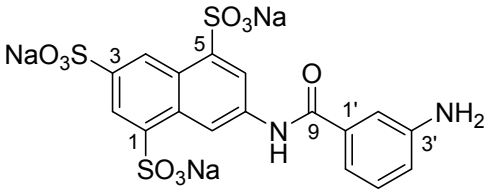

$C_{17}H_{11}N_2Na_3O_{10}S_3$ (568.4)

20 mg Palladium (10%) on charcoal were added as catalyst to a solution of 854.7 mg (1.4 mmol) compound 2a in water. The reaction was carried out according to GRP 3.

Yield: beige powder, 90.2 % (733 mg)
TLC: R_f = 0.77 (MP 1)
HPLC: 97.5 % (t_R = 3.34 min)
UV spectrum (phosphate buffer pH of 6.5): λ_{max} = 258.5 nm
NaCl: 3.60 %

Elemental analysis (%):

	C	H	N	C/N
Calculation:	35.9	1.9	4.9	7.3
Calculation with H_2O and NaCl:	27.6	3.7	3.8	7.3
Found:	27.6	3.4	3.9	7.2

Water content: 8 mol/mol

IR spectrum (cm^{-1}):

3444 (br, s)	1663 (m)	1577 (m)	1549 (m)
1473 (m)	1442 (w)	1329 (s)	1295 (m)
1189 (b, s)	1124 (s)	1076 (w)	1039 (vs)
882 (vw)	791 (m)	733 (m)	667 (s)
524.20 (m)			

500 MHz ^{1}H NMR spectrum (DMSO-*d*$_6$): δ (ppm), *J* (Hz)

10.92	NH-CO	s	1H exchangeable
9.12	H8	dd (^{4}J = 2.0, ^{5}J = 0.6)	1H
8.99	H4	dd (^{4}J = 2.1, ^{5}J = 0.6)	1H
8.39	H2	d (^{4}J = 2.1)	1H
8.27	H6	d (^{4}J = 2.0)	1H
7.19	H2′, H6′	m	2H
7.13	H5′	t (^{3}J = 7.9)	1H
6.74	H4′	dd (^{3}J = 7.9, ^{4}J = 2.0)	1H
5.23	-NH_2	s	2H exchangeable

125 MHz ^{13}C NMR spectrum (DMSO-*d*$_6$): δ (ppm)

166.4	C9	135.5	C3	121.3	C2
148.8	C3′	130.2	C8a	119.4	C4
145.1	C7	128.7	C5′	116.9	C4′
142.8	C5	126.4	C4a	115.2	C6′
142.5	C1	125.2	C8	113.4	C2′
135.8	C1′	123.4	C6		

Trisodium 7,7′-{carbonylbis[azanediyl(3,1-phenylene)carbonylazanediyl]}bis(naphthalene-1,3,5-trisulfonate) 2c

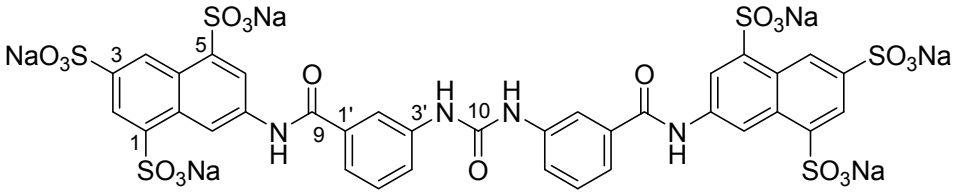

$C_{35}H_{20}N_4Na_6O_{21}S_6$ (1162.9)

A solution of 1.76 mmol phosgene (20 % in toluene) was slowly added to a solution of 500 mg (0.88 mmol) compound 2b under heavy stirring at room temperature. The reaction was carried out according to GRP 4.

Yield: beige powder, 88.2 % (902 mg)
TLC: R_f = 0.70 (MP 2)
HPLC: 98.0 % (t_R = 4.64 min)
UV spectrum (phosphate buffer pH of 6.5): λ_{max} = 258.5 nm
NaCl: 2.50 %

Elemental analysis (%):

	C	H	N	C/N
Calculation:	36.2	1.70	4.8	7.5
Calculation with H_2O and NaCl:	28.4	3.00	3.8	7.5
Found:	28.1	3.20	3.8	7.3

Water content: 16 mol/mol

ESI-MS negative mode: m/z
$[M-H]^-$: 1161.3, $[M-Na]^-$: 1139.3, $[M-2Na+H]^-$: 1117.3

IR spectrum (cm^{-1}):

3440 (br, s)	1591 (m)	1540 (s)	1472 (m)
1436 (m)	1402 (w)	1327 (m)	1192 (b.s)
1125 (m)	1079 (m)	1041 (vs)	897 (w)
796 (m)	746 (m)	668 (s)	614 (s)
613 (s)	526 (m)		

500 MHz ^{1}H NMR spectrum (DMSO-d_6): δ (ppm), J (Hz)

10.60	NH-CO	s	2H (exchangeable)
9.70	-NH-CO-NH-	s	2H (exchangeable)
9.14	H8	s	2H
9.06	H4	d (^4J = 2.1)	2H
8.45	H2	d (^4J = 2.1)	2H
8.29	H6	d (^4J = 1.6)	2H
8.01	H2′	pt	2H
7.80	H6′	d (^3J = 8.0)	2H
7.66	H4′	d (^3J = 8.0)	2H
7.42	H5′	t (^3J = 8.0)	2H

125 MHz ^{13}C NMR spectrum (DMSO-d_6): δ (ppm)

165.9	C9	135.7	C1′	123.5	C6
153.0	C10	135.4	C3	121.8	C4′, C6′
145.0	C7	130.2	C8a	121.1	C2
142.7	C5	128.8	C5′	119.3	C4
142.5	C1	126.4	C4a	117.8	C2′
140.8	C3′	125.3	C8		

Trisodium 7-[3-(3-nitrobenzamido)-benzamido]-naphthalene-1,3,5-trisulfonate
3a

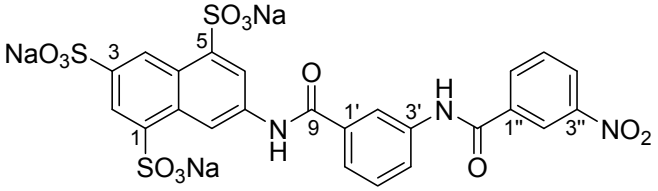

$C_{24}H_{14}N_3Na_3O_{13}S_3$ (717.6)

600.0 mg (3.2 mmol) 3-Nitrobenzoylchloride dissolved in 10 ml toluene were slowly added to the stirred solution of 568.4 mg (0.9 mmol) compound 2b in 50 ml water, until there was no amine left. The reaction was carried out according to GRP 2.

Yield: white powder, 89.5 % (609.9 mg)
TLC: R_f = 0.72 (MP 1)
HPLC: 99.1 % (t_R = 5.02 min)
UV spectrum (phosphate buffer pH of 6.5): λ_{max} = 260.5 nm
NaCl: 5.19 %

Elemental analysis (%):

	C	H	N	C/N
Calculation:	40.17	1.97	5.86	6.86
Calculation with H_2O and NaCl:	33.84	2.84	4.39	6.86
Found:	33.99	3.15	4.99	6.81

Water content: 5 mol/mol

IR spectrum (cm^{-1}):

3450 (br, s)	2918 (w)	1663 (s)	1558 (s)
1532 (s)	1433 (w)	1361 (m)	1329 (m)
1213 (vs)	1120 (m)	1041 (vs)	894 (w)
844 (w)	793 (w)	716 (m)	743 (m)
743 (m)	668(m)	614 (s)	528(m)

500 MHz ^{1}H NMR spectrum (DMSO-d_6): δ (ppm), J (Hz)

10.81	-NH-CO-	s	1H (exchangeable)
10.61	-NH-CO-	s	1H (exchangeable)
9.14	H8	d (^5J = 1.9)	1H
9.01	H4	d (^4J = 2.0)	1H
8.86	H2″	t (^3J = 2.0)	1H
8.47	H2	d (^4J =2.0)	1H
8.46	H6″	dd (^4J = 2.2, ^3J = 5.0)	1H
8.44	H4″	dd (^4J = 2.1, ^3J = 7.9)	1H
8.33	H2′	t (^4J = 2.0)	1H
8.28	H6	d (^4J = 1.9)	1H
8.09	H4′	dd (^3J = 8.4, ^3J = 1.6)	1H
7.87	H5″	t (^4J =7.9)	1H
7.85	H6′	d (^3J = 8.4)	1H
7.55	H5′	t (^3J = 8.4)	1H

125 MHz ^{13}C NMR spectrum (DMSO-d_6): δ (ppm)

165.5	C9	135.7	C1′	125.2	C8
163.6	C10	135.3	C3	123.6	C6′
147.9	C3″	134.4	C6″	123.5	C6
145.2	C7	130.4	C5″	122.6	C2″
142.9	C5	130.2	C8a	121.2	C2

142.6	C1	128.8	C5′	120.6	C2’
138.9	C3′	126.5	C4′′	119.5	C4
136.2	C1’’	126.4	C4a		

Trisodium 7-[3-(3-aminobenzamido)-benzamido]-naphthalane-1,3,5-trisulfonate
3b

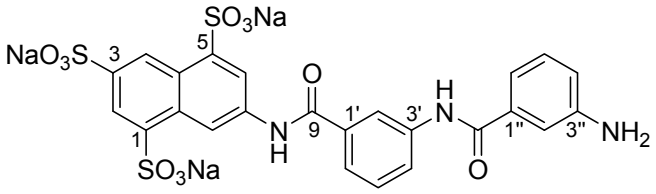

$C_{24}H_{16}N_3Na_3O_{11}S_3$ (687.6)

20 mg Palladium (10%) on charcoal were added as catalyst to a solution of 550 mg (0.8 mmol) compound 3a in water. The reaction was carried out according to GRP 3.

Yield: beige powder, 88.3 % (459.8 mg)
TLC: R_f = 0.54 (MP1)
HPLC: 97.7 % (t_R = 2.93 min)
UV spectrum (phosphate buffer pH of 6.5): λ_{max} = 260.5 nm
NaCl: 14.5 %

Elemental analysis (%):

	C	H	N	C/N
Calculation:	41.92	2.35	6.11	6.86
Calculation with H_2O and NaCl:	27.54	3.76	4.02	6.86
Found:	27.60	3.71	4.17	6.62

Water content: 11 mol/mol

IR spectrum (cm^{-1}):

3440 (br, s)	1636 (w)	1109 (w)	1039 (w)

500 MHz ^{1}H NMR spectrum (DMSO-d_6): δ (ppm), *J* (Hz)

10.57	-NH-CO-	s	1H (exchangeable)
10.25	-NH-CO-	s	1H (exchangeable)
9.13	H8	dd (^5J = 0.8, ^4J = 1.8)	1H
9.02	H4	dd (^5J = 0.8, ^4J = 2.2)	1H
8.45	H2	d (^4J = 2.2)	1H
8.33	H2′	t (^4J = 1.9)	1H
8.28	H6	d (^4J = 1.8)	1H
8.02	H4′	m	1H
7.76	H6′	d (^3J = 8.2)	1H
7.47	H5′	t (^3J = 8.2)	1H
7.16-7.13	H6′′, H5′′	m	2H
7.12	H2′′	t (^4J = 2.2)	1H

6.75	H4″	dd (^3J = 7.8, ^4J = 2.2)	1H
5.29	-NH_2	s	2H (exchangeable)

125 MHz ^{13}C NMR spectrum (DMSO-d_6): δ (ppm)

166.6	C9	135.6	C1′	123.3	C4′
165.8	C10	135.4	C3	122.8	C4A
148.9	C3″	130.2	C8a	121.1	C2
145.1	C7	128.9	C5″	120.3	C4″
142.9	C5	128.5	C4′	119.4	C4
142.6	C1	126.4	C4a	117.1	C6″
139.5	C3’	125.3	C8	114.9	C2′
135.8	C1″	123.4	C6	113.2	C2″

Hexasodium 7,7′-{carbonylbis[azanediyl-3,1-phenylenecarbonylazanediyl (3,1-phenylenecarbonylazanediyl]}bis(naphthalene-1,3,5-trisulfonate) 3c

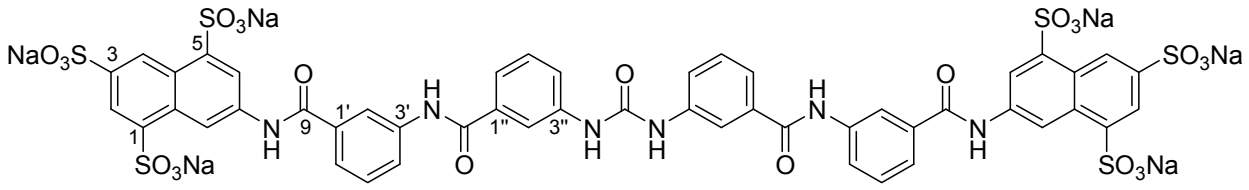

$C_{49}H_{30}N_6Na_6O_{23}S_6$ (1400.1)

A solution of 1.2 mmol phosgene (20 % in toluene) was slowly added to a solution of 400 mg (0.58 mmol) compound 3b under heavy stirring at room temperature. The reaction was carried out according to GRP 4.

Yield: beige powder, 72.5 % (290 mg)
TLC: R_f = 0.8 (MP2)
HPLC: 95.6 % (t_R = 5.58 min)
UV spectrum (phosphate buffer pH of 6.5): λ_{max} = 260.5 nm
NaCl: 6.69 %

Elemental analysis (%):

	C	H	N	C/N
Calculation:	42.00	2.16	6.00	7.00
Calculation with H_2O and NaCl:	32.68	3.41	4.67	7.00
Found:	32.76	4.01	4.70	6.98

Water content: 15 mol/mol

ESI-MS negative mode (m/z):
$[M+H]^-$: 1401.2, $[M-Na+H]^-$: 1377.4

IR spectrum (cm^{-1}):

3441 (br, s)	1540 (s)	1469 (m)	1436 (m)
1325 (m)	1305 (m)	1192 (br, s)	1041 (vs)
794 (w)	747 (m)	668 (m)	614 (s)

500 MHz ^{1}H NMR spectrum (DMSO-d_6): δ (ppm), J (Hz)

10.62	NH-CO	s		1H (exchangeable)
10.45	NH-CO	s		1H (exchangeable)
9.41	-NH-CO-NH-	s		1H (exchangeable)
9.15	H8	dd	(^{4}J = 1.6, ^{5}J = 0.6)	1H
9.05	H4	d	(^{4}J = 2.2)	1H
8.47	H2	d	(^{4}J = 2.2)	1H
8.35	H2″	pt		1H
8.30	H6	d	(^{4}J = 1.6)	1H
8.06	H4′	d	(^{3}J = 8.8)	1H
8.01	H2′	pt		1H
7.77	H6’, H6″	d	(^{4}J = 7.8)	2H
7.62	H4″	d	(^{3}J = 7.8)	1H
7.48	H5′, H5″	t	(^{3}J = 7.8)	2H

125 MHz ^{13}C NMR spectrum (DMSO-d_6): δ (ppm)

165.9	C9	135.8	C1′	123.6	C6
165.8	C10	135.7	C1″	123.7	C4′
152.9	C11	135.4	C3	123.1	C4″
145.1	C7	130.2	C8a	121.5	C6′
142.8	C5	129.0	C5′	121.2	C2 C6″
142.5	C1	128.5	C5″	120.4	C2′
140.1	C3′	126.4	C4a	119.4	C4
139.4	C3″	125.3	C8	117.8	C2″

Trisodium 7-[3-(4-nitrobenzamido)-benzamido]-naphthalene-1,3,5-trisulfonate
4a

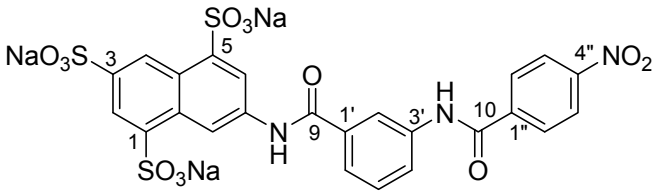

$C_{24}H_{14}N_3Na_3O_{13}S_3$ (717.6)

3.85 g (2.09 mmol) 4-Nitrobenzoylchloride dissolved in 10 ml toluene were slowly added to the stirred solution of 1 g (1.39 mmol) compound 2b in 20 ml water, until there was no amine left. The reaction was carried out according to GRP 2.

Yield: 72.7 % (719.7 mg)
TLC: R_f = 0.64 (MP1)

HPLC: 98.1 % (t_R = 4.45 min)
UV spectrum (phosphate buffer pH of 6.5): λ_{max} = 258.5 nm
NaCl: 10.5 %

Elemental analysis (%):

	C	H	N	C/N
Calculation:	40.17	1.97	5.86	6.86
Calculation with H_2O and NaCl:	33.42	2.34	4.87	6.86
Found:	33.43	2.64	4.89	6.83

Water content: 3 mol/mol

IR spectrum (cm^{-1}):

3418 (br, s)	1667 (m)	1602 (m)	1538 (s)
1474 (m)	1436 (m)	1401 (w)	1328 (m)
1302 (m)	1344 (m)	1328 (m)	1302 (m)
1258 (s)	1212 (vs)	1119 (m)	1051 (s)
852 (w)	798 (w)	743 (w)	713(w)
666 (s)	621 (s)	532 (m)	

500 MHz ^{1}H NMR spectrum (DMSO-d_6): δ (ppm), *J* (Hz)

10.79	-NH-CO-	s	1H (exchangeable)
10.61	-NH-CO-	s	1H (exchangeable)
9.13	H8	s	1H
9.01	H4	s	1H
8.46	H2	d (^4J = 2.0)	1H
8.36	H3″, H5″	d (^3J = 8.5)	2H
8.34	H2′	s	1H
8.28	H6	pd	1H
8.26	H2″, 6″	d (^3J = 8.5)	2H
8.07	H4′	d (^3J = 6.6)	1H
7.85	H6′	d (^3J = 7.3)	1H
7.52	H5′	t (^3J = 8.5)	1H

125 MHz ^{13}C NMR spectrum (DMSO-d_6): δ (ppm)

165.5	C9	138.9	C3′	125.3	C8
164.2	C10	135.7	C1′	123.7	C3″, 5″
149.4	C4″	135.3	C3	123.6	C6
145.2	C7	130.2	C8a	123.4	C6′
142.9	C5	129.5	C2″,C6″	121.1	C2
142.6	C1	128.7	C4′	120.5	C2′
140.5	C1″	126.5	C4a	119.5	C4

Trisodium 7-[3-(4-aminobenzamido)-benzamido]-naphthalene-1,3,5-trisulfonate
4b

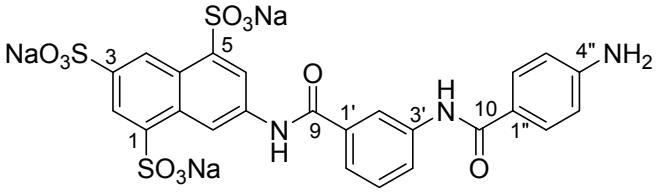

$C_{24}H_{16}N_3Na_3O_{11}S_3$ (687.6)

20 mg Palladium (10%) on charcoal were added as catalyst to a solution of 500 mg (0.70 mmol) compound 4a in water. The reaction was carried out according to GRP 3.

Yield: beige powder, 93.5 % (450 mg)
TLC: R_f = 0.54 (MP1)
HPLC: 99.2 % (t_R = 2.47 min)
UV spectrum (phosphate buffer pH of 6.5): λ_{max} = 262.5 nm
NaCl: 19.7 %

Elemental analysis (%):

	C	H	N	C/N
Calculation :	41.92	2.35	6.11	6.86
Calculation with H_2O and NaCl :	27.85	3.12	4.06	6.86
Found :	28.00	3.18	4.28	6.54

Water content: 8 mol/mol

IR spectrum (cm^{-1}):

3426 (br, s)	1436 (w)	1040 (s)	613 (m)
1544 (m)	1185 (s)	668 (m)	

500 MHz ^{1}H NMR spectrum (DMSO-*d*$_6$): δ (ppm), *J* (Hz)

10.55	-NH-CO-	s	1H (exchangeable)
9.95	-NH-CO-	s	1H (exchangeable)
9.13	H8	dd (^5J = 1.0, ^4J = 1.9)	1H
9.01	H4	dd (^4J = 2.2)	1H
8.45	H6	d (^4J = 2.2)	1H
8.29	H2'	pd	1H
8.28	H2	d (^4J = 1.0)	1H
8.03	H4'	t (^3J = 8.2)	1H
7.77	H2'', H6''	dd (^3J = 8.4, ^4J = 1.9)	2H
7.72	H6'	dd (^4J = 1.0, ^3J = 8.2)	1H
7.44	H5'	t (^3J = 8.2)	1H
6.61	H3'', H5''	d (^3J = 8.4)	2H
5.74	-NH_2	s	2H (exchangable)

125 MHz ^{13}C NMR spectrum (DMSO-d_6): δ (ppm)

165.8	C9	135.4	C3	122.3	C6
165.5	C10	130.2	C8a	121.2	C1″
152.4	C4″	129.6	C2″, C6′	121.0	C6′
145.1	C7	128.4	C5′	120.1	C2
142.9	C5	126.4	C4a	119.4	C4
142.6	C1	125.3	C8	112.7	C3″, 5″
139.9	C3′	123.4	C2′		
135.5	C1′	123.2	C4′		

Hexasodium 7,7′-{carbonylbis[azanediyl-4,1-phenylenecarbonylazanediyl]-(3,1-phenylene)carboylazanediyl]}bis(naphthalene-1,3,5-trisulfonate)
4c

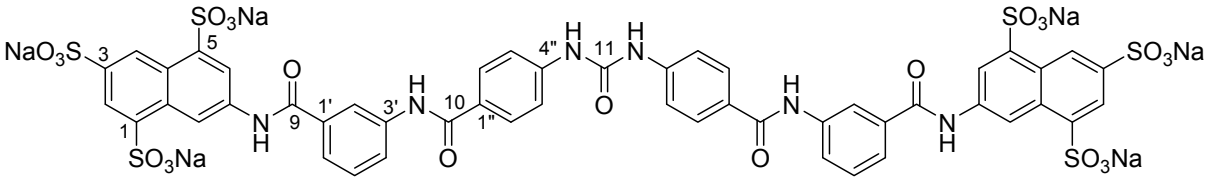

$C_{49}H_{30}N_6Na_6O_{23}S_6$ (1400.1)

A solution of 0.87 mmol phosgene (20 % in toluene) was slowly added to a solution of 400 mg (0.58 mmol) compound 4b in 20 ml water under heavy stirring at room temperature. The reaction was carried out according to GRP 4.

Yield: beige powder, 37.5 (300 mg)
TLC: R_f = 0.54 (MP2)
HPLC: 97.0 % (t_R = 5.31 min)
UV spectrum (phosphate buffer pH of 6.5): λ_{max} = 260.5 nm
NaCl: 27.3 %

Elemental analysis (%):

	C	H	N	C/N
Calculation:	42.00	2.16	6.00	7.00
Calculation with H_2O and NaCl:	25.25	2.63	3.60	7.00
Found:	25.32	3.13	3.68	6.88

Water content: 15 mol/mol

ESI-MS negative mode (m/z):
$[M-Na]^-$: 1379.2

IR spectrum (cm^{-1}):

3446 (br, s)	1534 (m)	1436 (m)	1302 (m)
1182 (m)	1038 (m)	798 (w)	

500 MHz ^{1}H NMR spectrum DMSO-d_6): δ (ppm), J (Hz)

10.60	-NH-CO-	s		1H
10.34	-NH-CO-	s		1H
10.18	-NH-CO-NH-	s		1H
9.14	H8	pdd	(^{5}J = 0.6)	1H
9.04	H4	pdd	(^{4}J = 2.2)	1H
8.47	H2	d	(^{4}J = 2.2)	1H
8.36	H2’	d	(^{4}J = 1.6)	1H
8.29	H6	d	(^{4}J = 1.6)	1H
8.05	H4’	d	(^{3}J = 7.9)	1H
8.01	H3’’, H5’’	d	(^{3}J = 8.8)	2H
7.76	H6’	d	(^{3}J = 7.9)	1H
7.62	H2’’, H6’’	d	(^{3}J = 8.8)	2H
7.52	H-5’	t	(^{3}J = 7.9)	2H

125 MHz ^{13}C NMR spectrum (DMSO-d_6): δ (ppm)

165.8	C9	135.6	C1′′	123.6	C2
165.4	C10	135.4	C3	123.4	C4
152.6	C11	130.2	C8a	122.9	C6
145.1	C7	129.1	C2′′, C6′′	121.2	C6′
143.2	C5	128.6	C1′′	120.4	C2
142.8	C1	127.7	C4′	119.4	C4
142.5	C4′′	126.4	C4a	117.1	C3′′, 5′′
139.8	C3′	125.3	C8		

4-Fluoro-nitrobenzoic acid (Ullmann *et al.*, 2005)

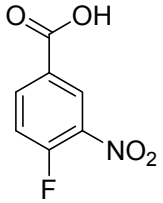

$C_7H_4FNO_4$ (185.1)

24 ml (280 mmol) 82 % Nitric acid were slowly dropped into a chilled solution of 45 ml conc. sulphuric acid at a temperature of -15 °C. 8.0 g (57 mmol) 4-fluorobenzoic acid were added as a small portion in to the solution at 0 °C. The mixture was stirred at this temperature for an hour and at room temperature overnight. The solution was poured into 150 g ice water and the white precipitate was filtered and washed many times with water.

Yield: pale yellow powder, 77.7 %

Elemental analysis (%):

	C	H	N	C/N
Calculation:	45.42	2.18	7.57	6.00
Found:	43.82	2.13	7.12	6.16

500 MHz ^{1}H NMR spectrum (DMSO-*d*$_6$): δ (ppm), *J* (Hz)

13.0	-OH	s	1H exchangeable
8.54-8.53	H2	dd (^{4}J = 7.6, ^{4}J = 2.2)	1H
8.29	H6	m	1H
7.69	H5	dd (^{3}J = 11.0, ^{3}J = 8.8)	1H

125 MHz ^{13}C NMR spectrum (DMSO-*d*$_6$): δ (ppm)

164.9	C7	136.9	C3	127.3	C2
157.3	C4	128.2	C1	119.3	C5
137.1	C6				

4-Fluoro-3-nitrobenzoyl chloride (Ullmann *et al.*, 2005)

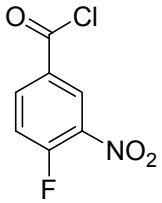

$C_7H_3ClFNO_3$ (203.6)

3.5 ml (50 mmol) of Thionylchloride was slowly dropped into a suspension of 7.22 g (39.66 mmol) of 4-fluoro-3-nitrobenzoic acid dissolved in 30 ml toluene and 6 drops of DMF. The reaction was carried out according to GRP 1.

Trisodium 7-(3-amino-4-fluorobenzamido)-naphthalene-1,3,5-trisulfonate 5a

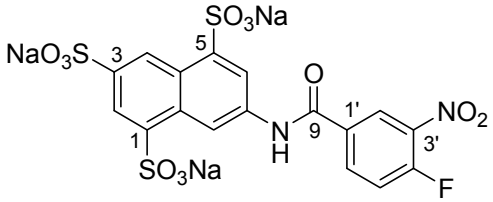

$C_{17}H_8FN_2Na_3O_{12}S_3$ (616.4)

814.2 mg (4 mmol) 4-Fluoro-nitrobenzoylchloride dissolved in 10 ml toluene were slowly added to the stirred solution of 1.0 g (2.2 mmol) trisodium 7-aminonaphthalene-1,3,5-trisulfonate in 50 ml water, until there was no amine left. The reaction was carried out according to GRP 2.

Yield: white powder, 80.2 % (1.1 g)
TLC: R_f = 0.64 (MP1)
HPLC: 98.3 % (t_R = 3.47 min)
UV spectrum (phosphate buffer pH of 6.5): λ_{max} = 256.5 nm
NaCl: 3.84 %

Elemental analysis (%):

	C	H	N	C/N
Calculation:	33.1	1.3	4.5	7.3
Calculation with H_2O and NaCl:	26.8	2.8	3.7	7.3
Found:	26.6	2.7	3.8	6.9

Water content: 6 mol/mol

ESI-MS negative mode (m/z):
$[M\text{-}Na]^-$: 593.3

IR spectrum (cm^{-1}):

3441 (br, s)	1679 (s)	1617 (m)	1576 (m)
1540 (s)	1467 (w)	1437 (w)	1330 (s)
1359 (m)	1190 (b.s)	1114 (s)	1078 (m)
1042 (vs)	817 (vw)	793 (m)	668 (m)
613 (vs)	526 (m)		

500 MHz ^{1}H NMR spectrum (DMSO-d_6): δ (ppm), J (Hz)

10.80	NH-CO	s	1H (exchangeable)
9.14	H8	dd (^4J = 1.8, ^5J = 0.8)	1H
9.06	H4	d (^4J = 2.0)	1H
8.86	H2′	dd (^4J = 1.9, ^4J = 7.2)	1H
8.49	H6′	m	1H
8.45	H2	d (^4J = 2.0)	1H
8.28	H6	d (^4J = 1.8)	1H
7.75	H5′	dd (^3J = 8.5, ^3J = 11.3)	1H

125 MHz ^{13}C NMR spectrum (DMSO-d_6): δ (ppm)

162.5	C9	135.0	C6′	125.2	C8
156.4	C4′	134.7	C3	123.5	C6
145.3	C7	131.8	C1′	120.7	C2
143.0	C5	130.1	C8a	119.5	C4
142.8	C1	126.6	C2′	118.8	C5′
136.8	C3′	126.1	C4a		

Trisodium 7-(3-amino-4-fluorobenzamido)-naphthalene-1,3,5-trisulfonate 5b

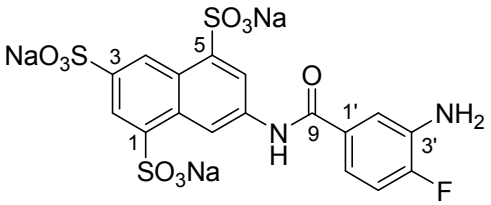

$C_{17}H_{10}FN_2Na_3O_{10}S_3$ (586.4)

20 mg Palladium (10%) on charcoal were added as catalyst to a solution of 901.6 mg (1.5 mmol) compound 5a in water. The reaction was carried out according to GRP 3.

Yield: beige powder, 84.3 % (685 mg)
TLC: R_f = 0. 58 (MP1)
HPLC: 95.6 % (t_R = 2.24 min)
NaCl: 5.50 %
UV spectrum (phosphate buffer pH of 6.5): λ_{max} = 258.5 nm

Elemental analysis (%):

	C	H	N	C/N
Calculation:	34.8	1.7	4.8	7.3
Calculation with H_2O and NaCl:	27.1	3.2	3.7	7.3
Found:	26.9	3.1	3.9	6.9

Water content: 7 mol/mol

ESI-MS negative mode (m/z):
$[M-Na]^-$: 563.8, $[M-2Na+H]^-$: 541.6, $[M-3Na+H]^-$: 519.6

IR spectrum (cm^{-1}):

3422 (br, s)	1652 (m)	1580 (m)	1551 (m)
1516 (m)	1467 (w)	1473 (w)	1438 (w)
1327 (m)	1200 (b.s)	1126 (m)	1041 (vs)
898 (w)	785 (w)	749 (m)	674 (m)
602 (s)	503 (m)		

500 MHz ^{1}H NMR spectrum (DMSO-d_6): δ (ppm), J (Hz)

10.40	NH-CO	s	1H exchangeable
9.12	H8	dd (^5J = 1.0, ^4J = 1.9)	1H
8.98	H4	dd (^5J = 1.0, ^4J =2.2)	1H
8.39	H2	d (^4J = 2.2)	1H
8.26	H6	d (^4J = 2.2)	1H
7.44	H2′	d (^4J = 1.9)	1H
7.25	H6′	m	1H
7.09	H5′	dd (^3J = 8.5, ^3J = 11.3)	1H
5.30	$-NH_2$	s	2H exchangeable

125 MHz ^{13}C NMR Spectrum (DMSO-d_6): δ (ppm)

165.4	C9	135.4	C3	121.2	C2
152.5	C4′	131.6	C1′	119.4	C4
145.1	C7	130.2	C8a	116.4	C2′
142.7	C5	126.4	C4a	115.9	C6′
142.5	C1	125.2	C8	114.6	C5′
136.5	C3′	123.3	C6		

Hexasodium 7,7′-{carbonylbis[azanediyl(4-fluoro-3,1-phenylene) carbonylazanediyl]}bis(naphthalene-1,3,5-trisulfonate)
5c

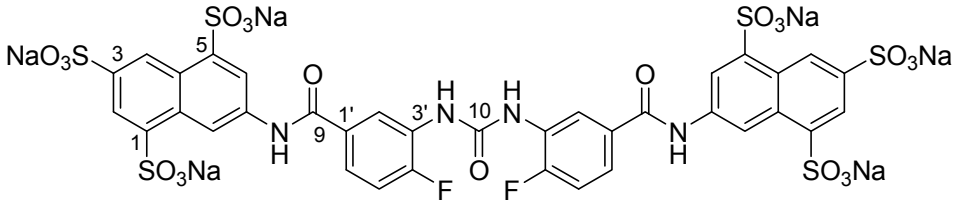

$C_{35}H_{18}F_2N_4Na_6O_{21}S_6$ (1198.9)

A solution of 1.4 mmol phosgene (20 % in toluene) was slowly added to a solution of 400 mg (0.7 mmol) compound 5b under heavy stirring at room temperature. The reaction was carried out according to GRP 4.

Yield: beige powder, 66.0 % (537.9 mg)
TLC: R_f = 0.58 (MP2)
HPLC: 96.5 % (t_R = 4.98 min)
UV spectrum (phosphate buffer pH of 6.5): λ_{max} = 258.5 nm
NaCl: 2.70 %

Elemental analysis (%):

	C	H	N	C/N
Calculation:	35.0	1.5	4.8	7.2
Calculation with H_2O and NaCl:	28.7	2.9	3.8	7.5
Found:	28.8	3.2	4.0	7.2

Water content: 12 mol/mol

ESI-MS negative mode (m/z):
$[M-Na]^-$: 1176.1

IR spectrum (cm^{-1}):

3438 (br, s)	1610 (m)	1539 (m)	1472 (m)
1436 (m)	1327 (m)	1201 (vs)	1120 (m)
1041 (vs)	898 (w)	794 (m)	669 (m)
614 (s)			

500 MHz ^{1}H NMR spectrum (DMSO-d_6): δ (ppm), *J* (Hz)

10.61	-NH-CO-	s	1H (exchangeable)
9.16	-NH-CO-NH-	s	1H (exchangeable)
9.14	H8	dd (^5J =1.6, ^4J = 1.9)	1H
9.05	H4	d (^4J = 1.6)	1H
8.73	H2′	d (^4J =1.6)	1H
8.42	H2	d (^4J = 2.2)	1H
8.28	H6	d (^4J =1.9)	1H
7.81	H6′	m	1H
7.41	H5′	dd (^3J =8.5, ^2J = 11.3)	1H

125 MHz ^{13}C NMR Spectrum (DMSO-d_6): δ (ppm)

164.5	C9	135.3	C3	123.5	C6
154.6	C4′	130.1	C8a	123.2	C6′
152.1	C10	127.2	C3′	121.8	C2′
145.1	C7	131.6	C1′	121.1	C2
142.7	C5	126.4	C4a	119.3	C4
142.6	C1	125.2	C8	115.1	C5′

Trisodium 7-[4-fluoro-3-(3-nitrobenzamido)-benzamido]-naphthalene-1,3,5-trisulfonate
6a

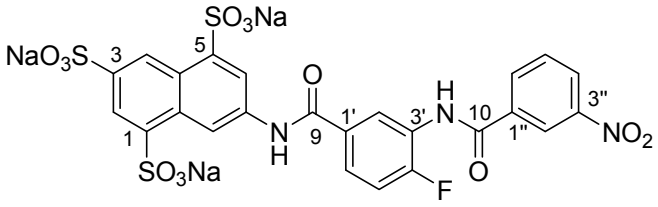

$C_{24}H_{13}FN_3Na_3O_{13}S_3$ (735.5)

97.5 mg (0.5 mmol) 3-Nitrobenzoylchloride dissolved in 5 ml toluene were slowly added to the stirred solution of 149.5 mg (0.3 mmol) 5b in 20 ml water, until there was no amine left. The reaction was carried out according to GRP 2.

Yield: pale yellow powder, 77.1 % (152.3 mg)
TLC: R_f = 0.76 (MP1)
HPLC: 97.5 % (t_R = 5.11 min)
UV spectrum (phosphate buffer pH of 6.5): λ_{max} = 258.5 nm
NaCl: 16.0 %

Elemental analysis (%):

	C	H	N	C/N
Calculation:	39.19	1.78	5.71	6.86
Calculation with H_2O and NaCl:	23.43	3.76	3.41	6.86
Found:	23.46	2.97	3.67	6.40

Water content: 16 mol/mol

IR spectrum (cm^{-1}):

3446 (br, s)	1636 (w)	1141 (vs)	622 (w)

500 MHz ^{1}H NMR Spectrum (DMSO-*d*$_6$): δ (ppm), *J* (Hz)

10.79	-NH-CO-	s	1H (exchangeable)
10.66	-NH-CO-	s	1H (exchangeable)
9.13	H8	dd (^5J = 1.0, ^4J = 1.9)	1H
9.05	H4	d (^4J = 1.6)	1H
8.84	H2′	t (^4J = 1.9)	1H
8.48	H2	d (^4J = 1.6)	1H
8.47	H2″	dd (^4J = 1.0, ^4J = 2.2)	1H
8.45	H6″	dd (^4J = 1.0, ^4J = 2.2)	1H
8.31	H4″	d (^4J = 2.5)	1H
8.30	H6	d (^4J = 2.2)	1H
8.07-8.04	H6′	m	1H
7.87	H5″	t (^3J = 8.50)	1H
7.50-7.47	H5′	m (^3J = 8.50)	1H

125 MHz ^{13}C NMR Spectrum (DMSO-*d*$_6$): δ (ppm)

166.3	C9	135.3	C3	126.5	C8
164.3	C10	135.2	C1′	123.5	C6
158.2	C4′	134.4	C6″	122.8.	C6′
148.0	C3″	130.5	C1′	121.0	C2, C2″
145.1	C7	130.2	C8a,C5″	119.4	C4, C3′
142.9	C5	127.5	C4″	116.1	C2′
142.6	C1	126.7	C4a	115.9	C5′

Trisodium 7-[3-(3-aminobenzamido)-4-fluoro-benzamido]-naphthalene-1,3,5-trisulfonate
6b

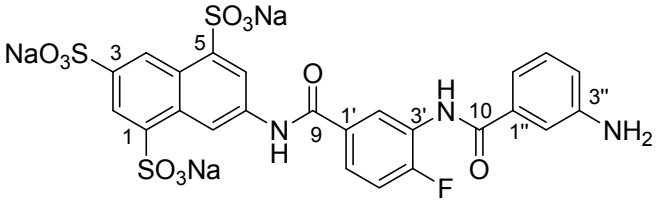

$C_{24}H_{15}FN_3Na_3O_{11}S_3$ (705.6)

20 mg Palladium (10%) on charcoal were added as catalyst to a solution of 128 mg (0.2 mmol) compound 6a in water. The reaction was carried out according to GRP 3.

Yield: white powder, 90.2 % (115.5 mg)
TLC: R_f = 0.44 (MP1)
HPLC: 97.5 % (t_R = 3.56 min)
UV spectrum (phosphate buffer pH of 6.5): λ_{max} = 258.5 nm
NaCl: 14.1 %

Elemental analysis (%):

	C	H	N	C/N
Calculation:	40.86	2.14	5.96	6.86
Calculation with H_2O and NaCl:	23.22	4.47	3.38	6.86
Found:	22.62	3.56	4.14	5.46

Water content: 20 mol/mol

IR spectrum (cm-1):
3446 (br, s) 1636 (w)

500 MHz ^{1}H NMR Spectrum (DMSO-*d*$_6$): δ (ppm), *J* (Hz)

10.62	-NH-CO-	s	1H (exchangeable)
10.04	-NH-CO-	s	1H (exchangeable)
9.13	H8	dd (^{5}J = 0.9, ^{4}J = 1.9)	1H
9.04	H4	d (^{4}J = 1.6)	1H
8.43	H2	d (^{4}J = 2.2)	1H
8.27	H6	d (^{4}J = 1.6)	1H
8.26	H2″	d (^{4}J = 1.6)	1H
8.00-7.97	H6″	m	1H
7.43	H5″	t (^{3}J = 7.6)	1H
7.17	H2′	dd (^{3}J = 7.6, ^{4}J = 2.1)	1H
7.15	H6′	d (^{4}J = 2.1)	1H
7.14	H4″	d (^{4}J = 1.6)	1H
6.77-6.75	H5′	m	1H
5.31	-NH_2	s	2H (exchangeable)

125 MHz ^{13}C NMR Spectrum (DMSO-*d*$_6$): δ (ppm)

166.3	C9	135.2	C3	123.4	C6
164.3	C10	134.8	C1″	121.0	C2
163.9	C4′	130.2	C8a, C1′	119.4	C4, C3′
149.0	C3″	128.9	C5″	117.3	C4″, C2′
145.1	C7	127.3	C6′	115.7	C6″
142.9	C5	126.5	C4a	114.9	C5′
142.6	C1	125.2	C8	113.3	C2″

Hexasodium 7,7′-{carbonylbis[azanediyl-3,1-phenylenecarbonylazanediyl(4-fluoro-3,1-phenylene)carbonylazanediyl]}bis(naphthalene-1,3,5-trisulfonate) 6c

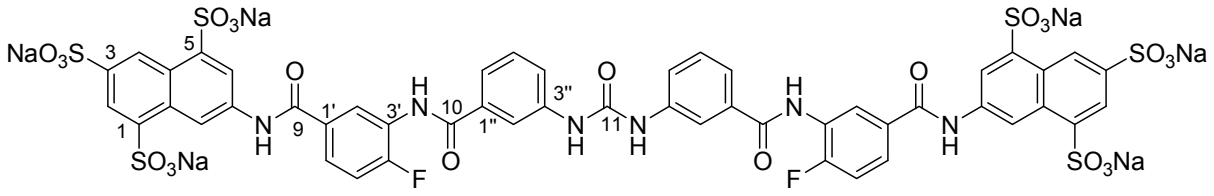

$C_{49}H_{28}F_2N_6Na_6O_{23}S_6$ (1437.1)

A solution of 0.4 mmol phosgene (20 % in toluene) was slowly added to a solution of 90 mg (0.2 mmol) compound 6b under heavy stirring at room temperature. The reaction was carried out according to GRP 4.

Yield: beige powder, 89.0 % (80.2 mg)
TLC: R_f = 0.25 (MP2)
HPLC: 97.1 % (t_R = 5.57 min)
UV spectrum (phosphate buffer pH of 6.5): λ_{max} = 260.5 nm
NaCl: 44.2 %

Elemental-Analysis (%):

	C	H	N	C/N
Calculation:	40.95	1.96	5.85	7.00
Calculation with H_2O and NaCl:	20.55	1.62	2.93	7.00
Found:	20.60	2.61	2.99	6.88

Water content: 9 mol/mol

IR spectrum (cm^{-1}):

3446 (br, s)	1662 (s)	1558 (m)	1216 (m)
1041 (m)	614 (m)		

ESI-MS negative mode (m/z):
$[M-Na]^-$: 1414.9

500 MHz ^{1}H NMR spectrum (DMSO-*d*$_6$): δ (ppm), *J* (Hz)

10.66	-NH-CO-	s		1H (exchangeable)
10.32	-NH-CO-	s		1H (exchangeable)
9.91	-NH-CO-NH-	s		1H (exchangeable)
9.13	H8	d	(^4J = 1.9)	1H
9.07	H4	d	(^4J = 2.0)	1H
8.44	H2	d	(^4J = 2.0)	1H
8.30.	H2′	d	(^4J = 2.2)	1H
8.28	H6	d	(^4J = 1.9)	1H
8.03	H2′′	pd		1H
8.02-8.00	H4′′	m		1H
7.79	H6′	d	(^3J = 7.9)	1H

7.61	H6″	d	(^3J = 6.5)	1H
7.47	H5″	t	(^3J = 6.5)	1H
7.45-7.43	H5′	m		1H

125 MHz ^{13}C NMR spectrum (DMSO-d_6): δ (ppm)

165.8	C9	131.1	C1″	121.1	C2
164.3	C10	130.2	C8a	120.9	C4
158.1	C4′	129.1	C5″	119.3	C3′
153.0	C11	127.4	C1′	117.6	C2″
145.1	C7	126.4	C4a	116.0	C2′
142.8	C5	126.0	C4″	115.9	C5′
142.6	C1	125.9	C6′	121.4	C6″
140.3	C3″	125.3	C8	123.5	C6
134.8	C3				

Trisodium 7[4-fluoro-3-(4-nitrobenzamido)-benzamido]-naphthalene-1,3,5-trisulfonate
7a

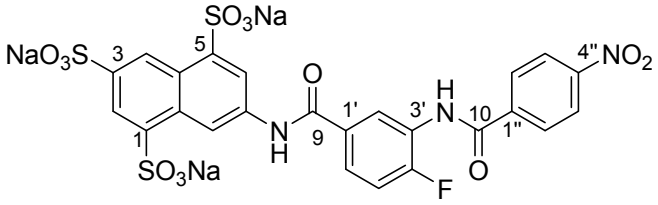

$C_{24}H_{13}FN_3Na_3O_{13}S_3$ (735.5)

1.88 g (1.02 mmol) 4-Nitrobenzoylchloride dissolved in 10 ml toluene were slowly added to the stirred solution of 400 mg (0.68 mmol) compound 5b in 50 ml water, until there was no amine left. The reaction was carried out according to GRP 2.

Yield: yellow powder, 90 % (460 mg)
TLC: R_f = 0.37 (MP1)
HPLC: 98.9 % (t_R = 5.77 min)
UV spectrum (phosphate buffer pH of 6.5): λ_{max} = 258 nm
NaCl: 18.9 %

Elemental analysis (%):

	C	H	N	C/N
Calculation:	39.19	1.78	5.71	6.86
Calculation with H_2O and NaCl:	29.62	1.97	4.32	6.86
Found:	29.64	2.15	4.28	6.93

Water content: 3 mol/mol

IR spectrum (cm^{-1}):

3425 (br. s)	1610 (m)	1535 (m)	1475 (m)
1211 (br, vs)	1051 (s)	853 (w)	619 (m)

500 MHz ^{1}H NMR spectrum (DMSO-d_6): δ (ppm), *J* (Hz)

10.77	-NH-CO-	s		1H (exchangeable)
10.70	-NH-CO-	s		1H (exchangeable)
9.15	H8	pd		1H
9.07	H4	pd		1H
8.47	H2′, H2	d	(^4J = 1.5)	2H
8.34	H2″, H6″	d	(^3J = 8.6)	2H
8.28	H3″, H5″	d	(^3J = 8.5)	2H
8.26	H6	pd		1H
8.09-8.06	H6′	m		1H
7.53	H5′	t	(^3J= 9.2)	1H

125 MHz ^{13}C NMR spectrum (DMSO-d_6): δ (ppm)

164.4	C9	139.7	C1″	125.5	C3'
164.3	C10	135.4	C3	124.1	C3″, C5″
157.2	C4′	131.5	C1’	123.7	C6
149.8	C4″	130.4	C8a	121.2	C2
145.3	C7	127.8	C2″, C6″	119.6	C4
143.1	C5	126.7	C4a	116.4	C2′
142.8	C1	125.6	C8	116.2	C5′

Trisodium 7-[3-(4-aminobenzamido)-4-fluoro-benzamido]-naphthalene-1,3,5-trisulfonate
7b

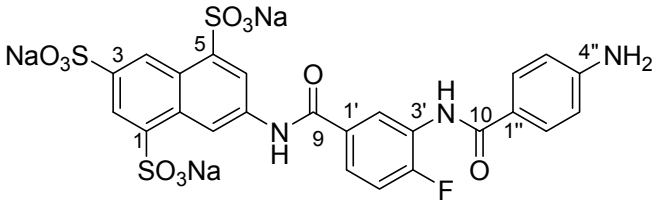

$C_{24}H_{15}FN_3Na_3O_{11}S_3$ (705.6)

20 mg Palladium (10%) on charcoal were added as catalyst to a solution of 410 mg (0.58 mmol) compound 7a in water. The reaction was carried out according to GRP 3.

Yield: brown powder, 95.12 % (390 mg)
TLC: R_f = 0.33 (MP1)
HPLC: 97.2 % (t_R = 3.27 min)
UV spectrum (phosphate buffer pH of 6.5): λ_{max} = 263 nm
NaCl: 32.8 %

Elemental analysis (%)

	C	H	N	C/N
Calculation:	40.86	2.14	5.96	6.86
Calculation with H_2O and NaCl:	22.09	2.57	3.25	6.86
Found:	21.89	2.14	3.24	6.76

Water content: 9 mol/mol

IR spectrum (cm^{-1}):

3439 (br. s)	1636 (m)	1188 (w)	1039 (m)

500 MHz ^{1}H NMR spectrum (DMSO-d_6): δ (ppm), J (Hz)

10.69	-NH-CO-	s	1H (exchangeable)
9.85	-NH-CO-	s	1H (exchangeable)
9.18	H8	s	1H
9.08	H4	d (^4J = 2.0)	1H
8.48	H2	d (^4J = 1.5)	1H
8.33	H2′	s	1H
8.31	H6	s	1H
8.03	H6′	m	1H
7.81	H2′′, H6′′	d (^3J = 8.4)	2H
7.49-7.45	H5′	t (^3J = 9.4)	1H
6.66	H3′′, H5′′	d (^3J = 8.4)	2H
5.86	-NH_2	s	2H (exchangeable)

125 MHz ^{13}C NMR spectrum (DMSO-d_6): δ (ppm)

165.5	C9	135.5	C3	123.6	C6
164.9	C10	130.4	C8A	121.3	C2
156.3	C4′	129.9	C1’	120.3	C3′
152.8	C4′′	126.7	C2′′, C6′′	119.6	C4, C2′
145.3	C5	126.5	C4a	114.9	C3′′, C5′′
143.1	C7	125.4	C8, C6′	112.9	C5′
142.8	C1	124.8	C1′′		

Hexasodium 7,7′-{carbonylbis[azanediyl-4,1-phenylenecarbonylazanediyl(4-fluoro-3,1-phenylene)carbonylazanediyl]bis(naphthalene-1,3,5-trisulfonate) 7c

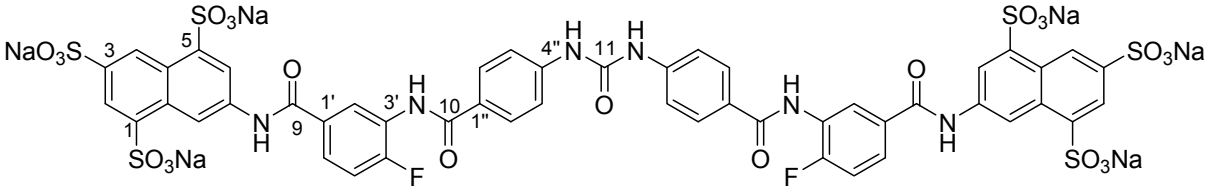

$C_{49}H_{28}F_2N_6Na_6O_{23}S_6$ (1437.1)

A solution of 0.86 mmol phosgene (20 % in toluene) was slowly added to a solution of 300 mg (0.43 mmol) compound 7c in 20 ml water under heavy stirring at room temperature. The reaction was carried out according to GRP 5.

Yield: beige powder, 49.2 % (300.12 mg)
TLC: R_f = 0.22 (MP2)
HPLC: 93.1 % (t_R = 7.20 min)
UV spectrum (phosphate buffer pH of 6.5): λ_{max} = 261 nm

NaCl: 67.5 %

Elemental analysis (%):

	C	H	N	C/N
Calculation:	40.95	1.96	5.85	7.00
Calculation with H_2O and NaCl:	10.64	1.24	1.52	7.00
Found:	10.44	0.88	1.69	6.20

Water content: 20 mol/mol

ESI-MS negative mode (m/z):
$[M-H]^-$: 1436.7

IR spectrum (cm^{-1}):

3444 (br, s)	1609 (m)	1534 (s)	1475 (m)
1437 (m)	1323 (m)	1189 (br, vs)	1126 (m)
1042 (s)	795 (w)	669 (m)	616 (m)

500 MHz ^{1}H NMR spectrum (DMSO-d_6): δ (ppm), J (Hz)

10.64	-NH-CO-	s	1H (exchangeable)
10.32	-NH-CO-	s	1H (exchangeable)
10.18	-NH-CO-NH-	s	1H
9.12	H8	pd	1H
9.06	H4	pd	1H
8.44	H2	d (^4J = 2.2)	1H
8.30	H2’	pd	1H
8.28	H6	d (^4J = 1.6)	1H
8.00	H6′, H3′′, H5′′	d (^3J = 8.8)	3H
7.63	H2′′, H6′′	d (^3J = 8.8)	2H
7.45-7.42	H5′	t (^3J = 8.5)	1H

125 MHz ^{13}C NMR spectrum (DMSO-d_6): δ (ppm)

164.7	C9	140.3	C1′	123.8	C6
164.3	C10	139.7	C4′′	123.2	C2
156.3	C4′	135.2	C3	122.1	C3′′, C5′′
154.5	C4′′	129.2	C8a,C1′′	119-3	C4
145.3	C5	126.2	C2′′, C6′′	117.1	C2′
143.1	C7	125.3	C4a	115.1	C5′
142.9	C1				

Trisodium 7-(4-nitrobenzamido)-naphthalene-1,3,5-trisulfonate
8a

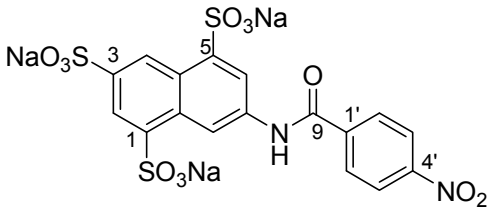

$C_{17}H_9N_2Na_3O_{12}S_3$ (598.42)

1.81 g (4.9 mmol) 4-Nitrobenzoylchloride dissolved in 10 ml toluene were slowly added to the stirred solution of 2 g (4.9 mmol) trisodium 7-aminonaphthalene-1,3,5-trisulfonate in 50 ml water, until there was no amine left. The reaction was carried out according to GRP 2.

Yield: yellow powder, 90.44 % (2.65 g)
TLC: R_f = 0.56 (MP1)
HPLC: 99.8 % (t_R = 3.47 min)
UV spectrum (phosphate buffer pH of 6.5): λ_{max} = 249 nm
NaCl: 3.41 %

Elemental analysis (%):

	C	H	N	C/N
Calculation:	34.12	1.52	4.68	7.29
Calculation with H_2O and NaCl:	28.65	2.69	3.93	7.30
Found:	28.61	2.41	3.99	7.17

Water content: 5 mol/mol

IR spectrum:

3455 (br, s)	2360 (w)	1604 (m)	1579 (m)
1526 (m)	1551 (m)	1472 (w)	1438 (w)
1331 (w)	1196 (vs)	1129 (m)	1104 (m)
1078 (w)	1042(vs)	853 (w)	794 (w)
713 (m)	668 (s)	615 (s)	530 (m)

500 MHz ^{1}H NMR spectrum (DMSO-d_6): δ (ppm), J (Hz)

10.99	-NH-CO-	s	1H (exchangeable)
9.14	H8	dd (^5J = 1.0, ^4J = 1.9)	1H
9.07	H4	d (^4J = 2.2)	1H
8.47	H2	d (^4J = 2.2)	1H
8.39	H3′, H5′	d (^3J = 8.5)	2H
8.30	H6	d (^4J = 1.6)	1H
8.28	H2′, H6′	d (^3J = 8.5)	2H

125 MHz ^{13}C NMR spectrum (DMSO-*d*$_6$): δ (ppm)

165.1	C9	135.8	C3	123.5	C6
159.8	C4′	132.1	C8a	122.5	C2
143.3	C7	129.8	C2′, C6′	119.8	C4
143.1	C5	126.9	C4a	112.7	C3′, C5′
142.6	C1	125.3	C8		

Trisodium 7-(4-aminobenzamido)-naphthalene-1,3,5-trisulfonate
8b

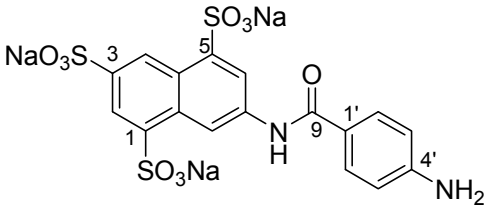

$C_{17}H_{11}N_2Na_3O_{10}S_3$ (568.44)

20 mg Palladium (10%) on charcoal were added as catalyst to a solution of 2.4 g (4.0 mmol) compound 8a in water. The reaction was carried out according to GRP 3.

Yield: white powder, 88.0 % (2 g)
TLC: R_f = 0.34 (MP1)
HPLC: 99.8 % (t_R = 1.60 min)
UV spectrum (phosphate buffer pH of 6.5): λ_{max} = 254.5 nm
NaCl: 3.46 %

Elemental analysis (%):

	C	H	N	C/N
Calculation:	35.92	1.95	4.93	7.29
Calculation with H_2O and NaCl:	31.22	2.78	4.28	7.30
Found:	30.95	2.45	4.28	7.24

Water content: 3 mol/mol

IR spectrum (cm^{-1}):

3422 (br, s)	2362 (w)	1653 (m)	1611 (m)
1577 (w)	1548 (w)	1519 (w)	1473 (m)
1399 (m)	1278 (m)	1212 (vs)	1128 (m)
1107 (m)	1056 (s)	904 (w)	842 (w)
800 (w)	759 (w)	689 (m)	668 (m)
625 (s)	602 (m)	534 (w)	

500 MHz ^{1}H NMR spectrum (DMSO-*d*$_6$): δ (ppm), *J* (Hz)

10.09	-NH-CO-	s	1H (exchangeable)
9.11	H8	dd (^5J = 0.9, ^4J = 1.9)	1H
9.00	H4	d (^4J = 2.2)	1H
8.38	H2	d (^4J = 2.2)	1H
8.26	H6	d (^4J = 1.6)	1H
7.84	H2′, H6′	d (^3J = 8.5)	2H
6.59	H3′, H5′	d (^3J = 8.5)	2H
5.70	-NH_2	s	2H (exchangeable)

125 MHz ^{13}C NMR spectrum (DMSO-*d*$_6$): δ (ppm)

165.5	C9	135.9	C3	123.4	C6
152.2	C4′	130.2	C8a	121.2	C2
144.9	C5	129.7	C2′, C6′	118.8	C4
142.6	C7	126.1	C4a	112.7	C3′, C5′
142.2	C1	125.3	C8		

Hexasodium 7,7′-[carbonylbis(azanediyl-4,1-carbonylazanediyl)]bis(naphthalene-1,3,5-trisulfonate)
8c

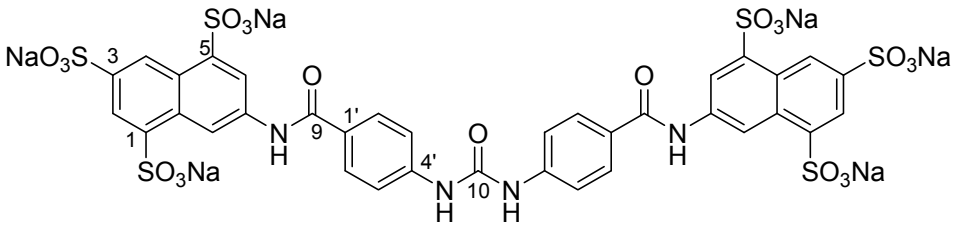

$C_{35}H_{20}N_4Na_6O_{21}S_6$ (1162.88)

A solution of 1.12 mmol phosgene (20 % in toluene) was slowly added to a solution of 320 mg (0.56 mmol) compound 8b in 20 ml water under heavy stirring at room temperature. The reaction was carried out according to GRP 4.

Yield: white powder, 90.1 % (330 mg)
TLC: R_f = 0.31 (MP2)
HPLC: 98.2 % (t_R = 5.45 min)
UV spectrum (phosphate buffer pH of 6.5): λ_{max} = 265 nm
NaCl: 19.3 %

Elemental analysis (%):

	C	H	N	C/N
Calculation :	36.15	1.73	4.82	7.50
Calculation with H_2O and NaCl :	23.38	2.92	3.11	7.50
Found :	23.28	2.78	3.27	7.12

Water content: 16 mol/mol

ESI-MS negative mode (m/z):
$[M-Na]^-$**:** 1139.4

IR spectrum (cm^{-1}):

3442 (br, s)	1594 (m)	1540 (m)	1510 (m)
1472 (w)	1439 (w)	1412 (w)	1324 (m)
1189 (br.vs)	1128 (m)	1040 (vs)	796 (w)
669 (m)	614 (m)		

500 MHz ^{1}H NMR spectrum (DMSO-*d*$_6$): δ (ppm), *J* (Hz)

10.43	-NH-CO	s	2H (exchangeable)
9.69	-NH-CO-NH-	s	2H (exchangeable)
9.13	H8	dd (^5J = 1.0, ^4J = 1.9)	2H
9.06	H4	dd (^5J = 1.0, ^4J = 2.2)	2H
8.43	H2	d (^4J = 2.2)	2H
8.28	H6	d (^4J = 1.9)	2H
8.04	H3′, H5′	d (^3J = 8.8)	4H
7.63	H2′, H6′	d (^3J = 8.8)	4H

125 MHz ^{13}C NMR spectrum (DMSO-*d*$_6$): δ (ppm)

165.2	C8	135.6	C3	123.4	C6
152.5	C9	130.2	C8a	121.2	C2
145.0	C5	129.2	C1′	119.2	C4
143.0	C7	127.9	C2′,C6′	117.3	C3′,C5′
142.7	C1	126.3	C4a		
142.0	C4′	125.3	C8		

Trisodium 7-[4-(3-nitrobenzamido)-benzamido]-naphthalene-1,3,5-trisulfonate
9a

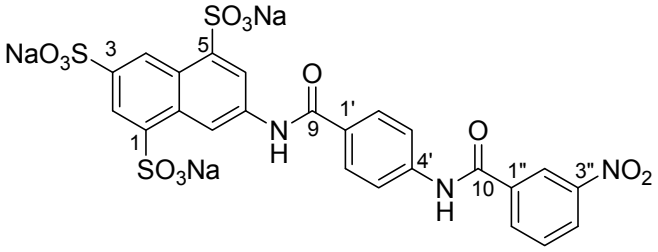

$C_{24}H_{14}N_3Na_3O_{13}S_3$ (717.54)

440 mg (2.4 mmol) 3-Nitrobenzoylchloride dissolved in 5 ml toluene were slowly added to the stirred solution of 0.91 g (1.6 mmol) compound 8b in 50 ml water until there was no amine left. The reaction was carried out according to GRP 2.

Yield: white powder, 78.4 % (900 mg)
TLC: R_f = 0.64 (MP1)
HPLC: 98.1 % (t_R = 5.66 min)
UV spectrum (phosphate buffer pH of 6.5): λ_{max} = 258 nm
NaCl: 6.22 %

Elemental analysis (%):

	C	H	N	C/N
Calculation:	40.17	1.97	5.86	6.86
Calculation with H_2O and NaCl:	32.39	3.06	4.72	6.86
Found:	32.17	2.98	4.77	6.75

Water content: 6 mol/mol

IR spectrum (cm^{-1}):

3442 (br, s)	1662 (m)	1602 (m)	1576 (m)	1527 (s)
1468 (w)	1436 (w)	1409 (w)	1357 (m)	1326 (m)
1192 (br, s)	1129 (m)	1108 (m)	1078 (w)	1043 (vs)
901 (w)	850 (w)	759 (w)	793 (w)	759 (w)
711 (m)	673 (s)	614 (s)	529 (m)	

500 MHz ^{1}H NMR spectrum (DMSO-d_6): δ (ppm), J (Hz)

10.84	-NH-CO-	s	1H (exchangeable)
10.52	-NH-CO-	s	1H (exchangeable)
9.13	H8	d (^4J = 0.9)	1H
9.06	H4	d (^4J = 1.9)	1H
8.82	H2″	t (^4J = 2.2)	1H
8.46	H2	d (^4J = 2.2)	1H
8.44	H6″, H4″	d (^4J = 2.2)	2H
8.28	H6	d (^4J = 1.9)	1H
8.12	H3′, H5′	dd (^3J =6.9, ^4J = 1.9)	2H
7.95	H2′, H6′	dd (^3J = 6.9, ^4J = 1.9)	2H
7.85	H5″	t (^3J = 6.9)	1H

125 MHz ^{13}C NMR spectrum (DMSO-d_6): δ (ppm)

164.9	C9	135.4	C1″	125.3	C8
163.8	C10	134.5	C6″	123.4	C6
147.9	C3″	130.4	C1′	122.7	C3′, C5′
145.1	C7	130.2	C5″	121.2	C2
142.8	C5	130.1	C8a	119.8	C2″
142.5	C1	128.9	C2′, C6′	119.3	C4
141.8	C4′	126.5	C4″		
136.3	C3	126.4	C4a		

Trisodium 7-[4-(3-aminobenzamido)-benzamido]-naphthalene-1,3,5-trisulfonate
9b

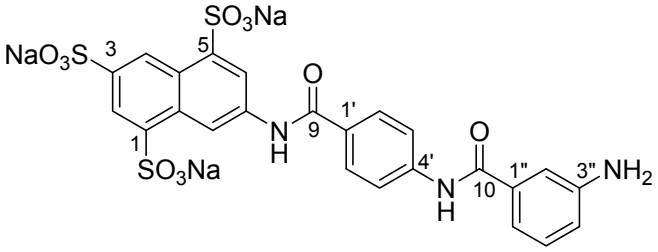

$C_{24}H_{16}N_3Na_3O_{11}S_3$ (687.56)

20 mg Palladium (10%) on charcoal were added as catalyst to a solution of 700 mg (0.98 mmol) compound 9a in water. The reaction was carried out according to GRP 3.

Yield: beige powder, 93.3 % (625 mg)
TLC: R_f = 0.37 (MP1)
HPLC: 98.0 % (t_R = 2.38 min)
UV spectrum (phosphate buffer pH of 6.5): λ_{max} = 254.5 nm
NaCl: 5.90 %

Elemental analysis (%):

	C	H	N	C/N
Calculation:	41.92	2.35	6.11	6.86
Calculation with H_2O and NaCl:	32.27	3.72	4.70	6.86
Found:	32.19	3.87	4.73	6.81

Water content: 8 mol/mol

IR spectrum (cm^{-1}):
3432 (br, s) 1636 (m) 1526 (m) 1187 (m) 1039 (m)

500 MHz ^{1}H NMR spectrum (DMSO-d_6): δ (ppm), *J* (Hz)

10.46	-NH-CO	s	1H (exchangeable)
10.31	-NH-CO	s	1H (exchangeable)
9.13	H8	dd (^4J = 0.9, ^4J = 1.0)	1H
9.05	H4	d (^4J = 0.9)	1H
8.43	H2	d (^4J = 0.9)	1H
8.28	H6	d (^4J = 0.9)	1H
8.08	H3′, H5′	d (^3J = 7.9)	2H
7.92	H2′, H6′	d (^3J = 7.9)	2H
7.15	H5′′	t (^3J = 7.5)	1H
7.12	H2′′	t (^4J = 1.5)	1H
7.09	H6′′	dd (^3J = 6.5, ^4J = 1.0)	1H
6.76	H4′′	d (^4J = 2.2, ^3J = 7.5)	1H
5.31	-NH_2	s	2H (exchangeable)

125 MHz ^{13}C NMR spectrum (DMSO-d_6): δ (ppm)

166.8	C9	135.4	C1″	123.4	C6
165.1	C10	130.2	C8a	121.2	C2
148.9	C3″	129.4	C1′	119.3	C3′, C5′
145.1	C7	128.9	C5″	117.2	C4
142.8	C5	128.7	C2′, C6′	116.7	C4″
142.5	C1	126.4	C4a	115.0	C6″
135.8	C4′	125.3	C8	113.2	C2″
135.7	C3				

Hexasodium 7,7′-{carbonylbis[azanediyl-3,1-phenylenecarbonyl-azanediyl(4,1-phenylene)carbonylazanediyl]}bis(naphthalene-1,3,5-trisulfonate)
9c

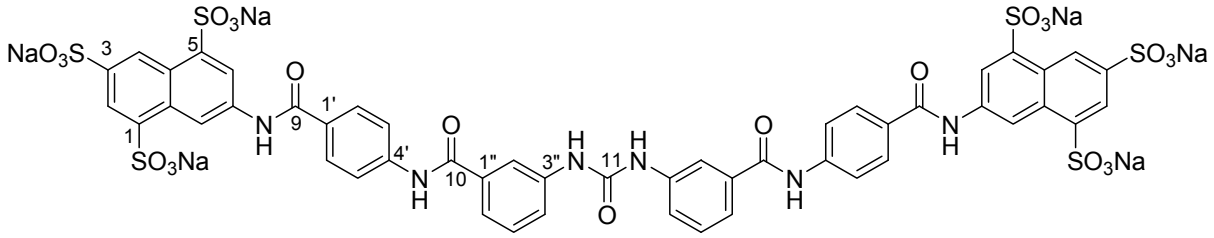

$C_{49}H_{30}N_6Na_6O_{23}S_6$ (1400.1)

A solution of 1.46 mmol phosgene (20 % in toluene) was slowly added to a solution of 500 mg (0.73 mmol) compound 9b in 20 ml water under heavy stirring at room temperature. The reaction was carried out according to GRP 4.

Yield: grey powder, 89 % (910 mg)
TLC: R_f = 0.6 (MP2)
HPLC: 98.3 % (t_R = 5.08 min)
UV spectrum (phosphate buffer pH of 6.5): λ_{max} = 260.5 nm
NaCl: 6.35 %

Elemental analysis (%):

	C	H	N	C/N
Calculation :	42.00	2.16	6.00	7.00
Calculation with H_2O and NaCl :	27.99	3.02	3.99	7.00
Found :	27.72	3.16	3.95	7.02

Water content: 16 mol/mol

ESI-MS negative mode (m/z):
$[M-Na]^-$: 1379.2, $[M-2Na+H]^-$: 1357.1, $[M-3Na-H]^-$: 1335.2

IR spectrum (cm^{-1}):

3433 (br, s)	2363 (w)	1526(m)	1186 (m)	1040 (s)
612 (m)	422 (w)			

500 MHz ^{1}H NMR spectrum (DMSO-*d*$_6$): δ (ppm), *J* (Hz)

10.56	-NH-CO	s	1H (exchangeable)
10.52	-NH-CO	s	1H (exchangeable)
9.89	-NH-CO-NH-	s	1H (exchangeable)
9.14	H8	d (^{4}J = 1.6)	1H
9.08	H4	d (^{4}J = 0.9)	1H
8.43	H2	d (^{4}J = 0.9)	1H
8.28	H6	d (^{4}J = 0.9)	1H
8.08	H3′, H5′	d (^{3}J = 8.8)	2H
8.02	H2″	s	1H
7.96	H2′, H6′	d (^{3}J = 8.8)	2H
7.77	H4″	d (^{3}J = 7.9)	1H
7.61	H6″	d (^{3}J = 8.2)	1H
7.46-7.43	H5″	t (^{3}J = 8.5)	1H

125 MHz ^{13}C NMR spectrum (DMSO-*d*$_6$): δ (ppm)

166.2	C9	135.7	C3	125.3	C8
165.1	C10	135.5	C1″	123.4	C6
153.0	C11	130.2	C8a	121.4	C4″
145.0	C7	129.5	C3″	121.2	C2
142.7	C5	129.0	C1′	121.1	C6″
142.4	C1	128.9	C5″	119.5	C3′, C5′
142.3	C4′	128.8	C2′, C6′	119.2	C4
140.3	C6′	126.3	C4a	117.6	C2″

Trisodium 7-[4-(4-nitrobenzamido)-benzamido]-naphthalene-1,3,5-trisulfonate
10a

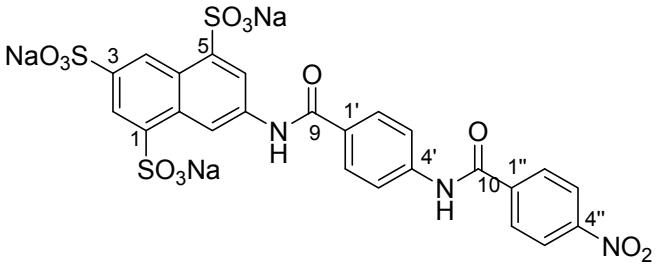

$C_{24}H_{14}N_3Na_3O_{13}S_3$ (717.54)

444 mg (2.4 mmol) 4-Nitrobenzoylchloride dissolved in 5 ml toluene were slowly added to the stirred solution of 0.9 g (1.6 mmol) compound 8b in 50 ml water until there was no amine left. The reaction was carried out according to GRP 2.

Yield: white powder, 87 % (1 g)
TLC: R_f = 0.43 (MP1)
HPLC: 99.3 % (t_R = 5.09 min)
UV spectrum (phosphate buffer pH of 6.5): λ_{max} = 264.5 nm
NaCl: 5.29 %

Elemental analysis (%):

	C	H	N	C/N
Calculation:	40.17	1.97	5.86	6.86
Calculation with H_2O and NaCl:	32.02	3.25	4.67	6.86
Found:	31.78	3.46	4.56	6.97

Water content: 7 mol/mol

IR spectrum (cm^{-1}):

3446 (br, s)	1674 (m)	1601 (m)	1540 (s)
1466 (w)	1436 (w)	1325 (m)	1193 (s)
1040 (vs)	866 (w)	792 (w)	760 (w)
714 (m)	670 (s)	613 (s)	

500 MHz ^{1}H NMR spectrum (DMSO-d_6): δ (ppm), J (Hz)

10.83	-NH-CO	s	(1H) exchangeable
10.56	-NH-CO	s	(1H) exchangeable
9.14	H8	d (^5J = 1.0)	(1H)
9.05	H4	d (^5J = 1.0)	(1H)
8.43	H2	d (^4J = 2.2)	(1H)
8.41	H3′, H5′	d (^3J = 9.0)	(2H)
8.27	H6	d (^4J = 1.9)	(1H)
8.25	H2′, H6′	d (^3J = 9.0)	(2H)
8.14	H2″, H6″	d (^3J = 8.7)	(2H)
7.97	H3″, H5″	d (^3J = 8.7)	(2H)

125 MHz ^{13}C NMR spectrum (DMSO-d_6): δ (ppm)

164.2	C9	139.8	C4′	125.8	C8
163.9	C10	135.3	C3	124.5	C3″, C5″
154.3	C4″	129.8	C8a	123.9	C6
143.9	C7	129.7	C1′	121.5	C3′, C5′
141.6	C5	129.0	C2″, C6″	120.4	C2
140.8	C1	128.0	C2′, C6′	119.9	C4
140.7	C1″	126.0	C4a		

Trisodium 7-[4-(4-aminobenzamido)-benzamido]-naphthalene-1,3,5-trisulfonate
10b

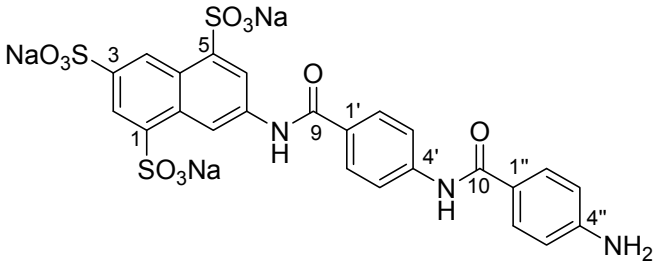

$C_{24}H_{16}N_3Na_3O_{11}S_3$ (687.56)

20 mg Palladium (10%) on charcoal were added as catalyst to a solution of 950 mg (1.3 mmol) compound 10a in water. The reaction was carried out according to GRP 3.

Yield: beige powder, 84.2 % (800 mg)
TLC: R_f = 0.69 (MP1)
HPLC: 98.5 % (t_R = 97.07 min)
UV spectrum (phosphate buffer pH of 6.5): λ_{max} = 260.5 nm
NaCl: 3.40 %

Elemental analysis (%):

	C	H	N	C/N
Calculation:	41.92	2.35	6.11	6.86
Calculation with H_2O and NaCl:	33.12	3.82	4.82	6.86
Found:	32.85	3.96	4.77	6.88

Water content: 8 mol/mol

IR spectrum (cm^{-1}):

3454 (br, s)	1667 (vs)	1608 (s)	1590 (s)
1539 (s)	1515 (s)	1470 (s)	1436 (s)
1409 (m)	1385 (m)	1357 (s)	1326 (vs)
1192 (br.vs)	1130 (s)	1079 (m)	1039 (vs)
1017 (m)	862 (m)	830 (m)	793 (s)
798 (vs)	666 (vs)	617 (s)	511 (s)

500 MHz ^{1}H NMR spectrum (DMSO-d_6): δ (ppm), *J* (Hz)

10.45	-NH-CO	s	1H (exchangeable)
10.00	-NH-CO	s	1H (exchangeable)
9.13	H8	dd (^5J = 1.0, ^4J = 1.6)	1H
9.08	H4	dd (^5J = 1.0, ^4J = 1.6)	1H
8.43	H2	d (^4J = 2.2)	1H
8.29	H6	d (^4J = 1.9)	1H
8.05	H3′, H5′	d (^3J = 9.0)	2H

7.91	H2′, H6	d (^3J = 9.0)	2H
7.75	H2′′, H6′′	d (^3J = 8.6)	2H
6.61	H3′′, H5′′	d (^3J = 8.6)	2H
5.79	-NH_2	s	1H

125 MHz ^{13}C NMR spectrum (DMSO-d_6): δ (ppm)

165.7	C9	142.5	C1′′	125.3	C8
165.2	C10	135.5	C3	123.4	C6
152.6	C4′′	130.2	C8a	121.2	C2
145.1	C7	129.7	C2′′, C6′′	120.8	C4
143.4	C4′	128.8	C1'	119.1	C3′, C5′
143.1	C5	128.7	C2′, C6′	112.8	C3′′, C5′′
142.8	C1	126.3	C4a		

Hexasodium 7,7′-{carbonylbis(azanediyl-4,1-phenylenecarbonylazanediyl (4,1-phenylene)carbonilazanediyl]}bis(naphthalene-1,3,5-trisulfonate) 10c

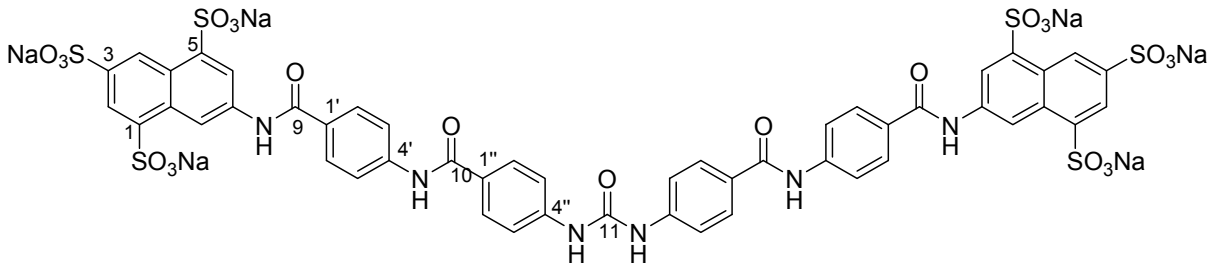

$C_{49}H_{30}N_6Na_6O_{23}S_6$ (1400.1)

A solution of 1.74 mmol phosgene (20 % in toluene) was slowly added to a solution of 600 mg (0.87 mmol) compound 10b in 20 ml water under heavy stirring at room temperature. The reaction was carried out according to GRP 4.

Yield: white powder, 44.6 % (500 mg)
TLC: R_f = 0.6 (MP2)
HPLC: 96.9 % (t_R = 4.99 min)
UV spectrum (phosphate buffer pH of 6.5): λ_{max} = 256.5 nm
NaCl: 4.37 %

Elemental analysis (%):

	C	H	N	C/N
Calculation:	42.00	2.16	6.00	7.00
Calculation with H_2O and NaCl:	22.78	2.42	3.25	7.00
Found:	23.03	2.82	3.29	6.99

Water content: 16 mol/mol

ESI-MS negative mode (m/z):
$[M-Na]^-$: 1377.2, $[M-2Na+H]^-$: 1355.3

IR spectrum (cm^{-1}):

3452 (br, s)	2361 (w)	1652 (s)	1595 (vs)
1531 (s)	1512 (s)	1472 (s)	1439 (m)
1411 (m)	1323 (s)	1188 (br, s)	1128 (s)
1042 (vs)	902 (w)	850 (m)	795 (m)
762 (m)	667 (s)	610 (vs)	532 (s)

500 MHz ^{1}H NMR spectrum (DMSO-d_6): δ (ppm), *J* (Hz)

10.50	-NH-CO	s	1H
10.42	-NH-CO	s	1H
10.26	-NH-CO-NH	s	1H
9.14	H8	d (^{5}J = 1.0)	1H
9.09	H4a	d (^{4}J = 1.9)	1H
8.44	H2	d (^{4}J = 2.2)	1H
8.29	H6	d (^{4}J = 1.9)	1H
8.10	H3′, H5′	d (^{3}J = 8.8)	2H
7.97	H2′, H6′ H2′′, H6′′	d (^{3}J = 8.8)	4H
7.66	H3′′, H5′′	d (^{3}J = 8.8)	1H

125 MHz ^{13}C NMR Spectrum (DMSO-d_6): δ (ppm)

165.4	C9	142.4	C4′, C4′′	125.3	C4A
165.1	C10	135.5	C3	123.4	C6
152.6	C11	130.2	C8a	121.1	C2
145.0	C7	129.3	C3′, C5′	119.5	C2′′, C6′′
143.3	C4′	128.8	C2′, C6′	119.2	C4′
142.7	C5	127.6	C1′, C1′′	117.1	C3′′, C5′′
142.7	C1	126.3	C4a		

Trisodium 7-(3-methyl-4-nitrobenzamido)-naphthalene-1,3,5-trisulfonate 11a

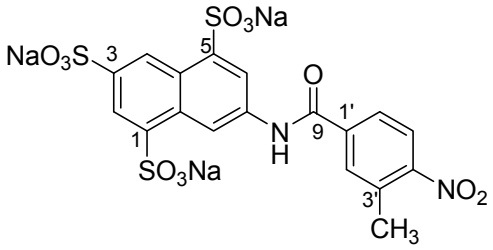

$C_{18}H_{11}N_2Na_3O_{12}S_3$ (612.5)

1.55 g (7.2 mmol) 3-Methyl-4-nitrobenzoylchloride was dissolved in 10 ml toluene and slowly added to the stirred solution of 1.5 g (3.7 mmol) trisodium 7-aminonaphthalene-1,3,5-trisulfonate in 50 ml water, until there is no amine left. The reaction was continued according to GRP 3.

Yield : 88.8 % (2.0 g)
TLC : R_f = 0.33 (MP1)
HPLC : 97.4 % (t_R = 5.17 min)

UV-Spectrum (Phosphate Buffer pH of 6.5): λ_{max} = 249 nm
NaCl : 47.3 %

Elemental-Analysis (%) :

	C	H	N	C/N
Calculation :	35.30	1.81	4.57	7.72
Calculation with H_2O and NaCl :	16.44	1.53	2.13	7.71
Found :	16.37	1.82	2.48	6.60

Water content : 4 mol/mol

IR spectrum :

3453.69 (br, s)	1635.93 (m)	1576.61 (m)	1546.29 (s)
1471.86 (w)	1436.75 (w)	1329.89 (m)	1200.32 (br, vs)
1130.81 (br, vs)	1114.89 (br, vs)	1042.38 (vs)	854.34 (w)
790.15 (w)	668.29 (s)	638.19 (s)	615.91 (s)
527.78 (w)			

500 MHz ^{1}H NMR spectrum (DMSO-d6) : δ (ppm), *J* (Hz)

10.809	-NH-CO-	s		1H (exchangeable)
9.14	H8	dd	(^5J = 0.8, ^4J = 1.7)	1H
9.06	H4	dd	(^5J = 0.8, ^4J = 2.3)	1H
8.45	H2	d	(^4J = 2.3)	1H
8.28	H6	d	(^4J = 1.7)	1H
8.16	H2′	dd	(^5J = 1.0, ^4J = 1.5)	1H
8.10	H6′	d	(^3J = 8.5)	1H
8.08	H5′	dd	(^4J = 2.0, ^3J = 8.5)	1H
2.59	-CH3	s		3H

125 MHz ^{13}C NMR spectrum (DMSO-d6) : δ (ppm)

164.0	C9	134.9	C3	125.2	C8
150.6	C4′	132.7	C3′	124.5	C5′
145.2	C7	132.3	C2′	123.5	C6
142.9	C5	130.1	C8a	120.8	C2
142.7	C1	126.9	C6′	119.5	C4
138.8	C1′	126.6	C4a	19.5	C10

Trisodium 7-(3-methyl-4-aminobenzamido)-naphthalene-1,3,5-trisulfonate 11b

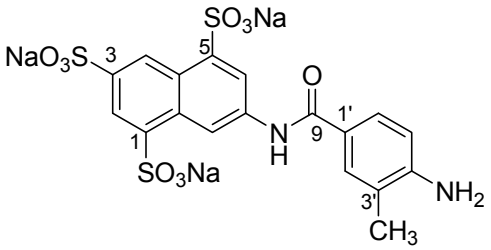

$C_{18}H_{13}N_2Na_3O_{10}S_3$ (582.5)

20 mg Palladium (10%) on charcoal was added as catalyst to a solution of 1.5 g (mmol) nitroderivative in water. The reaction was continued according to GRP 4.

Yield : 43.7 % (990 mg)
TLC : R_f = 0.51 (MP1)
HPLC : 98.7 % (t_R = 1.85 min)
UV-Spectrum (Phosphate Buffer pH of 6.5) : λ_{max} = 254 nm
NaCl : 25.8 %

IR spectrum :

3442.21 (br, s)	1636.13 (m)	1543.74 (m)	1508.21 (s)
1124.07 (br, vs)	1040.46 (s)	615.28 (s)	

500 MHz ^{1}H NMR spectrum (DMSO-d6) : δ (ppm), *J* (Hz)

10.809	-NH-CO-	s		1H (exchangeable)
9.14	H8	dd	(^5J = 0.8, ^4J = 1.7)	1H
8.97	H4	dd	(^5J = 0.8, ^4J = 2.3)	1H
8.38	H2	d	(^4J = 2.3)	1H
8.26	H6	d	(^4J = 1.7)	1H
7.36	H5′	dd	(^4J = 2.0, ^3J = 8.5)	1H
7.33	H2′	d	(^4J = 2.0)	1H
6.90	H6′	dd	(^3J = 8.5)	1H
2.59	-CH_3	s		3H

125 MHz ^{13}C NMR spectrum (DMSO-d6) : δ (ppm)

165.5	C9	130.3	C8a	121.5	C6′
150.2	C4′	132.7	C3′	121.3	C2
144.9	C7	127.3	C2′	119.8	C4
142.6	C5	126.0	C4a	118.8	C1′
142.3	C1	125.2	C8	112.8	C5′
135.8	C3	123.3	C6	19.5	C10

Hexasodium 7,7'-{carbonylbis[azanediyl(3-methyl-4,1-phenylene) carbonylazanediyl]}bis(naphthalene-1,3,5-trisulfonate)
11c

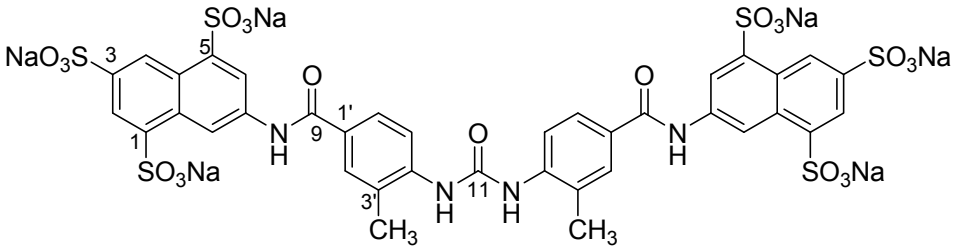

$C_{37}H_{24}N_4Na_6O_{21}S_6$ (1190.9)

A solution of 2.26 mmol phosgene (20 % in toluen) was slowly added to a solution of 660 mg (1.13 mmol) compound 11b in 20 ml water under heavy stirring at room temperature. The reaction was continued according to GRP 5.

Yield : 59.5 % (800 mg)
TLC : R_f = 0.29 (MP2)
HPLC : 95.1 % (t_R = 5.87 min)
UV-Spectrum (Phosphate Buffer pH of 6.5): λ_{max} = 257 nm
NaCl : 50.4 %

ESI-MS negative mode (m/z):
$[M-Na]^{-\cdot}$: 1168.7, $[M-2Na+H]^-$: 1144.7, $[M-3Na+H]^-$: 1122.7

IR spectrum :
3445.11 (br, s) 1636.03 (m) 1041.67 (w)

500 MHz ^{1}H NMR spectrum (DMSO-d6) : δ (ppm), *J* (Hz)

10.809	-NH-CO-	s		1H (exchangeable)
9.14	H8	dd	(^5J = 0.8, ^4J = 1.7)	1H
8.97	H4	dd	(^5J = 0.8, ^4J = 2.3)	1H
8.38	H2	d	(^4J = 2.3)	1H
8.26	H6	d	(^4J = 1.7)	1H
7.36	H6′	d	(^3J = 8.5)	1H
7.33	H2′	d	(^3J = 1.8)	1H
6.90	H5′	dd	(^4J = 1.8, ^3J = 8.5)	1H
2.59	-CH3	s		3H

125 MHz ^{13}C NMR spectrum (DMSO-d6) : δ (ppm)

164.0	C9	135.3	C3	126.3	C8
151.9	C11	133.8	C3′	125.7	C5′
149.0	C4′	132.0	C2′	121.6	C6
142.4	C7	130.1	C8a	120.3	C2
142.2	C5	128.1	C6′	119.1	C4
140.3	C1	127.0	C4a	18.9	C10
136.0	C1′				

Trisodium 7-(2-methyl-3-nitrobenzamido)-naphthalene-1,3,5-trisulfonate 12a

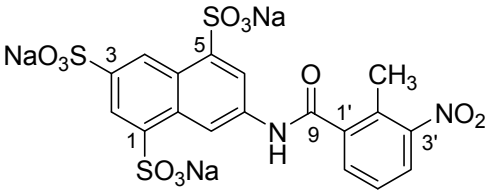

$C_{18}H_{11}N_2Na_3O_{12}S_3$ (612.5)

2.08 g (9.65 mmol) 2-Methyl-3-nitrobenzoylchloride which was obtained by GRP1, were slowly added to the stirred solution of 2.5 g (mmol) trisodium 7-aminonaphthalene-1,3,5-trisulfonate in 50 ml water, until there was no amine left. The reaction was continued according to GRP 2.

Yield: 80 % (3.02 g)
TLC: R_f = 0.33 (MP1)
HPLC: 96.0 % (t_R = 3.74 min)
UV spectrum (phosphate buffer pH of 6.5): λ_{max} = 254 nm
NaCl: 14.8 %

Elemental analysis (%):

	C	H	N	C/N
Calculation:	35.30	1.81	4.57	7.72
Calculation with H_2O and NaCl:	27.26	2.28	3.53	7.72
Found:	26.92	2.62	3.91	6.90

Water content: 3 mol/mol

ESI-MS negative mode:
$[M-Na]^-$: 590.3, $[M-2Na]^-$: 589.3, $[M-3Na]^-$: 567.3

IR spectrum (cm^{-1}):

3450 (br,s)	1684 (w)	1636 (w)	1576 (m)
1526 (m)	1465 (w)	1436 (w)	1324 (m)
1355 (w)	1326 (w)	1196 (br,vs)	1113 (m)
1077 (w)	1043 (vs)	791 (w)	719 (w)
665 (m)	617 (m)	527 (m)	

500 MHz ^{1}H NMR spectrum (DMSO-d_6): δ (ppm), *J* (Hz)

10.78	-NH-CO-	s		1H
9.14	H8	s		1H
9.04	H4	d	(^4J = 1.6)	1H
8.55	H2	d	(^4J = 1.9)	1H
8.31	H6	d	(^4J = 1.5)	1H
7.61	H4′, H5′	d	(^3J = 7.9)	2H
7.22	H6′	d	(^3J = 7.9)	1H
2.35	$-CH_3$	s		3H

125 MHz ^{13}C NMR spectrum (DMSO-d_6): δ (ppm)

166.2	C9	135.0	C3	125.3	C8
149.5	C3′	131.6	C2′	124.7	C5′
145.4	C7	130.1	C8a	123.5	C6
142.9	C5	128.9	C6′	119.9	C2
142.6	C1	127.2	C4′	118.3	C4
140.5	C1′	126.5	C4a	15.6	C10

Trisodium 7-(3-amino-2-methylbenzamido)-naphthalene-1,3,5-trisulfonate 12b

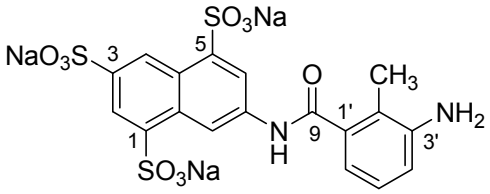

$C_{18}H_{13}N_2Na_3O_{10}S_3$ (582.5)

20 mg Palladium (10%) on charcoal were added as catalyst to a solution of 2 g (3.27 mmol) compound 12a in water. The reaction was continued according to GRP 3.

Yield: brown powder, 78.9 % (1.5 g)
TLC: R_f = 0.3 (MP1)
HPLC: 97.7 % (t_R = 1.47 min)
UV-Spectrum (phosphate buffer pH of 6.5): λ_{max} = 256 nm
NaCl: 16.4 %

Elemental analysis (%):

	C	H	N	C/N
Calculation :	37.12	2.25	4.81	7.72
Calculation with H_2O and NaCl :	27.24	2.79	3.53	7.71
Found :	27.62	2.94	4.13	6.70

Water content: 4 mol/mol

ESI-MS negative mode (m/z):
$[M-Na]^-$: 559.3, $[M-2Na-H]^-$: 537.3, $[M-3Na-H]^-$: 515.3

500 MHz ^{1}H NMR spectrum (DMSO-d_6): δ (ppm), J (Hz)

10.43	-NH-CO-	s		1H
9.12	H8	s		1H
8.99	H4	d	(^4J = 1.7)	1H
8.43	H2	d	(^4J = 2.2)	1H
8.27	H6	d	(^4J = 1.8)	1H
6.97-6.94	H4′	t	(^3J = 7.6)	1H
6.67	H5′, H6′	dd	(^3J = 8.0, ^3J = 7.6)	2H

4.98	$-NH_2$	s	2H
2.13	$-CH_3$	s	3H

125 MHz ^{13}C NMR spectrum (DMSO-*d_6*): δ (ppm)

169.0	C9	135.5	C3, C1′	120.4	C2
147.1	C3′	130.2	C8A	118.3	C4
145.2	C7	126.2	C4a	118.2	C2′
142.7	C5	125.8	C5′	115.2	C5′
142.3	C1	125.3	C8	115.1	C6′
138.6	C1′	123.4	C6	14.12	C10

Hexasodium 7,7′-{carbonylbis[azanediyl(2-methyl-3,1-phenylene)carbonylazanediyl]}bis(naphthalene-1,3,5-trisulfonate)
12c

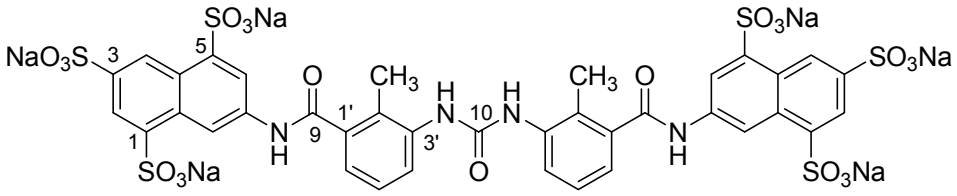

$C_{37}H_{24}N_4Na_6O_{21}S_6$ (1190.9)

A solution of 1.72 mmol phosgene (20 % in toluene) was slowly added to a solution of 500 mg (0.86 mmol) compound 12b in water under heavy stirring at room temperature. The reaction was continued according to GRP 4.

Yield: pale brown powder, 64.5 % (330 mg)
TLC: R_f = 3.48 (MP2)
HPLC: 94.6 % (t_R = 5.79 min)
UV spectrum (phosphate buffer pH of 6.5): λ_{max} = 258 nm
NaCl: 29.1 %

Elemental analysis (%):

	C	H	N	C/N
Calculation:	37.32	2.03	4.70	7.94
Calculation with H_2O and NaCl:	22.97	2.29	2.89	7.93
Found:	22.97	1.98	3.11	7.39

Water content: 10 mol/mol

ESI-MS negative mode (m/z):
$[M-H]^-$: 1190.0

IR spectrum (cm^{-1}):
3446 (br,s) 2360 (w) 1636 (w)

500 MHz ^{1}H NMR spectrum (DMSO-*d*$_6$): δ (ppm), *J* (Hz)

10.63	-NH-CO-	s		1H
9.12	H8	dd	(^{4}J = 0.9)	1H
9.00	H4	d	(^{4}J = 1.6)	1H
8.54	-NH-CO-NH-	s		1H
8.48	H2	d	(^{4}J =1.9)	1H
8.27	H6	d	(^{4}J =1.9)	1H
7.91	H4′	d	(^{3}J = 7.3)	1H
7.25	H5′	t	(^{3}J = 7.8)	1H
7.16	H6′	d	(^{3}J = 6.6)	1H
2.37	-CH_3	s		3H

125 MHz ^{13}C NMR spectrum (DMSO-*d*$_6$): δ (ppm)

168.3	C9	135.5	C3, C1′	123.4	C6
153.3	C10	130.2	C8a	123.1	C6′
145.2	C7	127.7	C2′	121.9	C4′
142.8	C5	126.3	C4a	120.3	C2
142.4	C1	125.6	C8	118.4	C4
138.8	C1′	125.3	C5’	15	-CH_2
138.0	C3′				

Trisodium 7-(4-methoxy-3-nitrobenzamido)-naphthalene-1,3,5-trisulfonate 13a

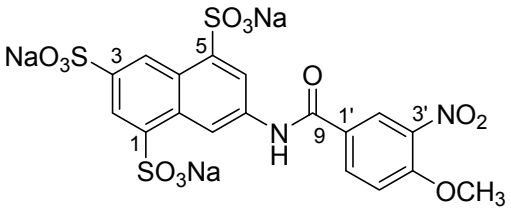

$C_{18}H_{11}N_2Na_3O_{13}S_3$ (628.5)

2.27 g (9.8 mmol) 4-Methoxy-3-nitrobenzoylchloride which was obtained by GRP1, were slowly added to the stirred solution of 2 g (mmol) trisodium 7-aminonaphthalene-1,3,5-trisulfonate in 50 ml water, until there was no amine left. The reaction was continued according to GRP 2.

Yield: white powder, 81.2 % (2.5 mg)
TLC: R_f = 0.29 (MP1)
HPLC: 99.1 % (t_R = 3.88 min)
UV spectrum (phosphate buffer pH of 6.5): λ_{max} = 265 nm
NaCl: 7.58 %

Elemental analysis (%):

	C	H	N	C/N
Calculation :	34.40	1.76	4.46	7.72
Calculation with H_2O and NaCl :	27.13	2.91	3.52	7.71
Found :	27.02	2.81	3.75	7.20

Water content: 6 mol/mol

IR spectrum (cm^{-1}):

3450 (br, s)	1618 (s)	1576 (m)	1466 (w)
1439 (w)	1358 (m)	1328 (m)	1273 (s)
1201(s)	1113 (m)	1077 (w)	1045 (vs)
822 (w)	790 (w)	749 (m)	668 (s)
612 (s)	528 (m)		

500 MHz ^{1}H NMR spectrum (DMSO-d_6): δ (ppm), J (Hz)

10.68	-NH-CO	s		1H
9.13	H8	dd	(^4J = 2.0, ^5J = 0.8)	1H
9.05	H4	d	(^4J = 2.2)	1H
8.63	H2′	d	(^4J = 2.4)	1H
8.42	H2	d	(^4J = 2.2)	1H
8.38	H6′	dd	(^4J = 2.4, ^3J = 8.8)	1H
8.27	H6	d	(^3J = 2.0)	1H
7.52	H5′	d	(^4J = 8.8)	1H
4.02	-OCH_3	s		3H

125 MHz ^{13}C NMR spectrum (DMSO-d_6): δ (ppm)

163.1	C9	134.9	C3′	124.9	C2′
154.4	C4′	134.2	C6′	123.4	C6
145.2	C7	130.1	C8A	119.4	C4
142.9	C5	126.8	C1′	114.3	C5′
142.7	C1	126.5	C4a	55.0	C9
138.9	C3	125.2	C8		

Trisodium 7-(3-amino-4-methoxybenzamido)-naphthalene-1,3,5-trisulfonate 13b

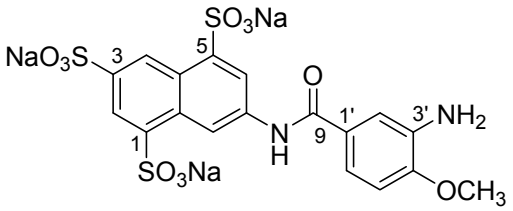

$C_{18}H_{13}N_2Na_3O_{11}S_3$ (598.47)

20 mg Palladium (10%) on charcoalwere added as catalyst to a solution of 1.5 g (2.38 mmol) compound 13a in water. The reaction was continued according to GRP 3.

Yield: white powder 81 % (1.15 mg)

TLC: R_f = 0.28 (MP1)
HPLC: 93.6 % (t_R = 2.15 min)
UV spectrum (phosphate buffer pH of 6.5): λ_{max} = 256 nm
NaCl: 20.4 %

Elemental analysis (%):

	C	H	N	C/N
Calculation:	36.12	2.19	4.68	7.72
Calculation with H_2O and NaCl:	17.46	4.56	2.26	7.72
Found:	17.53	1.71	2.22	7.89

Water content: 21 mol/mol

IR-spectrum (cm^{-1}):

3431 (br, s)	1646 (m)	1579 (m)	1551 (m)
1514 (m)	1358 (m)	1475 (w)	1438 (w)
1326 (m)	1278 (m)	1193 (br, vs)	1045 (vs)
1124 (s)	1043 (vs)	844 (w)	788 (w)
753 (m)	528 (m)	672 (s)	611 (s)
505 (m)			

500 MHz ^{1}H NMR spectrum (DMSO-d_6): δ (ppm), J (Hz)

10.23	-NH-CO	s		1H
9.11	H8	d		1H
8.96	H4	dd	(^4J = 1.6, ^4J = 0.9)	1H
8.38	H2	dd	(^4J = 1.6, ^4J = 0.9)	1H
8.26	H6	d	(^4J = 1.7)	1H
7.35	H2′	d	(^4J = 2.3)	1H
7.33	H6′	d	(^3J = 8.4)	1H
6.89	H5′	d	(^3J = 8.4)	1H
4.84	$-NH_2$	s		2H
3.84	$-OCH_3$	s		3H

125 MHz ^{13}C NMR spectrum (DMSO-d_6): δ (ppm)

165.8	C9	134.8	C3	125.2	C8
149.1	C4′	132.7	C5′	124.5	C2′
144.9	C7	132.3	C6′	123.5	C6
142.8	C5	130.1	C8a	120.8	C2
142.4	C1	126.9	C2′	119.5	C4
138.8	C1′	126.6	C4a	55.0	C10

Hexasodium 7,7′-{carbonylbis[azanediyl(4-methoxy-3,1-phenylene)carbonylazanediyl]}bis (naphthalene-1,3,5-trisulfonate)
13c

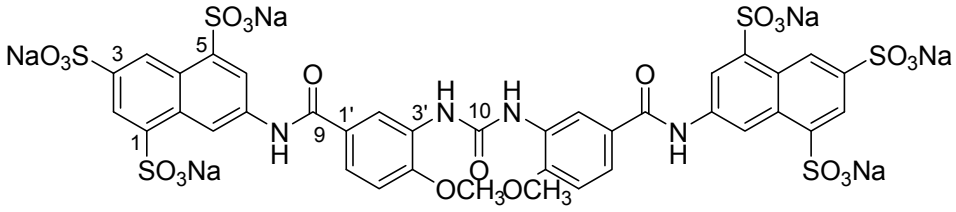

$C_{37}H_{24}N_4Na_6O_{23}S_6$ (1222.93)

A solution of 2.16 mmol phosgene (20 % in toluen) was slowly added to a solution of 649 mg (1.08 mmol) compound 13b in 20 ml water under heavy stirring at room temperature. The reaction was continued according to GRP 4.

Yield: white powder, 68.2 % (900 mg)
TLC: R_f = 0.76 (MP2)
HPLC: 98.3 % (t_R = 6.46 min)
UV spectrum (phosphate buffer pH of 6.5): λ_{max} = 265 nm
NaCl: 24.2 %

Elemental analysis (%):

	C	H	N	C/N
Calculation:	36.34	1.98	4.58	7.93
Calculation with H_2O and NaCl:	19.60	3.48	2.48	7.93
Found:	19.63	1.49	2.54	7.73

Water content: 27 mol/mol

ESI-MS negative mode (m/z):
$[M-Na]^-$: 1222.9

IR spectrum (cm^{-1}):
3442 (br, s) 1636 (m) 1222 (m) 1042 (m)

500 MHz ^{1}H NMR spectrum (DMSO-d_6): δ (ppm), *J* (Hz)

10.45	-NH-CO-	s		2H (exchangable)
9.12	H8	dd	(^5J = 1.0, ^4J = 1.9)	2H
9.03	H4	d	(^4J = 2.2)	2H
8.97	-NH-CO-NH-	s		2H (exchangable)
8.71	H2′	d	(^4J = 2.2)	2H
8.40	H2	d	(^4J = 2.2)	2H
8.27	H6	d	(^4J = 1.9)	2H
7.80	H6′	dd	(^4J = 2.2, ^3J = 8.7)	2H
7.14	H5′	d	(^3J = 8.7)	2H
3.98	$-CH_3$	s		3H

125 MHz ^{13}C NMR spectrum (DMSO-d_6): δ (ppm)

165.6	C9	135.1	C8a	121.3	C1′
151.8	C10	134.7	C3	119.2	C4
150.4	C4′	133.2	C3′	117.5	C6′
145.8	C7	130.2	C8a	116.9	C5′
142.6	C5	126.3	C4a	113.5	C2′
142.1	C1	123.4	C6	55.0	-CH_2
137.2	C1′	122.7	C2		

Trisodium 7-(4-nitrophenyl)acetamido-naphthalene-1,3,5-trisulfonate 14a

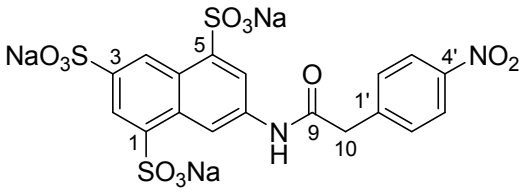

$C_{18}H_{11}N_2Na_3O_{12}S_3$ (612.45)

0.83 g (3.87 mmol) (4-Nitrophenyl)acetylchloride, which was obtained by GRP1, were slowly added to the stirred solution of 1.0 g (2.58 mmol) trisodium 7-aminonaphthalene-1,3,5-trisulfonate in 50 ml water, until there is no amine left. The reaction was continued according to GRP 2.

Yield: pink powder, 35.00 % (0.55 g)
TLC: R_f = 0.6 (MP1)
HPLC: 99.4 % (t_R = 4.05 min)
UV spectrum (phosphate buffer pH of 6.5): λ_{max} = 254 nm
NaCl: 30.7 %

Elemental analysis (%):

	C	H	N	C/N
Calculation:	35.30	1.81	4.57	7.72
Calculation with H_2O and NaCl:	20.79	2.23	2.69	7.72
Found:	20.81	1.86	2.93	7.10

Water content: 6 mol/mol

IR spectrum (cm^{-1}):

3448 (br, s)	1582 (w)	1551 (w)	1518 (m)
1474 (w)	1441 (w)	1351 (m)	1192 (br,s)
1122 (m)	1043 (vs)	798 (w)	664 (m)
612 (m)			

500 MHz ^{1}H NMR spectrum (DMSO-d_6): δ (ppm), *J* (Hz)

10.68	-NH-CO	s		1H
9.14	H-8	s		1H
8.88	H-4	s		1H
8.51	H-2	d	(^{4}J =1.9)	1H
8.30	H-6	d	(^{4}J =1.4)	1H
8.27	H3′, 5′	d	(^{3}J = 8.6)	2H
7.72	H2′, 6′	d	(^{3}J = 8.6)	2H
3.95	-CH_2	d		2H

125 MHz ^{13}C NMR spectrum (DMSO-d_6): δ (ppm)

168.3	C9	135.5	C3	123.7	C3′, C5′
155.9	C4′	130.9	C1′	123.6	C6
146.7	C6′	130.8	C2′, C6′	119.8	C4
145.5	C7	130.4	C8a	117.6	C2
144.7	C5	126.3	C4a	43.16	C10
142.9	C1	125.4	C8		

Trisodium 7-(4-aminophenyl)acetamido-naphthalene-1,3,5-trisulfonate 14b

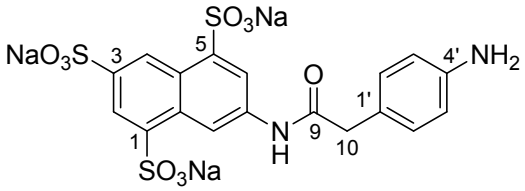

$C_{18}H_{13}N_2Na_3O_{10}S_3$ (582.47)

20 mg Palladium (10%) on charcoal were added as catalyst to a solution of 0.70 g (1.14 mmol) compound 14a in water. The reaction was continued according to GRP 3.

Yield: brown powder, 90.36 % (0.60 g)
TLC: R_f = 0.52 (MP1)
HPLC: 99.0 % (t_R = 1.19 min)
UV spectrum (phosphate buffer pH of 6.5): λ_{max} = 255 nm
NaCl: 37.0 %

Elemental analysis (%):

	C	H	N	C/N
Calculation:	37.12	2.25	4.81	7.72
Calculation with H_2O and NaCl:	19.22	2.42	2.50	7.68
Found:	19.00	1.79	2.90	6.55

Water content: 7 mol

ESI-MS negative mode (m/z):
$[M-Na]^-$: 559.3, $[M-2Na-H]^-$: 537.3, $[M-3Na-H]^-$: 515.5

IR spectrum (cm^{-1}):

3448 (br, s)	1618 (m)	1518 (w)	1475 (w)
1212 (br,vs)	1120 (s)	1044 (m)	669 (m)
614 (s)	530 (w)		

500 MHz ^{1}H NMR spectrum (DMSO-d_6): δ (ppm), *J* (Hz)

10.98	-NH-CO-	s		1H
9.06	H8	s		1H
8.75	H4	pd		1H
8.45	H2	d	(^4J = 2.0)	1H
8.22	H6	d	(^4J = 1.5)	1H
7.01	H3′, H5	d	(^3J = 8.2)	2H
6.52	H2′, H6′	d	(^3J = 8.3)	2H
4.89	$-NH_2$	s		2H
3.46	$-CH_2$	s		2H

Hexasodium 7,7′-{carbonylbis[azanediyl-4,1-(phenylenemethylene)carbonylazanedyl)]bis(naphthalene-1,3,5-trisulfonate) 14c

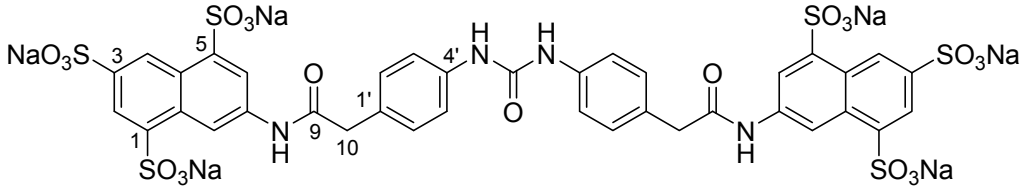

$C_{37}H_{24}N_4Na_6O_{21}S_6$ (1190.93)

A solution of 1.78 mmol phosgene (20% in toluen) was slowly added to a solution of 500 mg (0.89 mmol) compound 14b in 20 ml water under heavy stirring at room temperature. The reaction was continued according to GRP 4.

Yield: brown powder, 73.3 % (733 mg)
TLC: R_f = 0.66 (MP2)
HPLC: 95.2 % (t_R = 5.95 min)
UV spectrum (phosphate buffer pH of 6.5): λ_{max} = 258 nm
NaCl: 65.6 %

Elemental analysis (%):

	C	H	N	C/N
Calculation:	37.32	2.03	4.70	7.93
Calculation with H_2O and NaCl:	11.39	1.06	1.44	7.93
Found:	11.36	0.85	1.44	7.88

Water content: 8 mol/mol

ESI-MS negative mode (m/z):
$[M-H]^-$: 1190.0

IR spectrum (cm^{-1}):
3430 (br, s) 1628 (m) 1128 (w)

500 MHz ^1H NMR spectrum (DMSO-d_6): δ (ppm), *J* (Hz)

10.43	-NH-CO-	s	1H (exchangeable)
9.22	-NH-CO-NH	s	1H (exchangeable)
9.08	H-8	s	1H
8.82	H-4	d (^4J = 2.2)	1H
8.46	H-2	d (^4J = 1.9)	1H
8.24	H-6	d (^4J = 1.6)	1H
7.40	H-3′, H-5′	d (^3J = 8.8)	2H
7.25	H-2′, H-6′	d (^3J = 8.5)	2H
3.61	$-CH_2-$	d (^4J = 2.2)	2H

Sodium 4-(4-fluoro-3-nitrobenzamido)naphthalene-1-sulfonate
15a

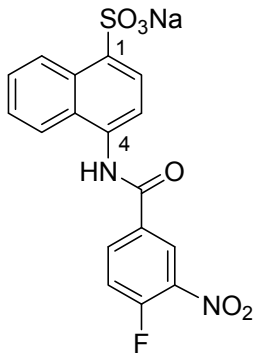

$C_{17}H_{10}FN_2NaO_6S$ (412.32)

1.64 g (8 mmol) 4-Fluoro-3-nitrobenzoylchloride, which was obtained by GRP1, were slowly added to the stirred solution of 1.5 g (6.1 mmol) sodium 4-amino-naphthalene-1-sulfonate in 50 ml water, until there was no amine left. The reaction was continued according to GRP 2.

Yield: pink powder, 83.6 % (2.1 g)
TLC: R_f = 0.85 (MP1)
HPLC: 98.6 % (t_R = 4.14 min)
UV spectrum (phosphate buffer pH of 6.5): λ_{max} = 297 nm
NaCl: 4.17 %

Elemental analysis (%):

	C	H	N	C/N
Calculation:	49.52	2.44	6.79	7.29
Calculation with H_2O and NaCl:	48.08	2.33	6.47	7.29
Found:	48.45	2.22	6.52	7.43

Water content: 1 mol/mol

IR spectrum (cm^{-1}):

3462 (br,s)	3200 (s)	1661 (s)	1640 (s)
1622 (s)	1595 (m)	1544 (vs)	1527 (s)
1490 (s)	1422 (w)	1409 (w)	1381 (m)
1347 (s)	1316 (w)	1300 (s)	1268 (s)
1195 (vs)	1161 (s)	1134 (m)	1064 (vs)
1026 (w)	904 (w)	881 (w)	843 (s)
814 (w)	778 (m)	764 (m)	747 (m)
693 (vs)	643 (m)	614 (m)	546 (m)
494 (m)			

500 MHz ^{1}H NMR spectrum (DMSO-d_6): δ (ppm), J (Hz)

10.85	-NH-CO	s		1H
8.97	H8	d	(^3J = 7.9)	1H
8.93	H2′	dd	(^4J = 1.9, ^4J = 7.1)	1H
8.57	H6′	m		1H
8.04	H5, H6	d	(^3J =7.6)	2H
7.88	H5′	d	(^3J = 8.5, ^3J = 9.8)	1H
7.62	H2, H3	d	(^4J = 2.0, ^3J = 11.5)	2H
7.59	H7	d	(^3J = 7.9)	1H

125 MHz ^{13}C NMR spectrum (DMSO-d_6): δ (ppm)

163.6	C9	131.6	C1′	126.0	C7
156.8	C4′	130.1	C8a	124.4	C3
143.1	C4	129.7	C4a	123.4	C5
137.1	C3′	128.3	C8	122.4	C2
136.2	C1	126.4	C2′	119.2	C5′
134.6	C6′	126.1	C6		

Sodium 4-(3-amino-4-fluorobenzamido)naphthalene-1-sulfonate
15b

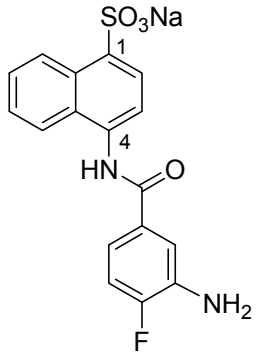

$C_{17}H_{12}FN_2NaO_4S$ (382.34)

20 mg Palladium (10%) on charcoal were added as catalyst to a solution of 0.8 g (1.94 mmol) compound 15a in water. The reaction was continued according to GRP 3.

Yield: grey powder, 91.76 % (680 mg)
TLC: R_f = 0.57 (MP1)
HPLC: 99.0 % (t_R = 1.88 min)
UV spectrum (phosphate buffer pH of 6.5): λ_{max} = 228 nm
NaCl: 57.7 %

Elemental analysis (%):

	C	H	N	C/N
Calculation:	53.40	3.16	7.33	7.29
Calculation with H_2O and NaCl:	17.61	2.08	2.42	7.29
Found:	17.72	1.18	2.43	7.29

Water content: 6 mol/mol

IR spectrum (cm^{-1}):

3445 (br,s)	1636 (s)	1500 (s)	1384 (w)
1309 (w)	1200 (vs)	1055 (s)	755 (m)
691 (s)	642 (m)	540 (w)	

500 MHz ^{1}H NMR spectrum (DMSO-d_6): δ (ppm), *J* (Hz)

10.34	-NH-CO-	s		1H
8.95	H8	d	(^3J = 7.9)	1H
8.02	H5	d	(^3J = 7.7)	1H
7.99	H6	d	(^3J = 7.8)	1H
7.59	H2	d	(^3J = 5.5)	1H
7.57	H2′	dd	(^4J = 1.9, ^3J = 8.0)	1H
7.53	H3, H7	d	(^3J = 2.4, 3.5)	2H
7.37-7.34	H6′	m		1H
7.19	H5′	dd	(^3J =8.4, ^3J =11.0)	1H
5.45	-NH_2	s		2H

125 MHz ^{13}C NMR spectrum (DMSO-d_6): δ (ppm)

166.4	C9	130.1	C8a	123.5	C5
152.8	C4′	129.9	C4a	122.6	C2
142.6	C4	128.3	C8	116.6	C6′
136.8	C3′	125.9	C6	115.8	C5′
135.4	C1	125.8	C7	114.9	C2′
131.5	C1′	124.5	C3		

Disodium 4,4′-{carbonylbis[azenediyl(4-fluoro-3,1-phenylene) carbonylazenediyl]}bis(naphthalene-1-sulfonate)
15c

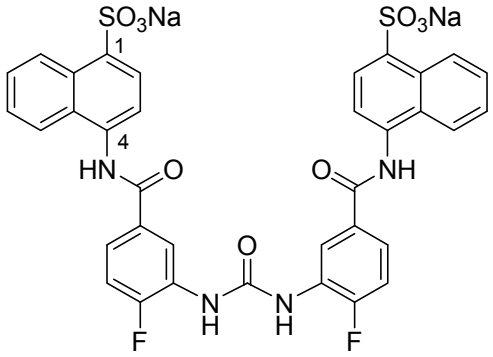

$C_{35}H_{22}F_2N_4Na_2O_9S_2$ (790.68)

A solution of 2.1 mmol phosgene (20 % in toluen) was slowly added to a solution of 400 mg (1.05 mmol) compound 15b in 20 ml water under heavy stirring at room temperature. The reaction was continued according to GRP 4.

Yield: grey powder, 19.34 % (160 mg)
TLC: R_f = 0.75 (MP2)
HPLC: 98.7 % (t_R = 7.64 min)
UV spectrum (phosphate buffer pH of 6.5): λ_{max} = 242 nm
NaCl: 10.6 %

Elemental analysis (%):

	C	H	N	C/N
Calculation:	53.17	2.80	7.09	7.50
Calculation with H_2O and NaCl:	44.04	3.06	5.87	7.50
Found:	44.07	3.99	5.88	7.49

Water content: 3 mol/mol

ESI-MS negative mode (m/z):
$[M-H]^-$: 789.5, $[M-Na]^-$: 767.7

IR spectrum (cm^{-1}):

3850 (m)	3444 (br, s)	1652 (m)	1558 (m)
1198 (w)	1049 (w)	622 (w)	

500 MHz ^{1}H NMR spectrum (DMSO-*d*$_6$): δ (ppm), *J* (Hz)

10.44	-NH-CO	s	(1H) exchangeable
9.25	-NH-CO-NH	s	(1H) exchangeable
8.89	H8	dd (^{3}J = 8.5, ^{4}J = 2.2)	(1H)
8.86	H2′	dd (^{4}J = 2.2, ^{4}J = 7.1)	(1H)
7.95	H6	d (^{3}J = 8.8)	(1H)
7.93	H5	dd (^{3}J = 8.5, ^{4}J = 1.9)	(1H)
7.82-7.79	H6′	m	(1H)
7.52	H3	d (^{4}J = 8.7)	(1H)
7.51	H2	d (^{3}J = 8.7)	(1H)
7.47	H7	dd (^{3}J = 8.5, ^{4}J = 1.9)	(1H)
7.44	H5′	dd (^{3}J =8.4, ^{3}J = 11.0)	(1H)

125 MHz ^{13}C NMR spectrum (DMSO-*d*$_6$): δ (ppm)

165.6	C9	129.7	C1′	123.2	C7
154.3	C4′	128.1	C8a	122.9	C3
152.1	C10	127.5	C4a	122.5	C5
142.6	C4	127.4	C8	121.3	C2
134.9	C3′	125.7	C2′	115.1	C5′
131.4	C1	124.3	C6		
129.9	C6′				

Sodium 8-(4-fluoro-3-nitrobenzamido)naphthalene-2-sulfonate
16a

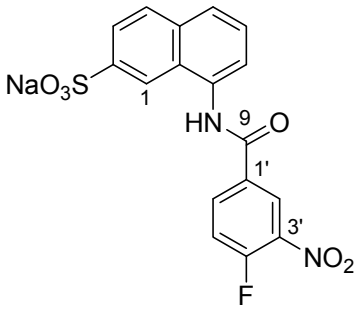

$C_{17}H_{10}FN_2NaO_6S$ (412.32)

1.64 g (8.07 mmol) 4-Fluoro-3-nitrobenzoylchloride, which was obtained by GRP1, were slowly added to the stirred solution of 1.48 g (5.38 mmol) Sodium 8-aminonaphthalene-2-sulfonate in 50 ml water, until there was no amine left. The reaction was continued according to GRP 2.

Yield: brown powder, 37.3 % (0.83 g)
TLC: R_f = 0.60 (MP1)
HPLC: 99.6 % (t_R = 3.97 min)
UV spectrum (phosphate buffer pH of 6.5): λ_{max} = 288 nm
NaCl: 2.59 %

Elemental analysis (%):

	C	H	N	C/N
Calculation :	49.52	2.44	6.79	7.29
Calculation with H_2O and NaCl :	46.22	2.74	6.34	7.29
Found :	46.54	2.61	6.33	7.34

Water content: 1 mol/mol

IR spectrum (cm^{-1}):

3424 (br,s)	2361 (m)	1647 (s)	1619 (s)
1534 (vs)	1490 (m)	1354 (s)	1267 (m)
1196 (br, s)	1114 (m)	1031 (m)	828 (m)
751 (w)	680 (s)	570 (w)	

500 MHz ^{1}H NMR spectrum (DMSO-d_6): δ (ppm), J (Hz)

10.93	-NH-CO	s		1H
8.96	H2′	d	(^4J = 1.5, ^4J = 7.8)	1H
8.56	H6′	m		1H
8.29	H1	s		1H
7.99	H4	d	(^3J = 8.5)	1H
7.93	H3	dd	(^4J = 3.1, ^4J = 6.1)	1H
7.88	H5′	dd	(^3J = 8.5, ^3J = 11.0)	1H
7.81	H5	d	(^3J = 8.5, ^4J = 1.0)	1H
7.64-7.62	H6, H7	dd	(^4J = 3.1)	2H

125 MHz ^{13}C NMR spectrum (DMSO-d_6): δ (ppm)

163.6	C9	134.3	C4a	125.2	C3
157.0	C4′	133.9	C7	124.6	C8a
146.2	C8	131.5	C1′	119.8	C5
137.2	C3′	128.9	C4	119.5	C1
136.1	C2	128.2	C6	119.3	C5′
136.0	C6′	126.4	C2′		

Sodium 8-(3-amino-4-fluorobenzamido)-naphthalene-2-sulfonate
16b

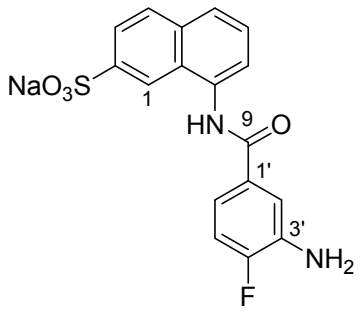

$C_{17}H_{12}FN_2NaO_4S$ (382.34)

20 mg Palladium (10%) on charcoal were added as catalyst to a solution of 0.5 g (1.21 mmol) compound 16a in water. The reaction was continued according to GRP 3.

Yield: brown powder, 97.26 % (0.45 g)
TLC: R_f = 0.54 (MP1)
HPLC: 96.1 % (t_R = 1.81 min)
UV spectrum (phosphate buffer pH of 6.5): λ_{max} = 293 nm
NaCl: 47.0 %

Elemental analysis (%):

	C	H	N	C/N
Calculation:	53.40	3.16	7.33	7.29
Calculation with H_2O and NaCl:	24.29	2.28	3.33	7.29
Found:	24.28	1.59	3.41	7.12

Water content: 3 mol/mol

IR spectrum (cm^{-1}):

3424 (s)	1654 (m)	1512 (m)	1490 (m)
1200 (m)	1028 (m)	681 (m)	

500 MHz ^{1}H NMR spectrum (DMSO-d_6): δ (ppm), *J* (Hz)

10.40	-NH-CO	s		1H
8.28	H1	s		1H
7.97	H4	d	(^3J = 8.0)	1H
7.89	H3	d	(^3J = 8.0)	1H
7.79	H5	dd	(^3J = 8.0, ^4J= 1.5)	1H
7.59	H7	t	(^3J = 7.5)	1H
7.55	H6	d	(^3J = 7.2)	1H
7.52	H2′	dd	(^4J = 1.9, ^3J = 8.8)	1H
7.37-7.35	H6′	m		1H
7.22	H5′	dd	(^3J =8.0, ^3J =11.0)	1H
5.45	-NH_2	s		2H

125 MHz ^{13}C NMR Spectrum (DMSO-d_6): δ (ppm)

166.4	C9	129.2	C7	116.6	C5
151.9	C4′	128.0	C1′	116.5	C1
145.9	C8	126.3	C4	115.8	C6′
135.3	C3′	125.2	C6	115.8	C5′
133.9	C2	124.5	C3	114.9	C2′
131.4	C4a	120.1	C8a		

Disodium 8,8′-{carbonylbis[azenedyl(4-fluoro-3,1-phenylene) carbonylazenediyl]}bis(naphthalene-2-sulfonate)
16c

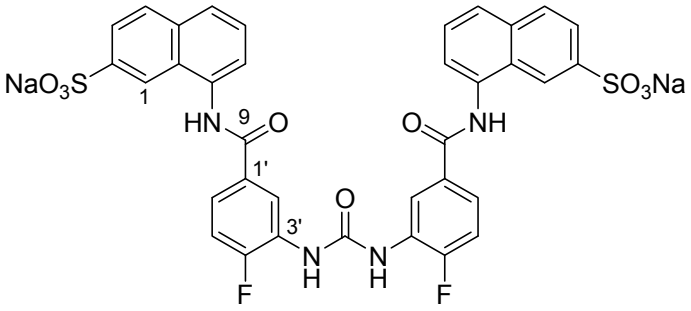

$C_{35}H_{22}F_2N_4Na_2O_9S_2$ (790.7)

A solution of 2.1 mmol phosgene (20% in toluen) was slowly added to a solution of 400 mg (1.05 mmol) compound 16b in 20 ml water under heavy stirring at room temperature. The reaction was continued according to GRP 4.

Yield: grey powder, 62.2 % (0.5 g)
TLC: R_f = 0.89 (MP2)
HPLC: 97.4 % (t_R = 7.76 min)
UV spectrum (phosphate buffer pH of 6.5): λ_{max} = 288 nm
NaCl: 62.5 %

Elemental analysis (%):

	C	H	N	C/N
Calculation:	53.17	2.80	7.09	7.49
Calculation with H_2O and NaCl:	16.55	1.58	2.21	7.53
Found:	16.50	1.19	1.16	9.93

Water content: 9 mol/mol

ESI-MS negative mode (m/z):
$[M-H]^-$: 789.5, $[M-Na]^-$: 768.5

IR spectrum (cm^{-1}):

3424 (br, s)	1610 (m)	1486 (m)	1200 (br, s)
1030 (m)	833 (w)	681 (m)	

500 MHz ^{1}H NMR spectrum (DMSO-d_6): δ (ppm), J (Hz)

10.58	-NH-CO-	s	1H
9.47	-NH-CO-NH-	s	1H
8.87	H2′	dd (^3J = 7. 6)	1H
8.23	H1	s	1H
7.91	H4	d (^3J = 8.3)	1H
7.85	H3	d (^3J = 8.3)	1H
7.82	H6′	m	1H
7.74	H5	d (^3J = 8.5)	1H
7.56	H7	d (^3J = 7.0)	1H
7.53	H6	d (^3J = 7.0)	1H
7.48-7.45	H5′	dd (^3J = 8.8, ^4J = 11.25)	1H

Disodium 3-(4-fluoro-3-nitrobenzamido)-naphthalene-1,5-disulfonate 17a

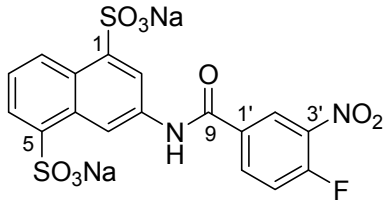

$C_{17}H_9FN_2Na_2O_9S_2$ (514.4)

1.4 g (6.9 mmol) 4-Fluoro-3-nitrobenzoylchloride, which was obtained by GRP1 were slowly added to the stirred solution of 1.5 g (4.6 mmol) Disodium 3-aminonaphthalene-1,5-disulfonate in 50 ml water, until there was no amine left. The reaction was continued according to GRP 2.

Yield: yellow powder, 90.67 % (2.14 g)
TLC: R_f = 0.57 (MP1)
HPLC: 99.6 % (t_R = 2.68 min)
UV spectrum (phosphate buffer pH of 6.5): λ_{max} = 258 nm
NaCl: 4.76 %

Elemental analysis (%):

	C	H	N	C/N
Calculation:	39.70	1.76	5.45	7.28
Calculation with H_2O and NaCl:	35.37	2.27	4.85	7.29
Found:	35.45	2.22	4.80	7.38

Water content: 2 mol/mol

IR spectrum (cm^{-1}):

3443 (br, s)	1670 (m)	1618 (s)	1583 (m)
1537 (vs)	1490 (m)	1437 (w)	1355 (s)
1207 (br, vs)	1079 (m)	1042 (vs)	868 (w)
812 (w)	794 (m)	740 (m)	614 (s)
527 (m)	494 (m)		

500 MHz ^{1}H NMR spectrum (DMSO-*d*$_6$): δ (ppm), *J* (Hz)

10.92	-NH-CO-	s		1H
9.08	H4	d	(^{4}J = 2.0.8)	1H
8.88	H2′	dd	(^{4}J = 2.9, ^{4}J = 7.3)	1H
8.8	H8	d	(^{3}J = 8.6)	1H
8.52-8.49	H6′	m		1H
8.43	H2	d	(^{4}J = 2.5)	1H
7.96	H6	d	(^{3}J = 7.2)	1H
7.77	H5′	dd	(^{3}J = 8.8, ^{4}J = 11.25)	1H
7.38-7.35	H7	t	(^{3}J =8.5)	1H

125 MHz ^{13}C NMR spectrum (DMSO-*d*$_6$): δ (ppm)

162.8	C9	131.9	C1′	123.4	C8a
155.7	C4′	130.4	C4a	120.8	C7
146.8	C1	129.3	C6′	119.9	C5′
143.8	C5	127.5	C8	119.2	C2
136.3	C3	126.4	C2′	118.9	C4
134.7	C3′	124.8	C6		

Disodium 3-(3-amino-4-fluorobenzamido)-naphthalene-1,5-disulfonate 17b

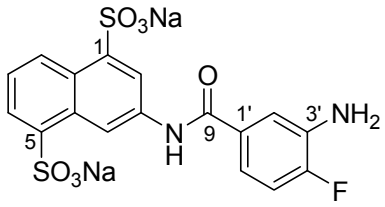

$C_{17}H_{11}FN_2Na_2O_7S_2$ (484.4)

20 mg Palladium (10%) on charcoal were added as catalyst to a solution of 1.2 g (2.33 mmol) compound 17a in water. The reaction was continued according to GRP 3.

Yield: beige powder, 96.1 % (1.07 g)
TLC: R_f = 0.51 (MP1)
HPLC : 99.3 % (t_R = 1.61 min)
UV spectrum (phosphate buffer pH of 6.5): λ_{max} = 269 nm
NaCl: 4.47 %

Elemental analysis (%):

	C	H	N	C/N
Calculation:	42.15	2.29	5.78	7.29
Calculation with H_2O and NaCl:	36,23	3,04	4.97	7,29
Found:	36.11	2.93	4.91	7.35

Water content: 3 mol/mol

IR spectrum (cm^{-1}):

3442 (br,s)	1628 (m)	1579 (w)	1543 (s)
1513 (s)	1499 (m)	1442 (m)	1338 (m)
1303 (w)	1205 (br, vs)	1158 (s)	1076 (w)
1041 (vs)	891 (w)	812 (m)	794 (m)
773 (w)	748 (m)	617 (s)	528 (m)
494 (m)			

500 MHz ^{1}H NMR spectrum (DMSO-*d*$_6$): δ (ppm), *J* (Hz)

10.39	-NH-CO	s		1H
8.99	H4	d	(^{4}J = 1.9)	1H
8.81	H8	d	(^{3}J = 8.0)	1H
8.36	H2	d	(^{4}J = 1.9)	1H
7.93	H6	d	(^{4}J = 8.0)	1H
7.44	H2′	dd	(^{4}J = 2.2, ^{3}J =7.0)	1H
7.33	H7	td	(^{4}J = 1.3, ^{3}J = 8.0)	1H
7.25-7.24	H6′	m		1H
7.12	H5′	dd	(^{3}J = 8.4, ^{3}J = 11.0)	1H
5.31	-NH_2	s		2H

125 MHz ^{13}C NMR Spectrum (DMSO-*d*$_6$): δ (ppm)

165.4	C9	130.3	C1’	119.6	C6’
153.5	C4’	129.1	C4a	116.4	C5’
143.5	C1	127.0	C8	116.0	C2
136.4	C5	124.5	C6	115.9	C4
136.3	C3	122.8	C8a	114.5	C2’
135.1	C3’	121.1	C7		

Disodium 3,3′-{carbonylbis[azanediyl(4-fluoro-3,1-phenylene)carbonylazanediyl]}bis(naphthalene-1,5-disulfonate)
17c

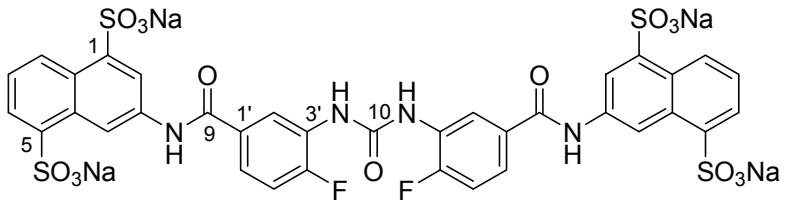

$C_{35}H_{20}F_2N_4Na_4O_{15}S_4$ (994.8)

A solution of 3.3 mmol phosgene (20 % in toluen) was slowly added to a solution of 800 mg (1.65 mmol) compound 17b in 20 ml water under heavy stirring at room temperature. The reaction was continued according to GRP 4.

Yield: pale pink powder, 75.0 % (1.23 g)
TLC: R_f = 0.49 (MP2)
HPLC: 99.1 % (t_R = 6.15 min)

UV spectrum (phosphate buffer pH of 6.5): λ_{max} = 258 nm
NaCl: 17.0 %

Elemental analysis (%):

	C	H	N	C/N
Calculation:	42.26	2.03	5.63	7.50
Calculation with H_2O and NaCl:	29.25	2.94	3.89	7.50
Found:	29.29	2.61	3.96	7.40

Water content: 11 mol/mol

ESI-MS positive mode (m/z):
$[M+Na]^+$: 1017.8

IR spectrum:

3446 (br,s)	1610 (s)	1541 (s)	1488 (s)
1432 (s)	1332 (m)	1255 (s)	1207 (vs)
1042 (vs)	810 (w)	793 (m)	738 (m)
664 (m)	614 (vs)	528 (m)	

500 MHz ^{1}H NMR spectrum (DMSO-d_6): δ (ppm), J (Hz)

10.63	-NH-CO	s		1H
9.47	-NH-CO-NH-	s		1H
9.06	H4	dd	(^5J = 0.5, ^4J = 2.2)	1H
8.82	H2′	dd	(^3J = 8.5)	1H
8.73	H8	dd	(^5J = 2.2, ^4J =7.5)	1H
8.38	H2	d	(^4J = 2.2)	1H
7.95	H6	dd	(^4J = 1.0, ^3J =7.5)	1H
7.81-7.78	H6′	m		1H
7.39	H5′	dd	(^3J = 8.5, ^3J = 11.0)	1H
7.33	H7	dd	(^3J = 7.3, ^3J = 6.9)	1H

125 MHz ^{13}C NMR spectrum (DMSO-d_6): δ (ppm)

164.9	C9	131.5	C1′	123.2	C8a
153.6	C4′	130.2	C4a	121.8	C2
152.3	C10	129.1	C7	120.9	C4
144.2	C1	127.3	C8	119.6	C3′
143.3	C5	127.0	C6′	115.1	C2′
134.9	C3	124.7	C6	114.9	C5′

Disodium 4-(4-fluoro-3-nitrobenzamido)-naphthalene-2,7-disulfonate
18a

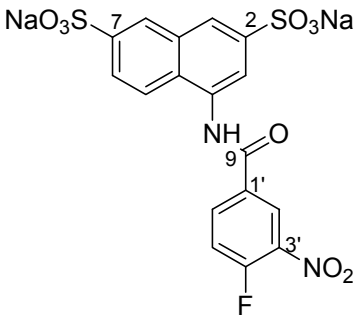

$C_{17}H_9FN_2Na_2O_9S_2$ (513.9)

872.9 mg (4.3 mmol) 4-Fluoro-nitrobenzoylchloride, which was obtained by GRP1, were slowly added to the stirred solution of 1.15 g (3.31 mmol) disodium 4-aminonaphthalene-2,7-disulfonate in 50 ml water, until there was no amine left. The reaction was continued according to GRP 2.

Yield: pale yellow powder, 70.59 % (1.20 g)
TLC: R_f = 0.60 (MP1)
HPLC: 95.0 % (t_R = 4.05 min)
UV spectrum (phosphate buffer pH of 6.5): λ_{max} = 232 nm
NaCl: 31.1 %

Elemental analysis (%):

	C	H	N	C/N
Calculation:	39.70	1.76	5.45	7.28
Calculation with H_2O and NaCl:	21.66	2.57	2.97	7.29
Found:	21.68	1.16	2.88	7.53

Water content: 7 mol/mol

IR spectrum (cm^{-1}):

3448 (br,s)	1675 (s)	1617 (m)	1533 (s)
1486 (m)	1390 (w)	1350 (m)	1266 (m)
1225 (s)	1193 (br,s)	1125 (br,s)	1040 (vs)
917 (w)	830 (w)	750 (m)	706 (m)
679 (s)	694 (m)	618 (m)	555 (m)
523 (w)			

500 MHz ^{1}H NMR spectrum (DMSO-*d*$_6$): δ (ppm), *J* (Hz)

10.88	-NH-CO-	s		1H
8.89	H2′	dd	(*J* = 2.2, *J* = 7.2)	1H
8.55	H6′	m		1H
8.18	H4	d	(*J* = 1.3)	1H
8.09	H5	s		1H
7.93	H1	d	(*J* = 8.8)	1H
7.82	H5', H7	dd	(*J* = 9.0, *J* = 10.4)	2H
7.75	H2	dd	(*J* = 1.6, *J* = 8.8)	1H

125 MHz ^{13}C NMR spectrum (DMSO-*d*$_6$): δ (ppm)

163.7	C9	133.4	C4a	124.9	C1
156.0	C4′	132.5	C1′	123.6	C3
146.4	C2	131.6	C8	122.8	C6′
145.4	C7	129.0	C8a	119.8	C2′
137.2	C3′	126.5	C6	119.2	C5′
136.2	C4	125.2	C5		

Disodium 4-(3-amino-4-fluorobenzamido)-naphthalene-2,7-disulfonate 18b

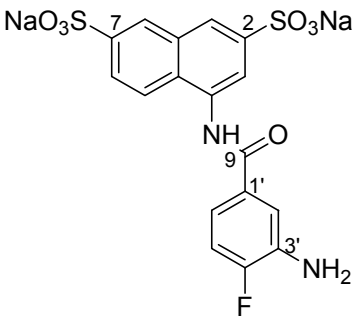

$C_{17}H_{11}FN_2Na_2O_7S_2$ (483.9)

20 mg Palladium (10%) on charcoal were added as catalyst to a solution of 1 g (1.94 mmol) compound 18a in water. The reaction was continued according to GRP 3.

Yield: brown powder, 91.4 % (860 mg)
TLC: R_f = 0.42 (MP1)
HPLC: 97.5 % (t_R = 1.5 min)
UV spectrum (phosphate buffer pH of 6.5): λ_{max} = 241 nm
NaCl: 28.9 %

Elemental analysis (%):

	C	H	N	C/N
Calculation:	42.15	2.29	5.78	7.29
Calculation with H_2O and NaCl:	21.26	3.46	2.92	7.29
Found:	20.98	1.65	2.84	7.38

Water content: 11 mol/mol

IR spectrum (cm^{-1}):

3430 (br,s)	2361 (w)	1636 (m)	1516 (m)
1196 (br,s)	1036 (s)	692 (m)	

500 MHz ^{1}H NMR spectrum (DMSO-*d*$_6$): δ (ppm), *J* (Hz)

10.32	-NH-CO	s		1H
8.16	H4	s		1H
8.05	H5	s		1H
7.86	H1	d	(^3J = 9.0)	1H
7.78-7.77	H7	s		1H
7.74	H2	d	(^3J = 9.0)	
7.48	H2′	d	(^4J = 1.8, ^4J = 9.0)	1H
7.32-7.30	H6′	m		1H
7.15	H5′	dd	(^3J = 8.5, ^3J = 11.0)	1H
5.41	-NH_2	s		2H

125 MHz ^{13}C NMR spectrum (DMSO-*d*$_6$): δ (ppm)

166.3	C9	132.5	C4a	123.2	C1
153.8	C4′	131.5	C1′	122.5	C3
146.3	C2	129.2	C8	116.6	C6′
145.9	C7	125.2	C8a	115.9	C5′
136.8	C3′	124.7	C6	115.0	C2′
134.1	C4	123.5	C5		

Disodium 4,4′-{carbonylbis[azanediyl-(4-fluoro-3,1-phenylene)carbonylazanediyl]}bis(naphthalene-2,7-disulfonate)
18c

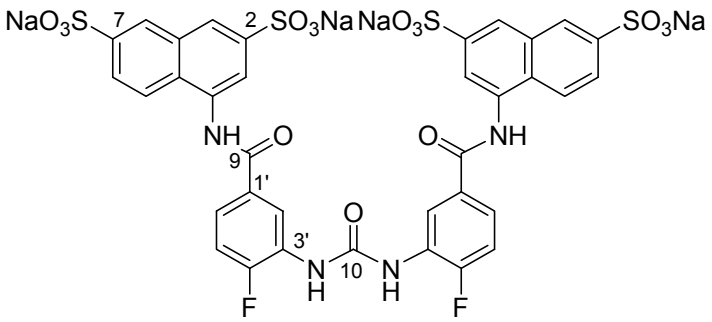

$C_{35}H_{20}F_2N_4Na_4O_{15}S_4$ (994.8)

A solution of 2.06 mmol phosgene (20 % in toluen) was slowly added to a solution of 500 mg (1.03 mmol) compound 18b in 20 ml water under heavy stirring at room temperature. The reaction was continued according to GRP 4.

Yield: beige powder, 53.7 % (550 mg)
TLC: R_f = 0.43 (MP2)
HPLC: 94.6 % (t_R = 5.59 min)
UV spectrum (phosphate buffer pH of 6.5): λ_{max} = 285 nm
NaCl: 30.1 %

Elemental analysis (%):

	C	H	N	C/N
Calculation:	42.26	2.03	5.63	7.50
Calculation with H_2O and NaCl:	24.28	2.56	3.24	7.50
Found:	24.28	2.55	3.37	7.21

Water content: 12 mol/mol

ESI-MS negative mode (m/z):
$[M-H]^-$: 993.6, $[M-Na]^-$: 971.6

IR spectrum (cm^{-1}):

3444 (br,s)	1609 (m)	1560 (m)	1484 (m)
1420 (w)	1196 (br, s)	1114 (m)	1036 (s)
751 (w)	691 (m)	613 (w)	

500 MHz ^{1}H NMR spectrum (DMSO-*d_6*): δ (ppm), *J* (Hz)

10.49	-NH-CO	s	1H exchangeable
9.41	-NH-CO-NH-	s	1H exchangeable
8.75	H2′	d (^4J = 2.2)	1H
8.15	H4	d (^4J = 1.6)	1H
8.05	H5	s	1H
7.86	H1	d (^3J = 8.8)	1H
7.84	H6′	m	1H
7.78	H7	d (^4J = 1.3)	1H
7.73	H2	d (^3J = 8.8)	1H
7.44	H5′	t (^3J = 8.4)	1H

125 MHz ^{13}C NMR spectrum (DMSO-*d_6*): δ (ppm)

165.5	C9	132.3	C4	124.6	C5
154.5	C4′	131.1	C4a	123.4	C1
152.2	C10	129.0	C1′	123.2	C3
146.1	C2	127.5	C8	122.5	C6′
145.7	C7	127.4	C8a	121.7	C2′
133.8	C3′	124.9	C6	115.3	C5′

Trisodium 8-(4-fluoro-3-nitrobenzamido)-naphthalene-1,3,6-trisulfonate 19a

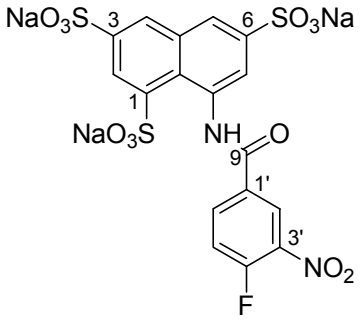

$C_{17}H_8FN_2Na_3O_{12}S_3$ (616.4)

812 mg (4 mmol) 4-Fluoro-nitrobenzoylchloride, which was obtained by GRP1, were slowly added to the stirred solution of 1 g (2.22 mmol) trisodium 8-aminonaphthalene-1,3,6-trisulfonate in 50 ml water, until there was no amine left. The reaction was continued according to GRP 2.

Yield: pale yellow powder, 76.7 % (1.05 g)
TLC: R_f = 0.5 (MP1)
HPLC: 98.7% (t_R = 5.5 min)
UV spectrum (phosphate buffer pH of 6.5): λ_{max} = 242 nm
NaCl: 10.7 %

Elemental analysis (%):

	C	H	N	C/N
Calculation:	33.12	1.31	4.54	7.30
Calculation with H_2O and NaCl:	26.48	2.09	3.63	7.29
Found:	26.54	1.91	3.56	7.46

Water content: 4 mol/mol

IR spectrum (cm^{-1}):

3448 (br,s)	1619 (m)	1535 (s)	1357 (m)
1390 (w)	1196 (br, s)	1050 (vs)	748 (w)
678 (s)	691 (s)	620 (m)	

500 MHz ^{1}H NMR spectrum (DMSO-*d*$_6$): δ (ppm), *J* (Hz)

12.75	-NH-CO-	s		1H
8.92	H2′	dd	(^{4}J = 2.0, ^{3}J = 7.3)	1H
8.63-8.62	H6′	m		1H
8.58	H4	d	(^{4}J = 1.5)	1H
8.45	H5	d	(^{4}J = 1.5)	1H
8.16	H2	d	(^{4}J = 1.5)	1H
8.02	H7	d	(^{4}J = 1.5)	1H
7.76	H5′	dd	(^{4}J = 2.2, ^{3}J= 11.0)	1H

125 MHz ^{13}C NMR spectrum (DMSO-*d*$_6$): δ (ppm)

162.8	C4′	136.1	C4a	126.5	C4
156.0	C9	134.8	C1′	123.6	C5
143.4	C6	133.0	C1	122.8	C7
143.9	C3	132.8	C8A	119.0	C2′
141.8	C8	128.4	C6′	118.9	C5′
137.1	C3′	126.8	C2		

Trisodium 8-(3-amino-4-fluorobenzamido)-naphthalene-1,3,6-trisulfonate 19b

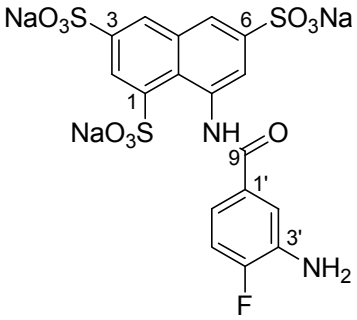

$C_{17}H_{10}FN_2Na_3O_{10}S_3$ (586.4)

20 mg Palladium (10%) on charcoal were added as catalyst to a solution of 700 mg (1.136 mmol) compound 19a in water. The reaction was continued according to GRP 3.

Yield: brown powder, 81 % (540 mg)
TLC: R_f = 0.36 (MP1)
HPLC: 97.3 % (t_R = 1.99 min)
UV spectrum (phosphate buffer pH of 6.5): λ_{max} = 235 nm
NaCl: 19.1 %

Elemental analysis (%):

	C	H	N	C/N
Calculation:	34.82	1.72	4.78	7.29
Calculation with H_2O and NaCl:	20.58	3.87	2.84	7.29
Found:	20.26	1.68	2.83	7.16

Water content: 12 mol/mol

IR spectrum (cm^{-1}):

3428 (br,s) 2361 (m) 1623 (m) 1196 (br,s)
1045 (s)

500 MHz ^{1}H NMR spectrum (DMSO-d_6): δ (ppm), *J* (Hz)

12.35	-NH-CO	s		1H
8.54	H4	d	(^4J = 1.7)	1H
8.37	H5	d	(^4J = 1.7)	1H
8.09	H2	d	(^4J = 1.7)	1H
7.93	H7	d	(^4J = 1.7)	1H
7.48	H2′	dd	(^4J = 2.0, ^3J = 8.9)	1H
7.41-7.39	H6′	m		1H
7.08-7.04	H5′	dd	(^3J = 8.5, ^3J = 11.0)	1H
5.26	$-NH_2$	s		2H

125 MHz ^{13}C NMR spectrum (DMSO-d^6): δ (ppm)

165.5	C9	133.5	C4a	122.0	C5
158.1	C4′	132.6	C1′	120.3	C7
145.5	C6	128.1	C1	119.5	C6′
142.1	C3	126.4	C8a	116.5	C5’
134.8	C8	122.8	C4	117.0	C2′
133.8	C3′	122.5	C2		

Trisodium 8,8′-{carbonylbis[azanediyl(4-fluoro-3,1-phenylene) carbonylazenediyl]}bis(naphthalene-1,3,6-trisulfonate)
19c

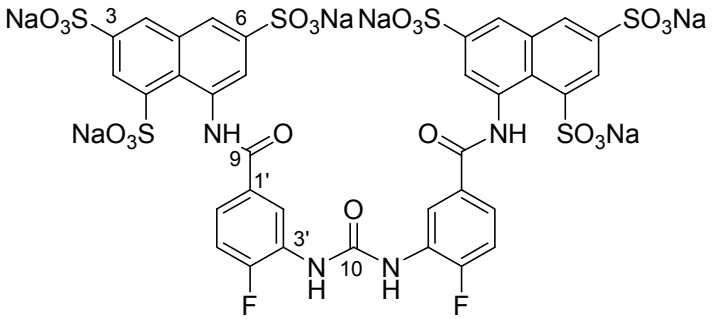

$C_{35}H_{18}F_2N_4Na_6O_{21}S_6$ (1198.9)

A solution of 1.36 mmol phosgene (20 % in toluen) was slowly added to a solution of 400 mg (0.68 mmol) compound 19b in 20 ml water under heavy stirring at room temperature. The reaction was continued according to GRP 4.

Yield: brown powder, 49.0 % (0.4 mg)
TLC: R_f = 0.17 (MP2)
HPLC: 95.4 % (t_R = 6.83 min)
UV spectrum (phosphate buffer pH of 6.5): λ_{max} = 260 nm
NaCl: 49.9 %

Elemental analysis (%):

	C	H	N	C/N
Calculation:	35.06	1.51	4.67	7.50
Calculation with H_2O and NaCl:	16.32	1.90	2.17	7.50
Found:	16.32	1.92	2.32	7.05

Water content: 5 mol/mol

ESI-MS negative mode (m/z):
$[M-H]^-$: 1197.7, $[M-Na]^-$: 1175.5

IR spectrum (cm^{-1}):

3432 (br,s)	1629 (m)	1430 (m)	1200 (br,s)
1028 (w)	681 (m)		

500 MHz ^{1}H NMR spectrum (DMSO-*d*$_6$): δ (ppm), *J* (Hz)

12.48	-NH-CO-	s	1H (exchangeable)
9.24	-NH-CO-NH-	s	1H (exchangeable)
8.70	H2′	dd (^4J = 2.2, ^3J = 8.2)	1H
8.56	H4	d (^4J = 1.9)	1H
8.44	H5	d (^4J = 1.9)	1H
8.12	H2	d (^4J = 1.9)	1H
8.01-7.98	H6′	m	1H
7.97	H7	d (^4J = 1.9)	1H
7.37-7.33	H5′	dd (^3J = 8.5, J = 11.0)	1H

125 MHz ^{13}C NMR spectrum (DMSO-*d*$_6$): δ (ppm)

164.7	C4′	141.8	C3′	123.0	C2
154.2	C9	133.6	C4a	122.7	C4
152.2	C10	132.3	C1′	122.4	C5
144.9	C6	128.1	C1	122.0	C7
143.7	C3	127.1	C8A	114.8	C2′
141.8	C8	126.4	C6′	114.6	C5′

Disodium 2-(4-fluoro-3-nitrobenzamido)benzene-1,4-disulfonate
20a

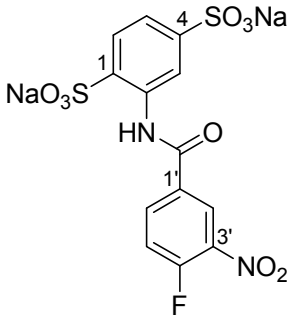

$C_{13}H_7FN_2Na_2O_9S_2$ (464.3)

1.26 g (6.75 mmol) 4-Fluoro-3-nitrobenzoylchloride, which was obtained by GRP1, were slowly added to the stirred solution of 1.15 g (4.50 mmol) disodium aminobenzene-1,4-disulfonate in 50 ml water, until there was no amine left. The reaction was carried out according to GRP 2.

Yield: pale yellow powder, 60.3 % (1.75 g)
TLC: R_f = 0.55 (MP1)
HPLC: 98.5 % (t_R = 2.37 min)
UV spectrum (phosphate buffer pH of 6.5): λ_{max} = 261 nm
NaCl: 15.7 %

Elemental analysis (%):

	C	H	N	C/N
Calculation:	33.62	1.52	6.03	5.58
Calculation with H_2O and NaCl:	19.60	3.87	3.51	5.57
Found:	19.44	1.32	3.38	5.75

Water content: 11 mol/mol

IR spectrum (cm^{-1}):

3465 (br,s)	1677 (s)	1620 (s)	1582 (s)
1537 (vs)	1499 (m)	1409 (vs)	1357 (s)
1316 (s)	1274 (s)	1224 (br,vs)	1192 (br,vs)
1125 (vs)	1050 (s)	1021 (s)	941 (w)
856 (w)	748 (m)	668 (vs)	639 (s)
617 (m)	559 (m)		

500 MHz ^{1}H NMR spectrum (DMSO-d_6): δ (ppm), J (Hz)

11.70	-NH-CO	s		1H
8.75	H3	s		1H
8.65	H2′	dd	(^4J = 1.0, ^4J = 7.0)	1H
8.31	H6′	m		1H
7.89	H5′	dd	(^3J = 11.0, ^3J = 9.0)	1H
7.69	H6	d	(^3J = 8.0)	1H
7.38	H5	d	(^3J = 8.0)	1H

125 MHz ^{13}C NMR spectrum (DMSO-d_6): δ (ppm)

161.2	C7	134.7	C1	125.8	C2′
156.9	C4′	134.3	C2	120.9	C5
150.0	C4	131.9	C1′	119.9	C3
137.5	C3′	126.8	C6	117.7	C5′
135.9	C6′				

Disodium 2-(3-amino-4-fluorobenzamido)benzene-1,4-disulfonate 20b

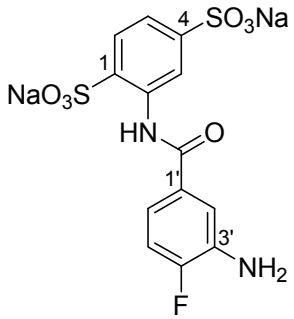

$C_{13}H_9FN_2Na_2O_7S_2$ (434.3)

20 mg Palladium (10%) on charcoal were added as catalyst to a solution of 700 mg (1.51 mmol) compound 20a in water. The reaction was carried out according to GRP 3.

.

Yield: beige powder, 88.5 % (0.58 g)
TLC: R_f = 0.56 (MP1)
HPLC: 98.5 % (t_R = 1.54 min)
UV spectrum (phosphate buffer pH of 6.5): λ_{max} = 257 nm
NaCl: 11.3 %

Elemental analysis (%):

	C	H	N	C/N
Calculation :	35.95	2.09	6.45	17.2
Calculation with H_2O and NaCl :	18.94	5.13	3.40	5.57
Found :	18.96	1.53	3.32	5.71

Water content: 17 mol/mol

IR spectrum (cm^{-1}):

3456 (br,m)	1582 (m)	1514 (m)	1409 (m)
1317 (m)	1202 (br, vs)	1123 (m)	1051 (m)
1019 (m)	662 (m)	644 (m)	

500 MHz ^{1}H NMR spectrum (DMSO-*d*$_6$): δ (ppm), *J* (Hz)

11.20	-NH-CO-	s		1H
8.75	H3	pd		1H
7.65	H6	d	(^{3}J =8.0)	1H
7.40	H2′	dd	(^{4}J =1.5, ^{4}J =9.0)	1H
7.30	H5	d	(^{3}J =8.0)	1H
7.13	H5′	dd	(^{3}J = 8.5, ^{3}J = 11.0)	1H
7.08	H6′	m		1H
5.46	-NH_2	s		2H

125 MHz ^{13}C NMR spectrum (DMSO-*d*$_6$): δ (ppm)

164.1	C7	135.1	C2	117.5	C3
152.5	C4′	131.8	C1′	115.9	C2′
149.9	C4	126.7	C6	115.4	C5′
137.1	C3′	119.9	C5	114.6	C6′
135.6	C1				

Tetrasodium 2,2′-{carbonylbis[azenediyl(4-fluoro-3,1-phenylene) carbonylazenediyl]}bis(benzene-1,4-disulfonate)
20c

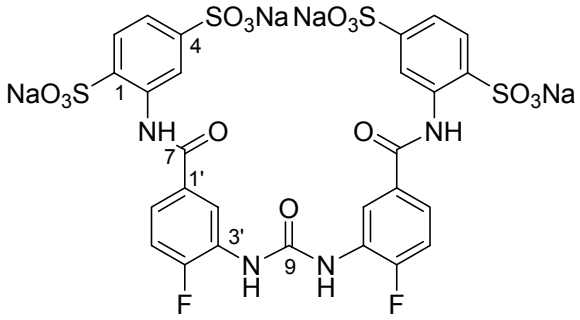

$C_{27}H_{16}F_2N_4Na_4O_{15}S_4$ (894.7)

A solution of 2.18 mmol phosgene (20 % in toluene) was slowly added to a solution of 475 mg (1.09 mmol) compound 20b under heavy stirring at room temperature. The reaction was carried out according to GRP 4.

Yield: beige powder, 76.5 % (0.75 g)
TLC: R_f = 0.47 (MP2)
HPLC: 96.6 % (t_R = 6.32 min)
UV spectrum (phosphate buffer pH of 6.5): λ_{max} = 261 nm
NaCl: 50.0 %

Elemental analysis (%):

	C	H	N	C/N
Calculation:	35.34	1.76	6.11	5.79
Calculation with H_2O and NaCl:	17.25	1.13	2.98	5.79
Found:	17.15	1.10	3.13	5.49

Water content: 2 mol/mol

ESI-MS negative mode (m/z):
$[M-Na]^-$: 871.2

IR spectrum (cm^{-1}):

3307 (br,m)	1694 (m)	1670 (m)	1613 (vs)
1579 (s)	1539 (s)	1492 (s)	1408 (s)
1340 (s)	1288 (s)	1267 (s)	1226 (br,vs)
1044 (s)	1020 (vs)	873 (w)	755 (m)
663 (vs)	636 (s)	617 (s)	563 (m)
533 (m)	532 (m)	422 (m)	

500 MHz ^{1}H NMR spectrum (DMSO-d_6): δ (ppm), J (Hz)

11.34	-NH-CO-	s	1H (exchangeable)
9.43	-NH-CO-NH-	s	1H (exchangeable)
8.77	H3	d (^4J = 1.5)	1H
8.72	H2′	dd (^4J = 2.0, ^4J = 8.0)	1H
7.67	H6	D (^3J = 7.9)	1H
7.60	H6′	M	1H
7.43	H5′	dd (^3J = 8.5, ^3J = 11.0)	1H
7.32	H5	dd (^3J = 7.9, ^4J = 1.5)	1H

125 MHz ^{13}C NMR spectrum (DMSO-d_6): δ (ppm)

163.2	C7	135.6	C1	121.1	C2′
154.6	C4′	134.8	C2	120.5	C5
152.1	C8	131.6	C1′	117.5	C3
149.5	C4	127.0	C6	115.7	C5′
137.3	C3′	126.5	C6′		

Sodium 2-(4-fluoro-3-nitrobenzamido)benzene-1-monosulfonate
21a

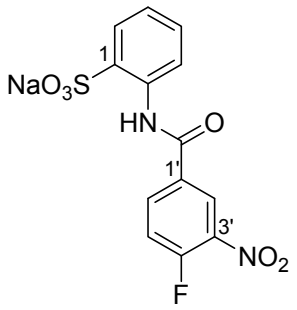

$C_{13}H_8FN_2NaO_6S$ (362.3)

1.28 g (6.75 mmol) 4-Fluoro-3-nitrobenzoylchloride, which was obtained by GRP1, were slowly added to the stirred solution of 1.00 g (5.77 mmol) sodium aminobenzene-1-sulfonate in 50 ml water, until there was no amine left. The reaction was carried out according to GRP 2.

Yield: white powder, 49.28 % (1.03 g)
TLC: R_f = 0.90 (MP1)
HPLC: 98.6 % (t_R = 5.84 min)
UV spectrum (phosphate buffer pH of 6.5): λ_{max} = 260 nm
NaCl: 19.1 %

Elemental analysis (%):

	C	H	N	C/N
Calculation:	43.10	2.23	7.73	5.58
Calculation with H_2O and NaCl:	32.45	2.30	5.82	5.57
Found:	32.77	2.03	5.75	5.58

Water content: 1 mol/mol

IR spectrum (cm^{-1}):

3671 (m)	3463 (br,s)	1672 (s)	1618 (s)
1590 (s)	1539 (br, vs)	1498 (m)	1466 (w)
1408 (w)	1441 (s)	1356 (s)	1328 (s)
1283 (m)	1261 (s)	1250 (s)	1190 (s)
1130 (m)	1082 (m)	1021 (s)	939 (w)
832 (w)	816 (w)	768 (m)	722 (m)
642 (m)	576 (m)	533 (m)	468 (w)

500 MHz ^{1}H NMR spectrum (DMSO-d^6): δ (ppm), *J* (Hz)

11.73	-NH-CO	s		1H
8.65	H2′	dd	(^4J = 2.0, ^4J = 7.0)	1H
8.44	H6	d	(^3J = 8.0)	1H
8.31-8.29	H6′	m		1H
7.88	H5′	dd	(^3J = 9.0, ^3J = 11.0)	1H
7.74	H3	d	(^3J = 7.5)	1H
7.44-7.41	H5	t	(^3J = 7.5)	1H
7.17-7.14	H4	t	(^3J = 7.5)	1H

125 MHz ^{13}C NMR spectrum (DMSO-d^6): δ (ppm)

161.4	C7	134.5	C4	123.8	C3
156.9	C4′	131.9	C1′	120.1	C2′
137.5	C3′	130.3	C6	119.8	C5′
136.1	C1	127.4	C5		
134.7	C2	125.8	C6′		

Sodium 2-(3-amino-4-fluorobenzamido)benzene-1- monosulfonate
21b

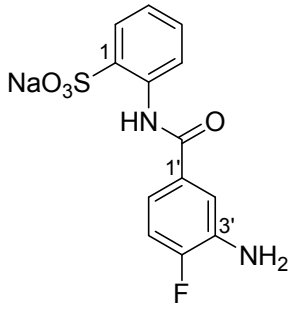

$C_{13}H_{10}FN_2NaO_4S$ (332.3)

20 mg Palladium (10%) on charcoal were added as catalyst to a solution of 700 mg (1.51 mmol) compound 21a in water, the reaction was carried out according to GRP 3.
.
Yield: grey powder, 50.17 % (0.56 g)
TLC: R_f = 0.72 (MP1)
HPLC: 98.6 % (t_R = 2.70 min)
UV spectrum (phosphate buffer pH of 6.5): λ_{max} = 252 nm
NaCl: 25.5 %

Elemental analysis (%):

	C	H	N	C/N
Calculation:	46.99	3.03	8.43	5.57
Calculation with H_2O and NaCl:	34.10	2.42	6.12	5.61
Found:	34.04	2.26	6.07	5.61

Water content: 1 mol/mol

IR spectrum:

3398 (br,m)	1546 (m)	1200 (m)	1019 (m)	572 (w)
3322 (m)	1512 (vs)	1176 (vs)	879 (w)	
1670 (m)	1440 (m)	1142 (m)	760 (m)	
1608 (m)	1321 (vs)	1112 (w)	715 (m)	
1590 (m)	1231 (m)	1089 (w)	617 (m)	

500 MHz ^{1}H NMR spectrum (DMSO-*d*$_6$): δ (ppm), *J* (Hz)

11.22	-NH-CO	s		1H
8.46	H6	d	(^3J = 8.0)	1H
7.71	H3	dd	(^3J = 7.7, ^4J = 1.5)	1H
7.41	H2′	dd	(^4J = 2.0, ^3J = 9.0)	1H
7.37	H5	dd	(^4J = 1.5, ^3J = 7.4)	1H
7.16	H5′	dd	(^3J = 8.5, ^3J = 9.0)	1H
7.10	H6′	m		1H
7.10	H4	td	(^2J = 7.7)	1H
5.49	-NH_2	s		2H

125 MHz ^{13}C NMR spectrum (DMSO-d^6): δ (ppm)

164.3	C7	131.7	C4	115.9	C6′
153.8	C4′	130.1	C1′	115.3	C5′
137.2	C3′	127.3	C6	114.6	C2′
135.7	C1	122.8	C5		
135.6	C2	120.1	C3		

Disodium 2,2′-{carbonylbis[azanediyl(4-fluoro-3,1-phenylene)carbonylazanediyl]bis(benzensulfonate)
21c

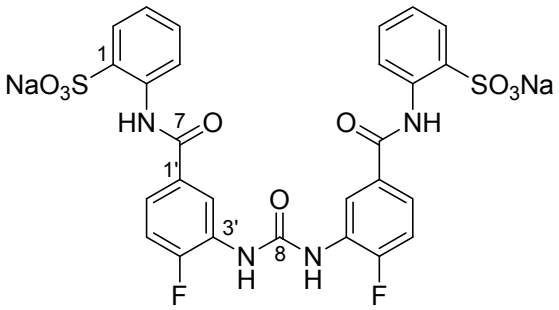

$C_{27}H_{18}F_2N_4Na_2O_9S_2$ (690.6)

A solution of 2.4 mmol phosgene (20 % in toluene) was slowly added to a solution of 400 mg (1.2 mmol) compound 21b under heavy stirring at room temperature. The reaction was carried out according to GRP 4.

Yield: beige powder, 61.59 % (510 mg)
TLC: R_f = 0.67 (MP1)
HPLC: 96.3 % (t_R = 8.39 min)
UV spectrum (phosphate buffer pH of 6.5): λ_{max} = 261 nm
NaCl: 40.1 %

Elemental analysis (%):

	C	H	N	C/N
Calculation:	46.96	2.63	8.11	5.79
Calculation with H_2O and NaCl:	20.80	2.91	3.59	5.79
Found:	20.71	1.51	3.64	5.69

Water content: 13 mol/mol

ESI-MS negative mode (m/z):
$[M-H]^-$: 689.3, $[M-Na]^-$: 667.5

IR spectrum (cm^{-1}):

3357 (br,m)	1610 (vs)	1590 (m)	1539 (m)
1439 (m)	1326 (m)	1216 (s)	1141 (m)
1117 (m)	1024 (m)	759 (m)	714 (m)
615 (m)	569 (w)	522 (w)	

500 MHz ^{1}H NMR spectrum (DMSO-d_6): δ (ppm), *J* (Hz)

11.37	-NH-CO-	s	1H (exchangeable)
9.51	-NH-CO-NH-	s	1H (exchangeable)
8.79	H2′	dd (^4J = 1.9, ^4J = 9.0)	1H
8.46	H6	d (^3J = 8.0)	1H
7.71	H3	dd (^3J = 8.0)	1H
7.59-7.45	H6′	m	1H
7.40	H5′	dd (^3J = 9.1, ^3J = 11.0)	1H
7.37	H5	dd (^3J = 7.5)	1H
7.08	H4	t (^3J= 7.5)	1H

125 MHz ^{13}C NMR spectrum (DMSO-d^6): δ (ppm)

163.4	C7	131.5	C2	120.1	C3
154.2	C4′	129.9	C4	119.9	C6′
152.1	C8	128.0	C1′	115.6	C5′
135.6	C3′	127.0	C6	115.4	C2′
135.3	C1	121.8	C5		

Trisodium 3-(2,4-disulfonatophenylcarbamoyl)-5-(4-nitrobenzamido) benzoate
22a

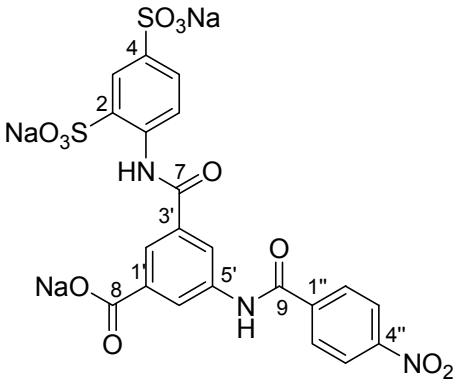

$C_{21}H_{12}N_3Na_3O_{12}S_2$ (631.4)

358 mg (1.94 mmol) 4-Nitrobenzoylchloride dissolved in 10 ml toluene were slowly added to the stirred solution of 626 mg (1.29 mmol) trisodium 5-amino-3-(2,4-disulfonato phenylcarbamoyl)benzoate in 50 ml water, until there was no amine left. The reaction was carried out according to GRP 2.

Yield: yellow powder, 85.3 % (0.70 g)
TLC: R_f = 0.5 (MP1)
HPLC: 98.6 % (t_R = 3.41 min)
UV spectrum (phosphate buffer pH of 6.5): λ_{max} = 277 nm
NaCl: 22.7 %

Elemental analysis (%):

	C	H	N	C/N
Calculation:	39.95	1.92	6.65	6.00
Calculation with H_2O and NaCl:	26.69	2.45	4.45	6.00
Found:	26.56	2.38	4.57	5.81

Water content: 5 mol/mol

IR spectrum:

3431 (br,m)	1685 (m)	1582 (m)	1526 (m)
1391 (m)	1318 (m)	1189 (br,m)	1080 (m)
1041 (m)	853 (w)	715 (m)	690 (m)
611 (m)	548 (m)		

500 MHz ^{1}H NMR spectrum (DMSO-d_6): δ (ppm), J (Hz)

11.42	-NH-CO	s		1H
10.84	-NH-CO	s		1H
8.52	H3	pd		1H
8.43	H6	d	(^3J = 8.5)	1H
8.38	H2′	s		1H
8.43	H3′′, H5′′	d	(^3J = 8.9)	2H
8.28	H2′′, H6′′	d	(^3J = 8.9)	2H
8.26	H4′	pd		1H
8.04	H6′	d	(^4J = 2.5)	1H
7.60	H5	dd	(^4J = 2.5, ^4J = 8.5)	1H

125 MHz ^{13}C NMR spectrum (DMSO-d_6): δ (ppm)

169.1	C8	139.5	C1	127.2	C2′
164.9	C7	138.7	C1′	125.2	C6′
164.2	C9	135.2	C5′	123.9	C3′′, 5′′
149.5	C4′′	134.9	C3′	120.6	C3
142.8	C4	134.7	C5	120.5	C6
140.8	C2	129.7	C2′′, 6′′	119.4	C4′
140.1	C1′′				

Trisodium 3-(2,4-disulfonatophenylcarbamoyl)-5-(4-aminobenzamido)benzoate
22b

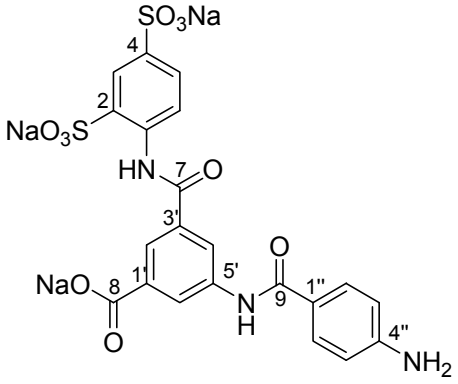

$C_{21}H_{14}N_3Na_3O_{10}S_2$ (601.5)

20 mg Palladium (10%) on charcoal were added as catalyst to a solution of 500 mg (0.79 mmol) compound 22a in water. The reaction was carried out according to GRP 3.

Yield: beige powder, 82.10 % (390 mg)
TLC: R_f = 0.52 (MP1)
HPLC: 98.2 % (t_R = 1.63 min)
UV spectrum (phosphate buffer pH of 6.5): λ_{max} = 295 nm
NaCl: 27.5

Elemental analysis (%):

	C	H	N	C/N
Calculation:	41.94	2.35	6.99	6.00
Calculation with H_2O and NaCl:	27.89	2.23	4.64	6.00
Found:	27.28	2.40	4.67	5.84

Water content : 3 mol/mol

IR spectrum (cm^{-1}):

3424 (br,m)	1674 (m)	1627 (m)	1586 (m)
1534 (m)	1317 (m)	1515 (m)	1442 (w)
1324 (m)	1286 (m)	1231 (s)	1184 (vs)
1081 (m)	1037 (m)	843 (w)	797 (w)
751 (m)	718 (m)	715 (m)	690 (m)
628 (m)	547 (m)		

500 MHz ^{1}H NMR spectrum (DMSO-*d*$_6$): δ (ppm), *J* (Hz)

11.34	-NH-CO	s		1H
9.98	-NH-CO	s		1H
8.44	H3	s		1H
8.42	H6	d	(^{2}J = 8.5)	1H
8.32	H2′	s		1H
8.19	H4′	s		1H
8.04	H6′	d	(^{4}J = 1.9)	1H
7.79	H2″, H6″	d	(^{3}J = 8.5)	2H
7.60	H5	dd	(^{3}J = 8.5, ^{4}J = 1.9)	1H
6.62	H3″, H5″	d	(^{3}J = 8.5)	2H
5.77	-NH_2	s		2H

125 MHz ^{13}C NMR spectrum (DMSO-*d*$_6$): δ (ppm)

169.8	C8	135.6	C3′	122.6	C1″
165.6	C7	134.8	C1′	121.5	C6
165.3	C9	134.5	C5′	120.4	C3
152.5	C4″	129.8	C2″, 6″	119.3	C4′
142.7	C4	127.2	C6′	112.9	C3″, 5″
141.5	C2	125.2	C5		
139.7	C1	125.1	C2′		

Hexasodium 5,5′-[carbonylbis(azanedyl-4,1-phenylenecarbonylazanediyl)] bis[3-(2,4)-disulfonatophenylcarbamoyl)benzoat]
22c

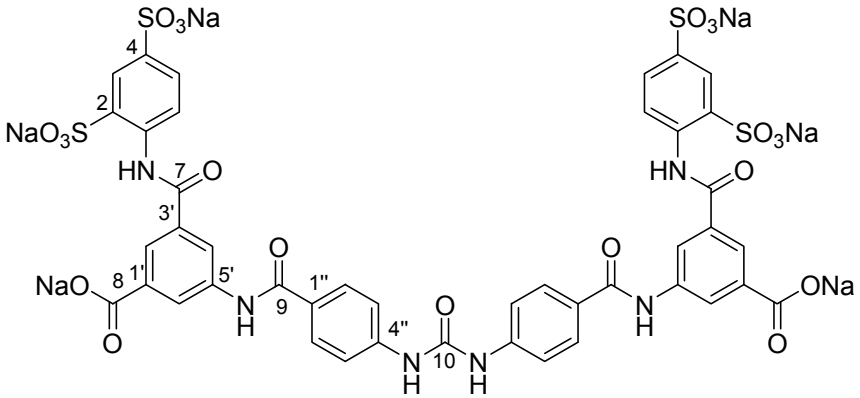

$C_{43}H_{26}N_6Na_6O_{21}S_4$ (1228.9)

A solution of 1.1 mmol phosgene (20 % in toluene) was slowly added to a solution of 333 mg (0.55 mmol) compound 22b under heavy stirring at room temperature. The reaction was carried out according to GRP 4.

Yield: pale orange powder, 75.56 % (510 mg)
TLC: R_f = 0.5 (MP2)
HPLC: 99.5 % (t_R = 5.87 min)
UV spectrum (phosphate buffer pH of 6.5): λ_{max} = 268 nm
NaCl: 45.1 %

Elemental analysis (%):

	C	H	N	C/N
Calculation:	42.03	2.13	6.84	6.15
Calculation with H_2O and NaCl:	18.35	2.18	2.99	6.15
Found:	18.32	2.09	3.04	6.10

Water content: 17 mol/mol

ESI-MS negative mode (m/z):
$[M\text{-}Na]^-$: 1205.3

IR spectrum (cm^{-1}):

3425 (br,m)	1593 (m)	1410 (m)	1190 (m)	617 (w)

500 MHz ^{1}H NMR spectrum (DMSO-d_6): δ (ppm), J (Hz)

11.37	-NH-CO-	s	1H (exchangeable)
10.45	-NH-CO-NH	s	1H (exchangeable)
10.30	-NH-CO-	s	1H (exchangeable)
8.48	H3	s	1H
8.43	H6	d (^2J = 8.5)	1H
8.37	H2′	s	1H
8.24	H4′	s	1H
8.04	H6′	d (^4J = 2.2)	1H
8.01	H2″, H6″	d (^3J = 8.5)	2H
7.70	H3″, H4″	d (^3J = 8.5)	2H
7.60	H5	dd (^3J = 8.5, ^4J = 2.0)	1H

125 MHz ^{13}C NMR spectrum (DMSO-d_6): δ (ppm)

169.1	C8	138.2	C4″	128.8	C2′
166.3	C7	138.1	C1′	126.8	C6′
162.5	C9	136.6	C5′	125.1	C6
151.0	C10	133.5	C3′	123.8	C3
142.2	C4	133.1	C5	121.9	C4′
141.5	C2	129.8	C1″	118.1	C3″, 5″
138.9	C1	129.6	C2″, 6″		

Trisodium 3-(2,4-disulfonatophenylcarbamoyl)-5-(4-fluoro-3-nitrobenzamido)benzoate
23a

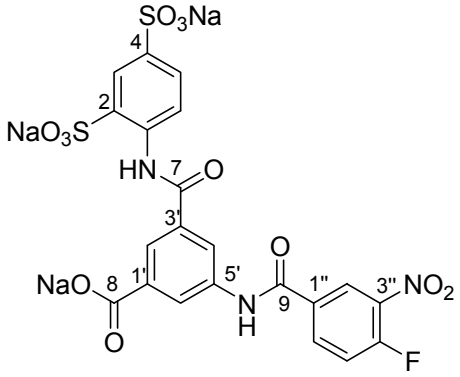

$C_{21}H_{11}FN_3Na_3O_{12}S_2$ (649.4)

0.4 g (1.94 mmol) 4-Fluoro-3-nitrobenzoylchloride, which was obtained by GRP1, were slowly added to the stirred solution of 626 mg (1.29 mmol) trisodium 5-amino-3-(2,4-disulfonato phenylcarbamoyl)benzoate in 50 ml water, until there was no amine left. The reaction was carried out according to GRP 2.

Yield: yellow powder, 88.83 % (0.75 g)
TLC: R_f = 0.6 (MP1)
HPLC: 95.5 % (t_R = 5.19 min)
UV spectrum (phosphate buffer pH of 6.5): λ_{max} = 268 nm
NaCl: 10.8 %

Elemental analysis (%):

	C	H	N	C/N
Calculation:	38.84	1.71	4.72	6.00
Calculation with H_2O and NaCl:	28.99	2.89	4.83	6.00
Found:	28.78	1.92	4.72	6.09

Water content: 7 mol/mol

ESI-MS negative mode: m/z
$[M-Na]^-$: 627.2, $[M-Na+H]^-$: 626.3, $[M-2Na+H]^-$: 604.3, $[M-3Na+H]^-$: 582.3

IR spectrum (cm^{-1}):

3441 (br,m)	1678 (m)	1622 (m)	1586 (m)
1536 (m)	1392 (m)	1318 (m)	1185 (br,vs)
1080 (m)	1040 (m)	840 (m)	797 (w)
749 (m)	720 (m)	689 (m)	610(m)
545 (m)			

500 MHz ^{1}H NMR spectrum (DMSO-d_6): δ (ppm), J (Hz)

11.44	-NH-CO	s		1H
10.81	-NH-CO	s		1H
8.86-8.47	H2″	dd	(^{3}J = 7.0, ^{4}J =2.0)	1H
8.52	H3	s		1H
8.50-8.47	H6″	m		1H
8.42	H6	d	(^{3}J = 8.5)	1H
8.37	H2′	s		1H
8.28	H6′	s		1H
8.03	H4′	d	(^{4}J = 2.0)	1H
7.81-7.77	H5″	dd	(^{3}J = 8.5, ^{3}J = 11.0)	1H
7.60	H5	dd	(^{3}J = 8.5, ^{4}J = 1.0)	1H

125 MHz ^{13}C NMR spectrum (DMSO-d_6): δ (ppm)

180.5	C8	135.9	C1	125.6	C2′
166.2	C7	135.8	C5′	125.1	C6′
164.9	C9	133.7	C1′	124.3	C6
157.7	C4″	130.2	C3′	123.0	C3
138.9	C4	129.6	C6″	122.0	C2″
138.2	C2	126.4	C5	119.5	C4′
136.6	C3″	126.3	C1″	119.3	C5″

Trisodium 3-(2,4-disulfonatophenylcarbamoyl)-5-(4-fluoro-3-aminobenzamido)benzoate
23b

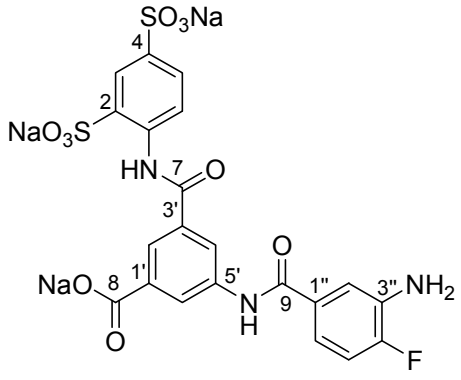

$C_{21}H_{13}FN_3Na_3O_{10}S_2$ (619.4)

20 mg Palladium (10%) on charcoal were added as catalyst to a solution of 500 mg (0.77 mmol) compound 23b in water. The reaction was carried out according to GRP 3.

Yield: brown powder, 94.53 % (0.45 g)

TLC: R_f = 0.57 (MP1)
HPLC: 99.7 % (t_R = 2.83 min)
UV spectrum (phosphate buffer pH of 6.5): λ_{max} = 270 nm
NaCl: 16.3%

Elemental analysis (%):

	C	H	N	C/N
Calculation:	40.72	2.12	6.78	6.00
Calculation with H_2O and NaCl:	28.68	2.98	4.78	6.00
Found:	28.83	2.73	4.77	6.04

Water content: 12 mol/mol

ESI-MS negative mode: m/z
$[M-Na]^-$: 597.4, $[M-Na+H]^-$: 596.3, $[M-2Na+H]^-$: 574.3, $[M-3Na+H]^-$: 552.4,

IR spectrum (cm^{-1}):

3424 (br,m)	1586 (m)	1391 (w)	1189 (m)
1038 (m)	690 (w)		

500 MHz ^{1}H NMR spectrum (DMSO-*d*$_6$): δ (ppm), *J* (Hz)

11.37	-NH-CO	s		1H
10.30	-NH-CO	s		1H
8.46	H3	s		1H
8.41	H6	d	(^4J = 8.5)	1H
8.29	H2′	s		1H
8.21	H6′	s		1H
8.02	H4′	d	(^4J =2.0)	1H
7.58	H5	dd	(^4J = 1.7, ^3J = 8.8)	1H
7.44	H2″	dd	(^4J = 1.7, ^3J = 8.5)	1H
7.24-7.21	H6″	m		1H
7.12	H5″	td	(^3J = 8.4, ^3J = 11.0)	1H
5.39	-NH_2	s		2H

125 MHz ^{13}C NMR spectrum (DMSO-*d*$_6$): δ (ppm)

187.7	C8	134.7	C1	124.3	C6′
168.5	C7	134.0	C5′	123.7	C6
166.9	C9	133.2	C1′	122.6	C3
157.7	C4″	130.3	C3′	119.5	C4′
139.0	C4	129.7	C5	117.6	C6″
138.4	C2	126.1	C1″	117.6	C5″
136.7	C3″	125.1	C2′	115.9	C2″

Hexasodium 5,5′-{carbonylbis[azanedyl(4-fluoro-1,3-phenylene)carbonylazanediyl]}bis[3-(2,4-disulfonatophenylene carbamoyl)benzoate]
23c

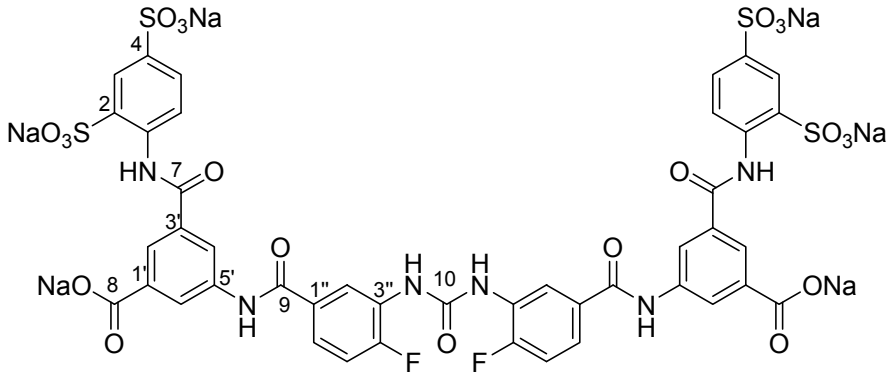

$C_{43}H_{24}F_2N_6Na_6O_{21}S_4$ (1264.8)

A solution of 1.22 mmol phosgene (20 % in toluene) was slowly added to a solution of 375 mg (0.61 mmol) compound 23b under heavy stirring at room temperature. The reaction was carried out according to GRP 4.

Yield: brown powder, 96.56 % (365 mg)
TLC: R_f = 0.53 (MP2)
HPLC: 97.4 % (t_R = 7.08 min)
UV spectrum (phosphate buffer pH of 6.5): λ_{max} = 265 nm
NaCl: 35.1 %

Elemental analysis (%):

	C	H	N	C/N
Calculation:	40.83	1.91	6.64	6.15
Calculation with H_2O and NaCl:	20.63	2.58	3.36	6.15
Found:	20.43	2.47	3.53	5.79

Water content: 20 mol/mol

ESI-MS negative mode (m/z):
$[M-Na]^-$: 1243.0, $[M-2Na-H]^-$: 1221.0

IR spectrum (cm^{-1}):

3426 (br,m)	1586 (m)	1394 (m)	1320 (m)
1188 (br,vs)	1081 (m)	1038 (m)	751 (w)
719 (m)	690 (m)	613 (m)	548 (m)

500 MHz ^{1}H NMR spectrum (DMSO-d_6): δ (ppm), *J* (Hz)

11.38	-NH-CO	s		1H
10.48	-NH-CO	s		1H
9.50	-NH-CO-CH	s		1H
8.80	H2″	dd	(^{4}J = 5.7)	1H
8.49	H3	s		1H
8.42	H6	d	(^{3}J = 8.5)	1H
8.33	H2′	s		1H
8.24	H4′	s		1H
8.04	H6′	d	(^{4}J = 1.9)	1H
7.74-7.72	H6″	m		1H
7.59	H5	d	(^{4}J = 1.9, ^{3}J =8.5)	1H
7.42-7.38	H5″	t	(^{3}J = 8.5, ^{3}J = 11.0)	1H

125 MHz ^{13}C NMR spectrum (DMSO-d_6): δ (ppm)

187.7	C8	134.8	C5′	125.1	C6′
168.5	C7	134.0	C1′	124.3	C6
166.9	C9	133.2	C3′	123.7	C3
153.7	C10	130.3	C6″	122.6	C4′
139.1	C4″	129.7	C5	119.5	C3″
138.5	C4	126.1	C1″	117.6	C2″
138.4	C2	126.0	C2′	115.8	C5″
136.7	C1				

Trisodium 3-(3-nitrobenzamido)-5-(2,4-disulfonatophenylcarbamoyl)benzoate 24a

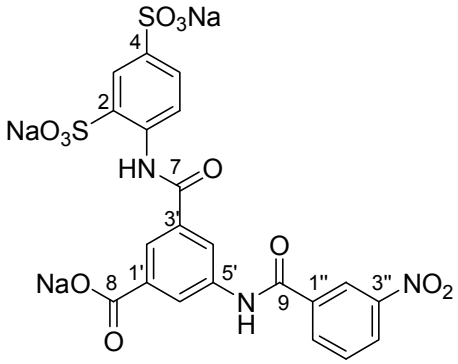

$C_{21}H_{12}N_3Na_3O_{12}S_2$ (631.4)

354.31 mg (1.92 mmol) 3-Nitrobenzoylchloride dissolved in 10 ml toluene were slowly added to the stirred solution of 620 mg (1.28 mmol) Trisodium 5-amino-3-(2,4-disulfonato phenylcarbamoyl) benzoate in 50 ml water, until there was no amine left. The reaction was carried out according to GRP 2.

Yield: pink powder, 53.2 % (0.43 g)
TLC: R_f = 0.41 (MP1)

HPLC: 99.0 % (t_R = 3.68 min)
UV spectrum (phosphate buffer pH of 6.5): λ_{max} = 270 nm
NaCl: 46.2 %

Elemental analysis (%):

	C	H	N	C/N
Calculation:	39.95	1.92	6.65	6.00
Calculation with H_2O and NaCl:	18.79	1.65	3.13	6.00
Found:	18.88	1.76	3.45	5.48

Water content: 5 mol/mol

ESI-MS negative mode (m/z):
$[M-Na]^-$: 608.7, $[M-Na+H]^-$: 607.7

IR spectrum (cm^{-1}):
3444 (br,m) 1527 (m) 1185 (m) 1038 (w)
690 (w)

500 MHz ^{1}H NMR spectrum (DMSO-d_6 δ (ppm), J (Hz)

11.4	-NH-CO-	s	1H (exchangeable)
10.8	-NH-CO-	s	1H (exchangeable)
8.89	H2″	d (^4J = 2.2)	1H
8.50	H4″	dd (^4J = 1.5, ^3J = 8.5)	1H
8.49	H3	s	1H
8.45	H6″	dd (^4J = 1.5, ^3J = 8.0)	1H
8.42	H6	d (^3J = 8.5)	1H
8.35	H2′	m	1H
8.25	H4′	s	1H
8.03	H6′	d (^4J = 2.0)	1H
7.86	H5″	t (^3J = 8.0)	1H
7.60	H5	dd (^4J = 2.0, ^3J = 8.5)	1H

Trisodium 3-(3-aminobenzamido)-5-(2,4-disulfonatophenylcarbamoyl) benzoate
24b

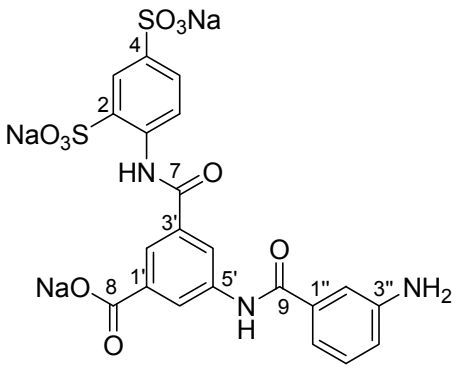

$C_{21}H_{14}N_3Na_3O_{10}S_2$ (601.5)

20 mg Palladium (10%) on charcoal were added as catalyst to a solution of 410 mg (0.70 mmol) compound 24a in water. The reaction was carried out according to GRP 3.

Yield: beige powder, 87.88 % (370 mg)
TLC: R_f = 0.5 (MP1)
HPLC: 97.5 % (t_R = 1.65 min)
UV spectrum (phosphate buffer pH of 6.5): λ_{max} = 258 nm
NaCl: 14.9 %

Elemental analysis (%):

	C	H	N	C/N
Calculation:	41.94	2.35	6.99	6.00
Calculation with H_2O and NaCl:	29.29	3.39	4.88	6.00
Found:	29.13	3.03	5.04	5.78

Water content: 7 mol/mol

ESI-MS negative mode (m/z):
$[M-H]^-$: 600.4, $[M-Na]^-$: 578.3, $[M-2Na+H]^-$: 556.3, $[M-3Na+H]^-$: 534.4

IR spectrum (cm^{-1}):

3414 (br,m)	1669 (s)	1608 (m)	1560 (w)
1530 (m)	1390 (m)	1318 (m)	1188 (br,m)
1136 (m)	1082 (m)	1040 (m)	806 (w)
756 (m)	690 (m)	612 (m)	552 (m)

500 MHz ^{1}H NMR spectrum (DMSO-*d*$_6$): δ (ppm), *J* (Hz)

11.36	-NH-CO	s		1H
10.26	-NH-CO	s		1H
8.47	H3	s		1H
8.42	H6	d	(^4J = 8.5)	1H
8.30	H2′	s		1H
8.21	H4′	s		1H
8.03	H6′	d	(^4J = 2.0)	1H
7.59	H6′′	dd	(^4J = 1.5, ^3J = 8.5)	1H
7.18	H2′′	s		1H
7.15	H5, H4′′	d	(^3J = 4.6)	2H
6.75-6.74	H5′′	m		1H
5.31	$-NH_2$	s		2H

125 MHz ^{13}C NMR spectrum (DMSO-*d*$_6$): δ (ppm)

173.8	C8	136.7	C1′	125.2	C6′
169.7	C7	134.9	C5′	124.5	C6
167.3	C9	134.3	C3′	123.9	C3
146.9	C3′′	133.5	C1′′	123.6	C4′
139.1	C4	130.1	C5	120.5	C4′′
138.6	C2	129.7	C5′′	118.5	C6′′
138.4	C1	126.4	C2′	115.2	C2′′

Hexasodium 5,5′-[carbonylbis(azanediyl-3,1-phenylene carbonylazanediyl]bis[3-(2,4-disulfonatophenylcarbamoyl)benzoate] 24c

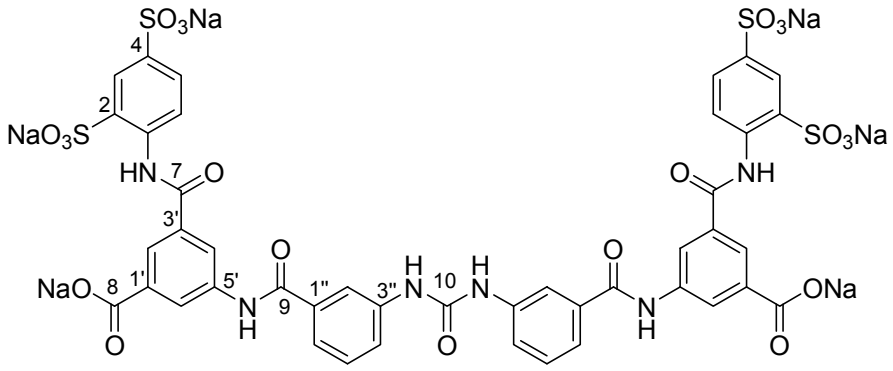

$C_{43}H_{26}N_6Na_6O_{21}S_4$ (1228.9)

A solution of 1.0 mmol phosgene (20 % in toluene) was slowly added to a solution of 300 mg (0.50 mmol) compound 24b under heavy stirring at room temperature. The reaction was carried out according to GRP 4.

Yield: grey powder, 89.5 % (550 mg)
TLC: R_f = 0.5 (MP2)
HPLC: 98.2 % (t_R = 6.68 min)
UV spectrum (phosphate buffer pH of 6.5): λ_{max} = 266 nm
NaCl: 66.4%

Elemental analysis (%):

	C	H	N	C/N
Calculation:	42.03	2.13	6.84	6.15
Calculation with H_2O and NaCl:	12.67	1.34	2.06	6.15
Found:	12.65	1.49	2.16	5.85

Water content: 14 mol/mol

IR spectrum (cm^{-1}):

3426 (br,m)	1589 (m)	1394 (m)	1320 (m)
1188 (m)	1390 (m)	1040 (m)	691 (m)
614 (m)	1039 (m)	552 (m)	

500 MHz ^{1}H NMR spectrum (DMSO-d_6): δ (ppm), *J* (Hz)

11.37	-NH-CO-	s	1H (exchangeable)
10.48	-NH-CO-	s	1H (exchangeable)
9.50	-NH-CO-NH-	s	1H (exchangeable)
8.79	H2′′	d (^4J = 2.2)	1H
8.48	H3	s	1H
8.42	H6	d (^3J = 8.5)	1H

8.32	H2′	s	1H
8.21	H4′	s	1H
8.03	H6′	d (^4J = 2.2)	1H
7.74-7.72	H6′′	dd (^4J = 2.2, ^3J = 8.5)	1H
7.60	H5′′, H4′′	d (^4J = 1.9)	2H
7.34-7.32	H5	t (^3J = 8.5)	1H

125 MHz ^{13}C NMR spectrum (DMSO-*d*$_6$): δ (ppm)

173.1	C8	136.4	C5′	124.0	C4′′
167.9	C7	133.1	C3′	122.8	C6
165.6	C9	132.7	C3′′	122.7	C3
152.4	C10	132.4	C1′′	122.6	C6′′
138.7	C4	129.6	C1	122.1	C4′
138.6	C2	129.5	C5′′	115.2	C2′′
138.1	C5	129.5	C2′		
138.0	C1′	125.2	C6′		

Trisodium 3-(2,4-disulfonatophenylcarbamoyl)-5-(4-methyl-3-nitrobenzamido)benzoate
25a

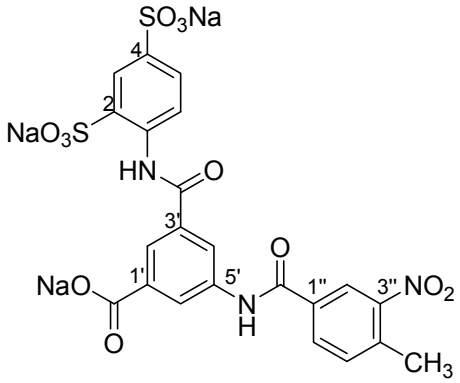

$C_{22}H_{14}N_3Na_3O_{12}S_2$ (645.5)

418 mg (1.95 mmol) 4-Methyl-3-nitrobenzoylchloride dissolved in 10 ml toluene were slowly added to the stirred solution of 626 mg (1.3 mmol) trisodium 5-amino-3-(2,4-disulfonato phenylcarbamoyl) benzoate in 50 ml water, until there was no amine left. The reaction was carried out according to GRP 2.

Yield: pale brown powder, 60.79 % (510 g)
TLC: R_f = 0.65 (MP1)
HPLC: 99.5 % (t_R = 6.05 min)
UV spectrum (phosphate buffer pH of 6.5): λ_{max} = 270 nm
NaCl: 23.8 %

Elemental analysis (%):

	C	H	N	C/N
Calculation:	40.94	2.19	6.51	6.29
Calculation with H_2O and NaCl:	27.37	2.51	4.35	6.29
Found:	27.35	2.36	4.49	6.10

Water content: 5 mol/mol

IR spectrum (cm^{-1}):

3440 (br,m)	1587 (m)	1530 (m)	1401 (m)
1341 (w)	1190 (m)	1040 (m)	690 (m)
627 (w)			

500 MHz ^{1}H NMR spectrum (DMSO-*d_6*): δ (ppm), *J* (Hz)

11.41	-NH-CO	s		1H
10.72	-NH-CO	s		1H
8.67	H2″	s		1H
8.51	H3	s		1H
8.43	H6	d	(^3J = 8.0)	1H
8.38	H2′	s		1H
8.30	H6″	dd	(^3J = 8.0, ^4J = 2.0)	1H
8.28	H4′	s		1H
8.04	H6′	dd	(^4J = 1.9)	1H
7.70	H5″	d	(^3J = 8.0)	1H
7.61	H5	dd	(^3J = 8.3, ^4J = 2.0)	1H
2.61	-CH_3	s		3H

125 MHz ^{13}C NMR spectrum (DMSO-*d_6*): δ (ppm)

174.8	C8	143.8	C1′	133.5	C5″
163.6	C7	142.8	C5′	132.6	C6′
163.5	C9	142.7	C3′	127.2	C2′
149.9	C3″	141.7	C4″	125.2	C6
149.8	C4	136.7	C6″	124.1	C3
149.2	C2	135.5	C1″	123.5	C2″
144.9	C5	133.9	C1	19.9	C11

Trisodium 3-(2,4-disulfonatophenylcarbamoyl)-5-(4-methyl-3-aminobenzamido)benzoate
25b

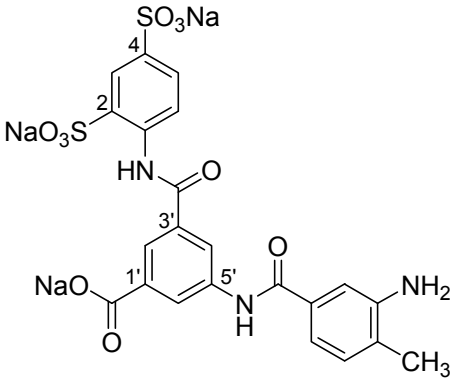

$C_{22}H_{16}N_3Na_3O_{10}S_2$ (615.6)

20 mg Palladium (10%) on charcoal were added as catalyst to a solution of 450 mg (0.70 mmol) compound 25a in water. The reaction was carried out according to GRP 3.

Yield: brown powder, 83.70 % (360 mg)
TLC: R_f = 0.38 (MP1)
HPLC: 96.6 % (t_R = 3.02 min)
UV spectrum (phosphate buffer pH of 6.5): λ_{max} = 271 nm
NaCl: 24.4%

Elemental analysis (%):

	C	H	N	C/N
Calculation:	42.93	2.62	6.83	6.29
Calculation with H_2O and NaCl:	26.30	3.20	4.18	6.29
Found:	26.20	2.50	4.49	5.84

Water content: 8 mol/mol

ESI-MS negative mode (m/z):
[M-Na]: 593.3, [M-Na-H]: 592.4

IR spectrum (cm^{-1}):

3427 (br,m)	1585 (m)	1391 (m)	1321 (w)
1188 (m)	1040 (m)	691 (m)	609 (m)

500 MHz ^{1}H NMR spectrum (DMSO-d_6): δ (ppm), *J* (Hz)

11.37	-NH-CO	s		1H
10.22	-NH-CO	s		1H
8.48	H3	s		1H
8.43	H6	d	(^3J = 8.5)	1H
8.33	H2′	s		1H

8.22	H4′	s		1H
8.04	H6′	d	(^4J = 2.0)	1H
7.60	H5	dd	(^3J = 8.5, ^4J = 1.5)	1H
7.27	H2″	s		1H
7.16	H6″	d	(^3J = 7.8, ^4J = 1.5)	1H
7.06	H5″	d	(^3J = 7.5)	1H
5.08	-NH_2	s		2H
2.13	-CH_3	s		3H

125 MHz ^{13}C NMR spectrum (DMSO-*d*$_6$): δ (ppm)

173.7	C8	136.7	C1′	125.1	C5′
169.9	C7	133.8	C3′	124.1	C3
166.7	C9	133.1	C4″	123.5	C2′
144.8	C3″	132.0	C5	122.5	C4′
138.9	C4	130.9	C1″	118.8	C6″
138.5	C2	129.6	C5″	114.9	C2″
138.4	C1	125.9	C6′	19.9	C11

Hexasodium 5,5′-{carbonylbis[azanediyl(4-methyl-3,1-phenylenecarbonylazanediyl]}bis[3-(2,4-disulfonatophenylenecarbamoyl]benzoate]
25c

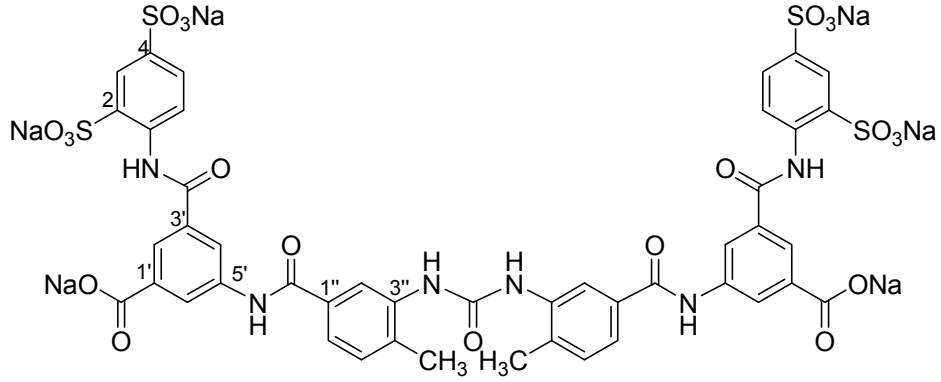

$C_{45}H_{30}N_6Na_6O_{21}S_4$ (1256.9)

A solution of 1.04 mmol phosgene (20 % in toluene) was slowly added to a solution of 323 mg (0.52 mmol) compound 25b under heavy stirring at room temperature. The reaction was carried out according to GRP 4.

Yield: pink powder, 53.56 % (350 mg)
TLC: R_f = 0.5 (MP2)
HPLC: 98.9 % (t_R = 6.75 min)
UV spectrum (phosphate buffer pH of 6.5): λ_{max} = 265 nm
NaCl: 56.5 %

Elemental analysis (%):

	C	H	N	C/N
Calculation:	43.00	2.41	6.69	6.43
Calculation with H_2O and NaCl:	14.86	1.83	2.31	6.43
Found:	14.83	1.64	2.41	6.16

Water content: 18 mol/mol

ESI-MS negative mode (m/z):
[M-Na-H]: 1232.9

IR spectrum (cm^{-1}):

3424 (br,m)	1183 (s)	610 (m)
1585 (m)	1080 (m)	548 (m)
1533 m)	1036 (m)	
1390 (w)	752 (m)	
1311 (m)	689 (m)	

500 MHz ^{1}H NMR spectrum (DMSO-d_6): δ (ppm), *J* (Hz)

11.53	-NH-CO-	s	1H (exchangeable)
10.52	-NH-CO-	s	1H (exchangeable)
9.19	-NH-CO-NH-	s	1H (exchangeable)
8.64	H2″	s	1H
8.51	H3	s	1H
8.43	H6	d (^3J = 8.0)	1H
8.41	H2′	s	1H
8.22	H4′	d (^4J = 1.5)	1H
8.03	H6′	d (^4J = 2.5)	1H
7.66	H6″	dd (^4J = 1.9, ^3J = 7.8)	1H
7.60	H5	dd (^4J = 2.0, ^3J = 8.5)	1H
7.33	H5″	d (^3J = 11.5)	1H
2.41	-CH_3	s	3H

10. References

Abbracchio MP (1996) Research overview: PI and P2 receptors in cell growth and differentiation. *Drug Dev Res* **39:** 393-406.

Abbrachio MP, Boeynaems M J, Barnard E A, Boyer J L, Kennedy C, Miras-Portugal M T, King B F, Gachet C, Jacobson K A, Weisman G, and Burnstock G (2003) Characterisation of the UDP-glucose receptor (re-named here the $P2Y_{14}$ receptor) adds diversity to the P2Y receptor family. *Trends in Pharmacol.l Sci.* **24:** 52-55.

Abbrachio MP, Burnstock G, Boeynaems M J, Barnard E A, Jose L B, Kennedy C, Knight G E, Fumagalli M, Gachet C, Jacobson K A, and Weisman G (2006) International Union of Pharmacology LVIII: Update on the P2Y G protein-coupled nucleotide receptors: from molecular mechanisms and pathophysiology to therapy. *Pharmacol Rev* **58:** 281-341.

Amisten S, Melander O, Wihlborg A, Berglund G, and Erlinge D (2006) Increased risk of acute myocardial infarction and elevated levels of C-reactive protein in carriers of the Thr87 Variant of the ATP receptor $P2Y_{11}$. *Purinergic Signaling* **2:** 234-235.

Angiolillo DJ, Costa M A, Shoemaker S B, Desai B, Bernardo E, Suzuki Y, Charlton R K, Zenni M M, Guzman L A, and Bass T A (2008) Functional effects of high clopidogrel maintenance dosing in patients with inadequate platelet inhibition on standard dose treatment. *Am J Cardiol* **101:** 440-445.

Arunlakshana O and Schild HO (1959) Some quantitative uses of drug antagonists. *Br J Pharmacol Chemother* **14:** 48-58

Balogh J, Wihlborg A K, Isackson H, Joshi B V, Jacobson K A, Arner A, and Erlinge D (2005) Phospholipase C and cAMP-dependent positive inotropic effects of ATP in mouse cardiomyocytes via $P2Y_{11}$-like receptors. *J of Mol and Cell Cardio* **39:** 1-8.

Barnard EA and Simon J (2001) An elusive receptor is finally caught: $P2Y_{12}$, an important drug target in platelets. *Trends Pharmacol Sci* **22:** 388-391.

Baurand A, Eckly A, Bari N, Leon C, Hechler B, Cazenave J P, and Gachet C (2000) Desensitization of the platelet aggregation response to ADP: differential down-regulation of the $P2Y_1$ and $P2_{cyc}$ receptors. *Thromb Haemost* **84:** 484-491.

Becker HGO, Berger W, Domschke G, Fanghaenel E, Faust J, Fischer M, Gentz F, Gewald K, Gluch R, Mayer R, Müller K, Pavel D, Schmidt H, Schollberg K, Schwetlick K, Seiler E, and Zeppenfeld G (2001) Organikum, organisch-chemisches grundpraktikum. *Wiley-VCH Weinheim* 351-392.

Boarder MR and Hourani S M (1998) The regulation of vascular function by P2 receptors: multiple sites and multiple receptors. *Trends Pharmacol Sci* **19:** 99–107.

Boeynaems JM, Robaye B, Janssens R, Suarez-Huerta N, and Communi D (2001) Overview of P2Y receptors as therapeutic targets. *Drug Dev Res* **52:** 187-189.

Boyer JL, Mohanram A, Camaioni E, Jacobson K A, and Harden T K (1998) Competitive and selective antagonism of $P2Y_1$ receptors by N^6-methyl 2'-deoxyadenosine 3',5'-bisphosphate. *Br J Pharmacol* **124:** 1-3.

Braun K, Rettinger J, Ganso M, Kassack M, Hildebrandt C, Ullmann H, Nickel P, Schmalzing G, and Lambrecht G (2001) NF449: A subnanomolar potency antagonist at recombinant rat $P2X_1$ receptors. *Naunyn-Schmiedeberg's Arch Pharmacol* **364:** 285-290.

Berchtold S, Ogilvie A L, Bogdan C, Muhl-Zurbes C, Ogilvie A, Schuler G, and Steinkasserer A (1999) Human monocyte derived dendritic cells express functional P2X and P2Y receptors as well as ecto-nucleotidases. *FEBS Lett* **458:** 424-428.

Brink CB, Harvey B H, Bodenstein J, Venter D P, and Oliver D W (2004) Recent advances in drug action and therapeutics: relevance of novel concepts in G protein-coupled receptor and signal transduction pharmacology. *Br J Clin Pharmacol* **57:** 373 - 387.

Brown SG, Kim Y C, Kim S A, Jacobson K A, Burnstock G, and King B F (2001) Actions of a series of PPADS analogues at $P2X_1$ and $P2X_3$ receptors. *Drug Dev Res* **53:** 281-291.

Burnstock G (1976) Purinergic receptors. *J of Th. Biol* **62:** 491-503.

Burnstock G (1978) A basis for distinguishing two types of purinergic receptor, in cell membrane receptors for drugs and hormones: A multidisciplinary approach. *Raven Press New York* 107-118.

Burnstock G (1981) Pathophysiology of migraine: A new hypothesis. *Lancet* 1397-1399.

Burnstock (2007) Purine and pyrimidine receptors. *Cellular and Molecular Life Science (CMLS)* **64:** 1471-1483.

Bultmann R, Wittenburg H, Pause B, Kurz G, Nickel P, Starke K. P2- purinoceptor antagonists: III. Blockade of P2-purinoceptor subtypes and ecto-nucleotidases by compounds related to suramin (1996) *Naunyn Schmiedebergs Arch Pharmacol* 1996; 354(4):498-504.

Caprie Steering Committee (1996) A randomized, blinded, trial of clopidogrel versus aspirin in patients at risk of ischaemic events. *Lancet* **16:** 1329-1339.

Carafoli E (2004) Calcium-mediated cellular signals: A story failures. *Trends in Biochem Sci* **29:** 371-378.

Cheek DJ, McHugh J M, Blood-Siegfried J, McFetridge J F, and Turner B S (2000) A historical perspective on the discovery of adenyl purines. *Biol Res Nurs* **1:** 265-275.

Chen CC, Akopian A N, Sivilottit L, Colquhoun D, Burnstock G, and Wood J N (1995) A P2X purinoceptor expressed by a subset of sensory neurons. *Nature* **377:** 428-431.

Cheng Y and Prusoff W H (1973) Relationship between the inhibition constant (K_i) and the concentration of inhibitor which cause 50 percent inhibition (IC_{50}) of an enzymatic reaction. *Biochem Pharmacol* **22:** 3099-3108.

Chhatriwala M, Ravi R G, Patel R I, Boyer J L, Jacobson K A, and Harden T K (2004) Induction of novel agonist selectivity for the ADP-activated $P2Y_1$ receptors versus the ADP-activated $P2Y_2$ and $P2Y_{13}$ receptors by conformational constrant of an ADP analogue. *J Pharmacol Exp Ther* **311:** 1038-1043.

Chizh BA and Illes P (2000) P2X receptors and nociception. *Pharm Rev* **53:** 553-568.

Clifford EE, Parker K, Humphreys B D, Kertesy S B, and Dubyak G R (1998) The $P2X_1$ Receptor, an adenosine triphosphate-gated cation channel, is expressed in human platelets but not in human blood leukocytes. *Blood* **91:** 3172-3181.

Communi, D, Motte S, Boeynaems J M, and Pirotton S (1996) Pharmacological characterization of the human $P2Y_4$ receptor. *Eur J of Pharmacol* **317:** 383–389.

Communi D, Robaye B, and Boeynaems J M (1999) Pharmacological characterization of the human $P2Y_{11}$ receptor. *Br J Pharmacol* **128:** 1199-1206.

Communi D, Suarez-Huerta N, Dussossoyi D, Savi P, and Boeynaems J M (2001) Cotranscription and intergenic splicing of human $P2Y_{11}$ and SSF1 genes. *The J of Biol Chem* **276:** 16561–16566.

Cruse MJ (2003) Illustrated dictionary of immunology. *CRC Press Boca Raton* 193-194.

Damer S (2002) Pharmacological evaluation of NF279 as a P2 receptor antagonist. *Dissertations Johann Wolfgang Goethe-Universitaet Frankfurt/Main.*

Dangelmaier C, Jin J, Daniel J L, Smith J B, and Kunapuli S P (2000) The $P2Y_1$ receptor mediates ADP-induced p38 kinase-activating factor generation in human platelets. *Eur J Biochem* **267:** 2283-2289.

Egan TM, Cox J A, and Voigt M M (2004) Molecular structure of P2X receptors. *Curr Topics Med Chem* **4:** 821-829.

Flower DR (1999) Modelling G-protein-coupled receptors for drug design. *Biochimica et Biophysica Acta* **1422:** 207-234.

Fredholm BB, Abbrachio M P, Burnstock G, Dubyak G R, Harden T K, Jacobson K A, Schwabe U, and Williams M (1997) Towards a revised nomenclature for P1 and P2 receptors. *Trends Pharmacol Sci* **18:** 79-82.

Fredholm BB, Hoekfelt T, and Milligan G (2007) G protein-coupled receptors: an update. *Acta Physiol* **190:** 3-7.

Fyffe REW and Perl E R (1984) Is ATP a central synaptic mediator for certain primary afferent fibres from mammalian skin? *Proc Natl Acad Sci* **81:** 6890-6893.

Fujihara T, Murakami T, Fujita H, Nakamura M, and Nakata K (2001) Improvement of corneal barrier function by the P2Y(2) agonist INS365 in a rat dry eye model. *Investigative Ophtalmology & Visual Science* **42:** 96-100.

Gachet C (2005) The platelet P2 receptors as molecular targets for old and new antiplatelet drugs. *Pharmacol and Ther* **108:** 180 - 192.

Gever J, Cockayne D, Dillon M, Burnstock G, and Ford A (2006) Pharmacology of P2X channels. *Pfluegers Archiv European Journal of Physiology* **452:** 513-537.

Glaenzel M, Bueltmann K, and Frahm A W (2005) Structure-activity relationships of novel P2-receptor antagonists structurally related to reactive blue 2. *European Journal of Medicinal Chemistry* **40:** 1262-1276.

Haughland RP (2006) Handbook of Fluorescent Probes and Research Products, Invitrogen Orlando, 819-820.

Hausmann R, Rettinger J, Gerevich Z, Meis S, Kassack MU, Illes P, Lambrecht G, and Schmalzing G (2006) The suramin analogue NF110 potently blocks $P2X_3$ receptors: subtype selectivity is determined by location of sulfonic acid groups. *Mol Pharmacol* **69:** 2058-2067.

Hollopeter G, Jantzen H M, Vincent D, Li G, England L, Ramakrishnan V, Yang R B, Nurden A, Julius D, and Conley P B (2001) Identification of the platelet ADP receptor targeted by antithrombotic drugs. *Nature* **409:** 202–207.

Hongwiset D (2008) Development of potent and selective antagonist at $P2Y_{11}$ receptors: Symmetrical and asymmetrical derivatives of NF340. Dissertation Heinrich Heine-Universität Düsseldorf.

Jacobson KA, Jarvis M F, and Williams M (2002) Purine and pyrimidine (P2) receptors as drug targets. *J Med Chem* **45:** 4057-4093.

Jacoby E, Bouhelal R, Gerspacher M and Seuwen K 2006. The 7 TM G-protein-coupled receptor target family. *Chem Med Chem* 1, 761–782.

Jahr CE and Jessell T M (1983) ATP excites a subpopulation of rat dorsal horn neurones. *Nature* **304:** 730-733.

Jin J, Dasari VR, Sistare FD, and Kunapuli SP (1998b) Distribution of P2Y receptor subtypes on haematopoietic cells. *Br J Pharmacol* **123:** 789–794.

Kassack M and Nickel P (1996) Rapid, highly sensitive gradient narrow-bore high-performance liquid chromatographic determination of suramin and its analogues. *J Chrom Biomed Appl* **15:** 275-284.

Kassack MU, Hoefgen B, Lehmann J, Eckstein N, Quillan J M, and Sadée W (2002) Functional screening of G protein-coupled receptors by measuring intracellular calcium with a fluorescence microplate reader. *J Biomol Screen* **7:** 233-246.

Kassack MU, Braun K, Ganso M, Ullmann H, Nickel P, Boeing B, Müller G, and Lambrecht G (2004) Structure-activity relationships of analogues of NF449 confirm NF449 as the most potent and selective known $P2X_1$ receptor antagonist. *Eur J Med Chem* **39:** 345-357.

Kennedy C (2005) P2X receptors: targets for novel analgesics? *Neuroscientist* **11:** 345-356.

Kim YC, Brown S G, Harden T K, Boyer J L, Dubyak G, King B F, Burnstock G, and Jacobson K A (2001) Structure-activity relationships of pyridoxal phosphate derivatives as potent and selective antagonists of P2X1 receptors. *J Med Chem* **44:** 340-349.

King BF and Towsend-Nicholson A (2003) Nucleotide and nucleoside receptors. *Tocris Rev* **23:** 1-11.

Kostenis E, Waelbroeck M, and Milligan G (2005) Techniques: Promiscuous Gα proteins in basic research and drug discovery trends in Pharmacol Sci **26:** 595-602.

Lewis C, Neidhart S, Holy C, North R A, Buell G, and Surprenant A (1995) Coexpression of $P2X_2$ and $P2X_3$ receptor subunits can account for ATP-gated currents in sensory neurons. *Nature* **377:** 432-435.

Lin K, Sadee W, and Quillan J M (1999) Rapid measurements of intracellular calcium using a fluorescence plate reader. *Biotechniques* **26:** 318-326.

Manfred H, Meier H, and Zeeh B (1979) Spektroskopische Methoden in der Organischen Chemie. *Thimie* 72-227.

Marteau F, Le-Poul E, Communi D, Labouret C, Savi P, Boeynaems J M, and Gonzales N S (2003) Pharmacological characterization of the human $P2Y_{13}$ receptor. *Mol Pharmacol* **64:** 104–112.

Meis S (2008) Molekulare und funktionelle Charakterisierung des $P2Y_{11}$ rezeptors sowie pharmakologische Evaluierung neuer Agonisten und Antagonisten. Dissertation Heinrich Heine-Universität Düesseldorf

Michelson AD (2008) $P2Y_{12}$ antagonism promises and challenges. *Arterioscler Thromb Vasc Bio* **28:** 33-38.

Milligan G (2003) Constitutive activity and inverse agonists of G protein-coupled receptors: a current perspective. *Mol Pharmacol* **64:**1271-1276

Mitka M (2001) Results of CURE trial for acute coronary syndrome. *JAMA* **285:** 1828-1829.

Müller CE (2002) P2-pyrimidinergic receptors and their ligands. *Curr Pharm Des* **8:** 2353-2369.

Monteith G and Bird G J (2005) Techniques: high-throughput measurement of intracellular Ca^{2+}-back to basics. *Trends in Pharmacol Sci* **26:** 218-223.

Moore DJ, Chambers J K, Wahlin J P, Tan K B, Moore G B, Jenkins O, Emson P C, and Murdock P R (2001) Expression pattern of human P2Y receptor subtypes: a quantitative reverse transcription polymerase chain reaction study. *Biochimica et Biophysica Acta* **1521:** 107-119.

Moore DJ, Murdock P R, Watsonc J M, Faull R M, Waldvogeld H J, Szekerese P G, Wilsone S, Freeman K B, and Emsona P C (2003) GPR105, a novel $G_{i/o}$-coupled UDP-glucose receptor expressed on brain glia and peripheral immune cells, is regulated by immunologic challenge: Possible role in neuroimmune function. *Mol Brain Res* **118:** 10–23.

Mundasad MV, Novack G D, Allgood V E, Evans R M, Gorden J C, Yerxa B R (2001) Ocular safety of INS365 ophthalmic solution: a $P2Y_2$ agonist, in healthy subjects. *J. Ocul. Pharmacol. Ther.* **17:** 173.

North RA (2002) Molecular physiology of P2X receptors. *Physiol Rev* **82:** 1013-1067.

Parr CE, Sullivan D M, Paradiso A M, Lazarowski E R, Burch L H, Olsen JC, Erb L, Weisman G A, Boucher R C, and Turner J T (1994) Cloning and expression of a human P2U nucleotide receptor, a target for cystic fibrosis pharmacotherapy. *Proc Natl Acad Sci* **91:** 3275.

Patrick GL (1995) An introduction to medicinal chemistry. *Oxford University Press, Oxford* 68-70.

Qi AD, Kennedy C, Harden K, and Nicholas R A (2001) Diferential coupling of the human $P2Y_{11}$ receptor to phospholipase C and adenylyl cyclase. *Brit J of Pharmacol* **132:** 318-326.

Ralevic V and Burnstock G (1998) Receptors for purines and pyrimidines. *Pharmacol Rev* **50:** 415-475.

Robaye B, Ghanem E, Wilkin F, Fokan D, Van Driessche W, Schurmans S, Boeynames J M, and Beauwens R (2003) Loss of nucleotide regulation of epithelial chloride transport in the jejunum of $P2Y_4$-null mice. *Mol Pharmacol* **63:** 777–783.

Romagnoli R, Baraldi P G, Cruz-Lopez O, Lopez-Cara C, Preti D, Borea P A, and Gessi S (2008) The $P2X_7$ receptor as a therapeutic target. *Expert Opin on Ther Targets* **12:** 647-661.

Rudolf R, Mongillo M, Rizzuto R, and Pozzan T (2003) Innovation: Looking forward to seeing calcium. *Nature Rev Mol Cell Biol* **4:** 579-586.

Salter MW and Henry J L (1985) Effects of adenosine 5′-monophosphate and adenosine 5′-triphosphate on functionally identified units in the cat spinal dorsal horn. Evidence for a differential effect of adenosine 5′ triphosphate on nociceptive vs non-nociceptive units. *Neurosci* **15:** 815-825.

Sandros MG, Sarraf C B, and Tabrizian T (2008) Prodrugs in cardiovascular therapy. *Molecules* **13:** 1156-1178.

Sasaki Y, Hoshi M, Akazawa C, Nakamura Y, Tsuzuki H, Inoue K, and Kohsaka S (2003) Selective expression of $G_{i/o}$-coupled ATP receptor $P2Y_{12}$ in microglia in rat. Brain. *GLIA* **44:** 242–250.

Schäfer R, Sedehizade F, Welte T, and Reiser G (2003) ATP- and UTP-activated P2Y receptors differently regulate proliferation of human lung epithelial tumor cells. *Am J Physiol Lung Cell Mol Physio* **285:** L376–L385.

Schnurr M, Then F, Galambos P, Scholz P, Siegmund B, Endres S, and Eigler A (2000) Extracellular ATP and TNF-α synergize in the activation and maturation of human dendritic cells. *J Immunol* **165:** 4704-4709.

Schnurr M, Toy T, Stoitzner P, Cameron P, Shin A, Beecroft T, Davis I D, Cebon J and Maraskovsky E (2003) ATP gradients inhibit the migratory capacity of specific human dendritic cell types: implications for $P2Y_{11}$ receptor signaling. *Blood* **102:** 613-620.

Schoeneberg T, Hermsdorf T, Engemaier E, Engel K, Liebscher I, Thor D, Zierau K, Roempler H, and Schulz A (2007) Structural and functional evolution of the $P2Y_{12}$-like receptor group. *Purinergic Signal* **3:** 255-268.

Steinhilber D, Schubert-Zsilavecz M, and Roth J H (2005) Medizinische chemie: Targets und Arzneistoffe, *Deutscher Apotheker Verlag Stuttgart.*

Swennen ELR, Bast A, and Dagnelie PC (2006) Purinergic receptors involved in the immunomodulatory effects of ATP in human blood. *Biochemical and biophysical research communications* **348:** 1194–1199.

Takahashi T, Camacho P, Lechleiter J D, and Herman B (1999) Measurement of intracellular calcium. *Physiol Rev* **79:**1089-1125.

Takasaki J, Kamohara M, Saito T, Matsumoto M, Matsjumoto S, Ohishi T, Soga T, Matsushime H, and Furuichi K (2001) Molecular cloning of the platelet P2TAC ADP receptor: pharmacological comparison with another ADP receptor, the $P2Y_1$ receptor. *Mol Pharmacol* **60:** 432–439.

Tuluc F, Bültmann R, Glaenzel M, Frahm A W, and Starke K (1998) P2-receptor antagonists: IV. Blockade of P2-receptor subtypes and ecto-nucleotidases by compounds related to reactive blue 2. *Naunyn-Schmiedeberg's Arch Pharmaco*l **357:**111–120.

Ullmann H (2001) NF449, ein $G_{s\alpha}$-selektiver G protein Antagonist. Synthesis von NF449 and analogueen. Diploma-Thesis Universität Bonn.

Ullmann H, Meis S, Hongwiset D, Marzian C, Wiese M, Nickel P, Communi D, Boeynaems J M, Wolf C, Hausmann R, Schmalzing G, and Kassack M U (2005) Synthesis and structure-activity relationship of suramin-derived $P2Y_{11}$ receptors antagonist with nanomolar potency. *J Med Chem* **48:** 7040-7048.

Wilkin F, Duhant X, Bruyns C, Suarez-Huerta N, Boeynaems J M, and Robaye B (2001) The $P2Y_{11}$ receptor mediates the ATP-induced maturation of human monocyte-derived dendritic cells. *J Immunol* **166:** 7172-7177.

Zambon AC, Brunton L L, Barrett K A, Hughes R J, Torres R, and Insel P A (2001) Cloning, expression, signaling mechanisms and membrane targeting of $P2Y_{11}$ receptors in madin darby canine kidney cells. *Mol Pharmacol* **60:** 26-35.

Zhang FL, Luo L, C Gustafson, Palmer K, Qiao X, Fan X, Yang S, Laz T M, Bayne M, and Monsma Jr F (2002) $P2Y_{13}$: Identification and characterization of a novel $G_{\alpha i}$-coupled ADP receptor from human and mouse. *J Pharm and Exp Ther* **301:** 705–713.

Zylberg J, Ecke D, Fischer B, and Reiser G (2007) Structure and ligand binding site characteristics of the human $P2Y_{11}$ nucleotide receptor deduced from computational modelling and mutational analysis. *Biochem J* **405:** 277-286.

11. Abbreviations

ADP	Adenosin 5′-diphosphat
AMP	Adenosine 5′-monophosphat
A3P5PS	Adenosine-3′-phosphat-5′-phosphosulphate
A3P5P	Adenosine-3′-phosphat-5′-phosphate
ATP	Adenosin 5′-triphosphate
ATPγS	Adenosin 5′-[γ-thio]triphosphate
BAPTA	1,2-Bis-(2aminophenoxy)ethan-N,N,N',N'-tetraacetic acid
cAMP	cyclic Adenosine 5′-monophosphat
D	Doublet
DAG	Diacylglicerol
DMEM	Dulbecco's Modified Eagle's Medium
DMSO	Dimethylsulfoxide
DMF	N, N' dimethylformamide
EC_{50}	Effective concentration 50 %
EDTA	Ethylendiamintetraaceticacid
ESI	Electron spray ionization
et al.	et alii
g	Gram
G418	Geneticindisulphate
GPCRs	G Protein-Coupled Receptors
GRP	General reaction procedure
GTP	Guanosin 5′-triphosphat
HEK	Human embrio kidney
HEPES	N-(2-Hydroxyethyl)piperazine-N'-(2-ethanesulfonicacid)
HPLC	High performance liquid chromatography
Hz	Herz
IC_{50}	Inhibition concentration 50 %
IP_3	Inositol triphosphate
IR	Infra red
J	Coupling constant
K_i	Constant of inhibition
KHP	Krebs HEPES puffer
mAu	Milli absorption unit
2-MeSADP	2-(Methylthio) adenosin 5′-diphosphat
2-MeATP	2-(Methylthio) adenosin 5′-triphosphat
m	multiplet
M	Molar
µM	Mikromolar
MRS2179	2′-Deoxy-N^6-methyl adenosine-3′-5′-diphosphate
MRS2279	2′-Chloro-N^6-methyl-(N)-methanocarba-2′-deoxyadenosine-3′-5′-biphosphate
m/z	Mass per charge
MeOH	Methanol
Min	Minute
ml	mililiter

MP	Mobile phase
MS	Mass spectrometry
n.d.	not determined
nM	nanoMolar
nm	nanometer
NMR	Nuclear magnetic resonance
OG	Oregon green®
p	Pseudo
p.a	pro analyse
ppm	part per million
Prep.grade	Preparation grade
Rf	Retention factor
RP	Reversed phase
RPM	Round per minute
Rt	Retention time
RT	Room temperature
s	singlet
SD	Standard deviation
t	triplet
TLC	Thin layer chromatography
UDP	Uridindiphosphate
UTP	Uridintriphosphate
UV	Ultraviolet

12. Appendix

Appendix A1 Agonist activities of the synthesized nitro (xa)-, amino (xb)-, and urea (xc) derivatives at concentrations of 10 µM and 100 µM are shown as percent response of 31.6 nM 2-MeSADP at $P2Y_1$ receptors. Data shown are mean ± SEM of the pooled data ($n \geq 2$, each experiment was performed with three replicates).

Comp.	10 µM	100 µM	Comp.	10 µM	100 µM
1c	6.2 ± 13.6	11.2 ± 22.2	14a	0 ± 23.0	7.0 ± 17.0
2a	0 ± 12.1	0 ± 10.0	14b	14.3 ± 17.0	15.6 ± 13.1
2b	3.1 ± 10.1	0 ± 7.1	14c	0 ± 7.4	21.7 ± 10.4
2c	0 ± 7.3	0 ± 5.4	15a	0 ± 7.4	50.3 ± 6.2
3a	0 ± 13.9	0 ± 5.2	15b	0 ± 5.4	0 ± 14.6
3b	0 ± 6.9	0 ± 3.3	15c	2.4 ± 4.5	0 ± 23.1
3c	1.9 ± 8.7	13.9 ± 28.3	16a	33.7 ± 9.0	25.4 ± 1.4
4a	0 ± 9.8	0 ± 5.0	16b	0 ± 7.6	0 ± 5.5
4b	0 ± 17.3	3.2 ± 9.7	16c	0 ± 9.5	19.3 ± 6.6
4c	0 ± 8.5	0 ± 5.0	17a	0 ± 15.7	0 ± 8.4
5a	9.4 ± 16.4	0 ± 9.6	17b	0 ± 11.8	0 ± 7.0
5b	0 ± 15.5	0 ± 12.9	17c	0 ± 9.3	0 ± 9.8
5c	1.8 ± 18.7	0 ± 29.5	18a	0 ± 3.6	31.1 ± 5.6
6a	0 ± 5.7	4.5 ± 8.9	18b	0 ± 7.6	0 ± 6.1
6b	5.4 ± 1.9	0 ± 8.5	18c	0 ± 12.5	16.2 ± 9.1
6c	5.6 ± 3.7	31.1 ± 9.5	19a	0 ± 6.1	0 ± 31.5
7a	11.9 ± 11.3	0 ± 22.2	19b	0 ± 11.8	0 ± 3.6
7b	12.3 ± 1.5	21.2 ± 2.03	19c	0 ± 11.7	0 ± 21.2
7c	21.2 ± 7.5	37.3 ± 4.0	20a	0 ± 6.66	0 ± 8.7
8a	0 ± 8.6	0 ± 13.7	20b	32.4 ± 10.0	31.1 ± 9.1
8b	0 ± 4.3	0 ± 15.1	20c	0 ± 4.7	0 ± 31.4
8c	0 ± 7.4	0 ± 3.6	21a	0 ± 9.1	0 ± 3.1
9a	0 ± 9.0	0 ± 5.3	21b	0 ± 12.6	49.4 ± 8.5
9b	0 ± 4.3	0 ± 6.1	21c	24.5 ± 4.5	7.4 ± 22.6
9c	0 ± 3.7	0 ± 11.0	22a	0 ± 3.1	0 ± 3.1
10a	0 ± 4.6	0 ± 16.1	22b	13.2 ± 4.4	24.0 ± 11.1
10b	0 ± 8.0	0 ± 8.0	22c	0 ± 24.0	9.3 ± 16.4
10c	0 ± 7.0	0 ± 8.7	23a	4.0 ± 8.8	27.7 ± 13.4
11a	0 ± 8.7	0 ± 18.1	23b	3.1 ± 1.0	70.1 ± 8.0
11b	0 ± 6.5	0 ± 14.8	23c	4.4 ± 10.4	80.8 ± 14.3
11c	0 ± 7.1	0 ± 9.1	24a	30.9 ± 20.3	17.5 ± 3.2
12a	0 ± 10.5	0 ± 2.2	24b	31.7 ± 8.0	35.1 ± 18.9
12b	0 ± 2.8	0 ± 9.3	24c	0 ± 15.8	19.7 ± 7.7
12c	0 ± 6.8	0 ± 9.5	25a	23.3 ± 21.7	35.5 ± 19.9
13a	3.9 ± 10.1	0 ± 5.7	25b	10.5 ± 13.6	10.8 ± 19.5
13b	0 ± 8.6	0 ± 4.4	25c	0 ± 1.6	9 ± 32.3
13c	0 ± 8.7	0 ± 2.8			

Appendix A2 Percent inhibition of the 2-MeSADP induced calcium signal by compounds in concentrations of 10 µM and 100 µM at $P2Y_1$ receptors. 31.6 nM 2-MeSADP was used as standard agonist. Data shown are mean ± SEM of the pooled data ($n \geq 2$, each experiment was performed with three replicates).

Comp.	10 µM	100 µM	Comp.	10 µM	100 µM
1c	0 ± 15.0	0 ± 8.2	14a	27.0 ± 10.1	29.2 ± 13.9
2a	3.8 ± 12.9	25.9 ± 7.7	14b	26.0 ± 11.6	5.6 ± 6.7
2b	12.9 ± 11.2	20.1 ± 4.9	14c	28.1 ± 14.9	0 ± 8.3
2c	0 ± 10.2	0 ± 18.5	15a	0 ± 8.0	0 ± 4.0
3a	31.0 ± 8.1	15.2 ± 8.7	15b	0 ± 8.4	0 ± 19.0
3b	10.4 ± 17.3	17.1 ± 5.6	15c	0 ± 1.4	9.3 ± 16.2
3c	0 ± 14.1	0 ± 19.1	16a	0 ± 27.1	0 ± 1.5
4a	15.0 ± 5.1	5.6 ± 8.8	16b	8.8 ± 10.7	0 ± 9.5
4b	10.7 ± 17.4	0 ± 9.0	16c	12.4 ± 16.1	0.3 ± 13.3
4c	0 ± 14.3	0 ± 10.1	17a	0 ± 4.5	0 ± 15.1
5a	13.3 ± 5.5	24.9 ± 5.5	17b	0 ± 13.5	0 ± 14.1
5b	3.1 ± 5.9	25.0 ±11.0	17c	0 ± 1.4	0 ± 16.2
5c	0 ± 20.1	0 ± 13.8	18a	14.8 ± 10.8	0 ± 13.4
6a	18.0 ± 14.8	18 ± 11.7	18b	0 ± 17.5	3.5 ± 2.9
6b	8.9 ± 4.2	24.6 ± 16.6	18c	0 ± 5.8	0 ± 9.5
6c	1.3 ± 8.6	0 ± 10.2	19a	0 ± 9.5	0 ± 7.3
7a	5.2 ± 3.3	24.3 ± 17.1	19b	0 ± 5.5	0 ± 4.1
7b	0 ± 5.1	8.2 ± 8.6	19c	0 ± 17.8	4.0 ± 7.3
7c	0 ± 8.21	0 ± 7.2	20a	0 ± 11.2	0 ± 8.0
8a	20.7 ± 5.7	29.4 ± 4.1	20b	8.9 ± 2.7	0 ± 14.3
8b	13.6 ± 6.3	6.6 ± 13.7	20c	0 ± 19.5	0 ± 5.9
8c	0 ± 12.5	0 ± 12.7	21a	0 ± 19.0	0.1 ± 8.4
9a	13.5 ± 2.7	4.8 ± 3.8	21b	0 ± 14.8	19.8 ± 6.0
9b	16.0 ± 3.0	0 ± 5.1	21c	6.8 ± 18.0	11.7 ± 11.4
9c	0 ± 22.1	0 ± 23.7	22a	1.6 ± 6.8	0 ± 5.8
10a	6.2 ± 5.3	3.5 ± 2.7	22b	17.6 ± 8.3	19.2 ± 14.0
10b	0 ± 8.4	0 ± 3.1	22c	6.4 ± 4.5	0 ± 9.4
10c	0 ± 16.0	0 ± 0.6	23a	7.8 ± 11.6	0 ± 6.9
11a	0 ± 5.0	0 ± 8.3	23b	17.2 ± 13.0	0 ± 14.2
11b	0 ± 4.2	0 ± 9.9	23c	29.4 ± 9.3	14.5 ± 17.4
11c	0 ± 17.2	0 ± 11.4	24a	14.6 ± 7.6	5.1 ± 2.3
12a	0 ± 16.4	11.9 ± 11.9	24b	11.0 ± 12.3	34.0 ± 10.0
12b	36.1 ± 11.2	28.4 ± 21.5	24c	0 ± 3.0	0 ± 13.7
12c	0 ± 3.5	0 ± 3.5	25a	14.0 ± 15.2	5.1 ± 18.6
13a	28.8 ± 6.7	16.3 ± 13.2	25b	13.5 ± 13.9	25.2 ± 11.9
13b	10.3 ± 16.0	9.1 ± 19.2	25c	7.8 ± 4.7	10.6 ± 8.2
13c	8.1 ± 8.4	26.7 ± 2.0			

Appendix A3 Agonist activities of the synthesized nitro (xa)-, amino (xb)-, and urea (xc) derivatives at concentrations of 10 μM and 100 μM are shown as percent response of 1 μM UTP at $P2Y_2$ receptors. Data shown are mean ± SEM of the pooled data ($n \geq 2$, each experiment was performed with three replicates).

Comp.	10 μM	100 μM	Comp.	10 μM	100 μM
1c	15.6 ± 7.7	8.7 ± 3.3	14a	0 ± 4.0	2.4 ± 1.9
2a	14.1 ± 4.2	14.6 ± 4.6	14b	23.0 ± 9.4	17.5 ± 8.8
2b	18.0 ± 5.2	13.4 ± 6.1	14c	20.9 ± 1.6	26.3 ± 5.4
2c	0 ± 3.4	0 ± 2.6	15a	9.2 ± 9.5	6.9 ± 6.7
3a	14.3 ± 0.4	21.1 ± 3.2	15b	13.0 ± 4.8	0 ± 0.8
3b	21.6 ± 5.3	22.9 ± 1.0	15c	0 ± 1.7	0 ± 0.9
3c	0 ± 2.2	0 ± 7.6	16a	1.0 ± 5.1	10.7 ± 7.0
4a	28.0 ± 8.2	26.5 ± 3.9	16b	16.1 ± 4.6	30.3 ± 5.5
4b	13.9 ± 4.6	29.1 ± 7.2	16c	0 ± 6.7	5.7 ± 5.2
4c	0 ± 1.8	0 ± 2.1	17a	11.1 ± 5.1	6.0 ± 3.4
5a	19.7 ± 0.7	15.6 ± 6.0	17b	0 ± 3.4	2.5 ± 6.8
5b	19.8 ± 8.3	23.7 ± 4.0	17c	9.8 ± 9.9	4.0 ± 3.7
5c	0 ± 6.8	1.9 ± 9.8	18a	9.0 ± 3.3	22.2 ± 6.6
6a	21.9 ± 4.0	27.7 ± 6.8	18b	7.9 ± 7.0	15.5 ± 8.2
6b	26.4 ± 7.9	28.5 ± 5.4	18c	19.5 ± 1.2	24.8 ± 1.6
6c	23.7 ± 3.5	0 ± 9.0	19a	0.5 ± 0.8	0 ± 4.9
7a	0 ± 2.5	4.6 ± 7.0	19b	0 ± 10.6	25.3 ± 9.4
7b	11.4 ± 5.7	0 ± 0.9	19c	10.9 ± 1.3	0 ± 0.6
7c	23.3 ± 11.5	15.8 ± 5.7	20a	14.5 ± 6.7	19.5 ± 7.7
8a	0 ± 0.8	0 ± 1.7	20b	17.4 ± 3.7	6.1 ± 14.3
8b	24.4 ± 0.8	28.9 ± 3.7	20c	2.8 ± 5.5	7.7 ± 7.8
8c	1.6 ± 4.9	2.1 ± 3.8	21a	19.3 ± 6.2	16.3 ± 2.1
9a	0 ± 5.0	9.0 ± 3.1	21b	0 ± 5.8	0 ± 6.9
9b	8.4 ± 8.2	12.0 ± 5.9	21c	4.3 ± 4.0	1.5 ± 6.4
9c	0 ± 2.9	0 ± 6.8	22a	28.8 ± 5.6	0 ± 7.1
10a	5.7 ± 3.2	8.4 ± 4.5	22b	10.3 ± 4.7	14.5 ± 3.5
10b	6.8 ± 3.1	5.5 ± 3.4	22c	0 ± 3.6	2.0 ± 1.3
10c	0 ± 5.5	0 ± 3.0	23a	0 ± 6.6	8.9 ± 0.6
11a	7.0 ± 2.7	1.5 ± 0.8	23b	8.8 ± 1.2	29.3 ± 0.4
11b	0 ± 1.2	2.1 ± 2.0	23c	0 ± 1.8	9.5 ± 8.2
11c	15.3 ± 4.9	9.4 ± 12.3	24a	26.6 ± 6.4	0 ± 5.4
12a	10.9 ± 2.3	12.0 ± 1.0	24b	26.1 ± 7.6	25.1 ± 4.8
12b	3.5 ± 1.2	7.7 ± 4.5	24c	0 ± 4.5	0 ± 3.6
12c	2.8 ± 9.2	4.9 ± 5.5	25a	1.2 ± 0.3	1.6 ± 5.8
13a	1.2 ± 1.3	7.3 ± 3.8	25b	2.4 ± 1.5	6.5 ± 2.7
13b	1.5 ± 0.8	0 ± 3.5	25c	5.5 ±10.0	0 ± 3.2
13c	0 ± 5.6	0 ± 5.5			

Appendix A4 Percent inhibition of the UTP-induced calcium signal by compounds in concentrations of 10 µM and 100 µM at $P2Y_2$ receptors. 1 µM UTP was used as standard agonist. Data shown are mean ± SEM of the pooled data ($n \geq 2$, each experiment was performed with three replicates).

Comp.	10 µM	100 µM	Comp.	10 µM	100 µM
1c	12.9 ± 1.8	21.9 ± 12.5	14a	0 ± 3.1	10.9 ± 12.1
2a	0 ± 8.1	0 ± 6.2	14b	27.1 ± 6.9	28.1 ± 4.1
2b	33.5 ± 2.1	0 ± 3.8	14c	14.7 ± 5.8	11.8 ± 1.2
2c	18.4 ± 12.0	15.7 ± 12.6	15a	6.4 ± 4.9	0 ± 13.2
3a	13.3 ± 4.7	23.6 ± 3.0	15b	9.2 ± 16.4	4.3 ± 6.6
3b	18.8 ± 2.9	32.1 ± 4.8	15c	10.9 ± 8.2	18.9 ± 3.9
3c	20.6 ± 6.5	35.1 ± 2.8	16a	0 ± 4.7	18.6 ± 9.3
4a	21.1 ± 10.4	17.7 ± 4.6	16b	15.5 ± 6.4	33.9 ± 3.4
4b	0 ± 3.8	8.3 ± 12.8	16c	0 ± 8.5	30.7 ± 3.9
4c	30.4 ± 14.5	31.3 ± 4.0	17a	0.5 ± 16.1	4.6 ± 11.3
5a	0 ± 13.4	4.7 ± 14.2	17b	3.0 ± 5.2	0 ± 19.2
5b	21.2 ± 11.5	20.2 ± 2.2	17c	0 ± 8.5	11.7 ± 13.4
5c	0.8 ± 1.1	21.9 ± 1.5	18a	0.7 ± 11.2	13.2 ± 12.2
6a	19.4 ± 1.3	22.3 ± 8.9	18b	0 ± 2.3	23.8 ± 11.9
6b	1.1 ± 9.7	5.0 ± 11.4	18c	1.8 ± 1.2	18.0 ± 4.8
6c	18.7 ± 9.8	27.5 ± 9.9	19a	0 ± 9.3	3.9 ± 1.8
7a	10.2 ± 1.5	11.5 ± 3.2	19b	23.5 ± 5.2	22.5 ± 3.0
7b	12.8 ± 16.9	13.7 ± 7.2	19c	9.8 ± 5.5	19.8 ± 4.8
7c	0 ± 7.2	26.6 ± 3.5	20a	9.5 ± 7.1	6.2 ± 1.1
8a	19.0 ± 3.0	27.7 ± 4.5	20b	2.3 ± 3.0	12.9 ± 5.7
8b	13.7 ± 3.6	26.5 ± 5.2	20c	24.4 ± 2.3	26.0 ± 2.9
8c	25.2 ± 10.4	18.2 ± 6.4	21a	6.3 ± 8.2	12.9 ± 7.8
9a	0 ± 14.0	0 ± 5.1	21b	0 ± 5.1	10.9 ± 4.0
9b	0 ± 7.1	0 ± 19.1	21c	24.0 ± 11.7	20.7 ± 4.2
9c	24.4 ± 6.1	29.5 ± 2.6	22a	3.9 ± 0.9	17.5 ± 8.4
10a	16.3 ± 3.0	0 ± 5.0	22b	18.6 ± 7.8	21.0 ± 9.0
10b	0 ± 4.7	0 ± 10.5	22c	24.8 ± 2.5	26.6 ± 3.1
10c	26.2 ± 4.5	29.5 ± 2.6	23a	15.9 ± 4.1	21.9 ± 3.1
11a	0 ± 7.1	14.6 ± 2.9	23b	9.0 ± 2.4	17.5 ±3.8
11b	0 ± 9.1	0 ± 4.2	23c	13.2 ± 3.5	22.6 ± 3.6
11c	0 ± 3.1	10.9 ± 12.1	24a	0 ± 11.2	20.5 ± 2.3
12a	0 ± 3.1	0 ± 4.8	24b	0 ± 9.0	5.5 ± 8.8
12b	0 ± 7.9	0 ± 5.0	24c	0 ± 6.0	8.8 ± 7.1
12c	5.8 ± 5.3	19.5 ± 9.0	25a	0 ± 2.9	4.9 ± 7.0
13a	0 ± 15.0	0 ± 6.7	25b	23.0 ± 7.3	29.7 ± 8.4
13b	0 ± 10.3	0 ± 11.0	25c	26.2 ± 4.0	35.4 ± 1.2
13c	0 ± 4.0	15.1 ± 5.2			

Appendix A5 Agonist activities of the synthesized nitro (xa)-, amino (xb)-, and urea (xc) derivatives at concentrations of 10 μM and 100 μM are shown as percent response of 1 μM UTP at $P2Y_4$ receptors. Data shown are mean ± SEM of the pooled data ($n \geq 2$, each experiment was performed with three replicates).

Comp.	10 μM	100 μM	Comp.	10 μM	100 μM
1c	0 ± 10.8	2.0 ± 6.9	14a	7.9 ± 1.6	5.4 ± 8.0
2a	6.8 ± 5.3	12.5 ± 7.3	14b	0.5 ± 2.1	2.7 ± 5.0
2b	0 ± 2.6	4.4 ± 3.5	14c	19.2 ± 6.4	2.4 ± 5.9
2c	0 ± 5.5	0 ± 4.0	15a	1.6 ± 2.1	3.3 ± 3.5
3a	11.3 ± 1.4	4.8 ± 7.7	15b	3.4 ± 2.1	4.4 ± 2.4
3b	4.2 ± 4.1	1.0 ± 1.9	15c	0 ± 13.4	10.5 ± 11.8
3c	0 ± 3.0	0 ± 0.4	16a	4.7 ± 3.0	3.9 ± 3.1
4a	0 ± 8.3	0 ± 7.3	16b	0 ± 3.6	0.7 ± 2.4
4b	7.3 ± 3.8	4.1 ± 9.8	16c	0 ± 9.8	0 ± 2.0
4c	0 ± 14.2	0 ± 8.0	17a	0 ± 12.4	4.5 ± 2.8
5a	12.1 ± 2.9	15.4 ± 3.8	17b	7.0 ± 3.4	19.4 ± 3.6
5b	0 ±10.2	0 ± 4.3	17c	18.7 ± 10.6	12.4 ± 1.6
5c	0 ± 3.5	0 ± 7.9	18a	14.2 ± 3.5	4.6 ± 1.4
6a	6.5 ± 12.6	0 ± 7.1	18b	3.9 ± 5.2	8.1 ± 4.0
6b	6.6 ± 2.4	4.6 ± 7.9	18c	7.7 ± 9.3	21.3 ± 13.0
6c	0 ± 2.1	0 ± 7.5	19a	4.2 ± 1.8	0 ± 3.3
7a	8.2 ±1.5	0 ± 3.5	19b	0 ± 4.6	0 ± 4.9
7b	0 ± 3.4	1.4 ± 4.5	19c	8.1 ± 7.4	4.1 ± 5.6
7c	0 ± 9.8	0 ± 2.0	20a	0 ± 5.6	5.9 ± 1.9
8a	0 ± 4.4	0.1 ± 4.4	20b	10.7 ± 1.6	9.4 ± 5.9
8b	0.7 ± 2.7	2.0 ± 2.4	20c	0 ± 7.5	0 ± 8.2
8c	0 ± 8. 6	16.1 ± 5.0	21a	0 ± 2.1	0.9 ± 5.1
9a	0 ± 15.4	1.5 ± 4.2	21b	9.7 ± 1.9	15.9 ± 4.7
9b	2.7 ± 0.5	20.5 ± 5.7	21c	0 ± 13.3	8.0 ± 8.2
9c	5.1 ± 2.3	4.7 ± 4.3	22a	6.5 ± 4.8	6.7 ± 2.1
10a	7.2 ± 5.7	0 ± 2.3	22b	0 ± 3.5	0 ± 2.8
10b	11.5 ± 7.6	4.7 ± 5.1	22c	0.2 ± 2.5	2.6 ± 1.2
10c	1.9 ± 3.5	2.4 ± 5.8	23a	11.2 ± 2.0	8.1 ± 4.1
11a	1.25 ± 7.3	0 ± 1.3	23b	4.7 ± 8.9	20.4 ± 1.9
11b	0 ± 1.7	18.4 ± 13.6	23c	5.8 ± 6.5	24.6 ± 6.4
11c	19.2 ± 6.3	2.4 ± 5.9	24a	13.4 ± 5.5	8.5 ± 3.4
12a	7.6 ± 5.4	7.4 ± 8.0	24b	7.8 ± 4.7	8.4 ± 1.2
12b	9.8 ± 5.9	11.0 ± 4.5	24c	2.6 ± 3.5	1.9 ± 5.6
12c	0 ± 4.1	7.6 ± 7.6	25a	1.4 ± 1.8	0.3 ± 1.8
13a	2.8 ± 1.5	8.7 ± 7.0	25b	9.5 ± 1.8	0 ± 1.2
13b	0 ± 2.4	0 ± 7.1	25c	10.8 ± 7.3	4.1 ± 11.0
13c	1.7 ± 9.4	0 ± 9.5			

Appendix A6 Percent inhibition of the UTP-induced calcium signal by compounds in concentrations of 10 µM and 100 µM at $P2Y_4$ receptors. 1 µM UTP was used as standard agonist. Data shown are mean ± SEM of the pooled data ($n \geq 2$, each experiment was performed with three replicates).

Comp.	10 µM	100 µM	Comp.	10 µM	100 µM
1c	15.7 ± 16.4	19.0 ± 14.0	14a	5.2 ± 3.4	5.2 ± 3.7
2a	10.3 ± 14.1	13.9 ± 15.6	14b	0 ± 2.8	8.4 ± 10.2
2b	0 ± 14.8	0 ± 14.8	14c	10.5 ± 4.1	0 ± 8.3
2c	10.0 ± 7.7	0 ± 16.0	15a	0 ± 8.5	0 ± 1.5
3a	19.4 ± 2.4	0 ± 12.3	15b	0 ± 6.0	0 ± 10.0
3b	0 ± 3.2	14.9 ± 4.1	15c	0 ± 4.2	14.7 ±10.9
3c	19.7 ± 8.1	0 ± 1.1	16a	0 ± 17.2	8.7 ± 11.6
4a	0 ± 9.6	2.2 ± 7.2	16b	2.5 ± 1.7	12.6 ± 17.2
4b	12.3 ± 10.1	10.9 ± 11.5	16c	0 ± 2.3	0 ±1.1
4c	0 ± 15.2	0 ± 18.6	17a	0 ± 1.2	0 ± 8.3
5a	0.7 ± 12.1	16.1 ± 15.7	17b	0 ± 5.5	0 ± 4.6
5b	0.0 ± 11.0	0 ± 3.6	17c	0 ± 4.8	5.1 ± 8.2
5c	17.6 ± 9.5	13.0 ± 4.3	18a	0 ± 7.2	6.6 ± 6.5
6a	17.9 ± 4.0	24.7 ± 10.0	18b	0 ± 7.6	0 ± 9.7
6b	0 ± 12.8	0 ± 6.9	18c	0 ± 1.3	0 ± 2.4
6c	0.4 ± 2.2	4.4 ± 1.9	19a	0 ± 4.4	0 ± 2.6
7a	2.5 ± 6.3	0 ± 16.0	19b	5.9 ± 10.4	1.0 ± 9.7
7b	9.2 ± 12.0	22.5 ±12.6	19c	0 ± 5.9	10.9 ± 0.5
7c	10.4 ± 3.6	0 ± 1.7	20a	5.5 ± 6.5	16.3 ± 11.6
8a	5.4 ± 10.6	5.9 ± 4.3	20b	0 ± 4.6	14.9 ± 13.4
8b	13.9 ± 13.5	20.9 ± 13.4	20c	17.5 ± 4.5	0 ± 3.8
8c	0 ± 4.0	7.32 ± 13.3	21a	20.4 ± 19.5	18.5 ± 9.4
9a	9.6 ± 4.6	16.2 ± 11.8	21b	0 ± 4.4	0 ± 4.8
9b	0 ± 8.3	0 ± 6.0	21c	0 ± 4.5	0 ± 3.8
9c	0 ± 4.0	5.2 ± 6.5	22a	0 ± 5.5	17.6 ± 6.9
10a	0 ± 6.3	0 ± 6.9	22b	0 ± 9.3	0 ± 10.6
10b	0 ± 10.0	0 ± 8.5	22c	1.8 ± 3.7	0 ± 2.8
10c	0 ± 13.9	0 ± 6.8	23a	0 ± 8.9	16.2 ± 16.5
11a	0 ± 5.3	0 ± 10.6	23b	0 ± 9.3	0 ± 10.6
11b	6.1 ± 19.1	0 ± 7.9	23c	8.8 ± 3.7	0 ± 2.8
11c	0 ± 1.3	3.6 ± 7.6	24a	0 ± 6.9	0 ± 5.5
12a	0 ± 4.0	0 ± 3.7	24b	4.2 ± 8.1	2.8 ± 12.2
12b	0 ± 1.6	0 ± 7.1	24c	13.8 ± 1.7	8.6 ± 8.4
12c	0 ± 6.8	0 ± 8.7	25a	0 ± 2.2	0 ± 1.8
13a	0 ± 7.6	0 ± 6.4	25b	4.5 ± 3.9	17.0 ± 8.1
13b	0 ± 8.7	0 ± 4.7	25c	8.5 ± 3.9	0 ± 6.1
13c	0 ± 1.0	22.2 ± 6.3			

Appendix B: Newly synthesized compounds with MK-and SD-number

1c (MK-220 /SD-144)

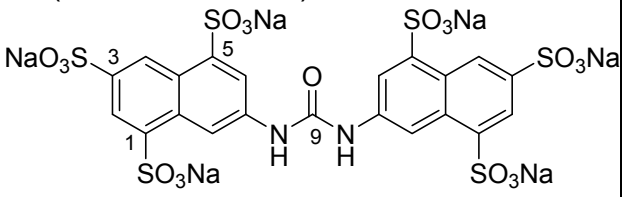

2a (MK-221/SD-126)

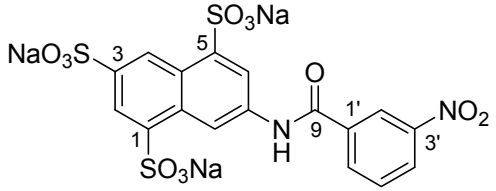

2b (MK-222/SD-128)

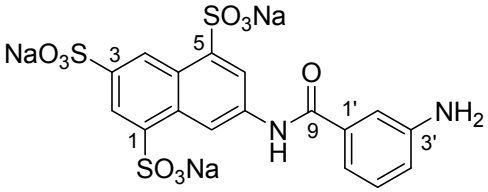

2c (MK-223/SD-133)

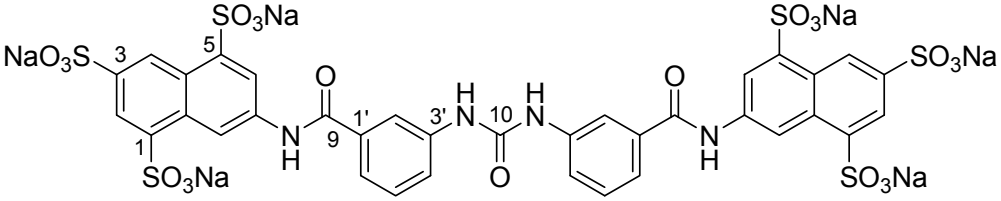

3a (MK-224/SD-141)

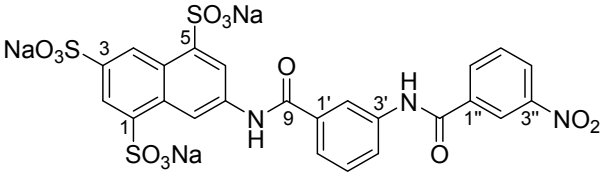

3b (MK-225/SD-148)

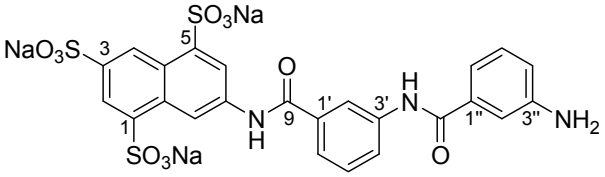

3c (MK-226/SD-149)

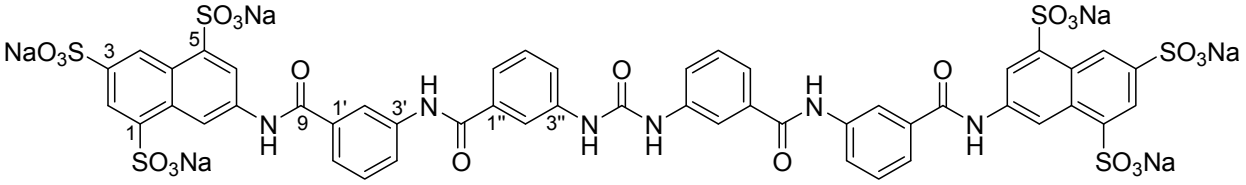

4a (MK-227/SD-142)

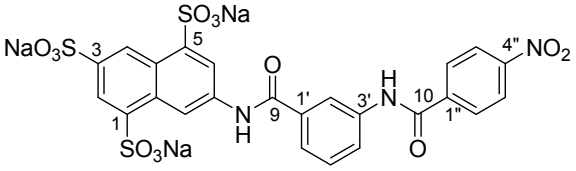

4b (MK-228/SD-147)

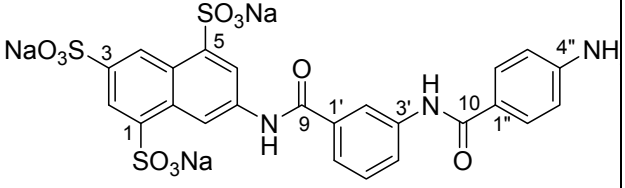

4c (MK-229/SD-152)

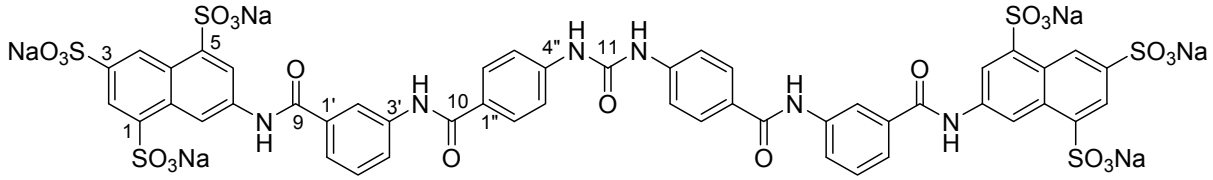

5a (MK-230/SD-127)

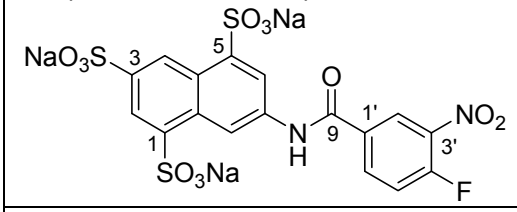

5b (MK-231/SD-131)

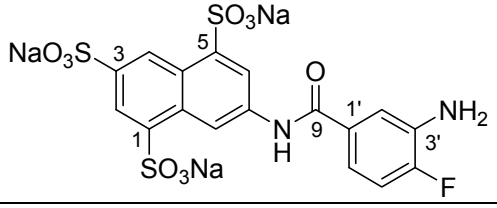

5c (MK-232/SD-134)

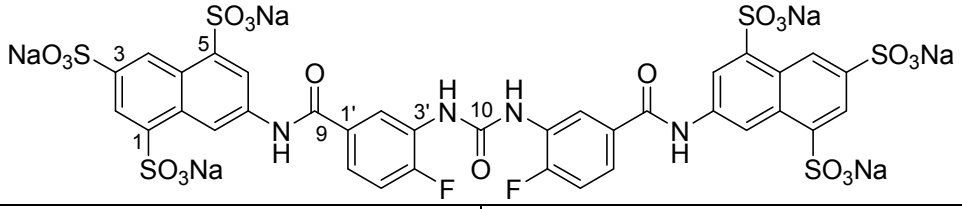

6a (MK-233/SD-139)

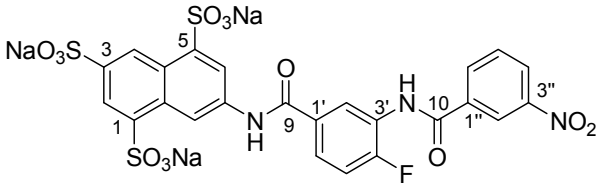

6b (MK-234/SD-143)

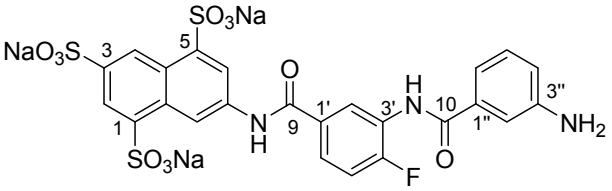

6c (MK-235/SD-146)

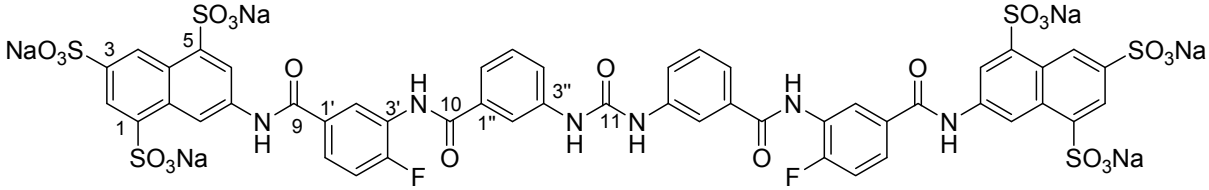

7a (MK-236/SD-275)

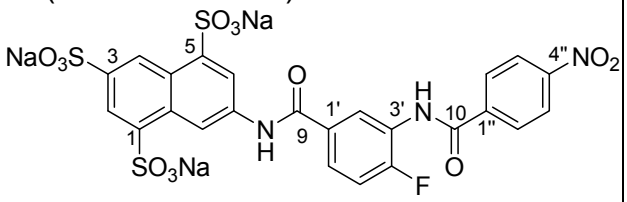

7b (MK-237/SD-280)

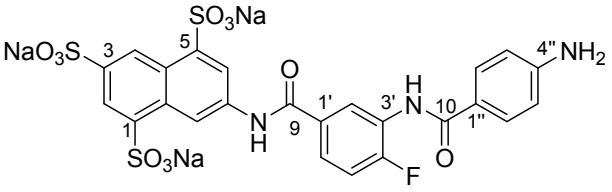

7c (MK-238/SD-291)

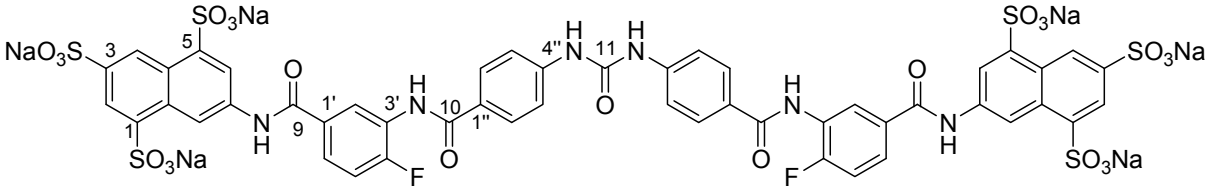

8a (MK-239/SD-201)

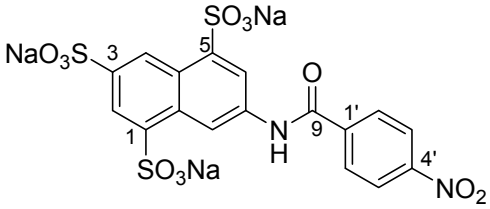

8b (MK-240/SD-204)

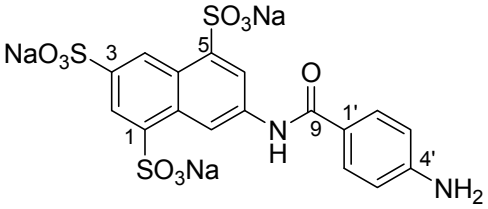

8c (MK-241/SD-242)

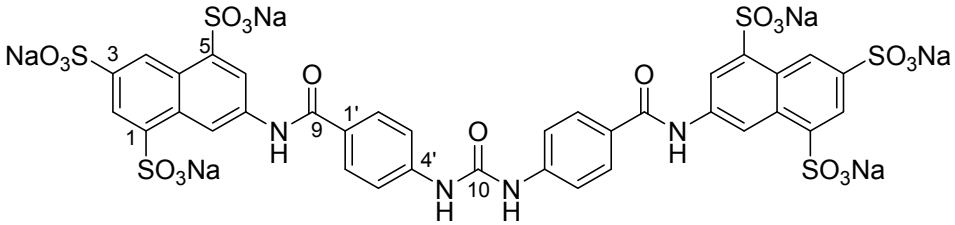

9a (MK-242/SD-206)

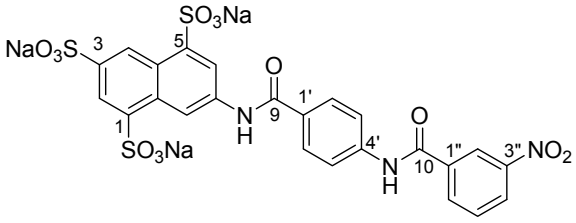

9b (MK-243/SD-209)

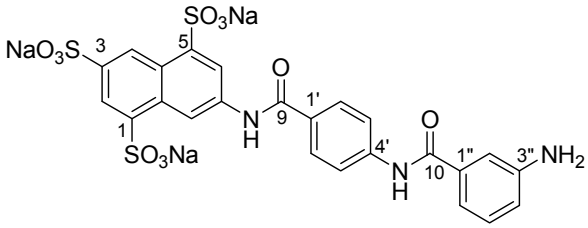

9c (MK-244/SD-211)

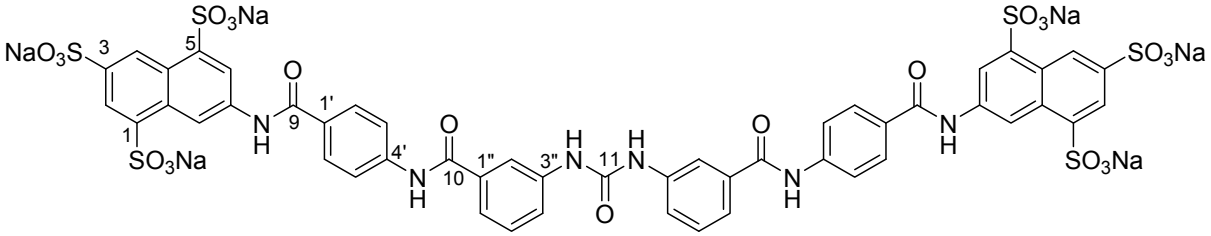

10a (MK-245/SD-207)

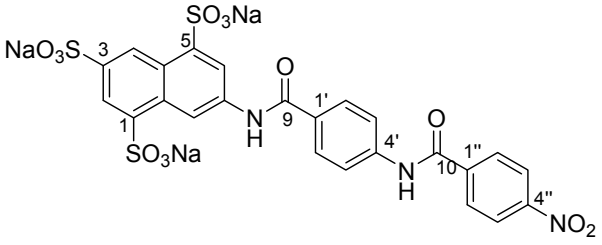

10b (MK-246/SD-213)

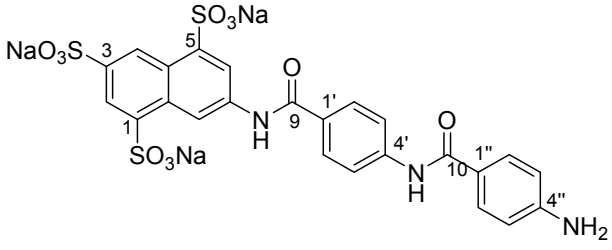

10c (MK-247/SD-214)

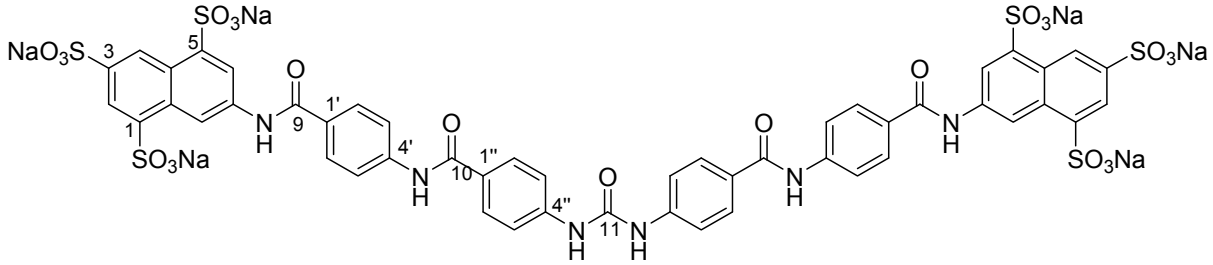

11a(MK-257/SD-240)

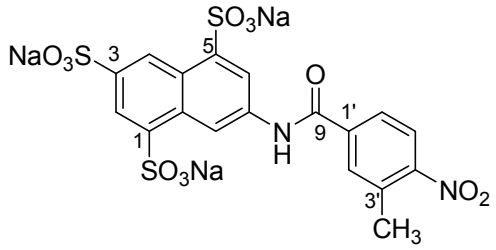

11b(MK-258/SD-245)

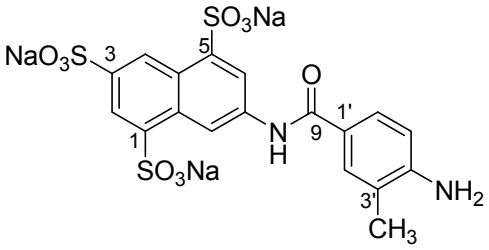

11c(MK-259/SD-246)

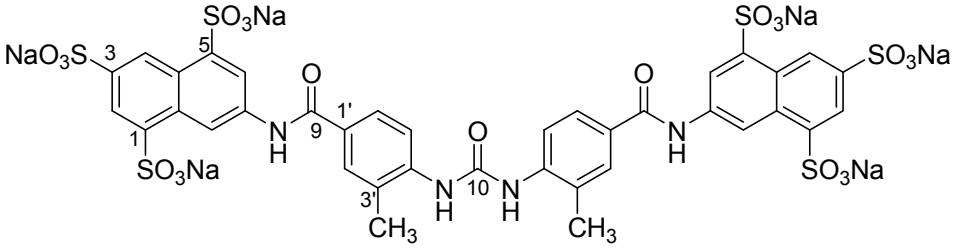

12a (MK-251/SD-218)

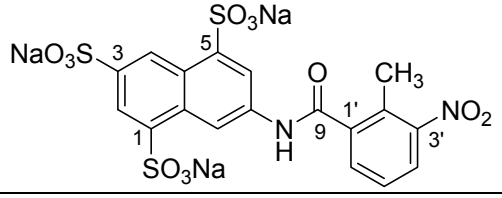

12b (MK-252/SD-228)

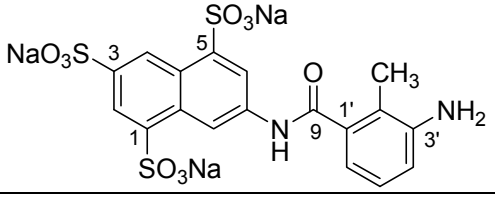

12C (MK-253/SD-230)

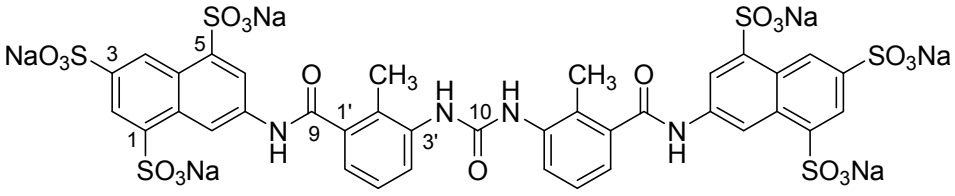

13a (MK-254/SD-235)

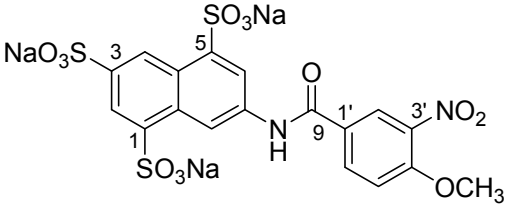

13b (MK-255/SD-236)

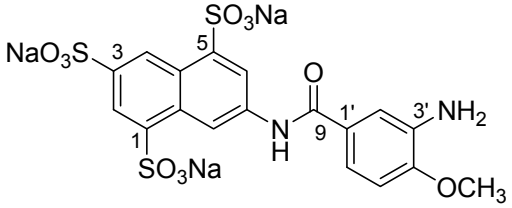

13c (MK-256/SD-237)

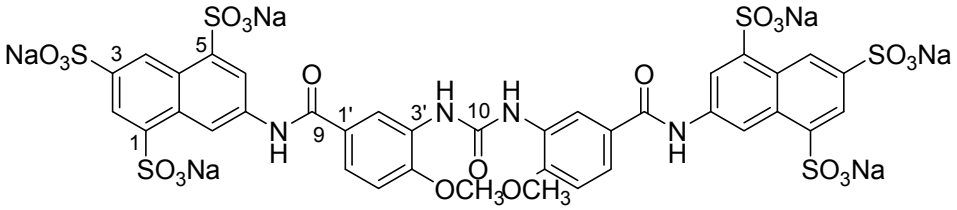

14a (MK-260/SD-263)

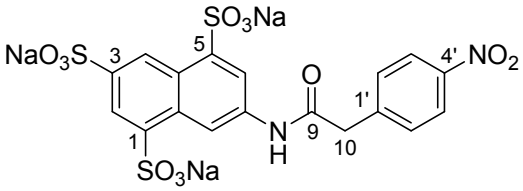

14b (MK-261/SD-303)

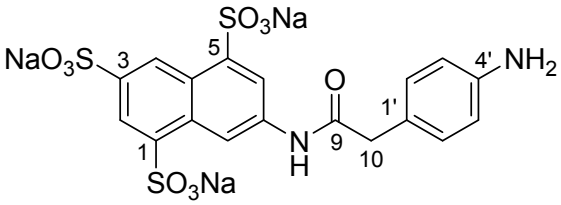

14c (MK-262/SD-314)

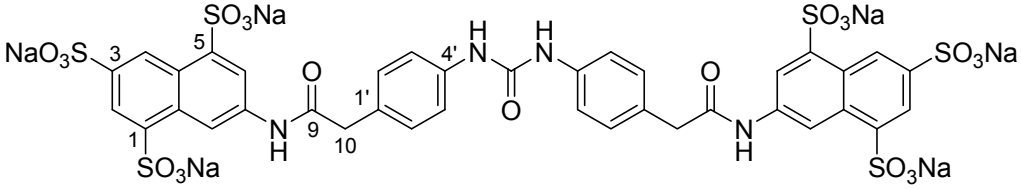

15a (MK-263/SD-257)

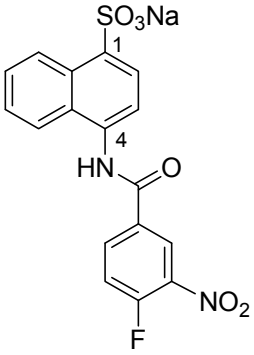

15b (MK-264/SD-261

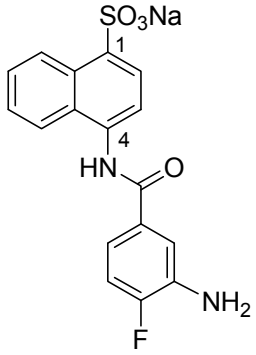

15c (MK-265/SD-269)

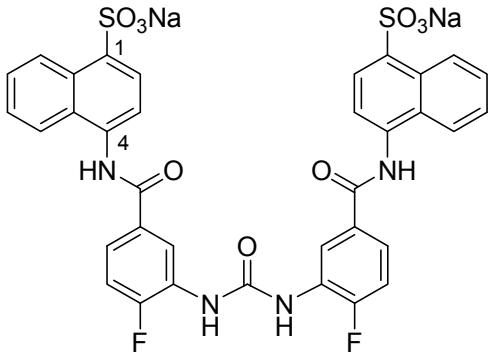

16a (MK-266/SD-278)

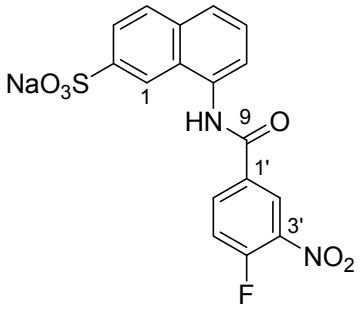

16b (MK-267/SD-292)

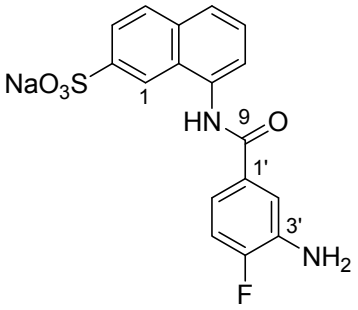

16c (MK-268/SD-299)

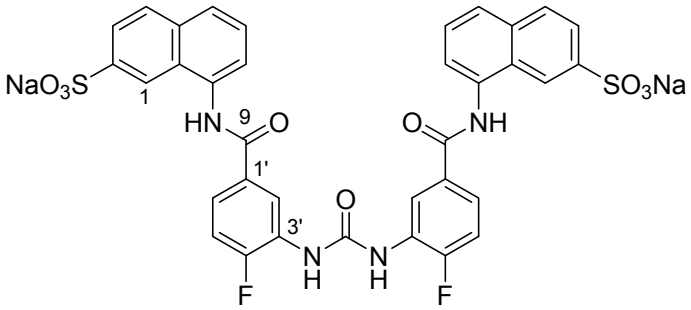

17a (MK-269/SD-253)

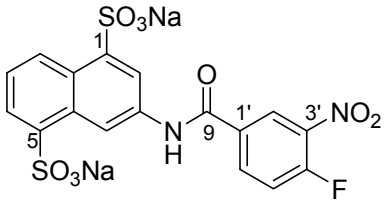

17b (MK-270/SD-256)

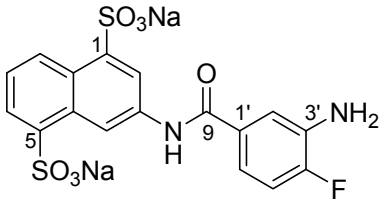

17c (MK-271/SD-258)

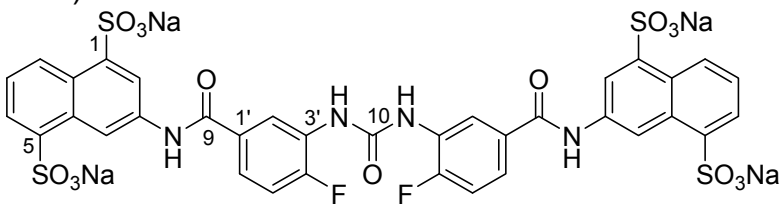

18a (MK-272/SD-265)

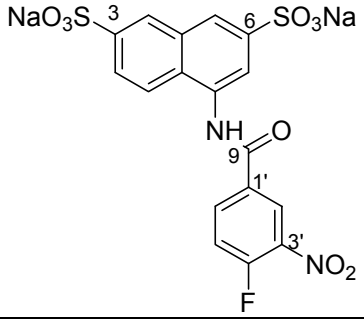

18b (MK-273/SD-268)

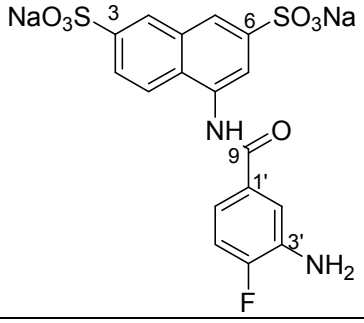

18c (MK-274/SD-272)

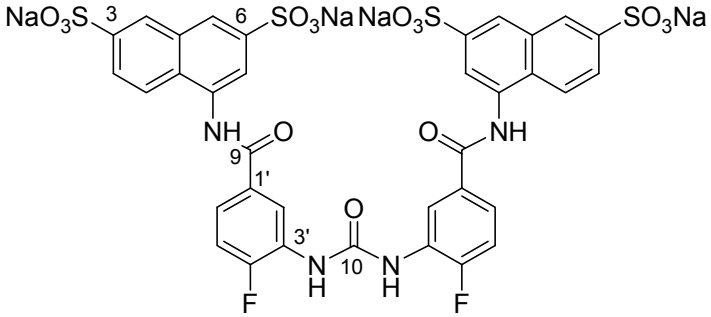

19a (MK-275/SD-271)

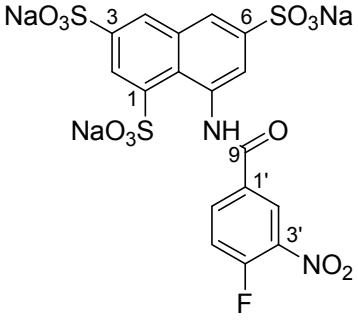

19b (MK-276/SD-282)

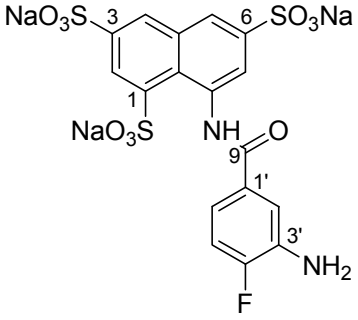

19c (MK-277/SD-290)

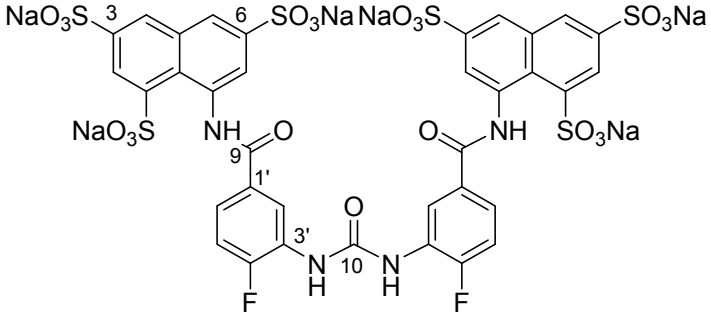

20a (MK-278/SD-297) 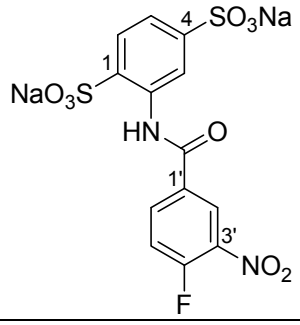	20b (MK-279/SD-306) 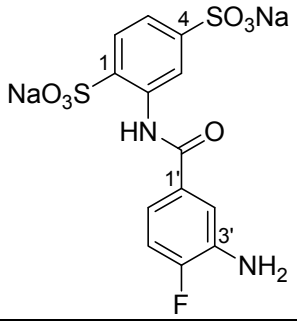
20c (MK-280/SD-310) 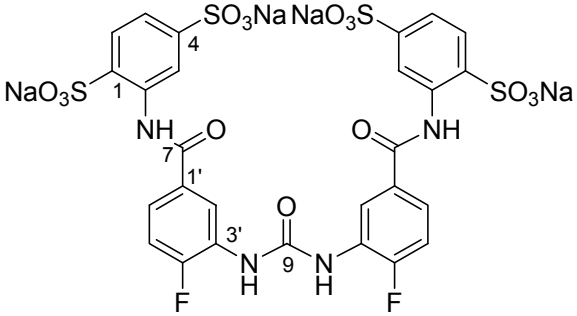	21a (MK-281/SD-298) 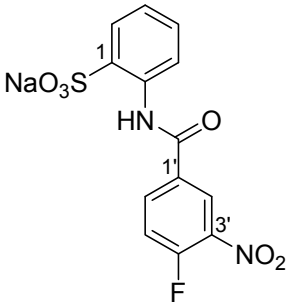
21b (MK282/SD-308) 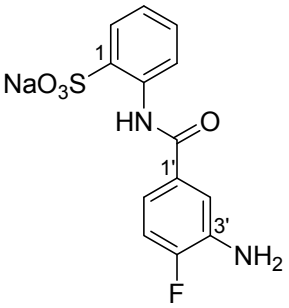	21c (MK283/SD-311) 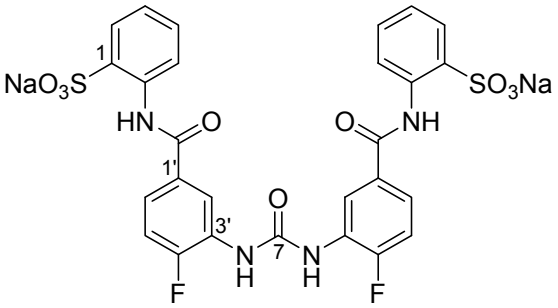
22a (MK-284/SD-312) 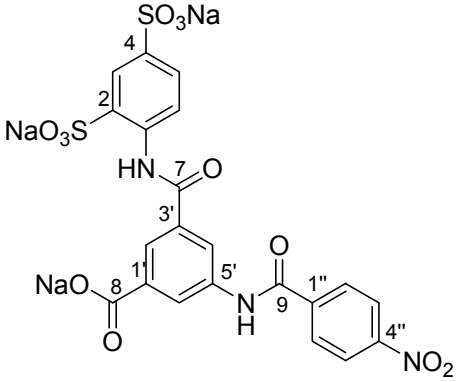	22b (MK-285/SD-316) 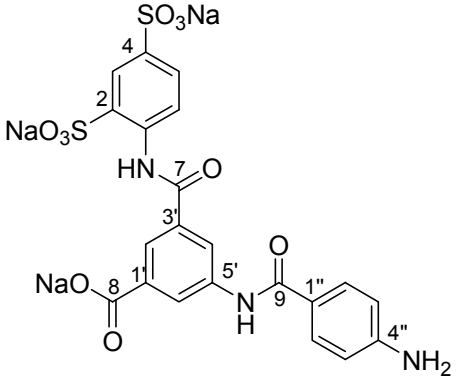

22c (MK-286/SD-317)

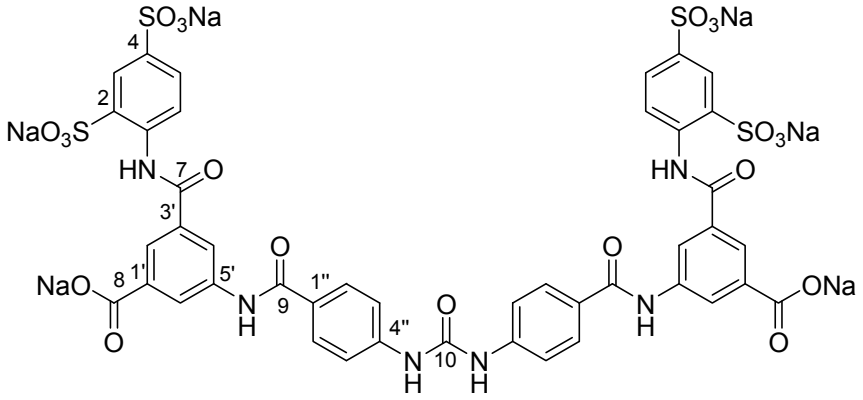

23a (MK-287/SD-313)

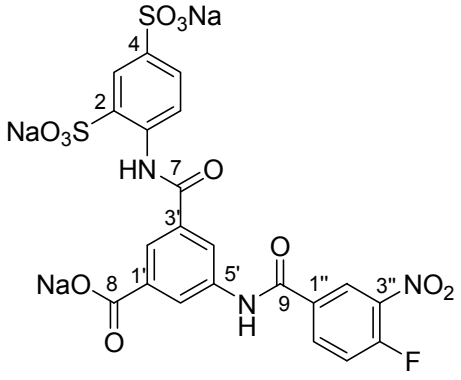

23b (MK-288/SD-318)

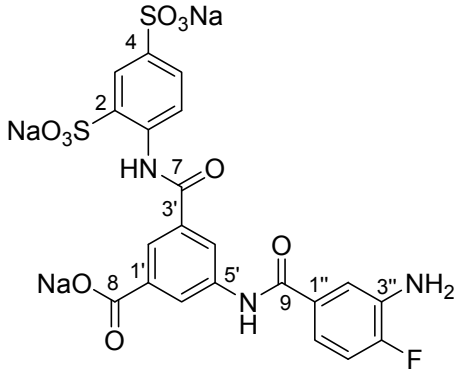

23c (MK-289/SD-320)

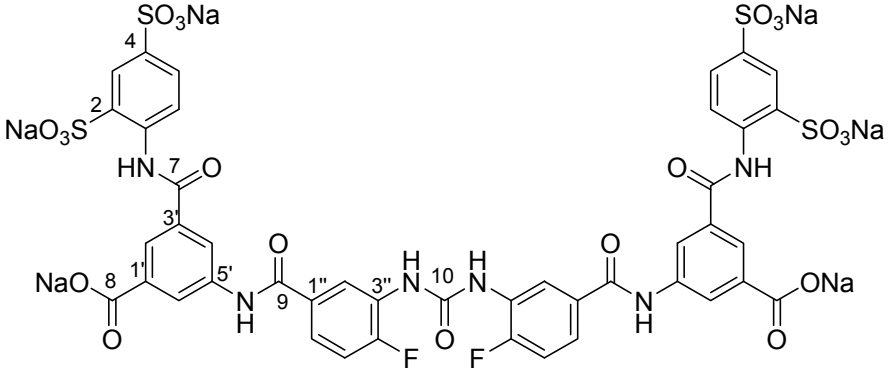

24a (MK-290/SD-304)

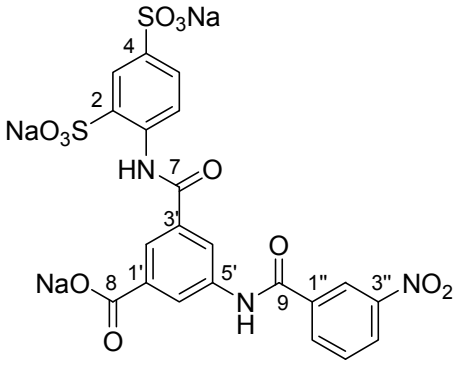

24b (MK-291/SD-315)

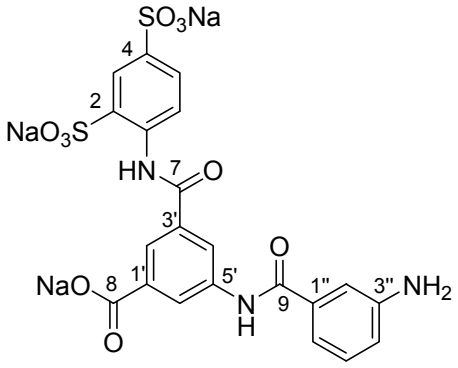

24c (MK-292/SD-322)

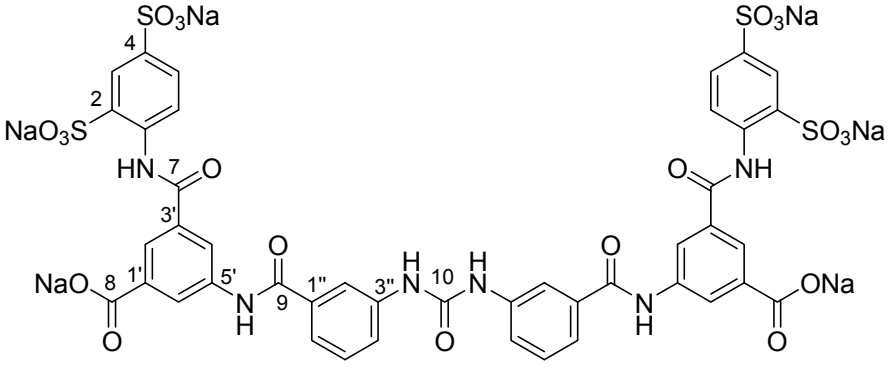

25a (MK-293/SD-321)

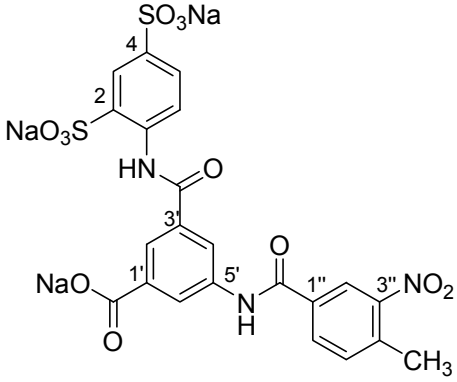

25b (MK-294/SD-323)

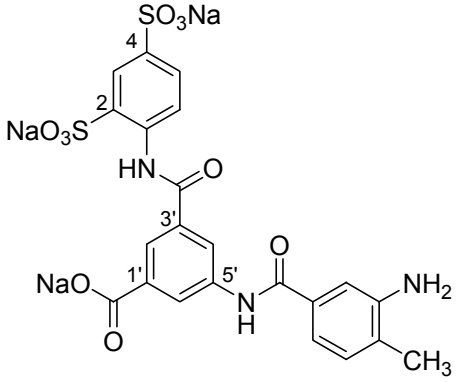

25c (MK-295 /SD-324)

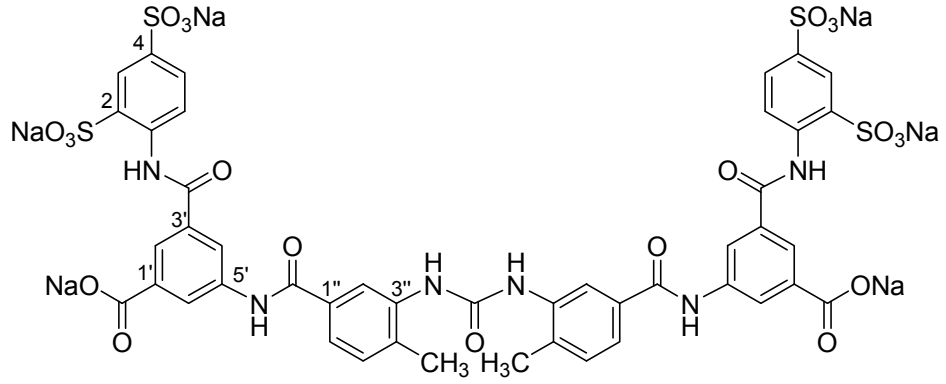

Curriculum Vitae

Personal data:

Name:	Sophi Damayanti
Date of Birth	20.02.1975
Place of Birth:	Bandung, Indonesia
Status:	Married (Spouse: M. Bayu Nurwicaksono)

Education background:

1981-1987	Elementary School, SD Merdeka 1 Bogor, West Java and SD Rajawali Banjarmasin, South of Borneo, Indonesia
1987-1990	Junior High School, SMPN 5 Tanjung Karang, Sumatra, Indonesia
1990-1993	Senior High School, SMAN 2 Tanjung Karang, Sumatra and SMAN 2 Denpasar, Bali, Indonesia

Pharmaceutical Background:

1993-1997 Pharmacy study at Institut Teknologi Bandung, ITB (Bandung Institute of Technology), West Java, Indonesia

1997-1998 Professional study (Apothecary) at ITB

Practices (all in Indonesia): Apotek Abadi, Pharmacy, Bandung; PT. Tanabe, Pharmaceutical Industry, Bandung; RSHS, Hospital, Bandung; Ditjen POM, Ministry of Health, Jakarta

1998 Apothecary examination

2000-2002 Master Study in Pharmaceutical Chemistry at ITB

Promotion:

02.2005-01.2007	Doctoral study at Prof. Kassack research group, Institute of Pharmaceutical, Friedrich-Willhelm-University of Bonn, Germany
02.2007-11.2008	Doctoral study at Prof. Kassack research group, Institute of Pharmaceutical and Medicinal Chemistry, Heinrich-Heine-University of Düsseldorf Germany.

Scholarship grants:

2000-2002	Master program scholarship, Ministry of Education Indonesia
2005-2008	Ph.D program scholarship, Islamic Development Bank, Saudi Arabia

Employment record:

1999-now	Academic staff at Sekolah Farmasi (School of Pharmacy) ITB, Bandung

Presentation:

Damayanti, S, Hongwiset, D, and Kassack MU, G protein-coupled receptors: NEW LIGANDS AT $P2Y_{11}$ RECEPTORS-Synthesis and Biological Testing, Poster Presentation, Italy-German Purine Meeting Club, September 2007, Leipzig-Germany

Acknowledgement

I would like to express my deep gratitude and sincere appreciation to Prof. Dr. Matthias U. Kassack who gave me the opportunity to be involved in his research group. I am deeply grateful for his excellent guidance, patience, attention, and encouragement during my doctoral study.

I wish to thank Prof. Dr. Thomas Kurz for his willingness to be my Co-supervisor and for his support at the end of my study.

The financial support from Islamic Development Bank (IDB) during my stay in Germany is gratefully acknowledged and thankful. To Mr. A.M. Shaharuqul Huq, I thank him for a fruitful cooperation as well as to other Indonesian IDB scholars for their assistance.

I would like to thank Prof. Dr. Michael Wiese for giving me facilities in the first two years of my study in University of Bonn.

Many thanks are assigned to School of Pharmacy, Bandung Institute of Technology, Indonesia, especially Department of Pharmaceutical Chemistry for supporting me before and during my study.

I would like to give my sincere thanks to Pharmaceutical Chemistry, University of Bonn, Dr. Peters and his colleagues for the NMR measurements and Dr. Ebel, Julia Kjer, Dr. Keck and Dr. Tommes from University of Düsseldorf for conducting ESI mass spectrometry analysis.

I wish to express my thankful for Dr. Günter Waldheim for his efforts and advices in the Nomen Clature of all new compounds.

I am indebt Dr. Alexandra Hamacher for her nice support and attention during my study especially at the important steps. For her encouragement and advices by my last edition manuscript, I thank her deeply.

I would like to express my thankful for Dr. Sabine Meis for introducing and guiding me how to work in cell laboratory and her advices and assistance during correction of my dissertation.

I appreciate and thank Heiko Ullmann and Darunee Hongwiset who introduced and assisted me how to work in the synthesis laboratory and also their advices by writing chemistry part.

Weiteren Dank gilt an Magdalene Matyja, die mir in ihre Büro adoptiert hat und für ihre ganz grosse Verstandniss und viele süße Fürsorge.

I am grateful to the group members I have mentioned before and to Daniel Esser, Susanne Kögel, Christian Urban, Katharina Keppner, Kathrin Christof, Omér Usta,

and all other members of AK Kassack for sharing a cooperative work, many laughters, and a very great support at the end. Vielen Dank, ich werde euch vermissen.

I would like to express my thankful for my “brother” Stefan Leyers for his warm friendship especially in the first two years in Bonn. Thank expression also given to all members of AK Wiese-Kassack research group University of Bonn.

Dr. Rahmana Emran Kartasasmita, Dr. Daryono Hadi Tjahjono, Dr. Diky Mudhakir, I thank them for their great supports in the last term of my study.

I would like to express my sincere thankful for Hr. and Fr. Supriyatna, Hossy Dwiyanto, Michi Zumbeck, Lili Irwani, Sri Haryani, Else Agustina, Henny Sutarto Adam Pamma, Rahmat Triandi, and all Indo-Bonn community for their friendship and encouragement, especially in our first two years in Bonn.

Special thanks are given for Dr. Ine Dewi Indriani, Arnulf Diesel, Triana Hertiani, Metta Yuniati, Edi Wahyu, Sri Yulis, Fr. Tilo, Fr. Niken Badruddin, and Ruhr-Gebiet Indonesian community for their support and friendship in our last two years in Duesseldorf. The same thanks are also given to Ria Wijayati, Trianti, Elin Julianti, Shinta Kania Wardhani, Lia Barra, Retmawati, Jessica Gaieb, Sandra Hornfischer, Peggy Seeger, Liane Schmidt, Jessica Martini, FA-93, Ex-UBG 92/93, WSAB and FFADGB for sharing our similar interests.

I would like to thank deeply my “sister” friends: Dewi Isnaniar, Dr. Lia Amalia, and Tribudiningdiyah Utami who always by my side in good times and especially bad times.

Uncountable thank goes to the late father Daday Sulaeman Kosasih and to my mother Dedeh Dahlia who bless me with the best support and pray can give. Thankful are also dedicated to the late mother in law and the late father in law who were always strengthen our will. The same amount of thank, I wish also for grandparents, sisters, brothers, and all our family.

At last, I feel blessed to have my husband M. Bayu Nurwicaksono for his unwavering encouragements, utmost sacrifices and uncountable patience for facing all comments and problems which were occurred during his accompanying here to reach our dream together. Ich bin froh, dass du hier bei mir bist.

Praise to The Mighty